Metabolic drivers of community dynamics in marine microorganisms

By

Max A. Jahns

B.A., Vasssar College, 2019

Submitted to the Department of Earth, Atmospheric, and Planetary Science

in partial fulfillment of the requirements for the degree of

Doctor of Philosophy

at the

MASSACHUSETTS INSTITUTE OF TECHNOLOGY

and

WOODS HOLE OCEANOGRAPHIC INSTITUTION

February, 2026

Authored by: Maxim Jahns
Earth, Atmospheric, and Planetary Sciences
September 25th, 2025

Certified by: Matthew D. Johnson
Biology Department
Woods Hole Oceanographic Institution
Thesis supervisor

Accepted by: Edward A. Boyle
Chair, Joint Committee for Chemical Oceanography
Massachusetts Institute of Technology/Woods Hole Oceanographic Institution

For Ben and Barbie,

Metabolic drivers of community dynamics in marine microorganisms

By: Max A. Jahns

Submitted to the Department of Earth, Atmospheric and Planetary Sciences on September 25th, 2025 in partial fulfillment of the requirements for the degree of Doctor of Philosophy.

ABSTRACT

Marine microorganisms adopt metabolic strategies, the biochemical means by which they acquire energy and nutrients, in part, because of the interactions between biological entities in their community. The eco-evolutionary strategies adopted by marine microbes both shape and are shaped by the environments in which they can live and remain competitive, the flow of carbon and nutrients through the environment, and the structure of the marine ecosystem. While many theories exist to explain the metabolic underpinnings of plankton ecology, there remains significant gaps in our understanding of how organisms fill metabolic niches and the mechanisms underlying these dynamics. This work focuses on three biotic relationships (parasitism, predation, and competition) and how these community dynamics both shape and are shaped by organismal metabolism using planktonic laboratory systems. To test the effects of parasitism and predation, we compared the cosmopolitan marine cyanobacteria *Prochlorococcus* MED4 lipidome under ideal conditions to its lipidome modulated due to top-down pressures from P-SSP7, a T7-like phage, and *Paraphysomonas bandaiensis*, a phagotrophic nanoflagellete predator. From cultures containing only *Prochlorococcus* MED4, we assemble the first complete lipidome of the abundant marine cyanobacteria *Prochlorococcus* MED4. Using this core lipidome as a baseline, we identify several characteristic ways phage infection alters the fatty acid, phospholipid, and other lipid metabolic pathways in *Prochlorococcus*. We also describe an unknown mechanism by which the energy storage metabolism of *Paraphysomonas bandaiensis* is affected by grazing on P-SSP7 infected prey. Next, to test how competitive dynamics shape metabolic niche partitioning, we assemble a novel model system using multiple strains of the marine mixotroph *Ochromonas*, with differing metabolic requirements. These mixotrophs were grown in competition with *Paraphysomonas bandaiensis* in batch and chemostatic culture. Generally, mixotrophic metabolism is assumed to confer a competitive advantage through the acquisition of energy and nutrients from multiple pools and the ability to relieve competitive pressures by switching trophic investments away from limiting pathways. Despite this, both obligately phagotrophic strains of *Ochromonas* tested instead 'doubled-down' on phagotrophy in response to competition with *Paraphysomonas bandaiensis*. Whereas the facultatively phagotrophic strain used in this study, *Ochromonas* 1391, followed typical mixotrophic competitive behavior of increased investment in phototrophy. These strains also experienced significant growth and energy efficiency tradeoffs because of this investment. We find evidence that this tradeoff may be due to prey nutrition needs or prey quotas in these organisms.

Additionally, we show how metabolic landscapes, i.e. multidimensional conceptualizations of metabolism, can inform metabolic tradeoffs and realized metabolic niches in response to community dynamics. Our results underscore the powerful effects of community interactions and metabolism, and vice versa. The dynamics captured within this dissertation research, inform microbial metabolic niches and how energy and nutrients flow through mixed planktonic communities with complex biotic interactions.

Thesis supervisor: Matthew Johnson

Title: Associate Scientist with Tenure, Woods Hole Oceanographic Institution

ACKNOWLEDGEMENTS

They say it takes a village to raise a PhD candidate- and they are right. I am so absolutely blessed to have been supported in my journey over the last six years by some of the most amazing people I could ever hope to meet.

Firstly, to acknowledge my funders: the NSF, the Simons Collaboration on Ocean Processes and Ecology, and WHOI. That money made it possible for me to even do this work.

Thank you to APO, WHOI facilities, WHOI IT, and everyone else at these two institutions who actually make this place function. That is not an easy task! A special shoutout to Christine and Julia who are just delightful human beings that I feel bad asking for help from, because I'd rather just talk with them about their lives! And thank you to Ann for helping me get my first teaching position.

I must also thank my mentors throughout all of my academic career- Teresa Garrett, Jill Schniedreman, Marshall Bowles, Jennifer Herrera, Chris Smart, Virginia Schutte, Mrs. Crothers, Mr. Taylor, Mrs. Schlobohm, and Mr. Mantra. Loving learning is a rare thing- thank you for helping me with it.

Next, thank you to Ben Van Mooy and the entire Ben Van Mooy lab for being my first science family and for welcoming me into WHOI with open arms. Special thank you to Helen who is the only reason that lab works. And Henry, Lydia, and Danny, you helped me find my footing, you listened to me vent, and you three were my first true mentors in graduate school.

My committee has been a wonderful support for me these past years. Harriet, Stephanie, and Holly all bring such a bright light with them whenever they go. They deserve eight million thanks for helping me fight JCCO to get an extension. To have the support and guidance of these accomplished scientists has been invaluable.

The ever-growing Johnson lab has also been instrument in my success during the past few years! Matt was right to say I was so excited to see Sophia, then Brittany, and then Julia join our team! You all have made working in the lab such an exciting prospect. You're all SO talented and I thank each of you for your insights. Y'all are just an incredible hype team.

Thank you to my summer family- the Bileckis for welcoming me into their crew. Especially, Mame, who gave me her love and support from the very start and has not let off the gas since. Mame is generous of spirit and with encouragement.

To my friends from college, especially Madeleine and Catherine, this is a path all three of us have taken together. Your love means the world to me. There are no two better people to complain or to celebrate with.

My friends from high school (who have now been my best friends for over a decade!) are just the best. I mean what else is there to say? Bailey, Lindsey, Kayla, Katherine and Morgan are just like amazing people. Like AMAZING amazing. Like I will go on at least one trip with them every year for the rest of my life. Like I'm going to be there to celebrate each of their wins and comfort them in each of the rough patches, as I know they will do for me. My cabin time family, I can't wait for our kids to grow up together.

Moving to the awe-inspiringly rare support network that is the JP-student community, there is no way I could have done this without all of you. This group of humans is like none I've ever met. You have been my sounding board, safe space to cry, and party central all at the same time.

To the folks in the WHOI Graduate Student Union- keep up the good fight! Veevee, Jacob, Noah, Cynthia, Chloe, Jonathon, Ciara, Jeanne, etc. thank you for stepping up and donating your valuable time to lead us. We are nothing without solidarity!

There are too many people who have been there for me in this process to name. Too many to thank, even if the words I'll write here could properly convey my gratitude. But I can't help but try.

Poonam - you've been a stellar roommate for almost three years! It's been so fun to come home and gab with you.

Iulia – Thank you for the wonderful dinner dates. You never hesitate to speak your mind and that's a remarkable quality I will always admire.

Brenna – there is no better enabler in the entire world! Brenna can hype me up to do literally anything. I miss our walks along the beach more than I can say. You're the type of person who can't help but be successful and I am so lucky to have met you!

Hannah – I honestly used to think you being so kind and so empathetic was at least in some part an act. But now, I am absolutely ashamed for ever thinking it wasn't possible for someone to be so understanding. My midwestern sister- I am so honored to work with you and to call you a friend!

Chloe – my lab little sister. There are so many words I could use to describe Chloe (goofy, sharp, flaky, witty, unpredictable, empathetic, etc.) but one in particular comes to mind: passionate. When Chloe sets her mind to something, especially when it involves helping someone else, there is nothing that can stop her. I am so lucky to love and be loved by you!

Samuel – the relationship we have developed is like nothing I have experienced before. It occurred to me recently, that when I jokingly say to 'yeah, bro', I truly am calling you my brother. You have an amazing ability to just be great to the people around you, and inspire those people, like me, want to want to treat others the way you treat them. You are funny and smart-more than I think you give yourself credit for. And in these few years I have known you, I have developed a relationship I cherish and never want to let go of. Thank you, bro.

Cora – What do you call Brad Pitt, but he just got his PhD? There is no other person on earth who can "yes and" like you do. Why? Because you have mastered the ability to listen and

empathize. Thank you for truly knowing me like few else do. The care and attention you give to your friends is inspiring.

Alan - thank you for being such a wonderful roommate and supportive friend. I believe Ciara once described you as being secretly funny- but I think you're downright hilarious. You are one of the best creative partners I've had. Thank you for joining me in the Avatar Megagame and Academia the Musical! And thank you for organizing jam band, TI night, etc. etc. You're amazing and singular!

Ciara – from the moment we *almost* held hands I knew I had a true friend. You (and your amazing animals!) have been so great to have around for support and comfort. You are as stubborn as I am, but you are even stronger, and you inspire me to be strong like you. Plus, your laugh is unique and there's nothing I quite love more than making you roll your eyes.

Shavonna – my lab twin! I cherish all the time I get to spend with you. In some ways we're a bit different (I have no artistic talents for example) but there is something about speaking with you where I just feel seen, understood. Your moral compass is unparalleled. And, I don't think your advice has ever steered me wrong. If there's one person in the world who deserves all of her blessings it is you. I just want to shout from the rooftops how great you are! You've been with me through literally every step of this journey and there's no way I can ever really thank you for everything you've given me.

Shawn – I mean, put the two of us in a room together and it's over. And, like APO knew, you were the first person I ever met or lived with at WHOI. From quoting Marvel movies to quoting… well basically anything, the two of us will take any catchphrase and beat it into the ground until we take it back to the "workshop". You're the kind of friend that most people just don't get to experience – one who is always there to support you (and even clean up your puke! Sorry!). But, I know I'm not special – Shawn is so stellar he is that kind and genuine and amazing to everyone he meets. You are like a brother to me, and it sucks that you are so far away, but I can't wait to see all the amazing things you do!

To all the many others I've met along the way – Owen, Nick, Digo, Ben, Evan, Chase, Michael, Lukas, Lina, Brendan, Kharis, Jin Si, Eleanor, other Ben, other Evan, Annaliese, Jordan, Eeshan, Shari, Charlie, Elizabeth, Trevor, Maddie, Mark, Jo, Mike, Ciara, etc. etc. thank you for being there for me. I hope you know I will be there for you too if you ever need it!

Finally, there is no blessing I cherish most than the blessing of such an amazing family. With a large and loud extended family, I learned to speak up and speak my mind. I learned that hard work is valuable and that giving up is the last resort. And most importantly, this family demonstrates how to love completely.

My sister is my rock in hard times and my light in dark times. She is always so much more than she gives herself credit for- because she is fucking amazing. Angie is the reason I've been able to stay true to myself through everything. She is funny and silly and annoying in all the right ways. I love you, sissy!!!!

Dad, you gave me a love for nature and for science. You were always teaching me the beauty and wonder of the natural world, from our garden (which always used native plants) to Phelps and beyond. And as I've grown up, you've become an amazing ear to bounce thoughts off of and truly a friend. I love you so much dad and I can't thank you enough for everything.

My ma, who always calls me the absent-minded professor, taught me how to celebrate myself and invest in my education. Twenty-eight years ago she chased around a tornado of a toddler who wanted to test everything, ask annoying questions, and learn everything I could get my hands on. And then, I watched her spend countless hours investing in her education in addition to being a mom. You taught me how to work hard, how to speak my mind, and how to value opportunities, like education, to better my life. I love you so, so, so, so much and I am PROUD (P-R-O-U-D) to be your son.

And finally, this thesis is dedicated to two people who wanted to badly to see this day come but did not get the chance, Barbie and Ben.

Barbie, you taught me to dance with joy, to preserve by loving yourself, and to invest in the ones you love. The world is dimmer without you in it.

Ben, my brother. I cannot find the world to place on this page to honor you in the way I want. Nothing can. I miss you everyday and love you so completely.

The two of you have created chambers in my heart I retreat to when I want to remind myself what true love is. I will cherish our reunion when my time comes as well.

Thank you.

TABLE OF CONTENTS

ACKNOWLEDGEMENTS 8

TABLE OF CONTENTS 13

LIST OF FIGURES 18

LIST OF TABLES 20

CHAPTER 1: INTERPLAY BETWEEN ORGANISMAL METABOLISM AND ECOLOGY 21

Ecology and metabolism 21

i. Metabolic foundations of life 21

ii. Interplay between metabolism, ecology, and the environment 21

Community dynamics and metabolic strategies 22

i. The metabolic niche 22

ii. Studying metabolic niches 23

Thesis overview and hypotheses 23

i. Aims and scope 23

ii. Chapter 2 24

iii. Chapter 3 26

iv. Chapter 4 27

v. Chapter 5 28

vi. Impact and merit 28

Figures 29

Figure 1.1 29

Figure 1.2 30

Tables 31

Table 1.1 31

References 31

CHAPTER 2: CYANOPHAGE INFECTION INDUCES CHARACTERISTIC CHANGES IN THE LIPIDOME OF *PROCHLOROCOCCUS* AND ITS PREDATOR 39

Abstract 39

Introduction 39

Methodology 40

i. Cultures and strains 40
ii. Field sampling 41
iii. Lipid extraction and mass spectrometry 41
iv. Untargeted lipidomics 41
v. Analytical methods 42
Results 42
i. The Prochlorococcus lipidome 42
ii. Changes in Prochlorococcus phosphorus metabolism in response to phage infection 44
iii. Phage-associated changes in oxylipin-like compounds and changes in fatty acid composition 44
iv. Cyanophage infection alters host energy storage metabolism and may decrease energy transfer to higher trophic levels 46
Discussion 47
i. The core lipidome of Prochlorococcus 47
ii. The modular lipidome of Prochlorococcus 47
iii. Infection induced alteration of phospholipid metabolism 47
iv. Changes to fatty acid composition and the identification of possible oxylipin-like biomarkers for phage infection 48
v. Indirect higher trophic level consequences of phage infection 49
Acknowledgements 50
Figures 51
Figure 2.1 51
Figure 2.2 52
Figure 2.3 53
Figure 2.4 54
Figure 2.5 55
Figure 2.6 56
Figure 2.7 58
Figure 2.8 59
Figure 2.9 59
Figure 2.10 60
Figure 2.11 61
Figure 2.12 62
Figure 2.13 63
Tables 63
Table 2.1 63
Table 2.2 64
References 64

CHAPTER 3: COMPETITION FOR PREY DRIVES A ‘DOUBLING DOWN’ ON PHAGOTROPHY IN THE MIXOTROPH *OCHROMONAS* 70
Abstract 70

Introduction 70
Methodology 72
i. Culture maintenance 72
ii. Experimental design 72
iii. Flow cytometry and fluorescence 72
iv. Analytical methods 73
Results 73
i. Solo experiments 73
ii. Competition experiments 74
Discussion 74
i. Environmental controls on growth and trophic mode 74
ii. Effects of competition on growth 75
iii. Trophic 'doubling down' in competition 76
iv. Implications for mixotrophic competitive ecology 77
Acknowledgements 79
Figures 80
Figure 3.1 80
Figure 3.2 81
Figure 3.3 82
Figure 3.4 85
Figure 3.5 87
Figure 3.6 89
Figure 3.7 90
Figure 3.8 91
Figure 3.9 92
Figure 3.10 93
References 93

CHAPTER 4: MIXOTROPHIC METABOLIC LANDSCAPES AND REQUIREMENTS SHAPE TROPHIC INVESTMENT IN COMPETITION 98
Abstract 98
Introduction 98
Methodology 100
i. Cultures and maintenance 100
ii. Chemostat design 100
iii. Experimental design and sampling 102
iv. Flow cytometry 102
v. Growth rates and equilibrium 102
vi. Bacteria and grazing: phagotrophic investment 103
vii. Photo-physiology and primary production: phototrophic investment 104
viii. Imaging and cell size 105

ix. Elemental analysis 105
x. Metabolic investments 106
xi. Analytical methods 106
Results 107
i. Chemostatic culturing 107
ii. Community composition 107
iii. Trophic displacement 107
iv. Growth efficiency and metabolic landscapes 108
Discussion 109
i. Trophic displacement due to competition explained through metabolic landscapes 109
ii. Mechanisms underlying metabolic tradeoffs 110
iii. Community-level impacts 112
iv. Evolutionary implications 113
v. Summary 114
Acknowledgements 114
Figures 114
Figure 4.1 115
Figure 4.2 115
Figure 4.3 116
Figure 4.4 116
Figure 4.5 118
Figure 4.6 120
Figure 4.7 121
Figure 4.8 123
Figure 4.9 125
Figure 4.10 125
Figure 4.11 126
Figure 4.12 127
Figure 4.13 128
Tables 128
Table 4.1 128
Table 4.2 129
Table 4.3 130
Table 4.4 130
Table 4.5 131
References 131
CHAPTER 5: CONCLUSIONS AND FURTHER WORK 138
Summary and implications 138
i. Chapter 2 138
ii. Chapter 3 139
iii. Chapter 4 140

Ochromonas as a non-traditional 'model system' for mixotrophic metabolism and ecology 141
i. The choice of mixotrophic study systems 141
ii. Importance of model systems 142
iii. Ochromonas as a non-model model system 144
iv. Research methods for using an Ochromonas model system 147
v. Looking towards the future 148
Future work 150
i. Investigating the pathways involved in T4-like phage lipid remodeling 150
ii. Cyanophage infection biomarker verification and field use 150
iii. Complex competitive communities in chemostat culturing 150
iv. Determining the metabolic pathways involved in mixotrophic competitive tradeoffs via transcriptomics 151
v. A model to predict competitive metabolic tradeoffs in mixotrophs 151
Concluding remarks on community dynamics and the metabolic niche 152
Tables 154
Table 5.1 154
Table 5.2 156
References 157

LIST OF FIGURES

CHAPTER 1: INTERPLAY BETWEEN ORGANISMAL METABOLISM AND ECOLOGY 21
Figure 1.1 29
Figure 1.2 30
CHAPTER 2: CYANOPHAGE INFECTION INDUCES CHARACTERISTIC CHANGES IN THE LIPIDOME OF *PROCHLOROCOCCUS* AND ITS PREDATOR 39
Figure 2.1 51
Figure 2.2 52
Figure 2.3 53
Figure 2.4 54
Figure 2.5 55
Figure 2.6 56
Figure 2.7 58
Figure 2.8 59
Figure 2.9 59
Figure 2.10 60
Figure 2.11 61
Figure 2.12 62
Figure 2.13 63
CHAPTER 3: COMPETITION FOR PREY DRIVES A 'DOUBLING DOWN' ON PHAGOTROPHY IN THE MIXOTROPH *OCHROMONAS* 70
Figure 3.1 80
Figure 3.2 81
Figure 3.3 82
Figure 3.4 85
Figure 3.5 87
Figure 3.6 89
Figure 3.7 90
Figure 3.8 91
Figure 3.9 92
Figure 3.10 93
CHAPTER 4: MIXOTROPHIC METABOLIC LANDSCAPES AND REQUIREMENTS SHAPE TROPHIC INVESTMENT IN COMPETITION 98
Figure 4.1 115
Figure 4.2 115
Figure 4.3 116
Figure 4.4 116
Figure 4.5 118
Figure 4.6 120

Figure 4.7 121
Figure 4.8 123
Figure 4.9 125
Figure 4.10 125
Figure 4.11 126
Figure 4.12 127
Figure 4.13 128
CHAPTER 5: CONCLUSIONS AND FURTHER WORK 138

LIST OF TABLES

CHAPTER 1: INTERPLAY BETWEEN ORGANISMAL METABOLISM AND ECOLOGY 21
Table 1.1 31
CHAPTER 2: CYANOPHAGE INFECTION INDUCES CHARACTERISTIC CHANGES IN THE LIPIDOME OF *PROCHLOROCOCCUS* AND ITS PREDATOR 39
Table 2.1 63
Table 2.2 64
CHAPTER 3: COMPETITION FOR PREY DRIVES A 'DOUBLING DOWN' ON PHAGOTROPHY IN THE MIXOTROPH *OCHROMONAS* 70
CHAPTER 4: MIXOTROPHIC METABOLIC LANDSCAPES AND REQUIREMENTS SHAPE TROPHIC INVESTMENT IN COMPETITION 98
Table 4.1 128
Table 4.2 129
Table 4.3 130
Table 4.4 130
Table 4.5 131
CHAPTER 5: CONCLUSIONS AND FURTHER WORK 138
Table 5.1 154
Table 5.2 156

CHAPTER 1: INTERPLAY BETWEEN ORGANISMAL METABOLISM AND ECOLOGY

Ecology and metabolism

i. Metabolic foundations of life

Life is made up of organized biochemical systems which are by-and-large thermodynamically unfavorable (Brown, Silby, and Kodric-Brown 2012). To create the biochemicals required for life, organisms must obtain and harness external energy to catalyze their synthesis (Alberts et al. 2002, Pontzer and McGrosky 2022).

There are three modes by which organisms produce energy: primary production (direct synthesis of biomolecules from inorganic materials), secondary production (catalyzing the synthesis of cellular components through the potential energy of ingested organic molecule catabolism), or a mix of the two (Heal and MacLean 1975, Selosse, Charpin, and Not 2017). Each form of production requires resources the cell cannot produce *de novo*, and thus the organism must obtain these nutrients and energy from the environment. The ability of the cell to obtain these materials is dependent on their availability in the environment (abiotic control on growth).

These resources are limited. As organisms exist within diverse communities and ecosystems, they often must compete with other lifeforms (biotic control on growth). For primary producers this means competition for materials required in their carbon fixation pathway. However, secondary producers are in constant battle with their prey for survival, as well as any other secondary producers for shared prey. Understanding the complex interactions between an organism's energy and nutrient requirements for growth and its biotic and abiotic environment form the foundation for understanding its ecology (Brown et al. 2004).

ii. Interplay between metabolism, ecology, and the environment

An organism's metabolism is inexorably intertwined with its ecology. The requirements of an organism for growth and carbon acquisition efficiency vary greatly across the tree of life, though they follow certain patterns within defined constraints (Crockford et al. 2023, Glazier 2024). Similarly, all organisms possess some extent of metabolic plasticity allowing them to respond to changing environments and needs (Brown et al. 2004, Norin and Metcalfe 2019, Venkataraman and Huffmyer 2025).

One central tenet of community ecology is that the distribution and abundance of energy and nutrients shapes species' metabolic strategies (Bernhardt et al. 2020, Gralka et al. 2020). As community structures shift due to changes in species abundance, competition, or environmental disturbance, so too do their metabolic demands (Gralka et al. 2020, Koffel, Daufresne, and Klausmeier 2021). For instance, when resources become scarce or unpredictable, organisms may

adjust their metabolic strategies, either by lowering energy expenditures or altering their resource-use efficiency (Amado et al. 2016). Similarly, a predator's metabolic investment in prey acquisition is in part determined by prey availability (Roller and Schmidt 2015). Current literature suggests that metabolic plasticity, ability of an organism to change its metabolic strategy, is an important factor in determining how species compete and persist in mixed communities (Donelson et al. 2019, Archibald et al. 2024).

Metabolism is not only shaped by ecological relationships but is itself a key factor that drives the nature and outcome of these relationships (Douglas 2010, Ponnudurai et al. 2016, McClain et al. 2020, Sørensen 2020, Yee et al. 2025). However, the underlying mechanisms which dictate how microbial community dynamics shape and are shaped by metabolism remain elusive (Klitgord and Segrè 2011, Stark et al. 2025). Metabolism is a complex process of thousands or more interconnected genes, not all of which are expressed at any given time. And though all two-species biotic ecological interactions can be boiled down to a set of fundamental relationships conceptually (Table 1.1), true ecosystem structure is multi-dimensional and can be in flux (Staehr et al. 2012, Ramon and Stelling 2023).

Biological entities also directly shape the abiotic characteristics of the environment (nutrients, heat, structure, etc.) (Wright and Jones 2006, Sutherland et al. 2013, Daniels, van Vilet, and Ackermann 2023, Sanders and Frago 2024). Organismal alteration of the environment depends on the chemical reaction its cells are able to catalyze (i.e. its metabolism). Thus, a thorough understanding of ecology and environmental science requires investigating the metabolism of environmental players.

Community dynamics and metabolic strategies

i. The metabolic niche

According to niche theory, species that occupy different ecological niches are less likely to exclude one another in competition for limited resources (Koffel, Daufresne, and Klausmeier 2021). While niche theory was classically applied to biogeographical niches, metabolic processes play a central role in niche differentiation (Baltar et al. 2019, Malard and Guisan 2023, Glazier 2024). Indeed, the idea of a niche is thought of more and more as a multidimensional space which includes metabolic investments and returns (Hutchinson 1957, Wilson et al. 2011, González et al. 2017, Sørensen et al. 2020, Carlson et al. 2021, Potapov et al. 2021). Species that specialize in certain metabolic pathways or competitive strategies may increase their eco-evolutionary fitness (Sánchez González 2023, Piriz, Niklitschek, and Maldonado 2025). Other species with generalist or plastic responses are less discriminatory in their metabolic strategies, which may confer a different competitive advantage (Archibald et al. 2024, Gubry-Rangin et al. 2024).

Understanding how biotic interactions influence these niches is a growing field in ecological and evolutionary research. One prevalent theory, the metabolic theory of ecology (MTE), puts forth that simple rules about the scaling of metabolic rates with body size, temperature, ecological interactions, etc. can be determinative of ecosystem structure and dynamics (Brown et al. 2004, Brown, Silby, and Kodric-Brown 2012). According to MTE, metabolic rates determine the

energy demands of organisms, which in turn influence species' ecological roles. Critics of classical MTE say its model of ecosystems may be too reductionist and not incorporate appropriate nuances of complex metabolism or community interactions (Valderrama and Fields 2017, Stark et al. 2025). Additionally, MTE traditionally focuses on abiotic forcing, and it remains unclear how competition, predation, and other biotic factors influence the metabolic strategies of species, particularly in complex communities (Montoya and Raffaelli 2010, Welti et al. 2017).

Other theories such as ecological stoichiometry focus on how environmental resource availability and cycling influences ecosystem structure and community dynamics (Van de Waal et al. 2018). Resource-ratio theory, for instance, theorizes competition is dictated in large part by resource availability (Wilson, Spijkerman, and Huisman 2007). This concept has been particularly applied to planktonic communities (Gallego and Narwani 2022, Behrenfield et al. 2025). In this view, under longer-term steady state conditions, it's not just the energy capture of the microbe that is dispositive of fitness. Instead of metabolic processes, the focus is on the competitors' resource requirements for growth.

While many ecological theories attempt to unify disparate observations into foundational rules that govern community structure, many studies of ecology employ a wholistic approach to evaluating metabolic interactions between microbes (Tecon et al. 2019, Prosser 2020). The metabolic strategies of organisms can sometimes be called the metabolic niche. The metabolic niche is an emerging tool for conceptualizing ecology with no clear definition, but generally relates to the multidimensional metabolic space organisms occupy under certain conditions (Massing et al. 2023). Perhaps one of the greater open questions in the field is determining what biotic and abiotic factors constrain a metabolic niche (Antwis et al. 2017).

ii. Studying metabolic niches

The realized niches and metabolic strategies of microbes in the marine system is important, as it greatly effects the structure, energy capture and transfer, and resilience of microbial communities (Donelson et al. 2019, Hu, Bourdeau, and Hollander 2024, Levine, Doblin, and Collins 2024). Because of this, model laboratory systems have been used to understand the fundamental drivers of trophic dynamics in marine plankton (Karl and Proctor 2007). Laboratory systems allow for greater experimental control and fewer confounding variables (Dupont and Metian 2023, Gazeau et al. 2024). These systems have a long history of being combined with field observations to create increasingly accurate models (Duarte, Gasol, and Vaqué 1997, Gerard et al. 2022, Graff et al. 2023). Laboratory experiments are therefore key to a greater understanding of marine microbial metabolism and ecology.

Thesis overview and hypotheses

i. Aims and scope

This thesis aims to better characterize the interplay between community ecology and microbial metabolism. The metabolic niche of a microbe is determined both by biotic and abiotic environmental constraints (Antwis et al. 2017). While a large body of work has explored the

effects of environmental limitations on marine microbial metabolism, notably less research has attempted to isolate and examine the influence of inter-species interactions, or the so-called 'interactome', on microbial ecology and biogeochemistry.

In each chapter we culture an environmentally relevant marine nano- or picoplankton in a controlled laboratory setting and explore its cellular biochemistry, energy capture, and nutrient acquisition. Then, we introduce new biological entities which form an ecological relationship with our subject, predatory, parasitic, or competitive, and observe how this new biotic force influences the metabolism of our subject (Figure 1.1).

Special care is taken in each experiment to control the abiotic environment's influence on microbial metabolism. Instead, by isolating the effects of the 'interactome' we were able to construct novel theories about biotic forcing on organismal metabolism, metabolic niches, and competitive dynamics in addition to community structure and productivity. In exploring these model and well-controlled mixed-community laboratory systems we form hypotheses about how these foundational interactions between species and their metabolism can shape evolutionary trajectories and aquatic ecosystems (Figure 1.1).

ii. Chapter 2

Viruses are the most abundant biological entity in the pelagic environment (Weynberg 2018). Viruses do not have their own metabolism, instead relying on the metabolism of their hijacked host to persist. The mechanism by which viruses use host machinery to replicate themselves vary (Vincent and Vardi 2023). However, most viruses carry host genes, called auxiliary metabolic genes (AMGs), in their genomes which they use to influence host metabolism (Tian et al. 2024). In the oligotrophic ocean, AMGs promote traits in their host advantageous for viral replication and lysis, often altering metabolic processes such as carbon acquisition, nutrient uptake, energy storage, and DNA replication (Thompson et al. 2011, Breitbart et al. 2018, Tsiola et al. 2023, Tian et al. 2024).

When cells are infected much of their cellular metabolism is altered to make phage capsids. The influence of viral infection on marine microbial metabolism is poorly characterized (Suttle 2007). However, viruses are hypothesized to alter many marine organisms such that the lysate of an infected cell is distinct from an uninfected cell (Hurwitz and U'Ren 2016, Yamada et al. 2018, Xiao et al. 2021). Studies have shown microorganisms rapidly take up viral lysate (Wilhelm and Suttle 1999). There have been suggestions that this change in composition of the cell lysate or when it is grazed may have implications for the transfer of energy to higher trophic levels, but so far there is no robust body of evidence to support this theory (Jacquet et al. 2010).

The cycling and fate of viral lysate is also an important matter of debate. Two conceptual models of viral impacts on the cycling of organic matter and nutrients in the ocean have emerged in the last few decades: the viral shunt and the viral shuttle. In the viral shunt model, viral lysate releases otherwise captured nutrients and dissolved organic matter (DOM) back into the environment which can be consumed, thus retaining the resources in the microbial loop (Wilhelm and Suttle 1999, Weitz et al. 2015). This model predicts increased transfer to higher trophic levels and community productivity (Weitz et al. 2015). On the other hand, the viral

shuttle hypothesizes aggregates created from viral lysate will sink out of the photic zone (Guidi et al. 2016, Yamada et al. 2018). Under this regime, export to the deep ocean is increased but total productivity is not (Guidi et al. 2016). As these theories predict different biogeochemical implications of virus-induced mortality, they also have varied ecological implications (Gilbert and Mitra 2022, Vincent and Vardi 2023). The fate of infected cells and lysate is important to understand the roll of viruses in the marine microbial ecosystem.

To understand how phages shape their host's metabolism on a biochemical level and affect the flow of energy and nutrients in the environment, Chapter 2 investigates changes to the lipid biochemistry of a marine microbe alone and in mixed communities containing phages. In this study, we chose to focus on the metabolism of *Prochloroccocus* as a model host. *Prochlorococcus* was chosen because it is an abundant, cosmopolitan cyanobacteria of global importance (). In many areas, *Prochlorococcus* is responsible for the majority of primary production (Scanlan and West 2002, Wu et al. 2022). Because of this, the metabolism of *Prochloroccocus* can have outsized effects on the carbon and nutrient cycling of the marine ecosystem (Partensky, Hess, and Vaulot 1999, Wu et al. 2022, Cai et al. 2024, Braakman et al. 2025).

We create a system containing *Prochloroccocus*, P-SSP7, a T7-like phage of *Prochlorococcus*, and *Paraphysomonas bandaiensis*, a eukaryotic predator of *Prochlorococcus* (Partensky, Hess, and Vaulot 1999). By examining a phage and a grazer interacting with *Prochlorococcus* and one another, we attempt to characterize the influence of top-down pressures on *Prochloroccocus* lipid metabolism.

Like many viruses, cyanophages have incorporated auxiliary metabolic genes from *Prochloroccocus* into their genomes (Sullivan et al. 2005). These auxiliary genes influence the metabolism of their host *Prochloroccocus* during infection (Lindell et al. 2007, Thompson et al. 2016, Ain et al. 2024). This confers an evolutionary advantage that maintains these genes in cyanophage populations across lineages, often through enhanced lysis, co-evolution, and phage production (Sullivan et al. 2005, Lindell et al. 2007, Thompson et al. 2011).

In many cases, these auxiliary genes interact with host lipid metabolism (Dammeyer et al. 2008, Roitman et al. 2018, Guillonneau et al. 2022). In fact, *phoH*, a hypothesized phospholipid metabolism gene, is one of the most abundant genes among marine phages (Goldsmith et al. 2011). Further, many cyanophages carry auxiliary fatty acid desaturases, leading to decreased saturation of fatty acids during infection (Roitman et al. 2018). The phage studied in this chapter, P-SSP7, contains no Pho-regulon or lipid metabolism genes (Lindell et al. 2007). However, P-SSP7 infection has led to the upregulation of phoH in *Prochlorococcus* in previous studies, suggesting the phage may still affect phospholipid synthesis or other phosphorus-stress pathways (Lindell et al. 2007). Yet, no upregulation of desaturases has been observed from P-SSP7 (Lindell et al. 2007). Therefore, we expect to see changes to *Prochloroccocus* phospholipids, but not to fatty acids in response to P-SSP7.

We also do not expect to see changes to the *Prochloroccocus* lipidome due to the presence of the grazer, as there is no known mechanism for a predator's presence altering lipid metabolism of

Prochloroccocus. However, previous studies suggest phage-induced alteration of host metabolism may change the nutritional quality of the host (Wilhelm and Suttle 1999, Thompson et al. 2011, Ankrah et al. 2014, Jin et al. 2024). If this is true, we anticipate seeing commensurate changes to the lipidome of *P. bandaiensis* when consuming infected prey, as lipids play an important role in energy and macronutrient storage (Becker et al. 2018, Melvin et al. 2019, Olsen, Thum, and Rohner 2021).

Finally, lipid biomarkers of viral infection have been found in other microbial systems (Fulton et al. 2013, Chatterjee et al. 2021). The presence of many auxiliary lipid metabolism genes in cyanophages suggests the creation of an infection-specific lipid is possible in *Prochloroccocus*. Therefore, we endeavor to find and verify possible biomarkers of P-SSP7 infection.

iii. Chapter 3

Traditional models of the marine microbial community focus only on the interactions between phyto- and zooplankton, and the environment. The simplest of which is the nutrient-phytoplankton-zooplankton model (NPZ) which is adapted from traditional terrestrial ecological models of primary producers and their consumers (Franks 2002, Caron 2016). This view of marine microbial ecology is obviously reductionist, but still a useful tool (Franks 2002). However, modelers have been updating the classical models of ecology borrowed from terrestrial science to include the unique metabolisms and ecological interactions more prevalent in the marine environment and improve model forecasts (Frank 2002, Baltar et al. 2019, Horn et al. 2021).

Mixotrophs, organisms which photosynthesize and phagocytize, complicate our understanding of the marine microbial food web. Mixotrophs occupy a unique metabolic niche- acting as both a primary producer and a secondary producer. The balance of each metabolic strategy in a mixotroph can have major effects on the ecology and biogeochemistry of the community (Caron 2016, Gilbert and Mitra 2022, Millette et al. 2024).

Continuing to use *P. bandaiensis*, we compete this representative single-guild phagotroph with two strains of a marine mixotroph, *Ochromonas* sp. In these competition experiments we observe changes to the trophic strategies of *Ochromonas*, and how environmental scarcity influences the realized niche of *Ochromonas* in competition.

Ochromonas is an abundant aquatic mixotroph found in a wide variety of freshwater and marine environments. It was chosen as a model mixotroph because of its metabolic plasticity, environmental relevance, relatively high growth rate, and ability to survive under scarce nutrient regimes (Lie et al. 2018, Barbaglia et al. 2024). Strains of *Ochromonas* vary greatly in their investment between phototrophy and heterotrophy, as well as their nutrient requirements (Holen 2010, Barbaglia et al. 2024). This allows us to examine a diverse variety of mixotrophic niche filling capabilities while controlling for cell size, genetic potential, etc. Similarly, *P. bandaiensis* and *Ochromonas* are closely related (in fact, *P. bandaiensis* is thought to be descended from a mixotroph) and often coexist in the same environment (Dorell et al. 2019, Terpis et al. 2025). By competing these two organisms in culture we can control for other lineage-related variables and directly investigate the results of competition on these organisms' metabolism.

Here, we use two strains of *Ochromonas*: CCMP 584 and CCMP 1148. While both are obligate phagotrophs and closely related, there are differences between the metabolic potential and efficiency of the two strains (Barbaglia et al. 2024). For example, *Ochromonas* 1148 has a much higher carbon use efficiency, and its growth is less controlled by prey availability than *Ochromonas* 584 (Barbaglia et al. 2024). From this, while we believe both will experience decreased growth, we predict *Ochromonas* 1148 will have a higher growth rate in competition with *P. bandaiensis* than *Ochromonas* 1148. We also anticipate that, in turn, *Ochromonas* 584, as a more voracious grazer, will decrease the growth of *P. bandaiensis* to a greater extent than *Ochromonas* 1148 (Barbaglia et al. 2024).

Because conventional wisdom suggests mixotrophy confers a competitive advantage when mixotrophs can leverage the least limiting trophic strategy, we predict both strains of *Ochromonas* will invest more in phototrophy and less in phagotrophy in the presence of single-guild phagotrophic competitor (Tittle et al. 2003, Edwards 2019, Chu, Moeller, and Archibald 2023). Relatedly, we anticipate the increased investment in phototrophy in competition will be more pronounced in prey-limiting environments compared to light-limiting environments.

iv. Chapter 4

In Chapter 4, we expand on this model system. Continuing to use *Ochromonas* 584 and *P. bandaiensis*, we include in this experiment the mixotroph *Ochromonas* 1391 as it is one of the few facultatively phagotrophic strains of *Ochromonas* (Barbaglia et al. 2024).

To control for environmental variables, we create a novel chemostatic culturing apparatus for the culturing of large volumes of *Ochromonas* and *P. bandaiensis*. In the chemostat, the environment is held constant through the regular introduction fresh media and dilution of old media. Our chemostat allows us to directly explore the competitive dynamics between mixotrophs and single-guild phagotrophs by controlling for confounding environmental variables (Pickell et al. 2009, Le Chevanton et al. 2016, Omta et al. 2017). In this controlled competitive system, we will again observe how competition causes niche displacement in mixotrophs. However, in this Chapter we explore not only the effect of competition on mixotrophic metabolism, but also the trade-offs associated with shifting trophic strategies.

The competitive dynamics of mixotrophic metabolism remains a major open question (Millette et al. 2024). Mixotrophs are often thought to have a competitive advantage when resources are limiting by taking advantage of the ability to obtain energy from multiple pools (Flynn and Mitra 2009, Caron 2016). However, while mixotrophs do make up the majority of primary or secondary production in some environments, they also coexist with their single-guild counterparts, showing there is also an ecological cost to mixotrophy (Sato, Shiozaki, and Hashihama 2017, Millette et al. 2024).

Many theories have emerged to explain the competitive costs of mixotrophic metabolism (Millette et al. 2024, Figure 1.2). Ward et al. (2011) propose that limited membrane space for the transporters and receptors needed for both phototrophy and phagotrophy decrease mixotrophic efficiency (Figure 1.2). Flynn and Mitra (2009) similarly take a biomechanical approach to

explaining mixotrophic tradeoffs, instead focusing on the limited intracellular space needed for plastids and vacuoles (Figure 1.2). Also prominent are the theories that dual metabolic machinery is metabolically costly or that mixotrophs are more limited in their capability to ingest or catabolize certain compounds or prey (Raven 1997, Christaki, Van Wambeke, and Dolan 1999, Figure 1.2).

To understand how inter-guild coexistence and niche filling dynamics materialize in scarce environments, we grow *Ochromonas* and *P. bandaiensis* in a co-limited low-phosphorus, low-organics medium simulating gyre-like environments. We predict, like in our batch experiment, *Ochromonas* will modulate its metabolism to relieve the competitive pressure for limited prey when grown with *P. bandaiensis*. As *Ochromonas* 1391 tends to invest more heavily in photosynthesis and has lower prey requirements, we hypothesize *Ochromonas* 1391 will fare better in competition with *P. bandaiensis* (Barbaglia et al. 2024). We also anticipate the total community production will be higher in the chemostat containing *Ochromonas* 1391 and *P. bandaiensis*, as these organisms will be able to obtain energy from different pools and likely not be deviate far from their ideal niche, allowing them to grow more efficiently.

v. Chapter 5

Finally, this thesis concludes with a look at the broader implications for marine microbiology, ecology, and metabolism that emerge from this work. Looking at phages, we discuss the use of lipidomics in evaluating the phage-host system in the environment, as well as how phage infection may cause trophic cascades. We present an argument for how the competitive system of *Ochromonas* developed here demonstrates *Ochromonas*'s usefulness as a model organism to study mixotrophic ecology, evolution, and metabolism. The implications of this thesis's findings for mixotrophic competitive ecology are also discussed. Finally, we close with some thoughts on how work from this thesis may be expanded and improved upon in the future to answer even more complex questions about marine microbial metabolism and ecology.

vi. Impact and merit

This thesis represents a novel approach to studying the metabolic niches of marine plankton. Through careful experimental design that isolates biotic forces on microbial metabolism this thesis qualifies and quantifies metabolic alteration across a range of biological interactions (Table 1.1) and proves that abiotic stress forces on single-species cultures cannot always accurately replicate competition or other inter-species interactions.

Additionally, this body of work confronts several obstacles to experimentation on the microbial metabolic niche and lays the groundwork for potentially easier and more accurate studies of multiple dimensions of marine microbial ecology and biogeochemistry in the future. Through the observation of the *Prochlorococcus* lipidome during phage infection, we identify a novel lipid compound with the potential to act as a proxy for phage infection in the pelagic environment (Chapter 2). Additionally, we demonstrate the ability to create competitive experiments that expose the competitive tradeoffs of mixotrophic competition directly through competition with a

single-guild competitor (and possibly other mixotrophs) by culturing large volumes of *Ochromonas* and *Paraphysomonas* in a chemostatic environment (Chapter 4).

Figures

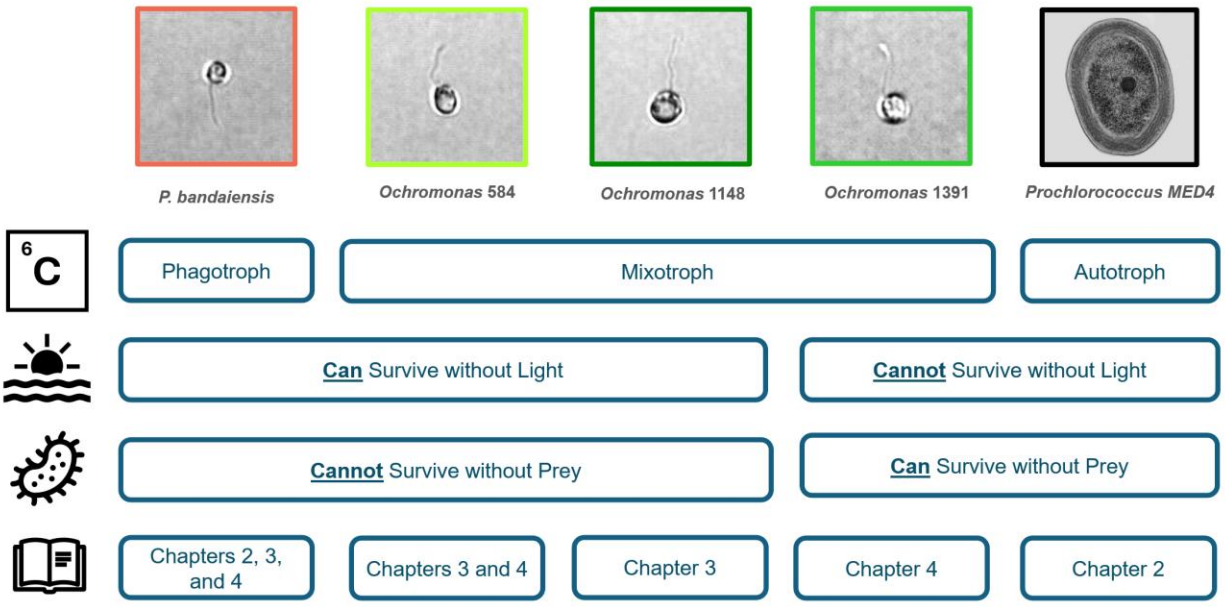

Figure 1.1 A conceptual overview of the organisms used in this thesis, their traits, and the chapters in which they appear. Picture of *Prochlorococcus marinus* used as a stand in for MED4 by Thompson and Watson (2007, Wikimedia Commons).

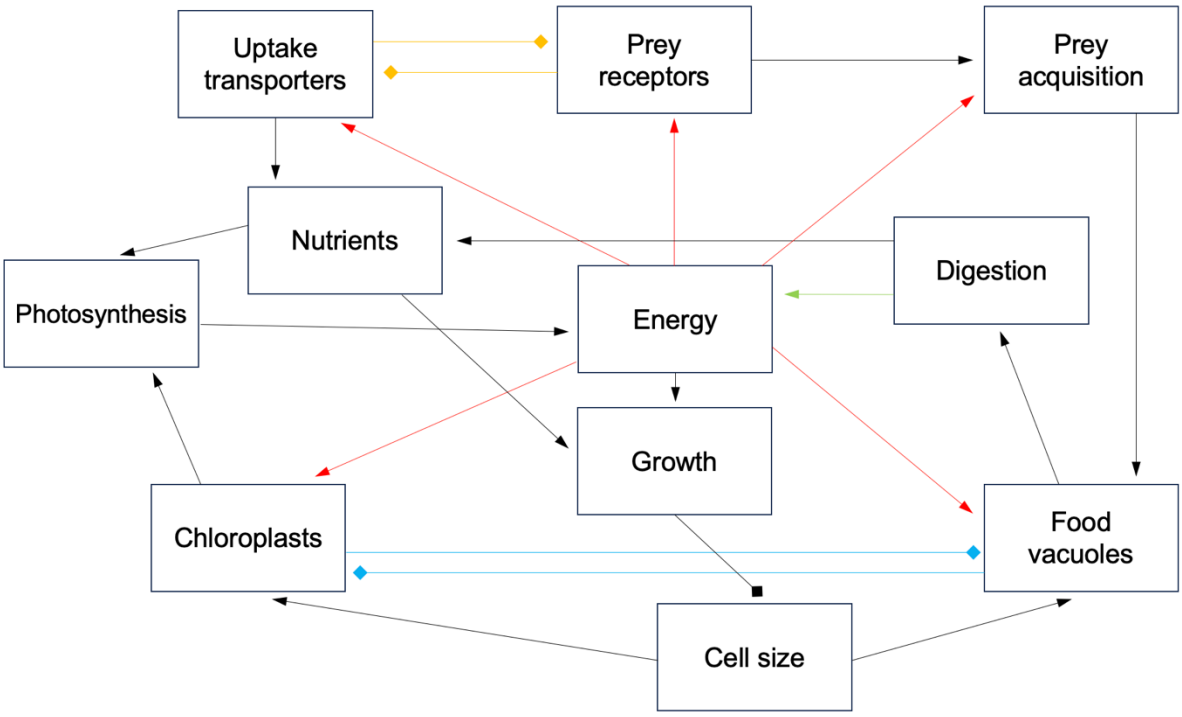

Figure 1.2 A simplified conceptual model of mixotrophic metabolism and its theorized tradeoffs. A pointed arrow indicates more of the source promotes more of the subject. A square arrow indicates more of the source inhibits increase of the subject. Four major theories of the "cost" of mixotrophy are marked by colored arrows. Yellow arrows indicate mixotrophs experience a tradeoff because of limited cellular membrane surface area for both nutrient uptake and prey receptors (Ward et al. 2011). Red arrows indicate the extra energetic costs of maintaining the machinery needed for both phagotrophy and photosynthesis (Raven 1997). The green arrow represents the theorized greater selectivity in prey and catabolism of complex molecules in mixotrophs (Christaki, Van Wambeke, and Dolan 1999). Finally, the blue arrows represent the theorized limitation in intracellular space which both chloroplasts and food vacuoles must occupy (Flynn and Mitra 2009).

Tables

Group 1	Group 2	Symbiotic Relationship
+	+	Mutualism
+	-	Parasitism, Predation
+	•	Commensalism
-	-	Competition
-	•	Amensalism
•	•	Neutralism

Table 1.1 The six fundamental symbiotic relationships (Douglas 2010). The first two columns show the effect success from the other biological group (often species) has on the other. A plus (+) sign indicates as the other group is successful, this group's success increases. A minus (-) sign indicates as the other group is successful, the success of this group declines. A dot (•) the other group's ecological success has no impact on the success of this group. Note, what is often called parasitism (one biological group benefits at the expense of another) is also descriptive of a predator-prey relationship. While some think of predation as a type of parasitism (Raffel, Martin and Rohr 2008), others define parasitism and predation as two different types of interactions depending on the underlying mechanisms for the relationship (Hesse et al. 2012), as such both are included here.

References

1. Ain, Q. ul, Wu, K., Wu, X., Bai, Q., Li, Q., Zhou, C.-Z., *et al.* (2024). Cyanophage-encoded auxiliary metabolic genes in modulating cyanobacterial metabolism and algal bloom dynamics. *Front. Virol.*, 4.
2. Alberts, B., Johnson, A., Lewis, J., Raff, M., Roberts, K. & Walter, P. (2002). Catalysis and the Use of Energy by Cells. In: *Molecular Biology of the Cell. 4th edition*. Garland Science.
3. Amado, A., Fernández, L., Huang, W., Ferreira, F.F. & Campos, P.R.A. (2016). Competing metabolic strategies in a multilevel selection model. *Royal Society Open Science*, 3, 160544.
4. Ankrah, N.Y.D., May, A.L., Middleton, J.L., Jones, D.R., Hadden, M.K., Gooding, J.R., *et al.* (2014). Phage infection of an environmentally relevant marine bacterium alters host metabolism and lysate composition. *ISME J*, 8, 1089–1100.
5. Antwis, R.E., Griffiths, S.M., Harrison, X.A., Aranega-Bou, P., Arce, A., Bettridge, A.S., *et al.* (2017). Fifty important research questions in microbial ecology. *FEMS Microbiol Ecol*, 93, fix044.
6. Archibald, K.M., Dutkiewicz, S., Laufkötter, C. & Moeller, H.V. (2024). Emergent trade-offs among plasticity strategies in mixotrophs. *Journal of Theoretical Biology*, 590, 111854.
7. Baltar, F., Bayer, B., Bednarsek, N., Deppeler, S., Escribano, R., Gonzalez, C.E., *et al.* (2019). Towards Integrating Evolution, Metabolism, and Climate Change Studies of Marine Ecosystems. *Trends in Ecology & Evolution*, 34, 1022–1033.
8. Barbaglia, G.S., Paight, C., Honig, M., Johnson, M.D., Marczak, R., Lepori-Bui, M., *et al.* (2024). Environment-dependent metabolic investments in the mixotrophic chrysophyte *Ochromonas*. *Journal of Phycology*, 60, 170–184.

9. Becker, K.W., Collins, J.R., Durham, B.P., Groussman, R.D., White, A.E., Fredricks, H.F., *et al.* (2018). Daily changes in phytoplankton lipidomes reveal mechanisms of energy storage in the open ocean. *Nat Commun*, 9, 5179.
10. Behrenfeld, M., Bisson, K., Boss, E. & Graff, J. (2025). Conceptualizing phytoplankton communities in the absence of resource based competitive exclusion. *Sci Rep*, 15, 23846.
11. Bernhardt, J.R., Kratina, P., Pereira, A.L., Tamminen, M., Thomas, M.K. & Narwani, A. (2020). The evolution of competitive ability for essential resources. *Philosophical Transactions of the Royal Society B: Biological Sciences*, 375, 20190247.
12. Braakman, R., Satinsky, B., O'Keefe, T.J., Longnecker, K., Hogle, S.L., Becker, J.W., *et al.* (2025). Global niche partitioning of purine and pyrimidine cross-feeding among ocean microbes. *Science Advances*, 11, eadp1949.
13. Breitbart, M., Bonnain, C., Malki, K. & Sawaya, N.A. (2018). Phage puppet masters of the marine microbial realm. *Nat Microbiol*, 3, 754–766.
14. Brown, J.H., Gillooly, J.F., Allen, A.P., Savage, V.M. & West, G.B. (2004). Toward a Metabolic Theory of Ecology. *Ecology*, 85, 1771–1789.
15. Brown, J.H., Sibly, R.M. & Kodric-Brown, A. (2012). Introduction: Metabolism as the Basis for a Theoretical Unification of Ecology. In: *Metabolic Ecology*. John Wiley & Sons, Ltd, pp. 1–6.
16. Cai, L., Li, H., Deng, J., Zhou, R. & Zeng, Q. (2024). Biological interactions with *Prochlorococcus*: implications for the marine carbon cycle. *Trends in Microbiology*, 32, 280–291.
17. Carlson, B.S., Rotics, S., Nathan, R., Wikelski, M. & Jetz, W. (2021). Individual environmental niches in mobile organisms. *Nat Commun*, 12, 4572.
18. Caron, D.A. (2016). Mixotrophy stirs up our understanding of marine food webs. *Proceedings of the National Academy of Sciences*, 113, 2806–2808.
19. Chatterjee, R., Chowdhury, A.R., Mukherjee, D. & Chakravortty, D. (2021). Lipid larceny: channelizing host lipids for establishing successful pathogenesis by bacteria. *Virulence*, 12, 195–216.
20. Christaki, U., Van Wambeke, F. & Dolan, J. (1999). Nanoflagellates (mixotrophs, heterotrophs and autotrophs) in the oligotrophic eastern Mediterranean: standing stocks, bacterivory and relationships with bacterial production. *Mar. Ecol. Prog. Ser.*, 181, 297–307.
21. Chu, T., Moeller, H.V. & Archibald, K.M. (2023). Competition between phytoplankton and mixotrophs leads to metabolic character displacement. *Ecological Modelling*, 481.
22. Crockford, P.W., On, Y.M.B., Ward, L.M., Milo, R. & Halevy, I. (2023). The geologic history of primary productivity. *Current Biology*, 33, 4741-4750.e5.
23. Dammeyer, T., Bagby, S.C., Sullivan, M.B., Chisholm, S.W. & Frankenberg-Dinkel, N. (2008). Efficient Phage-Mediated Pigment Biosynthesis in Oceanic Cyanobacteria. *Current Biology*, 18, 442–448.
24. Daniels, M., van Vliet, S. & Ackermann, M. (2023). Changes in interactions over ecological time scales influence single-cell growth dynamics in a metabolically coupled marine microbial community. *ISME J*, 17, 406–416.
25. Donelson, J.M., Sunday, J.M., Figueira, W.F., Gaitán-Espitia, J.D., Hobday, A.J., Johnson, C.R., *et al.* (2019). Understanding interactions between plasticity, adaptation and range shifts in response to marine environmental change. *Philos Trans R Soc Lond B Biol Sci*, 374, 20180186.

26. Dorrell, R.G., Azuma, T., Nomura, M., deKerdrel, G.A., Paoli, L., Yang, S., *et al.* (2019). Principles of plastid reductive evolution illuminated by nonphotosynthetic chrysophytes. *Proceedings of the National Academy of Sciences of the United States of America*, 116, 6914–6923.
27. Douglas, A.E. (2010). *The Symbiotic Habit*. Princeton University Press.
28. Duarte, C., Gasol, J. & Vaqué, D. (1997). Role of experimental approaches in marine microbial ecology. *Aquat. Microb. Ecol.*, 13, 101–111.
29. Dupont, S. & Metian, M. (2023). General considerations to experimental research on ocean alkalinity enhancement.
30. Edwards, K.F. (2019). Mixotrophy in nanoflagellates across environmental gradients in the ocean. *Proc Natl Acad Sci U S A*, 116, 6211–6220.
31. Flynn, K.J. & Mitra, A. (2009). Building the "perfect beast": modelling mixotrophic plankton. *Journal of Plankton Research*, 31, 965–992.
32. Franks, P.J.S. (2002). NPZ Models of Plankton Dynamics: Their Construction, Coupling to Physics, and Application. *Journal of Oceanography*, 58, 379–387.
33. Fulton, J.M., Fredricks, H.F., Bidle, K.D., Vardi, A., Kendrick, B.J., DiTullio, G.R., *et al.* (2014). Novel molecular determinants of viral susceptibility and resistance in the lipidome of *Emiliania huxleyi*. *Environmental Microbiology*, 16, 1137–1149.
34. Gallego, I. & Narwani, A. (2022). Ecology and evolution of competitive trait variation in natural phytoplankton communities under selection. *Ecol Lett*, 25, 2397–2409.
35. Gazeau, F., Urrutti, P., Dousset, A., Brodu, N., Richard, M., Villeneuve, R., *et al.* (2024). Toward an ecologically realistic experimental system to investigate the multigenerational effects of ocean warming and acidification on benthic invertebrates. *Limnology and Oceanography: Methods*, 22, 738–751.
36. Gerhard, M., Koussoroplis, A.-M., Raatz, M., Pansch, C., Fey, S.B., Vajedsamiei, J., *et al.* (2023). Environmental variability in aquatic ecosystems: Avenues for future multifactorial experiments. *Limnology and Oceanography Letters*, 8, 247–266.
37. Glazier, D.S. (2024). Power and Efficiency in Living Systems. *Sci*, 6, 28.
38. Glibert, P.M. & Mitra, A. (2022a). From webs, loops, shunts, and pumps to microbial multitasking: Evolving concepts of marine microbial ecology, the mixoplankton paradigm, and implications for a future ocean. *Limnology and Oceanography*, 67, 585–597.
39. Glibert, P.M. & Mitra, A. (2022b). From webs, loops, shunts, and pumps to microbial multitasking: Evolving concepts of marine microbial ecology, the mixoplankton paradigm, and implications for a future ocean. *Limnology and Oceanography*, 67, 585–597.
40. Goldsmith, D.B., Crosti, G., Dwivedi, B., McDaniel, L.D., Varsani, A., Suttle, C.A., *et al.* (2011). Development of phoH as a Novel Signature Gene for Assessing Marine Phage Diversity. *Applied and Environmental Microbiology*, 77, 7730–7739.
41. González, A.L., Dézerald, O., Marquet, P.A., Romero, G.Q. & Srivastava, D.S. (2017). The Multidimensional Stoichiometric Niche. *Front. Ecol. Evol.*, 5.
42. Graff, J.R., Nelson, N.B., Roca-Martí, M., Romanelli, E., Kramer, S.J., Erickson, Z., *et al.* (2023). Reconciliation of total particulate organic carbon and nitrogen measurements determined using contrasting methods in the North Pacific Ocean as part of the NASA EXPORTS field campaign. *Elementa: Science of the Anthropocene*, 11, 00112.

43. Gralka, M., Szabo, R., Stocker, R. & Cordero, O.X. (2020). Trophic Interactions and the Drivers of Microbial Community Assembly. *Curr Biol*, 30, R1176–R1188.
44. Gubry-Rangin, C., Aigle, A., Herrera-Alsina, L., Lancaster, L.T. & Prosser, J.I. (2024). Niche breadth specialization impacts ecological and evolutionary adaptation following environmental change. *ISME J*, 18, wrae183.
45. Guidi, L., Chaffron, S., Bittner, L., Eveillard, D., Larhlimi, A., Roux, S., *et al.* (2016). Plankton networks driving carbon export in the oligotrophic ocean. *Nature*, 532, 465–470.
46. Guillonneau, R., Murphy, A.R.J., Teng, Z.-J., Wang, P., Zhang, Y.-Z., Scanlan, D.J., *et al.* (2022). Trade-offs of lipid remodeling in a marine predator–prey interaction in response to phosphorus limitation. *Proceedings of the National Academy of Sciences*, 119, e2203057119.
47. Heal, O.W. & MacLean, S.F. (1975). Comparative productivity in ecosystems—secondary productivity. In: *Unifying Concepts in Ecology*. Springer, Dordrecht, pp. 89–108.
48. Hesse, O., Engelbrecht, W., Laforsch, C. & Wolinska, J. (2012). Fighting parasites and predators: How to deal with multiple threats? *BMC Ecology*, 12, 12.
49. Holen, D.A. (2010). Mixotrophy in two species of Ochromonas (Chrysophyceae). *Nova Hedwigia, Beihefte*, 153–165.
50. Horn, S., Meunier, C.L., Fofonova, V., Wiltshire, K.H., Sarker, S., Pogoda, B., *et al.* (2021). Toward Improved Model Capacities for Assessment of Climate Impacts on Coastal Bentho-Pelagic Food Webs and Ecosystem Services. *Front. Mar. Sci.*, 8.
51. Hu, N., Bourdeau, P.E. & Hollander, J. (2024). Responses of marine trophic levels to the combined effects of ocean acidification and warming. *Nat Commun*, 15, 3400.
52. Hurwitz, B.L. & U'Ren, J.M. (2016). Viral metabolic reprogramming in marine ecosystems. *Current Opinion in Microbiology*, Environmental microbiology * Special Section: Megaviromes, 31, 161–168.
53. Hutchinson, G.E. (1957). Concluding Remarks. *Cold Spring Harb Symp Quant Biol*, 22, 415–427.
54. Jacquet, S., Miki, T., Noble, R., Peduzzi, P. & Wilhelm, S. (2010). Viruses in aquatic ecosystems: important advancements of the last 20 years and prospects for the future in the field of microbial oceanography and limnology. *Advances in Oceanography and Limnology*, 1, 97–141.
55. Jin, M., Gong, Y., Geslin, C., He, T. & Zhang, X. (2024). Editorial: The role of viruses in marine environments. *Front Microbiol*, 15, 1437050.
56. Karl, D. & Proctor, L. (2007). Foundations of Microbial Oceanography. *Oceanog.*, 20, 16–27.
57. Klitgord, N. & Segrè, D. (2011). Ecosystems biology of microbial metabolism. *Current Opinion in Biotechnology*, Nanobiotechnology and Systems Biology, 22, 541–546.
58. Koffel, T., Daufresne, T. & Klausmeier, C.A. (2021). From competition to facilitation and mutualism: a general theory of the niche. *Ecological Monographs*, 91, e01458.
59. Le Chevanton, M., Garnier, M., Lukomska, E., Schreiber, N., Cadoret, J.-P., Saint-Jean, B., *et al.* (2016). Effects of Nitrogen Limitation on Dunaliella sp.–Alteromonas sp. Interactions: From Mutualistic to Competitive Relationships. *Front. Mar. Sci.*, 3.
60. Levine, N.M., Doblin, M.A. & Collins, S. (2024). Reframing trait trade-offs in marine microbes. *Commun Earth Environ*, 5, 219.

61. Lie, A.A.Y., Liu, Z., Terrado, R., Tatters, A.O., Heidelberg, K.B. & Caron, D.A. (2018). A tale of two mixotrophic chrysophytes: Insights into the metabolisms of two *Ochromonas* species (Chrysophyceae) through a comparison of gene expression. *PLOS ONE*, 13, e0192439.
62. Lindell, D., Jaffe, J.D., Coleman, M.L., Futschik, M.E., Axmann, I.M., Rector, T., *et al.* (2007). Genome-wide expression dynamics of a marine virus and host reveal features of co-evolution. *Nature*, 449, 83–86.
63. Malard, L.A. & Guisan, A. (2023). Into the microbial niche. *Trends in Ecology & Evolution*, 38, 936–945.
64. Massing, J.C., Fahimipour, A.K., Bunse, C., Pinhassi, J. & Gross, T. (2023). Quantification of metabolic niche occupancy dynamics in a Baltic Sea bacterial community. *mSystems*, 8, e00028-23.
65. McClain, C.R., Webb, T.J., Nunnally, C.C., Dixon, S.R., Finnegan, S. & Nelson, J.A. (2020). Metabolic Niches and Biodiversity: A Test Case in the Deep Sea Benthos. *Front. Mar. Sci.*, 7.
66. Melvin, S.D., Lanctôt, C.M., Doriean, N.J.C., Bennett, W.W. & Carroll, A.R. (2019). NMR-based lipidomics of fish from a metal(loid) contaminated wetland show differences consistent with effects on cellular membranes and energy storage. *Science of The Total Environment*, 654, 284–291.
67. Millette, N.C., Leles, S.G., Johnson, M.D., Maloney, A.E., Brownlee, E.F., Cohen, N.R., *et al.* (2024). Recommendations for advancing mixoplankton research through empirical-model integration. *Front. Mar. Sci.*, 11.
68. Montoya, J.M. & Raffaelli, D. (2010). Climate change, biotic interactions and ecosystem services. *Philosophical Transactions of the Royal Society B: Biological Sciences*, 365, 2013–2018.
69. Norin, T. & Metcalfe, N.B. (2019). Ecological and evolutionary consequences of metabolic rate plasticity in response to environmental change. *Philosophical Transactions of the Royal Society B: Biological Sciences*, 374, 20180180.
70. Olsen, L., Thum, E. & Rohner, N. (2021). Lipid metabolism in adaptation to extreme nutritional challenges. *Developmental Cell*, 56, 1417–1429.
71. Omta, A.W., Talmy, D., Sher, D., Finkel, Z.V., Irwin, A.J. & Follows, M.J. (2017). Extracting phytoplankton physiological traits from batch and chemostat culture data. *Limnology and Oceanography: Methods*, 15, 453–466.
72. Partensky, F., Hess, W.R. & Vaulot, D. (1999). *Prochlorococcus*, a Marine Photosynthetic Prokaryote of Global Significance. *Microbiol Mol Biol Rev*, 63, 106–127.
73. Pickell, L.D., Wells, M.L., Trick, C.G. & Cochlan, W.P. (2009). A sea-going continuous culture system for investigating phytoplankton community response to macro- and micro-nutrient manipulations. *Limnology and Oceanography: Methods*, 7, 21–32.
74. Piriz, G., Niklitschek, E. & Maldonado, K. (2025). Individual specialisation and niche variation in aquatic vertebrates: theoretical expectations and empirical evidence. *Authorea*.
75. Ponnudurai, R., Kleiner, M., Sayavedra, L., Petersen, J.M., Moche, M., Otto, A., *et al.* (2017). Metabolic and physiological interdependencies in the Bathymodiolus azoricus symbiosis. *ISME J*, 11, 463–477.
76. Pontzer, H. & McGrosky, A. (2022). Balancing growth, reproduction, maintenance, and activity in evolved energy economies. *Current Biology*, 32, R709–R719.

77. Potapov, A.M., Pollierer, M.M., Salmon, S., Šustr, V. & Chen, T.-W. (2021). Multidimensional trophic niche revealed by complementary approaches: Gut content, digestive enzymes, fatty acids and stable isotopes in *Collembola*. *Journal of Animal Ecology*, 90, 1919–1933.
78. Prosser, J.I. (2020). Putting science back into microbial ecology: a question of approach. *Philosophical Transactions of the Royal Society B: Biological Sciences*, 375, 20190240.
79. Raffel, T.R., Martin, L.B. & Rohr, J.R. (2008). Parasites as predators: unifying natural enemy ecology. *Trends in Ecology & Evolution*, 23, 610–618.
80. Ramon, C. & Stelling, J. (2023). Functional comparison of metabolic networks across species. *Nat Commun*, 14, 1699.
81. Raven, J.A. (1997). Phagotrophy in phototrophs. *Limnology and Oceanography*, 42, 198–205.
82. Roitman, S., Hornung, E., Flores-Uribe, J., Sharon, I., Feussner, I. & Béjà, O. (2018). Cyanophage-encoded lipid desaturases: oceanic distribution, diversity and function. *ISME J*, 12, 343–355.
83. Roller, B.R. & Schmidt, T.M. (2015). The physiology and ecological implications of efficient growth. *ISME J*, 9, 1481–1487.
84. Sánchez González, I., Hopper, G.W., Bucholz, J.R., Kubala, M.E., Lozier, J.D. & Atkinson, C.L. (2023). Niche specialization and community niche space increase with species richness in filter-feeder assemblages. *Ecosphere*, 14, e4495.
85. Sanders, D. & Frago, E. (2024). Ecosystem engineers shape ecological network structure and stability: A framework and literature review. *Functional Ecology*, 38, 1683–1696.
86. Sato, M., Shiozaki, T. & Hashihama, F. (2017). Distribution of mixotrophic nanoflagellates along the latitudinal transect of the central North Pacific. *J Oceanogr*, 73, 159–168.
87. Scanlan, D.J. & West, N.J. (2002). Molecular ecology of the marine cyanobacterial genera Prochlorococcus and Synechococcus. *FEMS Microbiology Ecology*, 40, 1–12.
88. Selosse, M.-A., Charpin, M. & Not, F. (2017). Mixotrophy everywhere on land and in water: the grand écart hypothesis. *Ecology Letters*, 20, 246–263.
89. Sørensen, M.E.S., Wood, A.J., Minter, E.J.A., Lowe, C.D., Cameron, D.D. & Brockhurst, M.A. (2020). Comparison of Independent Evolutionary Origins Reveals Both Convergence and Divergence in the Metabolic Mechanisms of Symbiosis. *Current Biology*, 30, 328-334.e4.
90. Staehr, P.A., Testa, J.M., Kemp, W.M., Cole, J.J., Sand-Jensen, K. & Smith, S.V. (2012). The metabolism of aquatic ecosystems: history, applications, and future challenges. *Aquat Sci*, 74, 15–29.
91. Stark, K.A., Clegg, T., Bernhardt, J.R., Grainger, T.N., Kempes, C.P., Savage, V., *et al.* (2025). Toward a More Dynamic Metabolic Theory of Ecology to Predict Climate Change Effects on Biological Systems. *The American Naturalist*, 205, 285–305.
92. Sullivan, M.B., Coleman, M.L., Weigele, P., Rohwer, F. & Chisholm, S.W. (2005). Three *Prochlorococcus* Cyanophage Genomes: Signature Features and Ecological Interpretations. *PLoS Biol*, 3, e144.
93. Sutherland, W.J., Freckleton, R.P., Godfray, H.C.J., Beissinger, S.R., Benton, T., Cameron, D.D., *et al.* (2013). Identification of 100 fundamental ecological questions. *Journal of Ecology*, 101, 58–67.

94. Suttle, C.A. (2007). Marine viruses — major players in the global ecosystem. *Nat Rev Microbiol*, 5, 801–812.
95. Tecon, R., Mitri, S., Ciccarese, D., Or, D., van der Meer, J.R. & Johnson, D.R. (2019). Bridging the Holistic-Reductionist Divide in Microbial Ecology. *mSystems*, 4, 10.1128/msystems.00265-18.
96. Terpis, K.X., Salomaki, E.D., Barcytė, D., Pánek, T., Verbruggen, H., Kolisko, M., *et al.* (2025). Multiple plastid losses within photosynthetic stramenopiles revealed by comprehensive phylogenomics. *Current Biology*, 0.
97. Thompson, L.R., Zeng, Q. & Chisholm, S.W. (2016). Gene Expression Patterns during Light and Dark Infection of *Prochlorococcus* by Cyanophage. *PLoS ONE*, 11, e0165375.
98. Thompson, L.R., Zeng, Q., Kelly, L., Huang, K.H., Singer, A.U., Stubbe, J., *et al.* (2011). Phage auxiliary metabolic genes and the redirection of cyanobacterial host carbon metabolism. *Proc Natl Acad Sci U S A*, 108, E757–E764.
99. Tian, F., Wainaina, J.M., Howard-Varona, C., Domínguez-Huerta, G., Bolduc, B., Gazitúa, M.C., *et al.* (2024). Prokaryotic-virus-encoded auxiliary metabolic genes throughout the global oceans. *Microbiome*, 12, 159.
100. Tittel, J., Bissinger, V., Zippel, B., Gaedke, U., Bell, E., Lorke, A., *et al.* (2003). Mixotrophs combine resource use to outcompete specialists: Implications for aquatic food webs. *Proceedings of the National Academy of Sciences*, 100, 12776–12781.
101. Tsiola, A., Michoud, G., Daffonchio, D., Fodelianakis, S., Giannakourou, A., Malliarakis, D., *et al.* (2023). Depth-driven patterns in lytic viral diversity, auxiliary metabolic gene content, and productivity in offshore oligotrophic waters. *Front Microbiol*, 14, 1271535.
102. Valderrama, D. & Fields, K.H. (2017). Flawed evidence supporting the Metabolic Theory of Ecology may undermine goals of ecosystem-based fishery management: the case of invasive Indo-Pacific lionfish in the western Atlantic. *ICES J Mar Sci*, 74, 1256–1267.
103. Van de Waal, D.B., Elser, J.J., Martiny, A.C., Sterner, R.W. & Cotner, J.B. (2018). Editorial: Progress in Ecological Stoichiometry. *Front. Microbiol.*, 9.
104. Venkataraman, Y.R. & Huffmyer, A.S. (2025). Interrogating metabolic plasticity in marine organisms: A framework for best practices using metabolomic and lipidomic approaches.
105. Vincent, F. & Vardi, A. (2023). Viral infection in the ocean—A journey across scales. *PLOS Biology*, 21, e3001966.
106. Ward, B.A., Dutkiewicz, S., Barton, A.D. & Follows, M.J. (2011). Biophysical Aspects of Resource Acquisition and Competition in Algal Mixotrophs. *The American Naturalist*, 178, 98–112.
107. Weitz, J.S., Stock, C.A., Wilhelm, S.W., Bourouiba, L., Coleman, M.L., Buchan, A., *et al.* (2015). A multitrophic model to quantify the effects of marine viruses on microbial food webs and ecosystem processes. *ISME J*, 9, 1352–1364.
108. Welti, N., Striebel, M., Ulseth, A.J., Cross, W.F., DeVilbiss, S., Glibert, P.M., *et al.* (2017). Bridging Food Webs, Ecosystem Metabolism, and Biogeochemistry Using Ecological Stoichiometry Theory. *Front. Microbiol.*, 8.
109. Weynberg, K.D. (2018). Chapter One - Viruses in Marine Ecosystems: From Open Waters to Coral Reefs. In: *Advances in Virus Research*, Environmental Virology and Virus Ecology (ed. Malmstrom, C.M.). Academic Press, pp. 1–38.

110. Wilhelm, S.W. & Suttle, C.A. (1999). Viruses and Nutrient Cycles in the Sea: Viruses play critical roles in the structure and function of aquatic food webs. *BioScience*, 49, 781–788.
111. Wilson, J.B., Spijkerman, E. & Huisman, J. (2007). Is there really insufficient support for Tilman's R* concept? A comment on Miller et al. *Am Nat*, 169, 700–706.
112. Wilson, R.P., McMahon, C.R., Quintana, F., Frere, E., Scolaro, A., Hays, G.C., *et al.* (2011). N-dimensional animal energetic niches clarify behavioural options in a variable marine environment. *J Exp Biol*, 214, 646–656.
113. Wright, J.P. & Jones, C.G. (2006). The Concept of Organisms as Ecosystem Engineers Ten Years On: Progress, Limitations, and Challenges. *BioScience*, 56, 203–209.
114. Wu, Z., Aharonovich, D., Roth-Rosenberg, D., Weissberg, O., Luzzatto-Knaan, T., Vogts, A., *et al.* (2022). Significant organic carbon acquisition by *Prochlorococcus* in the oceans.
115. Xiao, X., Guo, W., Li, X., Wang, C., Chen, X., Lin, X., *et al.* (2021). Viral Lysis Alters the Optical Properties and Biological Availability of Dissolved Organic Matter Derived from *Prochlorococcus* Picocyanobacteria. *Applied and Environmental Microbiology*, 87, e02271-20.
116. Yamada, Y., Tomaru, Y., Fukuda, H. & Nagata, T. (2018). Aggregate Formation During the Viral Lysis of a Marine Diatom. *Front. Mar. Sci.*, 5.
117. Yee, D.P., Juery, C., Toullec, G., Catacora-Grundy, A., Lekieffre, C., Wangpraseurt, D., *et al.* (2025). Physiology and metabolism of eukaryotic microalgae involved in aquatic photosymbioses. *New Phytologist*, 247, 71–89.

CHAPTER 2: CYANOPHAGE INFECTION INDUCES CHARACTERISTIC CHANGES IN THE LIPIDOME OF *PROCHLOROCOCCUS* AND ITS PREDATOR

Coauthors: Shavonna Bent, Helen Fredricks, Henry Holm, Joshua Sacks, David Demory, Dave Caron, Debbie Lindell, and Benjaman Van Mooy

Abstract

In the pelagic environment, *Prochlorococcus* is affected by a variety of top-down trophic pressures including grazing and viral infection. Given the prevalence of *Prochlorococcus* in the global oceans, the effects of these pressures on *Prochlorococcus* metabolism have important implications for the biogeochemical cycling of carbon, phosphorus, and other macronutrients. Here we present the first complete lipidome of *Prochlorococcus* MED4 and demonstrate how *Prochlorococcus* MED4 modulates its lipid metabolism in response to top-down pressures in co-cultures with P-SSP7, a T7-like phage, and *Paraphysomonas bandaiensis*, a eukaryotic predator. We demonstrate that *Prochlorococcus* phosphorus partitioning and phospholipid metabolism is significantly altered by phage infection. We also find, viral infection and mortality alter the fatty acid makeup of *Prochlorococcus*, including an increase in production of and unsaturated acyl chains. In the lipidomes of infected *Prochlorococcus* populations, we identify an unknown lipid compound that appears to track viral infection cycles of *Prochlorococcus* in the North Pacific Subtropical Gyre. Finally, we demonstrate a previously undescribed mechanism for indirect trophic effects on predator triacylglycerol (TAG) and fatty acid metabolism when prey *Prochlorococcus* cells are infected by T7-like phages.

Introduction

Phytoplankton are responsible for one-half of the primary production in the biosphere and are therefore an important counterbalance to rising anthropogenic CO_2 emissions (Flombaum et al. 2013). The marine cyanobacteria *Prochlorococcus* and *Synechococcus* are among the most abundant phytoplankton in the world's oceans (Partensky, Hess and Valout 1999). In many regions, *Prochlorococcus* is the dominant photosynthetic organism and may provide a majority of energy and carbon to higher trophic levels (Partensky, Hess and Valout 1999, Worden et al. 2004, Armengol et al. 2019).

Viral lysis and grazing are two important environmental controls on *Prochlorococcus* abundance, though the balance of contributions of lysis and grazing rates to *Prochlorococcus* mortality is currently debated (Mann 2003). Both top-down controls are thought to significantly

impact nutrient cycling in the gyres, as grazer excretion and viral lysis both release dissolved organic matter (DOM) and particulate organic matter (POM)1 into the microbial loop (Wilhelm and Suttle 1999, Nagata 2000, Anderson and Ducklow 2001, Weitz et al. 2015). Grazing and viral lysis are both very different sources of organic matter, as grazing preferences or host alteration from phage auxiliary metabolic genes may alter the composition of the released material (Wilhelm and Suttle 1999, Ankrah et al. 2014, Evans et al. 2021, Xiao et al. 2021). Similarly, the fates of organic matter produced via these top-down pressures may differ from each other. For example, the proposed viral shunt hypothesis, showing lysis leads to a recycling of organic matter, preventing it from reaching higher trophic levels (Sullivan, Weitz, and Wilhelm 2017).

Viral infection is known in many cases to alter lipid metabolism in eukaryotic phytoplankton, but comparably little is known about cyanobacteria (Fulton et al. 2014, Malitsky et al. 2016, Rossenwasser et al. 2016, Ziv et al. 2016, Fulton et al. 2017, Dughale et al. 2019). Many cyanophages encode for fatty acid desaturates, suggesting lipidome remodeling is evolutionarily advantageous and important in viral lysis and replication (Sullivan et al. 2005, Roitman et al. 2017). The exact effects of T7-like phages on the *Prochlorococcus* lipidome are currently unknown, but deciphering phage alteration of *Prochlorococcus* lipid metabolism is important for understanding the impact of viral infection and lysis on marine biogeochemical cycles. Additionally, in other marine host and virus systems, specific lipid indicators of infection, or biomarkers, have been identified which can allow for easier and more accurate quantification of viral infection or lysis rates in the open ocean (Vardi et al. 2009, Hunter et al. 2015). It is possible future studies of *Prochlorococcus* infection by T7-like phages may be enhanced by the identification of lipid biomarkers.

Because *Prochlorococcus* is responsible for a large portion of production within many marine environments, it is an important source of energy for higher trophic levels both through direct predation and catabolism of lysate (Armengol et al. 2019). However, because the effects on the *Prochlorococcus* lipidome from viral infection are poorly categorized, there is uncertainty regarding the lipidomic differences between infected and uninfected *Prochlorococcus* cells. These differences may alter the energy or nutrient composition of the cell, meaning grazing of infected *Prochlorococcus* cells may not provide similar amounts of energy or nutrients to grazers (Xiao et al. 2021). Most previous laboratory studies have focused either on *Prochlorococcus* cocultured with only a grazer, or only a virus, which may miss indirect dynamics of predation of infected host cells.

Here we present an analysis of the *Prochlorococcus* MED4 lipidome grown in batch culture alone (control), with a T7-like phage P-SSP7 (+phage), and *P. bandaiensis,* a eukaryotic grazer (+grazer), giving insight into the lipid metabolism of *Prochlorococcus* in response to these top-down pressures. This experiment is one of a series of experiments on *Prochlorococcus* mortality using this same system (Lindell et al. *in prep*). Here, we show how viral infection alters both the *Prochlorococcus* lipid metabolism, and, indirectly, the grazer's lipidome as well.

Methodology

i. Cultures and strains

The culturing and subsequent analysis, growth, infection and mortality rates were conducted by Lindell et al. (in prep) and used as a basis for the lipidomic work explored in this study. Briefly,

Prochlorococcus MED4 cultures were grown in batch cultures alone (control), with P-SSP7 (+phage), *Paraphysomonas bandaiensis* (+grazer), and in a mixed *P. bandaiensis* and phage community (+phage+grazer) as described (Lindell et al. *in prep*). *Prochlorococcus* was grown to a concentration of approximately 2 x 10^7 cells per mL in 10L batch cultures. Cultures were inoculated in the light with *P. bandaiensis*, P-SSP7, or a mixture of grazers and phages. Cultures were grown over the course of 48 hours in a 14-10 hour light-dark cycle. 38-300 mL samples were taken for lipidomic analysis every six to twenty-four hours by filtering sample water onto a 0.2 um Durapore filter via gentle vacuum filtration. Filters were folded, wrapped in aluminum foil, and stored at -80º C until extraction.

Prochlorococcus, *P. bandaiensis*, P-SSP7, and heterotrophic bacteria concentrations were measured every two hours as previously described (Lindell et al. *in prep*).

ii. Field sampling

Lipid samples from the North Pacific Subtropical Gyre, near Station ALOHA, were collected on the Simons Collaboration on Ocean Processes and Ecology (MESO-SCOPE) cruise during the summer of 2017 (KM1709) as described by Bent et al. (2024). Briefly, 1-2 liters of seawater were filtered onto 47 mm diameter 0.22 μm Durapore filters (MilliporeSigma, Burlington, MA) every six hours from the same water mass. Samples were taken at the surface (15m depth) or the deep chlorophyll maximum (ranging from 103m to 130m). Filters were foled, wrapped in aluminum foil, and stored in liquid nitrogen until extraction.

iii. Lipid extraction and mass spectrometry

Sample filters were extracted for their lipid content via a modified Bligh and Dyer extraction (Bligh and Dyer 1959) as described by Popendorf et al. (2013). Extracts were stored at -80º C under nitrogen gas until analysis to prevent lipid oxidation.

Extracts were run in the dark on a high-performance liquid chromatography (HPLC) Agilent 1200 reverse-phase system (Agilent Technologies, Santa Clara, CA, 149 USA), with a gradient between eluents composed of a 0.99 M ammonium acetate and 0.17 M acetic acid in Milli-Q filtered water solution, as well as a 7:3 acetonitrile/isopropyl alcohol mixture also containing 0.99 M ammonium acetate and 0.17 M acetic acid as described in Collins et al. (2016). The HPLC system was coupled with a Q Exactive Hybrid 151 Quadrupole - Orbitrap mass spectrometer (Thermo Fisher Scientific, Waltham, MA, USA). Mass spectrometer settings were identical to Collins et al. (2016).

iv. Untargeted lipidomics

Positive and negative mode mass spectra were screened with the LOBSTAHS pipeline developed by Collins et al. (2016) in R. Briefly, the ProteoWizard Toolkit (Chambers et al., 2012) was used for conversion to a .xzxml format and fed into the xcms (Smith et al., 2006; Tautenhahn et al.,2008; Benton et al., 2010) and CAMERA (Kuhl et al., 2012) R packages for peak detection, peak grouping, and retention time correction. Peaks were required to exceed a 20x noise threshold to be considered. Lipid peak and adduct detection was performed by the LOBSTAHS package within a 5-ppm mass certainty.

Final compound confirmation was done manually using ms2 fragmentation spectra and HPLC retention time patterns as previously shown (Becker et al., 2018) with the aid of the LOB_tools

package (https://github.com/hholm/LOB_tools). Some isomers were not distinguishable in our analysis, including the distinction between diacylglyceryltrimethylhomoserine (DGTS) and diacylglyceryl-hydroxymethyltrimethyl-β-alanine (DGTA), as well as the stereochemistry of fatty acids. These non-distinguishable isomers were grouped together in analysis. All data processing and analysis was performed in R studio (R studio team 2020) and R version 3.6.2 (R core team 2013) utilizing the tidyverse collection of packages (Wickham et al. 2019). In total 668 unique lipid compounds were identified.

Known concentrations of deuterated standards were analyzed on the HPLC-MS immediately prior to running samples to establish a quantitative relationship between peak area and lipid abundance, analogous to the procedure used Holm et al. (2022). Because a known, constant amount of each internal standard was added to each sample, lipid peak areas were corrected to account for the ionization factor of a chemically similar, deuterated standard (Table 2.1). In other words, the observed quantity of a given internal standard was compared to the actual amount added to the sample and the response of chemical-similar compounds was corrected for the response of the standard.

v. Analytical methods

Statistically significant differences, except where stated, are defined by p-values < 0.05 across analyses including student's t-test, ANOVA tests, multi-linear regressions, and Spearman rank correlations. Statistical analysis was conducted using the stats package in base R (R core team 2013). Except where stated all confidence intervals are plus or minus one standard error around the mean.

The pheatmap (Kolde 2015), dendsort (Sakai et al. 2014), and NbClust (Charrad et al. 2014) R packages were used for clustering analysis and heatmap creation. Unsupervised clustering analysis was performed on the concentrations of individual lipid compounds in log space. Compounds below the limit of detection were given values of the lowest peak that was detected. The optimal number of clusters was chosen via gap-statistic analysis using the NbClust package. NMDS analysis was done with the aid of the vegan R package (Oksanen et al. 2020).

Results

i. The Prochlorococcus *lipidome*

To obtain the complete lipidome of *Prochlorococcus* MED4, we averaged concentrations of individual lipids across all *Prochlorococcus* control cultures where the total concentration of *Prochlorococcus* was at least 100-fold greater than the concentration of background heterotrophic bacteria. Our analysis included a total of 7 cultures across biological replicates and time points, including *Prochlorococcus* in different phases of growth and division, ensuring an accurate, complete picture of the *Prochlorococcus* lipidome in the wild. We then excluded classes of lipids known not to be present in *Prochlorococcus* (Van Mooy et al. 2006, Popendorf, Lomas, and Van Mooy 2011).

A large majority of the *Prochlorococcus* lipidome is composed of glycolipids, specifically monogalactosyldiacylglycerols (MGDGs; 48 species) and sulfoquinovosyl-diacylglycerols (SQDGs; 47 species) (Figure 2.1). These two classes of lipid alone make up over 85% of the total lipidome. Divinyl chlorophyll a makes up $4.6 \pm 0.64\%$ of the total lipidome and pigments comprise approximately $4.9 \pm 0.66\%$. *Prochlorococcus* invests very little in phospholipids, with

phosphatidylglycerol (PGs; 27 species) composing only 1.4 ± 0.02% of the lipidome. These numbers agree with previous studies on the lipid-class makeup of the lipidome of *Prochlorococcus* MED4 (Van Mooy et al. 2006).

The *Prochlorococcus* lipidome is largely composed of lipids that contain short-chain fatty acids with few unsaturations (Table 2.2). The average fatty acid chain length across lipid compounds is 30.2 ± 0.021. The average number of double bonds is 0.77 ± 0.015. These measurements are consistent with previous fatty acid data on *Prochlorococcus* and other cyanobacteria (Goodloe and Light 1982, Brenton et al. 2019, Wlodarczyk et al. 2020).

Prochlorococcus divided synchronously, roughly doubling over the course of 12 hours, starting during the "dark" or "night" period, where the incubator light was turned off (10 hours each day) ((Lindell et al. *in prep*, Figure 2.2). Samples were taken two hours before the lights turned off (preparing for mitosis/growth) and right when the lights turned on, but cells were still dividing (mitosis/division). To determine how the *Prochlorococcus* lipidome is altered during growth and division, *Prochlorococcus* samples without the presence of grazers or phages were grouped into these two life cycle stages (growth and division). 37.5% of *Prochlorococcus* lipids increased significantly ($p < 0.05$) between growth and mitosis, and no compounds significantly declined.

Overall, the total per cell lipid content of *Prochloroccocus* increased by 97.4% ($p<0.05$), indicating a near doubling in lipid content per cell over the growth phase. This is consistent with the reported cell volumes during this experiment (Lindell et al. *in prep*). The five largest significant increases in per cell concentration were mainly among phospholipids and an MGDG, including a 3.22-fold increase in PG 32:0 ($p=0.0155$), 3.17-fold increase in MGDG 30:0 ($p=0.0060$), 2.81-fold increase in PG 30:1 ($p=0.0036$), 2.60-fold increase in PG 32:1 ($p=0.0036$), and a 2.34-fold increase in PG 31:2 ($p=0.0269$). However, overall lipid phosphorus content increased only by 85.3% ($p=0.0187$), less than the total lipid increase during growth.

To distinguish which lipids were mainly affected by growth or, alternatively, responded mainly to top-down pressures, we performed a clustering analysis of all lipid compounds across samples. Samples of the same treatment tended to cluster together, especially later in the experiment, indicating the ability for lipidomic analysis to resolve differences in *Prochlorcoccus* metabolism between top-down pressures (Figure 2.3). Compounds were grouped into 13 clusters (A-L), the ideal number of clusters according to gap-statistical analysis (Figure 2.4, Figure 2.6).

Concentrations of lipids within each cluster were compared to the concentrations of *Prochlorococcus, P. bandaiensis*, P-SSP7 phages, and heterotrophic bacteria across all samples (Figure 2.5A). Similarly, the per cell concentration of each cluster was compared to the increase or decline in the concentrations of *Prochlorococcus, P. bandaiensis*, phages, and heterotrophic bacteria in the preceding 12 hours (Figure 2.5B). Clusters A, B, C, K, and L all significantly correlated with the concentration of *Prochlorococcus* and contained almost entirely *Prochlorococcus* lipids identified in our core lipidome, except for a small amount of triacylglycerol (TAGs), phosphatidylcholine (TAGs), and phosphatidylethanolamines (PEs) (Figure 2.6, Figure 2.7A). Additionally, clusters A, C, K, and L were correlated with the increase in *Prochlorococcus* abundance over the previous twelve hours, suggesting they are lipids related to *Prochlorococcus* growth (Figure 2.6). Thus, we call the lipids in these clusters the "core" *Prochlorococcus* lipidome, as this portion of the lipidome is not correlated with grazing or viral mortality (Figure 2.7A).

The *Prochlorococcus* core lipidome is distinguished from the "modular" lipidome, or those lipids found in the *Prochlorococcus* lipidome which are highly responsive to top-down pressures (clusters D, E, F, G, H, I, J and M). The *Prochlorococcus* modular lipidome represents <1% of the total *Prochlorococcus* lipidome, meaning cell concentration is the main factor determining the abundance of most *Prochlorococcus* lipids in each sample. Indeed, a majority of the 25 most abundant *Prochlorococcus* lipids are contained within cluster K (Table 2.2).

The modular lipidome is mainly composed of PG (48.7 ± 17.0%) and SQDG (47.2 ± 33.3%) (Figure 2.7B). The large variance across samples in the makeup of the modular lipidome reflects the highly responsive nature of this portion of the lipidome to different experimental treatments and conditions. A greater proportion of poly-unsaturated and phosphorus containing lipids were found in the modular *Prochlorococcus* lipidome (Figure 2.7B).

ii. Changes in Prochlorococcus *phosphorus metabolism in response to phage infection*

In the marine environment, *Prochlorococcus* is known to substitute the phospholipid PG for the sulfur containing lipid SQDG with declining environmental phosphate (Van Mooy et al. 2006, Van Mooy et al. 2008). Therefore, the total SQDG:PG ratio reflects a metabolic response to phosphorus availability and stress (Van Mooy et al. 2006, Van Mooy et al. 2008). To investigate the impact of viral infection on phosphorus partitioning within the cell, we examined the changes in *Prochlorococcus* MED4 SQDG:PG ratio during phage infection.

To remove the effects of heterotrophic bacterial PGs on the SQDG:PG ratio we first excluded PGs contained in cluster M from our analysis (PG 31:1, PG 29:0, and PG 28:0), as they correlated with total abundance and change over time of these bacteria across treatments. Cluster M accounted for an average of 1.4% total PG concentration across all samples. With these lipids removed, the concentration of SQDG per *Prochlorococcus* cell was compared to the total concentration of PG per cell across replicates of same treatment to compute the SQDG:PG ratio. The SQDG:PG ratio of *Prochlorococcus* in control treatments stayed mostly constant throughout the course of the experiment, showing the cultures were not experiencing changes in P-stress, which is expected in a P-replete medium (Figure 2.2, Lindell et al. *in prep*).

The SQDG:PG ratio of the +phage and +phage+grazer treatments first differ significantly from the control 12 hours after the start of the experiment ($p = 0.0021$ and $p < 0.0001$ respectively), despite all cultures being grown in P-replete medium (Figure 2.2, Figure 2.8, Lindell et al. *in prep*). The SQDG:PG ratio in the +phage treatment was significantly lower than the control at t =12, yet the total concentration of *Prochlorococcus* did not significantly differ ($p=0.156$), meaning there was not a significant signal of mortality or lysis this early in the experiment (Figure 2.2, Figure 2.8).

Unfortunately, no sample was taken from the +grazer treatment at t = 12 hours; however, the +grazer treatment does not differ significantly from the control until t = 36 hours and based on the similar SQDG:PG of the +grazer and control samples at t = 24 hours ($p = 0.476$), it is reasonable to assume the +grazer would not differ significantly from the control at 12 hours into the experiment (Figure 2.8).

iii. Phage-associated changes in oxylipin-like compounds and changes in fatty acid composition

We then examined the *Prochlorococcus* lipids in the modular lipidome to investigate potential biomarkers of top-down mortality. Three unknown compounds with masses coinciding with

oxidized MGDGs were identified in the complete lipidome of *Prochlorococcus*. These compounds had masses corresponding to MGDG 30:0 + O, MGDG 32:0 + O, and MGDG 32:1 + O, however their exact structure could not be determined via ms2 (Figure 2.13). Here we investigate these compounds because of the previous linkages between phage infection and oxidative stress in phytoplankton demonstrated in several previous studies (Rosenwasser et al. 2014, Sheyn et al. 2016, Thompson, Zeng, & Chisholm 2016). Because these compounds share masses with MGDG oxylipins MGDG 30:0 + O, MGDG 32:0 + O, and MGDG 32:1 + O, we call these compounds MLOs (MGDG-like oxylipins) and refer to them as MLO300, MLO320, and MLO321 respectively.

Of the three compounds, MLO300 and MLO321 did not correlate with *Prochlorococcus* abundance ($p = 0.865$ and 0.606 respectively) but were present in the modular lipidome Cluster E. Cluster E is composed only of MLOs, and a small percentage of other compounds. Cluster E is the only cluster positively associated with the production of viruses. This supports a hypothesis that MLO300 and MLO321 are both associated with the T7-like phage induced mortality (i.e. lysis) of *Prochlorococcus* MED4.

A Spearman-rank comparison between these MLOs and the total abundance of phages across all samples revealed a positive correlation between phage abundance and the concentration MLO321 ($p \sim 0.00042$), but not MLO320 ($p \sim 0.561$) or MLO300 ($p \sim 0.105$). Spearman-rank correlation was chosen for the high number of samples that had little or no viruses, or MLOs below the limit of detection. P-values for this analysis are estimates and not exact values due to ties between samples containing no viruses. This evidence suggests that MLO321, is a potential biomarker of phage infection of *Prochlorococcus* by a T7-like phage.

To investigate the usefulness of this biomarker for detecting phage infection in *Prochlorococcus* in the open ocean, we examined samples from the same station in the North Pacific Subtropical Gyre (NPSG) over the course of several days (Bent et al. 2024). MLO321 was abundant in the NPSG and exhibited a pattern of diel cycling, with concentrations reaching a maximum around 6:00 pm and a minimum around 6:00 am (Figure 2.9).

In addition to the increase in MLOs, we found chain length and unsaturation of fatty acids increases as a result of viral infection in *Prochlorococcus*. We analyzed the average fatty acid chain length and number of double bonds in all intact polar lipids in the *Prochlorococcus* lipidome excluding pigments and the heterotrophic bacteria associated PGs (PG 31:1, PG 29:0, and PG 28:0). No treatment significantly diverged from the control in either total chain length or units of unsaturation during the first 24 hours of the experiment, with the exception of the +grazer treatment at t=0 which had an average of 0.0337 more double bonds per lipid ($p = 0.023$), and 0.00114 more double bonds per carbon ($p < 0.0001$). However, after 36 hours the +phage treatment significantly differed from the control in total fatty acid chain length ($p = 0.00095$), number of double bonds per lipid ($p = 0.00061$), and double bonds per carbon ($p = 0.0013$). On average the sum of both fatty acids in *Prochlorococcus* diacyl lipids contained 0.153 ± 0.0038 more double bonds, 1.47 ± 0.054 more carbons, and 0.0037 ± 0.0011 more double bonds per carbon in the high virus treatment than the control at $t = 36$ hours. No other treatment significantly differed carbon from the control in chain length, unsaturation, or unsaturation per carbon throughout the course of the experiment.

iv. Cyanophage infection alters host energy storage metabolism and may decrease energy transfer to higher trophic levels

The lipidome of *P. bandaiensis* was assembled from a culture containing only *P. bandaiensis* with *Prochlorococcus* or phages. Lipidomic analysis reveals *P. bandaiensis* invests a significant amount of carbon in triacylglycerols (TAGs), making up over a third of the lipidome (Figure 2.10).

TAGs are primarily eukaryotic energy storage molecules that can be membrane-bound or stored in lipid droplets. TAG concentrations tend to increase at the onset of carbon limitation, as TAGs are a long-term, stable energy storage mechanism, and then are often metabolized during extreme starvation (Yu et al. 2009, Juarez et al. 2017, Tajparast and Frigon 2018). TAGs are important in marine carbon cycling, constituting a major portion of particulate organic carbon (POC), so much so that the daily diel cycling of TAGs represents a flux of 2.4 Pg C yr^{-1} (Becker et al. 2018). Given the importance of TAGs to the global carbon cycle, we sought to investigate what effect prey *Prochlorococcus* concentrations and viral abundances had on TAG metabolism in *P. bandaiensis*.

Concentrations of TAGs were dynamic over the course of the experiment. Per cell TAG concentrations were slightly but not significantly different at the beginning of the experiment between the +grazer and +phage+grazer treatments. But, both treatments significantly diverged from their initial TAG concentrations 24 hours into the experiment [Figure 6A]. The +phage+grazer treatment had significantly higher per cell TAG concentrations than the +grazer treatment at 24 hours into the experiment. However, 12 hours later, at 36 hours into the experiment, the per cell concentration of the +grazer treatment was significantly higher than that of the +phage+grazer treatment (Figure 2.11A). Because of the significantly lower *Prochlorococcus* (prey) abundances in the +phage+grazer treatment at this timepoint compared to the +grazer, we hypothesize that the significant decrease in TAG concentrations between 24 and 36 hours into the experiment in the +phage+grazer treatment compared to the +grazer treatment reflects TAG catabolism in the face of prey scarcity and starvation.

Additionally, the total TAG concentrations between +grazer and +phage+grazer treatments significantly differ at 24 and 36 hours into the experiment in a similar way, with TAG concentrations in cultures with grazers and viruses higher than grazers alone at t = 24 hours, but lower at 36 hours (Figure 2.11B). This difference resulted in an approximately 3-fold larger concentration in TAGs in the +phage+grazer treatment, than the treatment with only *P. bandaiensis* (+grazer). Interestingly, the growth rates of *P. bandaiensis* do not differ greatly throughout the course of the experiment (Figure 2.12). This indicates phage presence alters the metabolism, but not necessarily the growth of its host's predator.

The increase or decline in TAGs changed disproportionally between specific compounds. Some TAGs increased between 24 and 36 hours during which the +phage+grazer treatment had significantly higher *P. bandaiensis* abundances than the +grazer and likely began to starve due to lack of prey. Differences between the responses of specific TAGs to starvation in the +phage+grazer treatment seemed to mainly reflect differences in fatty acid composition, with more unsaturated fatty acids becoming more common. Between 24 and 36 hours after inoculation the weighted average number of double bonds per TAG increased from 3.06 ± 1.88 to 6.12 ± 2.40 ($p = 0.015$) and the weighted average total fatty acid chain length per TAG increased from 49.7 ± 2.61 to 53.9 ± 2.27 ($p = 0.0020$) in the +phage+grazer treatment. The

number of double bonds and fatty acid chain length was also significantly greater at t = 36 hours in the +phage+grazer treatment than in the grazer alone treatment with an average difference of 4.441 ± 1.111 more double bonds and 7.249 ± 1.055 more carbons (p = 0.00012) per TAG.

Discussion

i. The core lipidome of Prochlorococcus

We present, to our knowledge, the first compound-specific resolution of the full lipidome of any strain of *Prochlorococcus* (Table 2.2). In total, we identified the *Prochlorococcus* MED4 lipidome is composed of 145 lipids.

The observed core lipidome of *Prochlorococcus*, which contained the lipid molecules not affected by top-down pressures in the experiment, agrees well with previously published studies on the elemental composition and lipid class make up of *Prochlorococcus* (Bertilsson et al. 2003, Van Mooy et al. 2006, Brenton et al. 2019). The *Prochlorococcus* lipidome reflects a frugal phosphorus usage strategy, as even in our P-replete cultures, phospholipids composed only about 1.5% of the total lipidome (Figure 2.1, Figure 2.7, Table 2.2). This is thought to be an evolutionary adaptation to the highly nutrient limiting environments of the open ocean (Van Mooy et al. 2006).

Interestingly, the core lipidome does vary during the cell cycle. During the growth and synthesis phases, phospholipids compose less of the lipidome. One explanation may be a decrease in phospholipid production during the synthesis phase allows the cell to free up more phosphorus for DNA replication, helping to lower the cellular phosphorus requirement which may be beneficial in the P-limited gyre environments.

ii. The modular lipidome of Prochlorococcus

The modular *Prochlorococcus* lipidome, which is responsive to top-down pressures in addition to mortality, composes less than 1% of the complete *Prochlorococcus* lipidome (Figure 2.7, Table 2.2). The modular lipidome is composed mainly of SQDGs and PGs and did not include any pigments (Figure 2.7). This seems to contradict previous studies suggesting phage infection causes an increase in divinyl chlorophyll production in *Prochlorococcus* (Dammeyer 2008, Thompson, Zeng, and Chisholm 2016, Sieradiski et al. 2019). However, it is possible this signal was lost due to the high rates of mortality ultimately controlling pigment abundances in our samples. Alternatively, this could be an example of the diversity of phage infection and lysis strategies.

iii. Infection induced alteration of phospholipid metabolism

The SQDG:PG ratio was affected by and is responsive to viral infection of *Prochlorococcus* (Figure 2.8). Further, the significant decrease in the SQDG:PG at only 12-hours into the experiment, before lysis affected growth in the cultures, suggests that viral infection alone can alter the phospholipid composition of the *Prochlorococcus* MED4 lipidome (Figure 2.2, Figure 2.8). Whether this reflects total cellular phosphorus being diverted into the membrane cannot be determined from our data. However, our data does indicate infection alone of a T7-like phage alters the cellular phosphorus metabolism of *Prochlorococcus* MED4, which is reflected in the lipidome by an increase in phospholipids, and a decrease in the SQDG:PG ratio.

The decrease in the SQDG:PG ratio in *Prochlorococcus* because of viral infection suggests a relief of phosphorus stress in the cell despite being grown in P-replete cultures, as phospholipid substitution is known to be induced by P-starvation (Van Mooy et al. 2009). Indeed, the SQDG:PG ratio is strongly inversely correlated with the total availability of inorganic phosphorus in the environment, suggesting it is a reliable reflection of cellular phosphorus content (Martin et al., 2014). Since P-SSP7 does not contain a lipid envelope, and studies from other model bacterial host systems show phospholipid degradation is often upregulated in the process of cellular lysis, there is no obvious advantage for P-SSP7 to increase the fraction of phospholipids within the lipidome (Cronan and Wulff 1969, Young 2014).

In a study of the same P-SSP7 T7-like phage and *Prochlorococcus* MED4 system, Lindell et al. (2007) discovered upregulation of genes homologous to ATPases and phosphate regulatory genes 3-7 hours post infection, including a phoH-like gene (PMM1284). PhoH is a well conserved member of the Pho regulon which responds to phosphorus stress by upregulating phosphate transporters and extracellular phosphate scavenging proteins (Hsieh and Wanner 2010, Santos-Beneit 2015). It may also lead to phospholipid synthesis (Goldsmith et al. 2011) Additionally, phosphorus stress genes and the Pho regulatory pathway are well-represented within phages in the marine environment, with Pho-like genes appearing in 40% of marine phage genomes as opposed to only 4% of non-marine phages, and phoH is the most prevalent of these genes (Sullivan et al. 2010, Goldsmith et al. 2011, Monier et al. 2012). This indicates there is likely an evolutionary advantage in the marine environment for alteration of host phosphorus metabolism, and we see evidence this extends to lipid metabolism specifically, at least in P-SSP7. Further studies should investigate the role of viral infection of phosphorus partitioning and acquisition in *Prochlorococcus* to determine to what extent the decrease in the SQDG:PG ratio represents total cellular phosphorus or an increase in phosphorus allocation to lipid synthesis.

Our results have wide-ranging implications for the cycling of phosphorus in the marine environment. The alteration of lipid phosphorus usage and partitioning in *Prochlorococcus* from P-SSP7 infection suggests the make-up of dissolved organic matter (DOM) and particulate organic matter (POM) resulting from phage-induced lysis differs significantly from that of grazer excretion or cell death. Though our study looked only at a single cyanobacteria/phage system, the prevalence of pho genes within marine phages, coupled with the fact that P-SSP7 contains no known host P-regulation genes but still altered host phosphorus metabolism, suggests this phenomenon could potentially occur in other systems with or without known pho genes (Sullivan et al. 2005). Given the prevalence of *Prochlorococcus* and T7-like phages in the pelagic environment and the possibility of phage phosphorus metabolism rewiring in other marine phytoplankton, our findings suggest viral infection may be a potentially important and overlooked factor in the biogeochemical cycling of organic phosphorus in the marine environment.

iv. Changes to fatty acid composition and the identification of possible oxylipin-like biomarkers for phage infection

MLOs were associated with viral production in our experiment and tracked with the lytic cycle of *Prochlorococcus* in the open ocean. The correlation was weaker in MLO300, and we found very low concentrations and no noticeable diel cycling of this compound in the NPSG. MLO321 was significantly correlated with viral production and total virus concentration in our cultures,

and analysis of diel samples taken over the course of two days in the NPSG indicated a peak in MLO321 near sunrise and a trough near sunset (Figure 2.9).

Previous studies in the NPSG have shown cyanophage concentration peaks around or nearly after sunset, and *Prochlorococcus* infection peaks around the same time (Chen and Zheng 2020, Mruwat et al. 2020). Synchrony of our observed MLO321 diel cycle, which had similar peaks and troughs, suggests MLO321 may be a potential biomarker for phage-induced mortality and cyanophage production in the environment. Future studies investigating this relationship directly in the field will help determine the usage potential of this possible biomarker.

We also saw an increase in fatty acid chain length, double bond content, and number of double bonds per carbon in *Prochlorococcus* when cultured with phages. This suggests viral infection and lysis is altering fatty acid metabolism within the cell. Many other phages contain desaturases or other auxiliary fatty acid genes however these genes are absent in P-SSP7 (Sullivan 2005, Roitman et al. 2017). It is possible a gene of unknown function in P-SSP7 encodes for a desaturase, a fatty acid synthase, or another gene involved in fatty acid metabolism. Alternatively, this may be a downstream effect of another metabolic process. Future studies probing the P-SSP7 genome, especially gene knockouts, may be able to answer this question. Interesting, despite the difference in fatty acid composition in the +phage treatment, the +phage+grazer treatment did not significantly differ from the control in fatty acid composition.

v. Indirect higher trophic level consequences of phage infection

The greater TAG concentrations earlier in the experiment, and steep fall later in the experiment, in the +phage+grazer treatment compared to *P. bandaiensis* in the +grazer treatment shows a more rapid buildup in non-polar energy storage molecules when in the presence of infected cells. This relationship held true in both per cell and total concentrations of TAGs (Figure 2.11). A possible explanation for this relationship may be the much higher rates of mortality in +phage+grazer treatments which induced starvation earlier in *P. bandaiensis* and lead to catabolism of TAG energy stores to compensate for prey limitation. Alternatively, since we have shown the lipid metabolism of *Prochlorococcus* is altered by viral infection, *P. bandaiensis* may derive different amounts of nutrients and energy from infected cells than they do from uninfected cells. Perhaps, the increase in cellular phosphorus due to viral infection could have increased the efficiency of *P. bandaienis* to acquire this nutrient (Figure 2.8). Changes in nutrient composition of *Prochlorococcus* cells have been shown to have similar effects on grazers (Worden and Binder 2003). However, if this is the case, this difference in prey quality does not seem to alter the growth rate *P. bandaiensis* to a large extent (Figure 2.12).

The change in TAG fatty acid composition in *P. bandaiensis* further demonstrates P-SS7 infection of *Prochlorococcus* leads to an indirect lipid metabolism alteration of *P. bandaiensis*. The increase in lipid unsaturation in *P. bandaiensis* in +phage+grazer treatments match an increase in lipid unsaturation in *Prochloroccocus* in the presence of phages. Increases in fatty acid unsaturation are also associated with a decline in *Prochlorococcus* abundances, so we suggest the changes in fatty acid composition are due to starvation of *P. bandaiensis* in times of extreme prey scarcity. However, there exists a possibility that viral alteration of the *Prochlorococcus* lipidome may in turn affect the metabolism of *P. bandaiensis* as it digests *Prochlorococcus*.

The large change in TAG concentrations may have important implications for the cycling of TAGs and other energy storage compounds in the NPSG. Becker et al. (2018) showed TAG concentrations undergo 2- to 3-fold changes in concentration on a diel cycle, with a peak in concentration at sunset, and that this cycling of TAGs in the NPSG is equivalent to 4-6% of global NPP. Our results indicate that in addition to eukaryotic phototrophs, eukaryotic grazers may significantly contribute to this TAG cycle. Indeed, in the phage and grazer combined treatment TAG concentration dropped over 95% in a matter of 12 hours (Figure 2.111).

It is worth noting that changes in the heterotrophic bacteria community may have contributed to the changes in lipid metabolism of *P. bandaienis*. While grazing of *P. bandaienis* on the heterotrophic bacterial community was not measured directly, it is reasonable to assume some amount of background bacteria grazing occurred (Lindell et al. *in prep*). There were changes in abundances of the bacteria in the experiments as compared to the control (Lindell et al. *in prep*). However, these abundances remained low, so if they did contribute to the changes in *P. bandaienis* herein must have had an incredibly outsized effect on compared to the generally much more abundant *Prochlorococcus* prey (Lindell et al. *in prep*).

To our knowledge this is one of the first studies demonstrating the lipidome of a eukaryotic grazer can be altered by infection and lysis of its prey. These results emphasize the importance of studying virus-host-grazer systems in coculture, as both the lipid metabolism of the host and grazer are altered by the presence of phages. The surface waters of subtropical gyres where *Prochlorococcus* is found are a mix of viruses, prokaryotes, and eukaryotes, and our results demonstrate synergies and indirect interactions between trophic levels can greatly alter the metabolism of grazers and prey. Future models of the microbial loop in these environments should consider the effects of viral infection on the transfer of energy and nutrients to higher trophic levels.

Acknowledgements

This work was funded by a grant to Benjamin A.S. Van Mooy from the Simons Foundation (#721229). Max Jahns's gradate stipend was funded in part by an NSF Graduate Fellowship. We would like to thank our Simons Foundation Collaboration on Ocean Processes and Ecology (SCOPE) colleagues for their help in this project. We would also like to thank Kelsey and the rest of the Van Mooy lab for their assistance with lipid extractions.

Figures

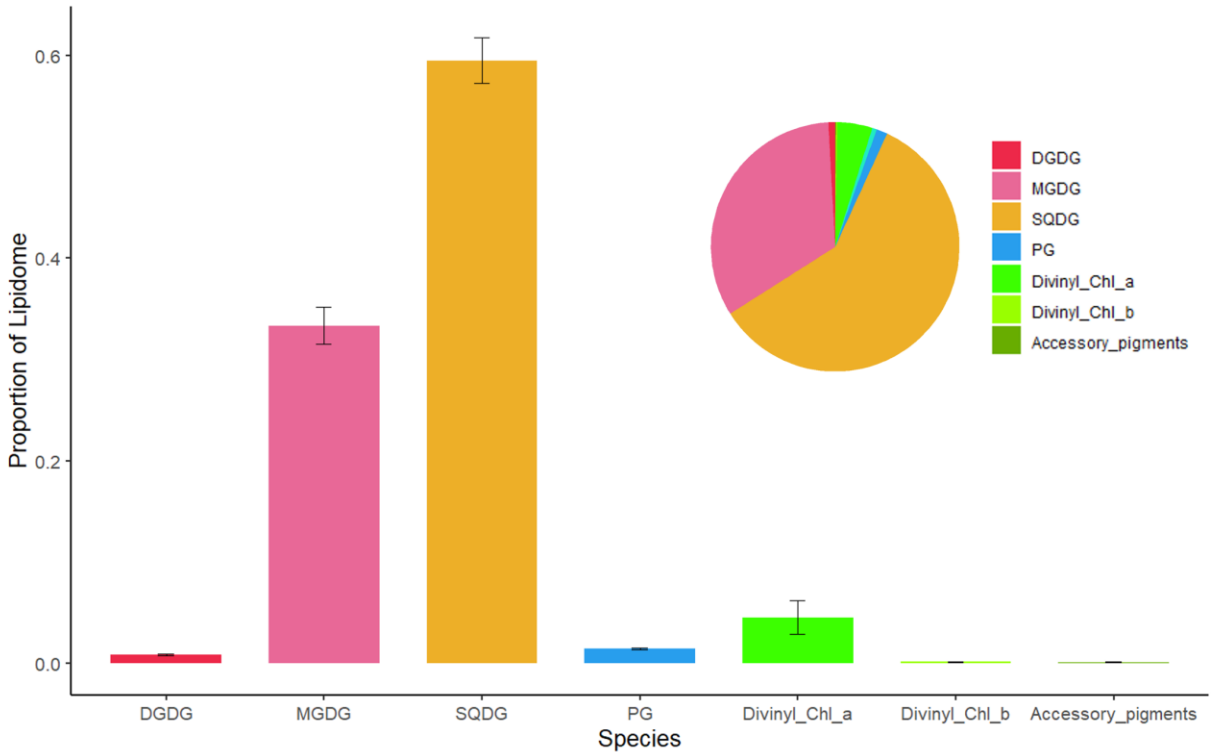

Figure 2.1. The relative contributions of major lipid classes to the *Prochlorococcus* MED4 lipidome. Lipid concentrations are an average across replicates and growth stages. Lipid classes are colored according to the legend and the inlay represents the same data in a different format. Error bars denote standard error (n = 7).

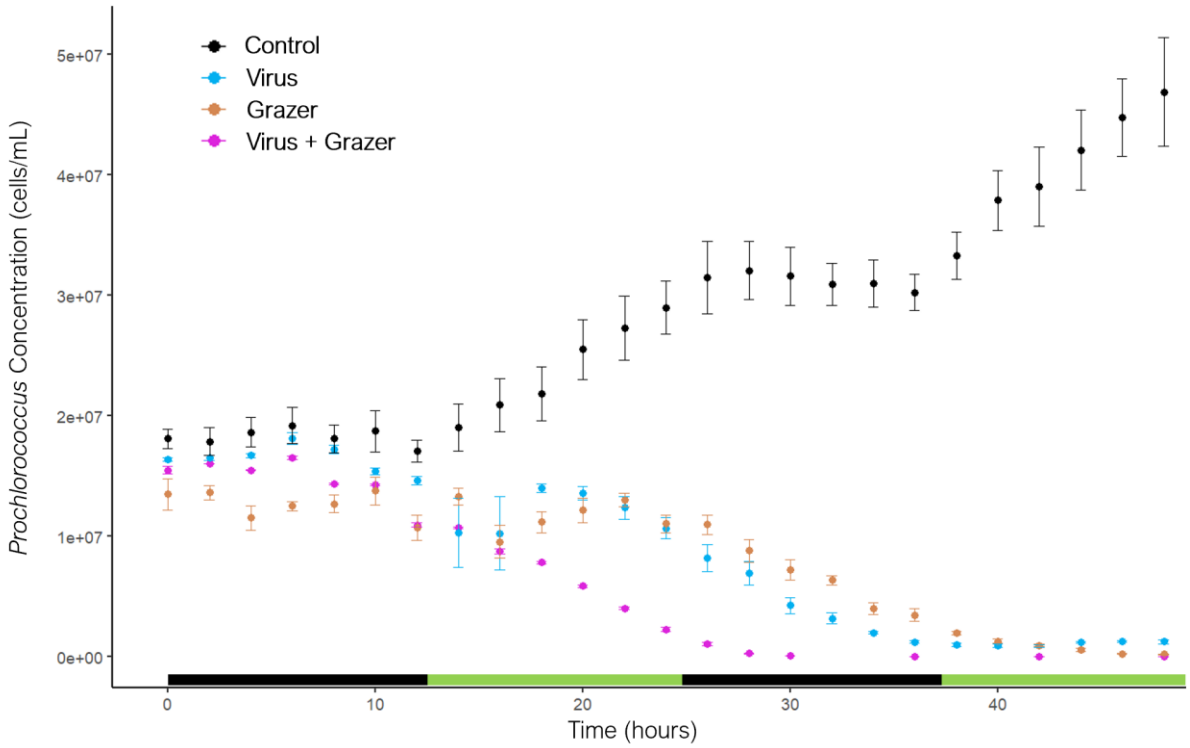

Figure 2.2. Growth of *Prochlorococcus* over time during the experiment across four different treatments (colors marked in the legend). Across the bottom axis the rough growth stages of *Prochlorococcus* are marked where green the culture in the process of dividing. In the control (black) *Prochlorococcus* divided synchronously on 12-hour cycles of growth and division with the light-dark cycle. Points are colored according to treatment: control (black), +phage+grazer (pink), +grazer (orange), and +phage (blue) Error bars are standard error. Data adapted from Lindell et al. (*in prep*).

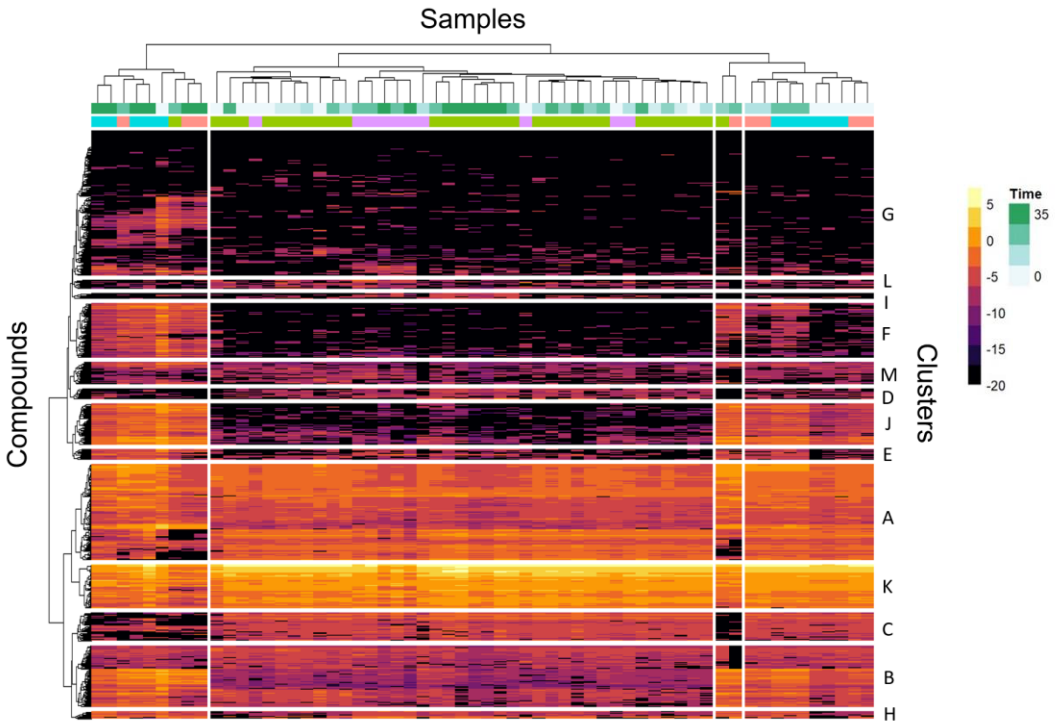

Figure 2.3. Heatmap of all identified lipid compounds (rows) across control, low grazer, high virus, and combined low grazer + high virus treatments. Dendograms denote relatedness of samples or lipids. Across the top, hours after inoculation are marked as a green scale, where white is 0 hours after inoculation. Below that, the colored bars indicate the different treatments analyzed: control (green), +phage+grazer (red), +grazer (blue), and +phage (purple). For an explanation of the treatment designations see (Lindell et al. *in prep*). Horizontal divisions are the 13 cultures determined by the NbClust R package (Figure 2.4). Coloration corresponds to the natural log pM concentration of each compound across samples.

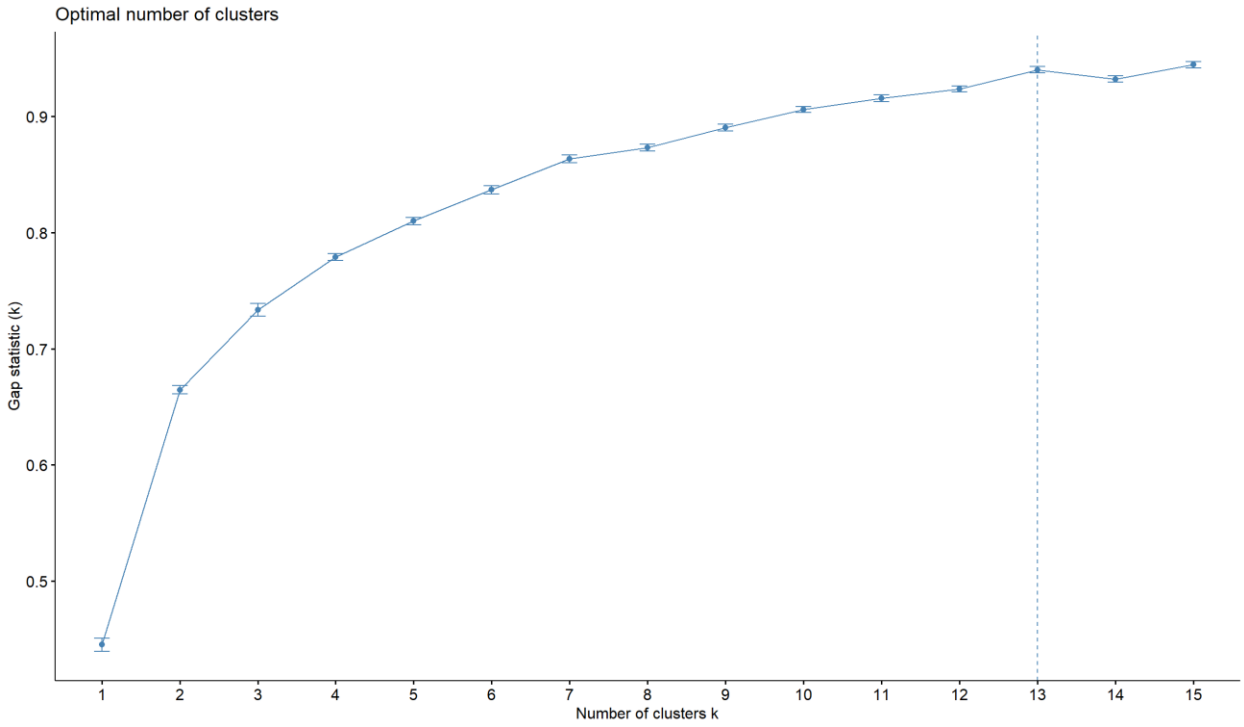

Figure 2.4. The optimal number of clusters as determined by gap-statistic analysis using the NbClust R package. The dashed line at 13 indicates the optimal number of clusters is 13.

2.5A

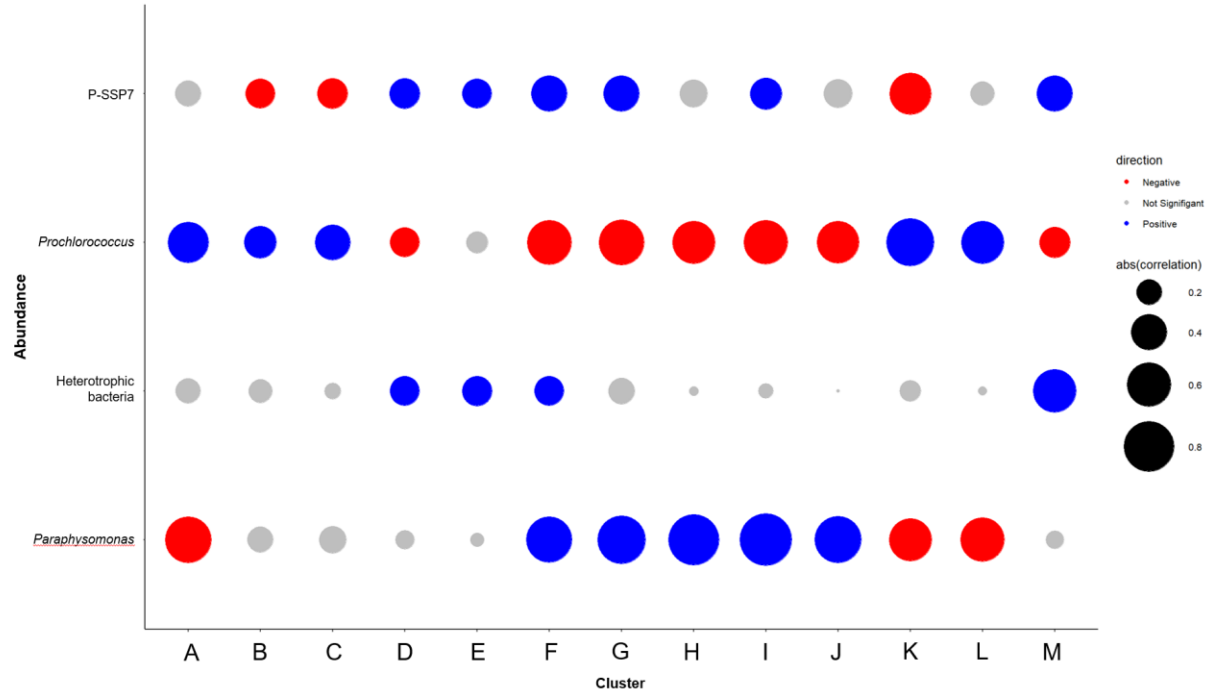

2.5B

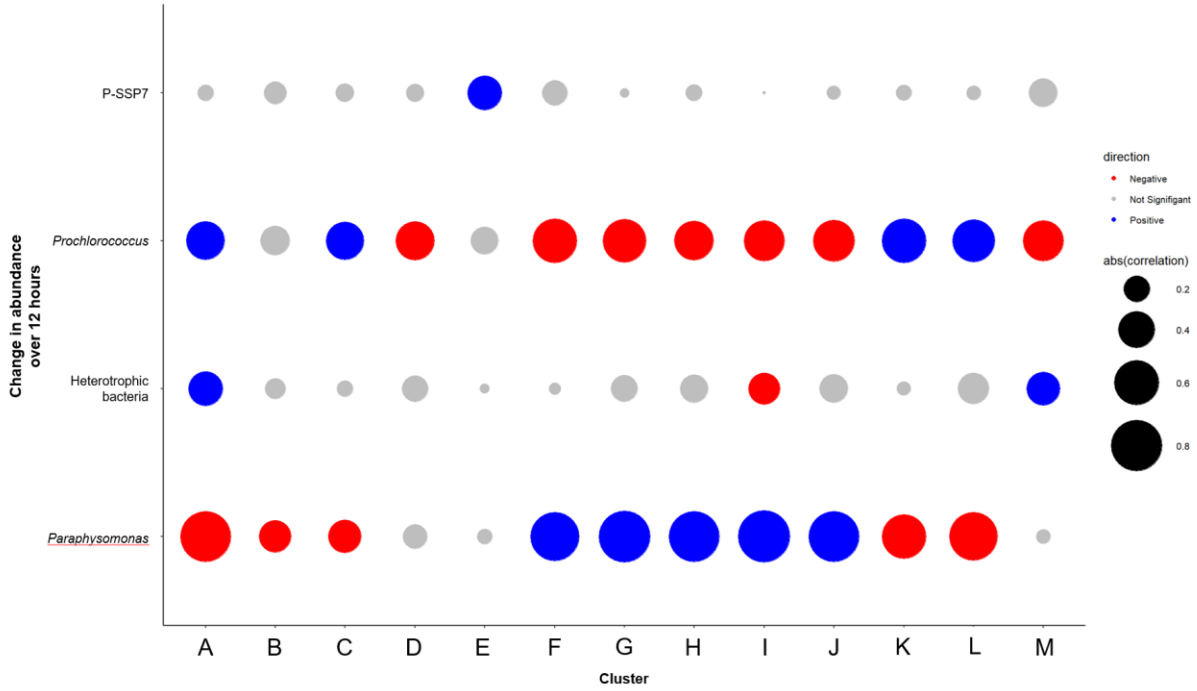

Figure 2.5. (A) Linear regression correlation of each cluster with concentrations of viruses, *Prochlorococcus*, heterotrophic bacteria, and a eukaryotic grazer (*Paraphysomonas bandaiensis*). (B) Spearman rank correlation of each cluster with change in concentration of viruses, *Prochlorococcus*, heterotrophic contaminants, and a eukaryotic grazer (*P. bandaiensis*) over the last twelve hours. Samples <12 hours into the experiment were excluded. In this case, a Spearman rank correlation was used due to the non-meaningful units of the relationship. The size of the bubble indicates magnitude of r-squared value. The color of the bubble indicates the sign of the correlation: negative correlation (red) or positive correlation (blue). Correlations that were not significant ($p > 0.05$) are marked in grey.

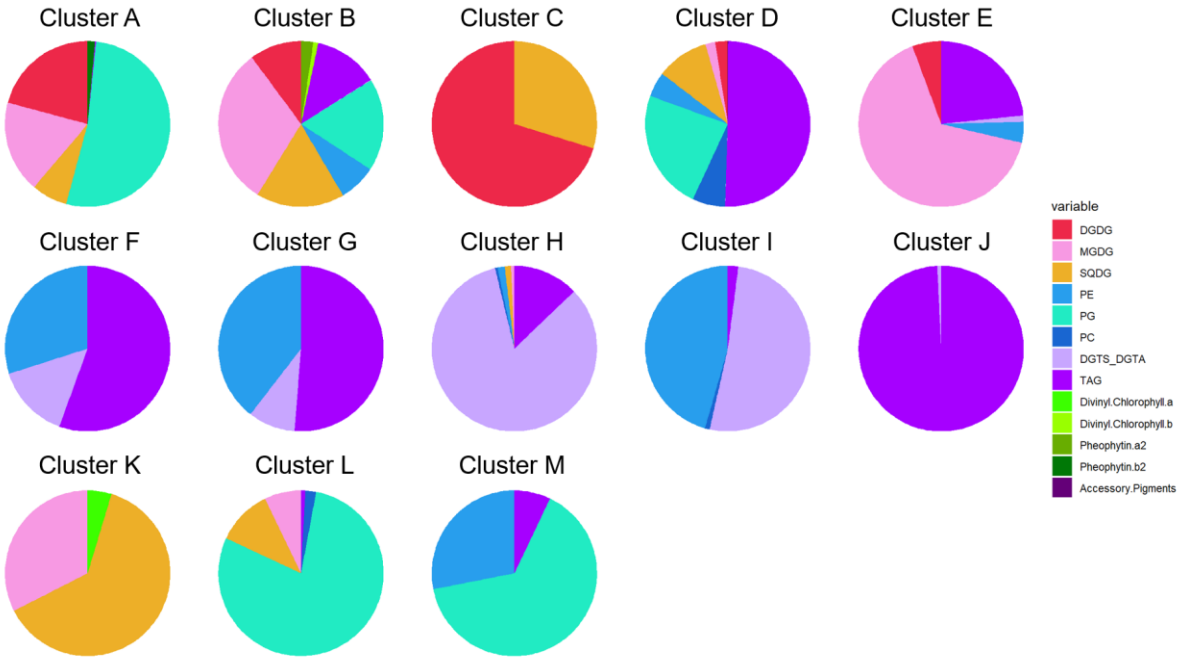

Figure 2.6. Average composition of each cluster by lipid class. Glycolipids are in red/orange, phospholipids are in blue, and pigments are in green/brown. The cyanobacterial lipids in clusters A, B, C, K and L are included in the core lipidome of *Prochlorococcus* MED4. The remaining clusters (D, E, F, G, H, I, J, and M) are made up primarily of eukaryotic or heterotrophic bacterial lipids, however the cyanobacterial lipids in this cluster are grouped into the *Prochlorococcus* MED4 modular lipidome.

2.7A

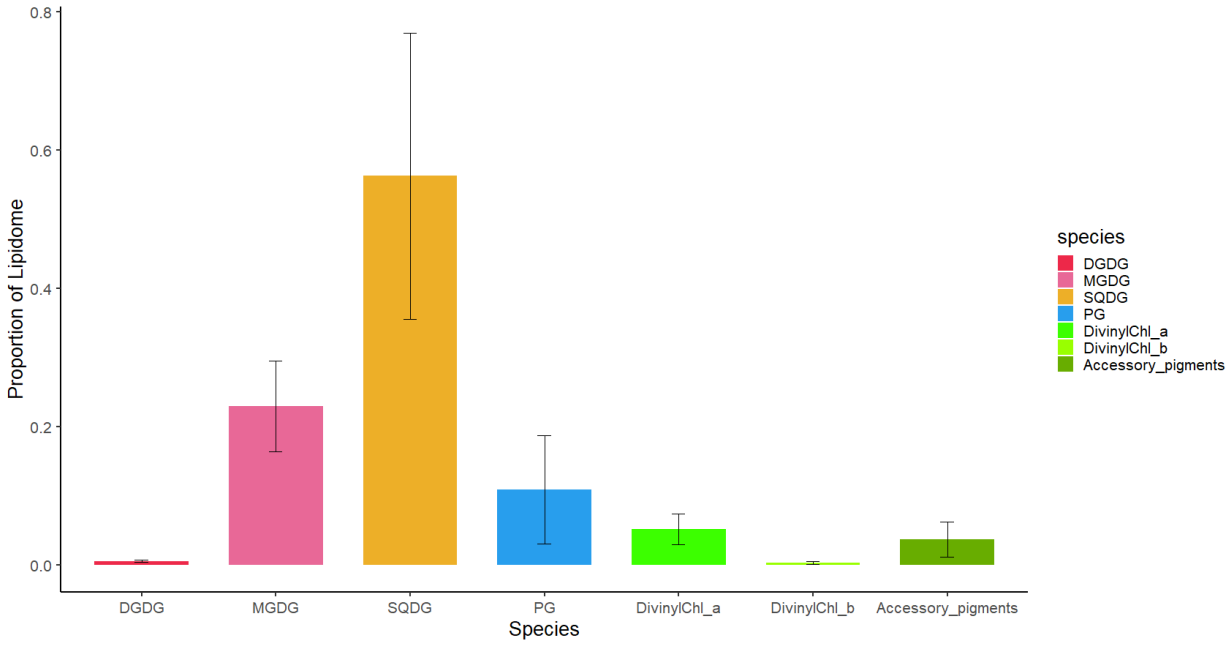
0.8
0.6
0.4
0.2
0.0
Proportion of Lipidome
DGDG
MGDG
SQDG
PG
DivinylChl_a
DivinylChl_b
Accessory_pigments
Species
species
DGDG
MGDG
SQDG
PG
DivinylChl_a
DivinylChl_b
Accessory_pigments

2.7B

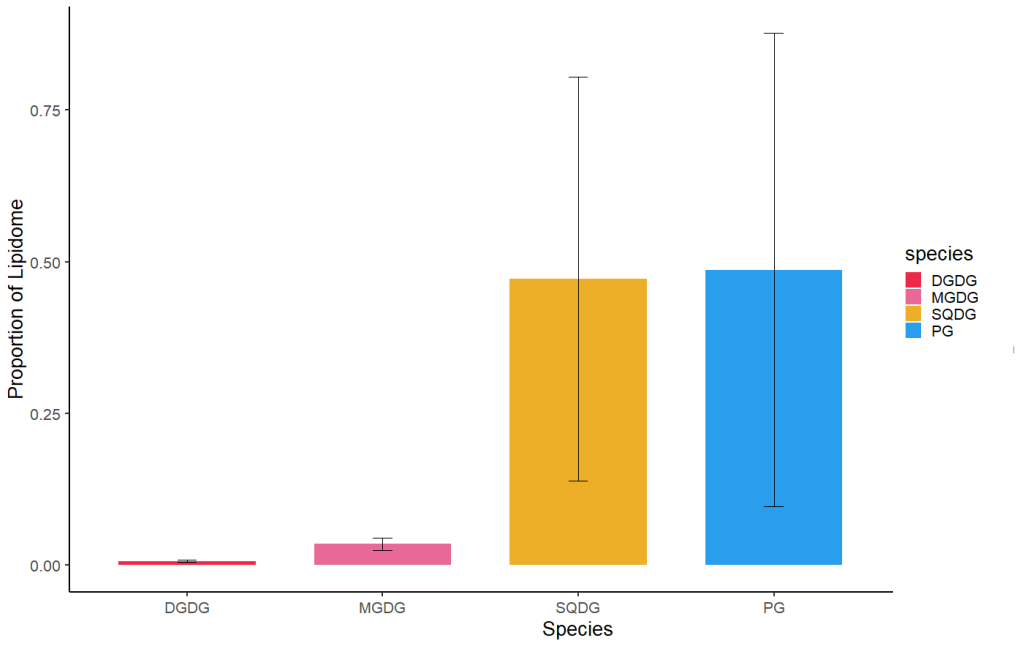

Figure 2.7. (A) The average proportion of each of the major classes of *Prochlorococcus* lipids found in clusters A, B, C, K, and L across all samples (the core *Prochlorococcus* lipidome). Note the similarity to the identified total lipidome of the control samples in Figure 1. Error bars represent standard error. (B) The average proportion of each of the major classes of *Prochlorococcus* lipids found in clusters D, E, F, G, H, I, J, and M across all samples (the modular lipidome). Glycolipids are in red/orange, phospholipids are in blue, and pigments are in green. Error bars represent standard error.

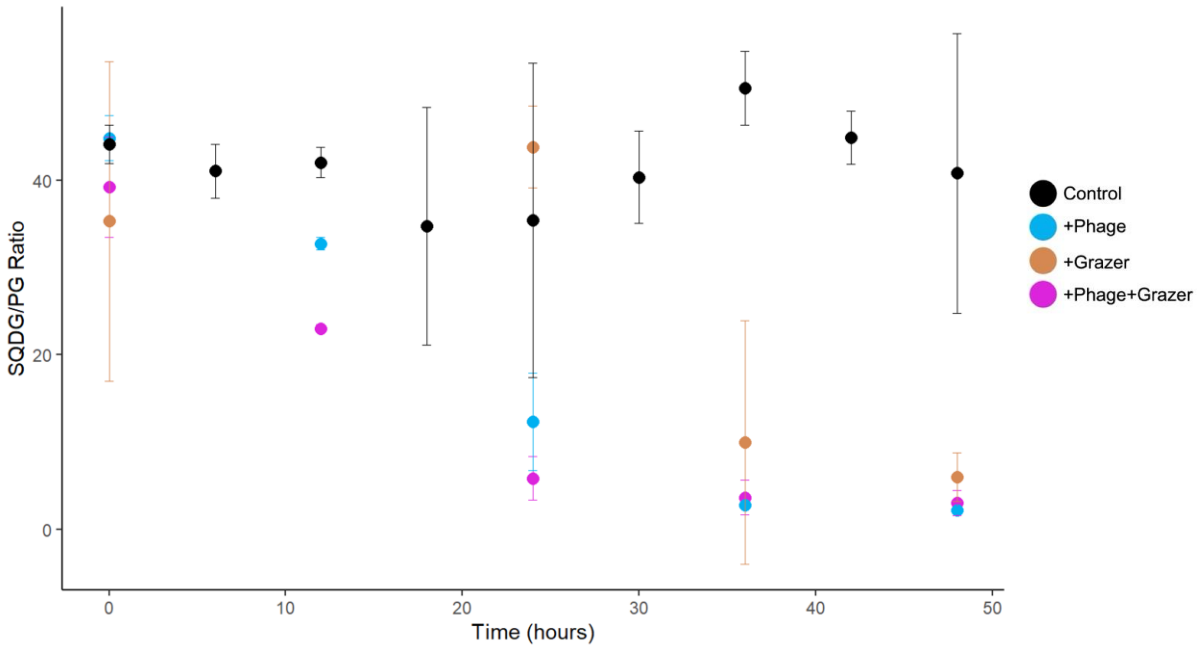

Figure 2.8. The ratio of SQDG to PG in the *Prochlorococcus* lipidome over the course of the experiment in the control (black), +phage (blue), +grazer (orange), and +phage+grazer (pink) treatments.

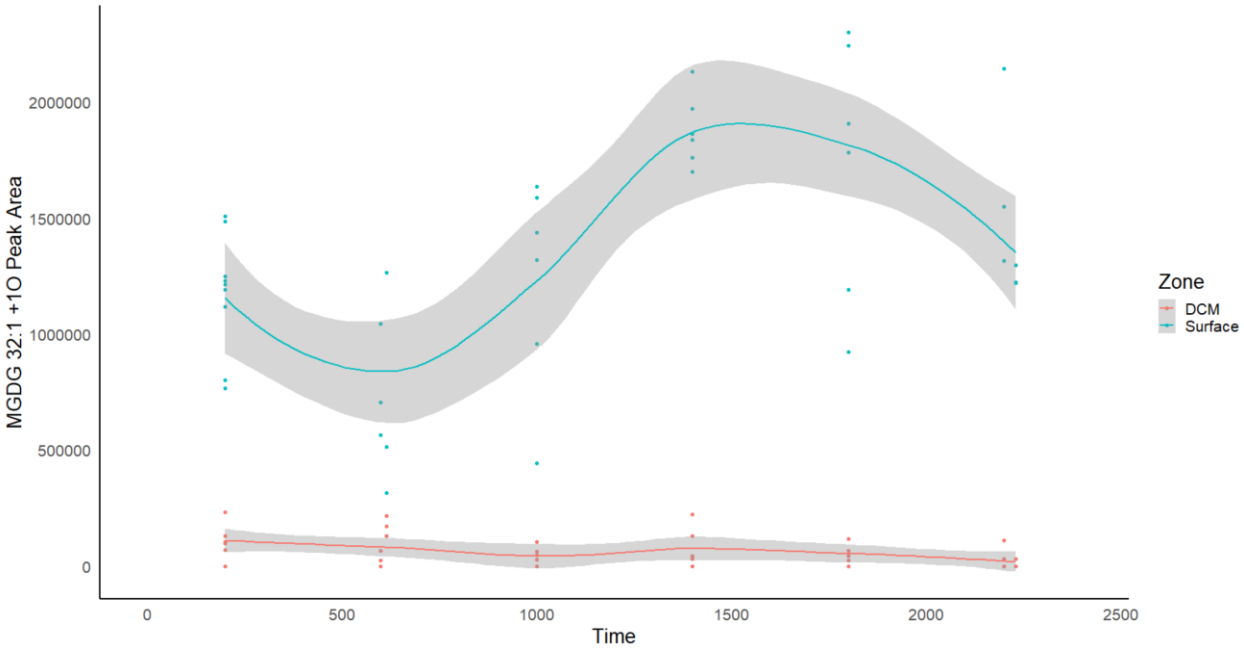

Figure 2.9. The peak area of MGDG 32:1 +O in the NPSG over a diel time frame in the surface (blue) and the deep chlorophyll maximum (red). Solid lines are smooth local regression, and the confidence interval is represented by the grey region.

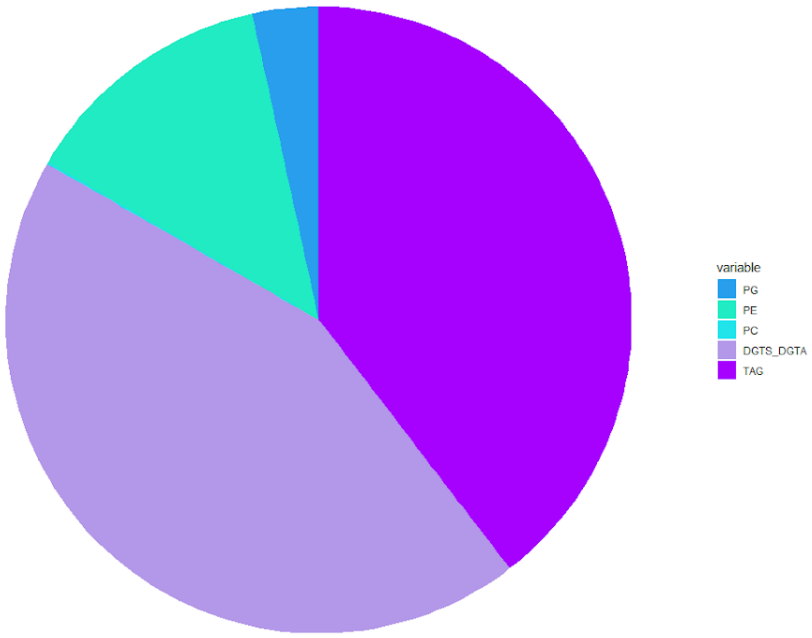

Figure 2.10. The relative contributions of major lipid classes to the *P. bandaiensis* lipidome. Lipid concentrations are an average across replicates, treatments, and growth stages. Lipid classes are TAGs (dark purple), DGTS/DGTA (light purple), PE (teal), and PG (blue).

2.11A

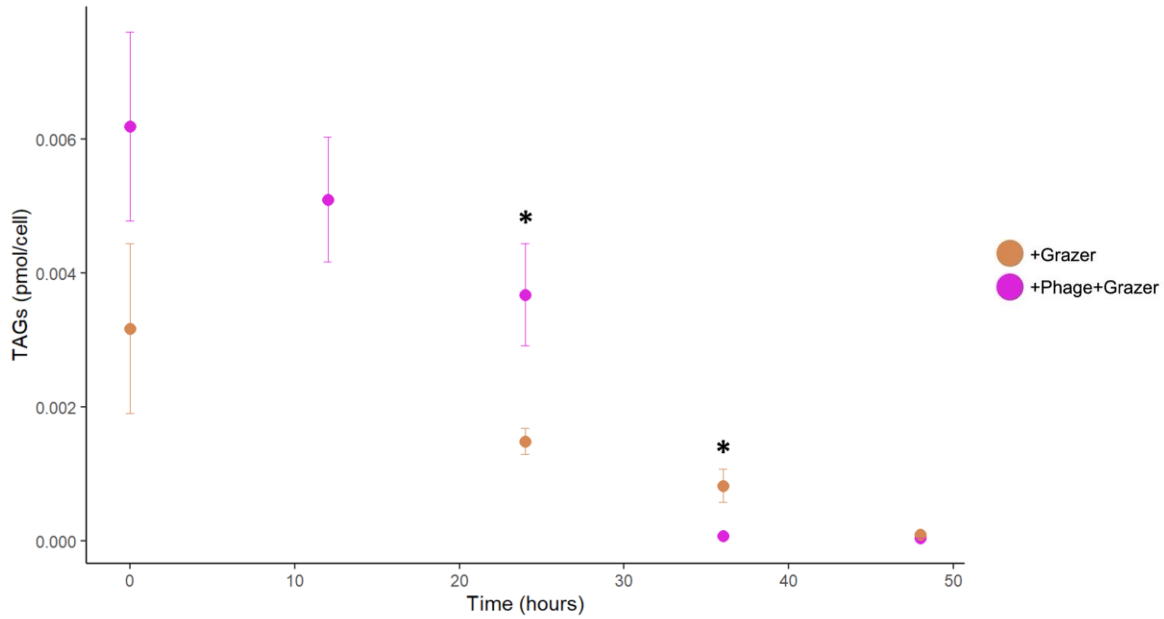

2.11B

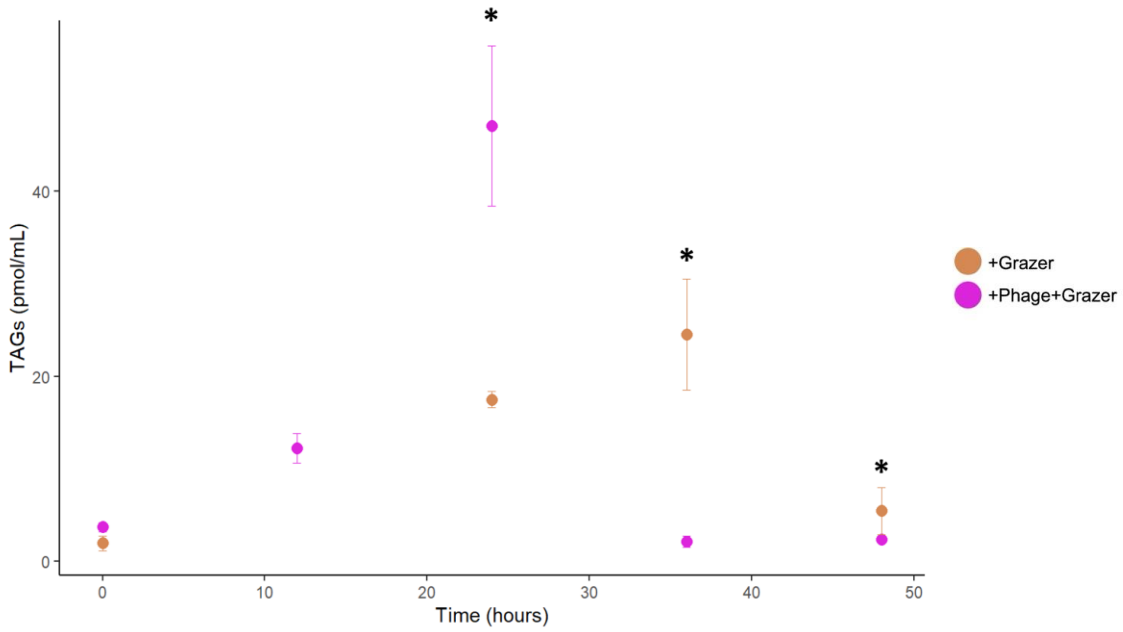

Figure 2.11. The concentration of TAGs (A) per cell and (B) per mL over time in the +grazer (orange) and the +phage+grazer (pink) treatments. Asterisks represent significantly different TAG concentrations between treatments ($p < 0.05$).

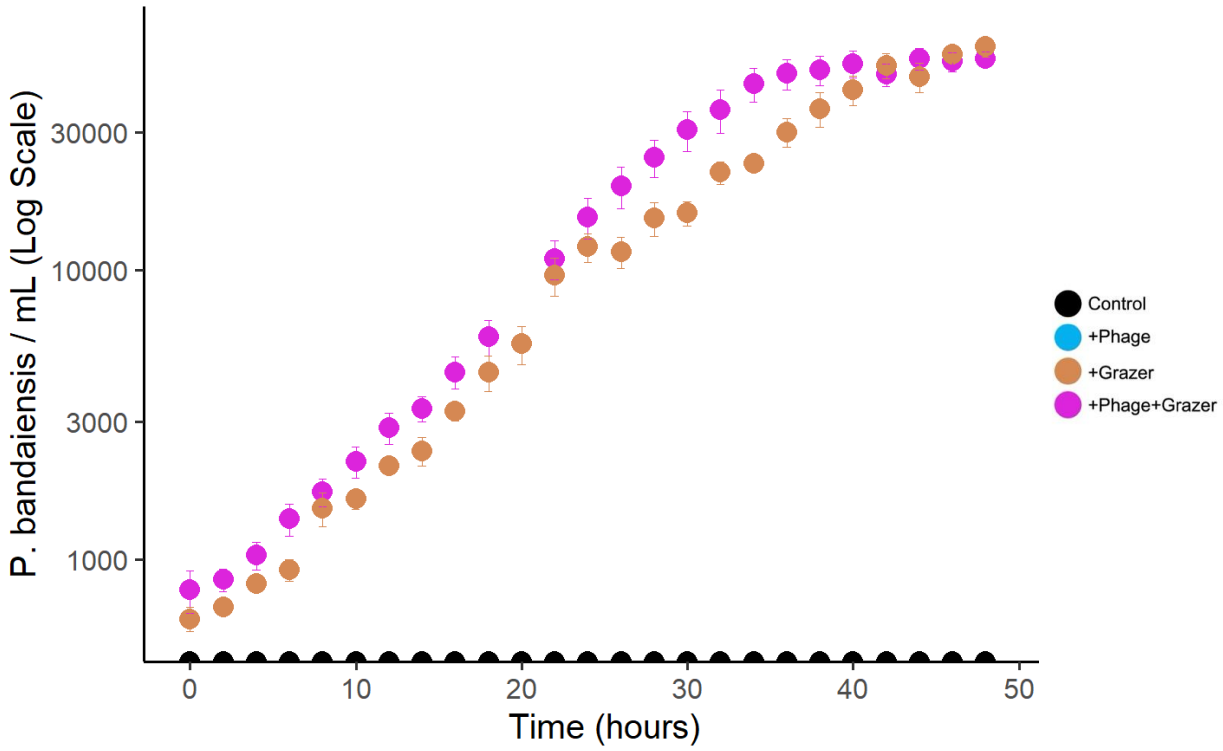

Figure 2.12. The concentration of *Paraphysomonas bandaiensis* over the course of the experiment in +grazer (orange) and +phage+grazer (pink) treatments. The control (black) and +phage (blue) treatments did not contain *P. bandaiensis*.

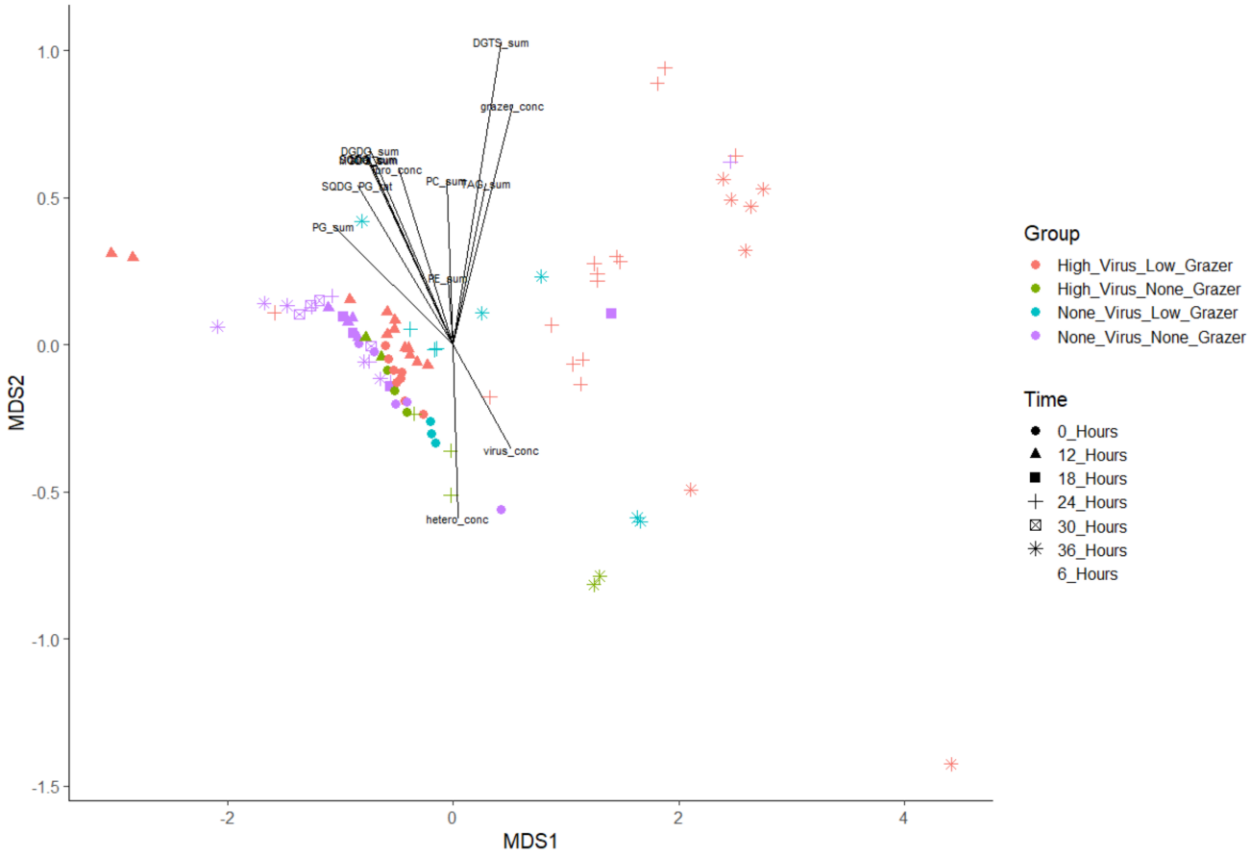

Figure 2.13. NMDS plot of the change of concentrations of all identified lipids in each experimental treatment over time. The color of the point corresponds to the treatment, while the shape indicates the time after inoculation. Samples mainly begin to diverge from the control around 12-24 hours. Treatments have distinct trajectories in this space from one another suggesting *Prochlorococcus* is highly responsive to different top-down pressures.

Tables

Lipid Class	**Deuterated Standard**
DGDG	C15_GSL_d7
DGTS_DGTA	DGTS-d9
DGTS-d9	DGTS-d9
MGDG	C15_GSL_d7
PC	15:0-18:1-d7-PC
PE	15:0-18:1-d7-PE
PG	16:0-18:1_D5_PG
SQDG	C15_GSL_d7
TAG	16:0-18:0-16:0_D5_TG
All other	DNPPE

Table 2.1. The internal, deuterated standard used to correct for the recovery of each lipid class as described in Holm et al. (2022).

COMPOUND	CONCENTRATION (PMOL/CELL)	PROPORTION OF LIPIDOME
MGDG 30:1	6.4755 x10^{-6}	24.73%
SQDG 30:0	5.9215 x10^{-6}	22.61%
SQDG 30:1	5.4149 x10^{-6}	20.68%
SQDG 32:1	1.3427 x10^{-6}	5.13%
Divinyl Chlorophyll a	1.1939 x10^{-6}	4.56%
SQDG 32:0	1.0190 x10^{-6}	3.89%
MGDG 30:2	8.3967 x10^{-6}	3.21%
MGDG 28:1	7.1738 x10^{-6}	2.74%
SQDG 30:2	1.0190 x10^{-6}	3.89%
SQDG 28:0	6.2028 x10^{-7}	2.37%
SQDG 32:2	2.3804 x10^{-7}	0.91%
MGDG 30:0	2.0129 x10^{-7}	0.77%
PG 32:2	1.8097 x10^{-7}	0.69%
MGDG 28:0	1.5727 x10^{-7}	0.60%
DGDG 30:1	1.4767 x10^{-7}	0.56%
SQDG 28:1	1.1386 x10^{-7}	0.43%
MGDG 32:1	1.0735 x10^{-7}	0.41%
SQDG 31:0	6.6247 x10^{-8}	0.25%
PG 36:2	6.2968 x10^{-8}	0.24%
SQDG 31:1	6.1521 x10^{-8}	0.23%
MGDG 30:3	3.8839 x10^{-8}	0.15%
SQDG 29:0	3.7740 x10^{-8}	0.14%
Pheophytin a2	3.7254 x10^{-8}	0.14%
MGDG 32:2	3.6223 x10^{-8}	0.14%
MGDG 28:2	3.1666 x10^{-8}	0.12%

Table 2.2. The average abundance and relative contribution of the 25 most prevalent lipid compounds in the *Prochlorococcus* MED4 lipidome. Together, these 25 compounds account for over 99% of the total lipidome. All are contained within Cluster K.

References

1. Anderson T, Ducklow H. Microbial loop carbon cycling in ocean environments studied using a simple steady-state model. *Aquat Microb Ecol*. 2001;26: 37–49. doi:10.3354/ame026037
2. Ankrah NYD, May AL, Middleton JL, Jones DR, Hadden MK, Gooding JR, et al. Phage infection of an environmentally relevant marine bacterium alters host metabolism and lysate composition. *ISME J.* 2014;8: 1089–1100. doi:10.1038/ismej.2013.216
3. Armengol L, Calbet A, Franchy G, Rodríguez-Santos A, Hernández-León S. Planktonic food web structure and trophic transfer efficiency along a productivity gradient in the tropical and subtropical Atlantic Ocean. *Sci Rep.* 2019;9: 2044. doi:10.1038/s41598-019-38507-9
4. Baer SE, Lomas MW, Terpis KX, Mouginot C, Martiny AC. Stoichiometry of *Prochlorococcus*, *Synechococcus*, and small eukaryotic populations in the western North

Atlantic Ocean. *Environmental Microbiology.* 2017;19: 1568–1583. doi:10.1111/1462-2920.13672
5. Becker KW, Collins JR, Durham BP, Groussman RD, White AE, Fredricks HF, et al. Daily changes in phytoplankton lipidomes reveal mechanisms of energy storage in the open ocean. *Nat Commun.* 2018;9: 5179. doi:10.1038/s41467-018-07346-z
6. Bent, S.M., Muratore, D., Becker, K.W., Barone, B., Clemente, T., Fredricks, H.F., *et al.* (2024). Lipid biochemical diversity and dynamics reveal phytoplankton nutrient-stress responses and carbon export mechanisms in mesoscale eddies in the North Pacific Subtropical Gyre. *Front. Mar. Sci.*, **11**.
7. Benton HP, Want EJ, Ebbels TMD. Correction of mass calibration gaps in liquid chromatography-mass spectrometry metabolomics data. *Bioinformatics*. 2010;26: 2488–2489. doi:10.1093/bioinformatics/btq441
8. Bertilsson S, Berglund O, Karl DM, Chisholm SW. Elemental composition of marine *Prochlorococcus* and *Synechococcus*: Implications for the ecological stoichiometry of the sea. *Limnology and Oceanography*. 2003;48: 1721–1731. doi:10.4319/lo.2003.48.5.1721
9. Bligh EG, Dyer WJ. A rapid method of total lipid extraction and purification. *Can J Biochem Physiol*. 1959;37: 911–917. doi:10.1139/o59-099
10. Breton S, Jouhet J, Guyet U, Gros V, Pittera J, Demory D, et al. Unveiling membrane thermoregulation strategies in marine picocyanobacteria. *New Phytologist*. 2019;225: 2396–2410. doi:10.1111/nph.16239
11. Chambers MC, Maclean B, Burke R, Amodei D, Ruderman DL, Neumann S, et al. A cross-platform toolkit for mass spectrometry and proteomics. Nat Biotechnol. 2012;30: 918–920. doi:10.1038/nbt.2377
12. Charrad M, Ghazzali N, Boiteau V, Niknafs A. NbClust: An R Package for Determining the Relevant Number of Clusters in a Data Set. *Journal of Statistical Software*. 2014;61: 1–36. doi:10.18637/jss.v061.i06
13. Chen Y, Zeng Q. Temporal transcriptional patterns of cyanophage genes suggest synchronized infection of cyanobacteria in the oceans. *Microbiome*. 2020;8: 68. doi:10.1186/s40168-020-00842-9
14. Collins JR, Edwards BR, Fredricks HF, Van Mooy BAS. LOBSTAHS: An Adduct-Based Lipidomics Strategy for Discovery and Identification of Oxidative Stress Biomarkers. *Anal Chem.* 2016;88: 7154–7162. doi:10.1021/acs.analchem.6b01260
15. Cronan JE, Wulff DL. A role for phospholipid hydrolysis in the lysis of *Escherichia coli* infected with bacteriophage T4. *Virology*. 1969;38: 241–246. doi:10.1016/0042-6822(69)90365-1
16. Dammeyer T, Bagby SC, Sullivan MB, Chisholm SW, Frankenberg-Dinkel N. Efficient phage-mediated pigment biosynthesis in oceanic cyanobacteria. *Curr Biol*. 2008;18: 442–448. doi:10.1016/j.cub.2008.02.067
17. Evans C, Brandsma J, Meredith MP, Thomas DN, Venables HJ, Pond DW, et al. Shift from Carbon Flow through the Microbial Loop to the Viral Shunt in Coastal Antarctic Waters during Austral Summer. *Microorganisms*. 2021;9: 460. doi:10.3390/microorganisms9020460

18. Flombaum P, Gallegos JL, Gordillo RA, Rincón J, Zabala LL, Jiao N, et al. Present and future global distributions of the marine Cyanobacteria *Prochlorococcus* and *Synechococcus*. PNAS. 2013;110: 9824–9829. doi:10.1073/pnas.1307701110
19. Fulton JM, Kendrick BJ, DiTullio GR, Van Mooy BAS. Alkenone unsaturation during virus infection of *Emiliania huxleyi*. *Organic Geochemistry*. 2017;111: 82–85. doi:10.1016/j.orggeochem.2017.06.001
20. Goldsmith DB, Crosti G, Dwivedi B, McDaniel LD, Varsani A, Suttle CA, et al. Development of phoH as a Novel Signature Gene for Assessing Marine Phage Diversity. *Applied and Environmental Microbiology*. 2011;77: 7730–7739. doi:10.1128/AEM.05531-11
21. Goodloe RS, Light RJ. Structure and composition of hydrocarbons and fatty acids from a marine blue-green alga, *Synechococcus sp. Biochimica et Biophysica Acta* (BBA) - Lipids and Lipid Metabolism. 1982;710: 485–492. doi:10.1016/0005-2760(82)90133-3
22. Hsieh Y-J, Wanner BL. Global regulation by the seven-component Pi signaling system. *Curr Opin Microbiol*. 2010;13: 198–203. doi:10.1016/j.mib.2010.01.014
23. Hunter JE, Frada MJ, Fredricks HF, Vardi A, Van Mooy BAS. Targeted and untargeted lipidomics of *Emiliania huxleyi* viral infection and life cycle phases highlights molecular biomarkers of infection, susceptibility, and ploidy. *Front Mar Sci*. 2015;0. doi:10.3389/fmars.2015.00081
24. Juarez A, Villa JA, Lanza VF, Lázaro B, de la Cruz F, Alvarez HM, et al. Nutrient starvation leading to triglyceride accumulation activates the Entner Doudoroff pathway in *Rhodococcus jostii* RHA1. *Microbial Cell Factories*. 2017;16: 35. doi:10.1186/s12934-017-0651-7
25. Kolde R. Pheatmap: Pretty Heatmaps. 2018.
26. Kuhl C, Tautenhahn R, Böttcher C, Larson TR, Neumann S. CAMERA: an integrated strategy for compound spectra extraction and annotation of liquid chromatography/mass spectrometry data sets. Anal Chem. 2012;84: 283–289. doi:10.1021/ac202450g
27. Lev S, Rupasinghe T, Desmarini D, Kaufman-Francis K, Sorrell TC, Roessner U, et al. The PHO signaling pathway directs lipid remodeling in Cryptococcus neoformans via DGTS synthase to recycle phosphate during phosphate deficiency. PLOS ONE. 2019;14: e0212651. doi:10.1371/journal.pone.0212651
28. Lindell D, Jaffe JD, Coleman ML, Futschik ME, Axmann IM, Rector T, et al. Genome-wide expression dynamics of a marine virus and host reveal features of co-evolution. Nature. 2007;449: 83–86. doi:10.1038/nature06130
29. Lindell, D., Carlson, M.C.G., Weissenbach, J., Kirzner, S., Sulcius, S., Hulata, Y., *et al.* (n.d.). Virus-grazer interplay results in enhanced virus production and particle aggregation during infection of *Prochlorococcus*. In prep.
30. Malitsky S, Ziv C, Rosenwasser S, Zheng S, Schatz D, Porat Z, et al. Viral infection of the marine alga Emiliania huxleyi triggers lipidome remodeling and induces the production of highly saturated triacylglycerol. New Phytol. 2016;210: 88–96. doi:10.1111/nph.13852
31. Mann NH. Phages of the marine cyanobacterial picophytoplankton. FEMS Microbiology Reviews. 2003;27: 17–34. doi:10.1016/S0168-6445(03)00016-0

32. Monier A, Welsh RM, Gentemann C, Weinstock G, Sodergren E, Armbrust EV, et al. Phosphate transporters in marine phytoplankton and their viruses: cross-domain commonalities in viral-host gene exchanges. Environ Microbiol. 2012;14: 162–176. doi:10.1111/j.1462-2920.2011.02576.x
33. Mruwat N, Carlson MCG, Goldin S, Ribalet F, Kirzner S, Hulata Y, et al. A single-cell polony method reveals low levels of infected Prochlorococcus in oligotrophic waters despite high cyanophage abundances. ISME J. 2021;15: 41–54. doi:10.1038/s41396-020-00752-6
34. Nagata T. Production Mechanisms of Dissolved Organic Matter. 1st ed. Microbial Ecology of the Oceans. 1st ed. John Wiley & Sons; 2020.
35. Oksanen J, Blanchet FG, Friendly M, Kindt R, Legendre P, McGlinn D, et al. vegan: Community Ecology Package. 2020. Available: https://CRAN.R-project.org/package=vegan
36. Partensky F, Hess WR, Vaulot D. Prochlorococcus, a Marine Photosynthetic Prokaryote of Global Significance. Microbiol Mol Biol Rev. 1999;63: 106–127.
37. Popendorf KJ, Fredricks HF, Van Mooy BAS. Molecular ion-independent quantification of polar glycerolipid classes in marine plankton using triple quadrupole MS. Lipids. 2013;48: 185–195. doi:10.1007/s11745-012-3748-0
38. Popendorf KJ, Lomas MW, Van Mooy BAS. Microbial sources of intact polar diacylglycerolipids in the Western North Atlantic Ocean. Organic Geochemistry. 2011;42: 803–811. doi:10.1016/j.orggeochem.2011.05.003
39. R Core Team. R: A Language and Environment for Statistical Computing. Vienne, Austria; 2020.
40. R Studio Team. RStudio: Integrated Development for R. Boston, MA: PBC; 2020. Available: http://www.rstudio.com/
41. Roitman S, Hornung E, Flores-Uribe J, Sharon I, Feussner I, Béjà O. Cyanophage-encoded lipid desaturases: oceanic distribution, diversity and function. ISME J. 2018;12: 343–355. doi:10.1038/ismej.2017.159
42. Rosenwasser S, Mausz MA, Schatz D, Sheyn U, Malitsky S, Aharoni A, et al. Rewiring Host Lipid Metabolism by Large Viruses Determines the Fate of Emiliania huxleyi, a Bloom-Forming Alga in the Ocean. The Plant Cell. 2014;26: 2689–2707. doi:10.1105/tpc.114.125641
43. Rosenwasser S, Ziv C, Creveld SG van, Vardi A. Virocell Metabolism: Metabolic Innovations During Host–Virus Interactions in the Ocean. Trends in Microbiology. 2016;24: 821–832. doi:10.1016/j.tim.2016.06.006
44. Roth-Rosenberg D, Aharonovich D, Omta AW, Follows MJ, Sher D. Dynamic macromolecular composition and high exudation rates in Prochlorococcus. Limnology and Oceanography. 2021;66: 1759–1773. doi:10.1002/lno.11720
45. Sakai R, Winand R, Verbeiren T, Moere AV, Aerts J. Dendsort: modular leaf ordering methods for dendrogram representations in R. F1000Res. 2014;3: 177. doi:10.12688/f1000research.4784.1
46. Santos-Beneit F. The Pho regulon: a huge regulatory network in bacteria. Front Microbiol. 2015;0. doi:10.3389/fmicb.2015.00402

47. Schieler, B.M., Soni, M.V., Brown, C.M., Coolen, M.J.L., Fredricks, H., Van Mooy, B.A.S., et al. (2019). Nitric oxide production and antioxidant function during viral infection of the coccolithophore Emiliania huxleyi. ISME J, 13, 1019–1031.
48. Sieradzki ET, Ignacio-Espinoza JC, Needham DM, Fichot EB, Fuhrman JA. Dynamic marine viral infections and major contribution to photosynthetic processes shown by spatiotemporal picoplankton metatranscriptomes. Nat Commun. 2019;10: 1169. doi:10.1038/s41467-019-09106-z
49. Smith CA, Want EJ, O'Maille G, Abagyan R, Siuzdak G. XCMS: processing mass spectrometry data for metabolite profiling using nonlinear peak alignment, matching, and identification. Anal Chem. 2006;78: 779–787. doi:10.1021/ac051437y
50. Sullivan MB, Coleman ML, Weigele P, Rohwer F, Chisholm SW. Three Prochlorococcus Cyanophage Genomes: Signature Features and Ecological Interpretations. PLOS Biology. 2005;3: e144. doi:10.1371/journal.pbio.0030144
51. Sullivan MB, Huang KH, Ignacio-Espinoza JC, Berlin AM, Kelly L, Weigele PR, et al. Genomic analysis of oceanic cyanobacterial myoviruses compared with T4-like myoviruses from diverse hosts and environments. Environmental Microbiology. 2010;12: 3035–3056. doi:10.1111/j.1462-2920.2010.02280.x
52. Sullivan MB, Weitz JS, Wilhelm S. Viral ecology comes of age. Environmental Microbiology Reports. 2017;9: 33–35. doi:10.1111/1758-2229.12504
53. Tajparast M, Frigon D. Predicting the accumulation of storage compounds by Rhodococcus jostii RHA1 in the feast-famine growth cycles using genome-scale flux balance analysis. PLOS ONE. 2018;13: e0191835. doi:10.1371/journal.pone.0191835
54. Tautenhahn R, Böttcher C, Neumann S. Highly sensitive feature detection for high resolution LC/MS. BMC Bioinformatics. 2008;9: 504. doi:10.1186/1471-2105-9-504
55. Thompson LR, Zeng Q, Chisholm SW. Gene Expression Patterns during Light and Dark Infection of Prochlorococcus by Cyanophage. PLOS ONE. 2016;11: e0165375. doi:10.1371/journal.pone.0165375
56. Van Mooy BAS, Moutin T, Duhamel S, Rimmelin P, Van Wambeke F. Phospholipid synthesis rates in the eastern subtropical South Pacific Ocean. Biogeosciences. 2008;5: 133–139. doi:10.5194/bg-5-133-2008
57. Van Mooy BAS, Rocap G, Fredricks HF, Evans CT, Devol AH. Sulfolipids Dramatically Decrease Phosphorus Demand by Picocyanobacteria in Oligotrophic Marine Environments. Proceedings of the National Academy of Sciences of the United States of America. 2006;103: 8607–8612.
58. Vardi A, Van Mooy BAS, Fredricks HF, Popendorf KJ, Ossolinski JE, Haramaty L, et al. Viral glycosphingolipids induce lytic infection and cell death in marine phytoplankton. Science. 2009;326: 861–865. doi:10.1126/science.1177322
59. Warwick-Dugdale J, Buchholz HH, Allen MJ, Temperton B. Host-hijacking and planktonic piracy: how phages command the microbial high seas. Virology Journal. 2019;16: 15. doi:10.1186/s12985-019-1120-1
60. Weitz JS, Stock CA, Wilhelm SW, Bourouiba L, Coleman ML, Buchan A, et al. A multitrophic model to quantify the effects of marine viruses on microbial food webs and ecosystem processes. ISME J. 2015;9: 1352–1364. doi:10.1038/ismej.2014.220

61. Wickham H, Averick M, Bryan J, Chang W, McGowan LD, François R, et al. Welcome to the Tidyverse. Journal of Open Source Software. 2019;4: 1686. doi:10.21105/joss.01686
62. Wilhelm SW, Suttle CA. Viruses and Nutrient Cycles in the Sea: Viruses play critical roles in the structure and function of aquatic food webs. BioScience. 1999;49: 781–788. doi:10.2307/1313569
63. Włodarczyk A, Selão TT, Norling B, Nixon PJ. Newly discovered Synechococcus sp. PCC 11901 is a robust cyanobacterial strain for high biomass production. Commun Biol. 2020;3: 1–14. doi:10.1038/s42003-020-0910-8
64. Worden AZ, Nolan JK, Palenik B. Assessing the Dynamics and Ecology of Marine Picophytoplankton: The Importance of the Eukaryotic Component. Limnology and Oceanography. 2004;49: 168–179.
65. Worden A, Binder B. Application of dilution experiments for measuring growth and mortality rates among Prochlorococcus and Synechococcus populations in oligotrophic environments. Aquatic Microbial Ecology. 2003;30: 159–174. doi:10.3354/ame030159
66. Xiao X, Guo W, Li X, Wang C, Chen X, Lin X, et al. Viral Lysis Alters the Optical Properties and Biological Availability of Dissolved Organic Matter Derived from Prochlorococcus Picocyanobacteria. Applied and Environmental Microbiology. 2021;87: e02271-20. doi:10.1128/AEM.02271-20
67. Young R. Phage lysis: three steps, three choices, one outcome. J Microbiol. 2014;52: 243–258. doi:10.1007/s12275-014-4087-z
68. Yu ET, Zendejas FJ, Lane PD, Gaucher S, Simmons BA, Lane TW. Triacylglycerol accumulation and profiling in the model diatoms Thalassiosira pseudonana and Phaeodactylum tricornutum (Baccilariophyceae) during starvation. J Appl Phycol. 2009;21: 669. doi:10.1007/s10811-008-9400-y
69. Ziv C, Malitsky S, Othman A, Ben-Dor S, Wei Y, Zheng S, et al. Viral serine palmitoyltransferase induces metabolic switch in sphingolipid biosynthesis and is required for infection of a marine alga. PNAS. 2016;113: E1907–E1916. doi:10.1073/pnas.1523168113

CHAPTER 3: COMPETITION FOR PREY DRIVES A 'DOUBLING DOWN' ON PHAGOTROPHY IN THE MIXOTROPH *OCHROMONAS*

Coauthors: Matthew D. Johnson

Abstract

Mixotrophy (i.e. photophagotrophy) as a trophic strategy is thought to confer a competitive advantage when resources are limiting by obtaining nutrients and energy from multiple pools. To test this, we grew two strains of the marine mixotrophic nanoflagellete *Ochromonas* alone and in competition with a solely-phagotrophic competitor, *Paraphysomonas bandaiensis*, in light- and prey-limiting environments. Surprisingly, both strains of *Ochromonas* divested from phototrophy and increased their investment in phagotrophy while in competition. This "doubling down" when competing for a limited resource in competition contrasts with previous studies suggesting the optimal strategy for plastic mixotrophs in competition is to relieve resource limitation. While *P. bandaiensis* experienced no change in growth rate in competition with *Ochromonas* CCMP 1148, its growth rate decreased in competition with the comparatively more phagotrophic strain, *Ochromonas* CCMP 584, highlighting the differing impacts of competition between these closely related mixotrophs.

Introduction

Mixotrophy, defined here as the ability to derive energy from photosynthesis and phagotrophy, is a widespread metabolic strategy in marine microbial communities. In some areas of the ocean plastid containing organisms can account for the majority of bacterivory or grazing, highlighting the importance of mixotrophs in the marine food web (Safi et al. 1999, Hartmann et al. 2012). Studies demonstrate mixotrophic niche partitioning can help determine community structure (Katechakis & Stibor 2006, Crane and Grover 2010, Våge et al. 2013, Wilken et al. 2014), succession (Berge et al. 2016), diversity (Katechakis & Stibor 2006, Crane and Grover 2010, Ward and Follows 2016), community productivity (Hammer and Pitchford 2005, Ward and Follows 2016, Leles et al. 2018, Wieczynski, Moeller and Gibert 2023), energy transfer to higher trophic levels (Katechakis & Stibor 2006, Weithoff and Wacker 2007, Ward and Follows 2016, Honig et al. 2024), and resilience (Jost et al. 2004, Shade et al. 2012).

Mixotrophic metabolic strategies were, for a long period, not included in ecological and biogeochemical models of the ocean, as much of our basic understanding of ecological interactions are derived from terrestrial ecology that dichotomizes producers (plants) from

consumers (animals) (Flynn et al. 2013, Crop and Norbury 2015, Caron 2016, Ward 2019, Wilken et al. 2019). Given the prevalence of mixotrophs in the global oceans, and the large impact of mixotrophs on microbial communities, there is an urgent need to improve our understanding of the competitive ecology of mixotrophic organisms.

The ubiquity of mixotrophy in the world's oceans is often attributed to the flexibility of mixotrophic metabolism and the ability to obtain carbon and limiting nutrients from multiple sources. Mixotrophs can be highly plastic in their elemental stoichiometries and metabolic investments, leveraging their dual energy acquisition pathways to survive in a variety of nutrient regimes under competition (Smalley, Coats, and Stoecker 2003, Villanova et al. 2017, Curien et al. 2021, Chu, Moeller, and Archibald 2023). When competition for one pool of resources increases, a competitive benefit for mixotrophs arises if the mixotroph can shift its investment to alleviate this limitation. Indeed, many studies have shown mixotrophs are highly competitive with single-guild (i.e. solely phototrophy or phagotrophic) species under varied nutrient or light-limited environments (Tittle et al. 2003, Ghyoot et al. 2017, Edwards 2019, Moeller, Neubert and Johnson 2019). However, predicting mixotrophic response to competitive pressures is complicated by the absence of a direct trade-off between phagotrophy and phototrophy in many species; that is, mixotrophs often do not decrease their investment in one trophic mode in a way that is commensurate to an increase in the other trophic mode (Moeller, Neubert and Johnson 2019, Barbaglia et al. 2024, Mitra et al. 2024).

While many studies have explored environmental limitations such as prey, nitrogen, or light limitation as a proxy for competitive pressures, we attempt to more directly qualify the competitive benefits and costs of mixotrophy in *Ochromonas*, a mixotrophic chrysophyte, with a closely related single-guild phagotrophic competitor, *Paraphysomonas bandaiensis*. Species of *Ochromonas* can be found in a wide range of aquatic environments and can have a significant impact on the productivity and bacterivory in some communities (Posch et al. 1999, Boenigk et al. 2005, Katechakis and Stibor 2006, Schmidtke, Bell, and Weithoff 2006, Wilken at al. 2018). Though all are thought to be mixotrophic, species of *Ochromonas* differ greatly in their plasticity and relative metabolic investments (Holen 2010, Lie et al. 2018, Barbaglia et al. 2024). For example, some species of *Ochromonas* are obligately phagotrophic and rely on phototrophy only when prey is limiting (Terrado et al. 2017), while other species cannot survive without light and rely primarily on photosynthesis for carbon acquisition under normal conditions (Wilken, Choi, and Worden 2020).

Our experiment uses two relatively similar marine strains of *Ochromonas* isolated from the North Atlantic oligotrophic gyre, CCMP 584 and CCMP 1148, to compare different mixotrophic strategies in competition. Despite their close evolutionary and ecological relationship, *Ochromonas* CCMP 584 and 1148 have contrasting metabolic strategies, carbon use efficiencies, and plasticity (Barbaglia et al. 2024). *P. bandaiensis* was chosen as a single-guild, phagotrophic competitor for *Ochromonas* because it is a colorless chrysophyte of a similar size and is closely related to *Ochromonas* (Scoble and Cavalier-Smith 2014, Dorrell et al. 2019, Terpis et al. 2025).

In this study, we demonstrate the resilience of mutual coexistence between a mixotroph and single-guild phagotroph in limiting environments. Our results also suggest *Ochromonas* may

benefit from an increased investment in phagotrophy when prey is limited by competition (i.e. 'doubling-down' on phagotrophy) rather than increasing its investment in phototrophy.

Methodology

i. Culture maintenance

Ochromonas sp. CCMP 584 (*Ochromonas* 584) and *Ochromonas* sp. CCMP 1148 (*Ochromonas* 1148) were obtained from the Bigelow National Center for Marine Algae (NCMA). *Paraphysomonas bandaiensis* cultures were provided by the lab of David Caron at the University of Southern California. All cultures were maintained in a synthetic ocean water (SOW) media made of "Aquil salts" as described by Anderson (2004) adjusted to 32 practical salinity units (PSU) via refractometer. This media was appended with the addition of K/10 (from a "K media kit" sold by NMCA), a sterile grain of rice, and 5 µL of liquid broth (LB) per mL of media (Keller et al. 1987). Cultures were maintained at ~70 µmol photons m^{-2} sec^{-1} and 23°C. Cultures were grown this way for at least eight transfers in this media prior to the start of the experiment.

ii. Experimental design

Sterile 75 mL flasks containing 30 mL of SOW with K/10 were inoculated to an initial concentration of ~10^3 cells/mL of each competitor. "High light" treatments were cultured at 70 µmol photons m^{-2} sec^{-1}. "Low light" treatments were cultured at 12 µmol photons m^{-2} sec^{-1}. To control prey growth, maintain growth of the competitors through the duration of the experiment, and approximate the steady state of marine environments, "high prey" treatments were given 30 µL of LB daily and "low prey" treatments were given 0.5 µL of LB daily. Cultures of each strain were either grown alone, or in one of the following competitive environments: *Ochromonas* 584 + *P. bandaiensis* or *Ochromonas* 1148 + *P. bandaiensis* (Figure 3.1). Each experiment was run for 12 days.

iii. Flow cytometry and fluorescence

Cell abundance was measured via flow cytometry on a Guava easyCyte HT. *Ochromonas* was identified from other particulate matter using chlorophyll red fluorescence. Because *P. banaiensis* lacks pigments, to identify *P. banaiensis* from other particulate matter, cultures with *P. banaiensis* were stained with SYBR Green I Nucleic Acid Gel Stain (ThermoFisher Scientific) and *P. banaiensis* was identified via green fluorescence from the SYBR stain. The final concentration of SYBR Green was 0.5x and cells were incubated at room temperature in the dark for at least 15 minutes prior to flow cytometry. Growth rates were calculated by the slope of a least-squares regression of log cell abundance versus days since inoculation while the culture was in exponential phase.

Separate aliquots of cultures were stained with the acidic vacuole stain Lysotracker Green DND-26 (ThermoFisher Scientific) at a concentration of 100 nM immediately prior to flow cytometry. From previous experiments, we find that Lysotracker fluorescence can be used as proxy for cellular acidic food vacuole content in these organisms. Although many studies have demonstrated the utility of Lysotracker for studying mixotrophic, we also recognize the literature suggesting relying on Lysotracker (Rose et al. 2004, Anderson, Jürgens, and, Hansen 2017,

Costa et al. 2022, Millette et al. 2023, Florenza, Divne, and Bertilsson 2024). For example, Costa et al. (2022) found the percent of cells stained with Lysotracker in *Ochromonas tuberculate* did not correlate with ingestion rate. However, Sintes and Del Georgio (2010) showed heterotrophic activity has a relationship with per cell LysoTrakcer fluorescence. Additionally, some studies have cautioned that an acidic thylakoid membrane in mixotrophs may produce false positives using Lysotracker (Wilken et al. 2019, Millette et al. 2023), but we do not find evidence for this in our organisms based on microscopy (Figure 3.2). Further, while we used a low prey treatment, we did not starve our competitors, therefore it is unlikely that LysoTracker fluorescence could be attributed to stress-induced autophagy.

Cell abundances, chlorophyll fluorescence, and acidic vacuole content, approximated by Lysotracker Green fluorescence (LGF), were measured every day for the first six days and every 1-2 days thereafter.

Chlorophyll fluorescence and acidic vacuole content (LGF) are presented in Figure 3.7 as relative changes from an initial baseline (first two days) versus corresponding fluorescence in log phase (first two days after the onset of exponential phase). We used this normalization approach because of the high variance in initial cell red fluorescence and green fluorescence between and within cultures due to changing cell size and the low number of particles counted during lag phase in *Ochromonas*, as well as to better contextualize the arbitrary units of fluorescence measured by flow cytometry.

iv. Analytical methods

Data analysis was conducted in RStudio (version 2023.12.0) using R (version 4.3.2), or in Microsoft Excel for Microsoft 365 (Version 2502). Analysis in R utilized the packages dplyr (Wickham et al. 2025), lubridate (Grolemond and Wickham 2011), readr (Wickham, Hester and Bryan 2024), and reshape2 (Wickham 2020) for data handling, as well as ggpattern (FC, Davis, and Wickham 2025) and ggplot2 (Wickham 2016) for figure production. Except where stated, all error bars and confidence intervals represent standard error (SE), and statistical significance was determined using an alpha of 0.05.

Results

i. Solo experiments

Grown alone, *P. bandaiensis* had the highest maximum growth rates of the three strains studied, reaching an average growth rate of 2.21 ± 0.45 day^{-1} in high prey conditions (Figure 3.3C). In high light and high prey conditions, both strains of *Ochromonas* experienced their highest growth rates (Figure 3.3). Under these ideal conditions, *Ochromonas* CCMP 584 had an average growth rate of 0.82 ± 0.02 day^{-1} and *Ochromonas* CCMP 1148 had an average growth rate of 0.67 ± 0.006 day^{-1} (Figure 3.3).

When grown alone, both strains of *Ochromonas* had a significantly lower growth rate in low light conditions compared to high light conditions (Figure 3.3). The growth rates of both strains of *Ochromonas* were unaffected by the amount of prey in the media (Figure 3.3). The growth rates of *P. bandaiensis* were significantly lower in low prey conditions and its growth was

unaffected by light level (Figure 3.3C).

The chlorophyll fluorescence per cell during exponential phase of both strains of *Ochromonas* was generally higher in low light treatments than high light treatments, with one exception (Figure 3.4C). The chlorophyll fluorescence of *Ochromonas* 584 was unaffected by prey level, but *Ochromonas* 1148 had significantly higher chlorophyll fluorescence in high prey environments compared to low prey environments when grown in high light (Figure 3.4B).

The acidic vacuole content, as measured by LGF, during exponential phase of *Ochromonas* 1148 was higher in low light treatments compared to high light treatments at the same prey level (Figure 3.4). Under high light conditions, *Ochromonas* 1148 had higher LGF when prey was high, but there was no significant difference between prey levels in LGF when light was low (Figure 3.4). Acidic vacuole content (LGF) in *Ochromonas* 584 was not statistically different across treatments (Figure 3.4).

ii. Competition experiments

Across all environmental conditions, both strains of *Ochromonas* grew significantly slower in the presence of the phagotrophic single-guild competitor, *P. bandaiensis* (Figure 3.5). *Ochromonas* 584 grew particularly slow in competition with *P. bandaiensis* under low light and low prey conditions, achieving a growth rate of only 0.20 ± 0.002 day^{-1} (Figure 3.5A).

P. bandaiensis experienced a decline in growth rate in competition with *Ochromonas* 584 but did not grow significantly slower in competition with *Ochromonas* 1148 (Figure 3.5C). The decline in growth rate of *P. bandaiensis* due to competition with *Ochromonas* 584 was greater in low light treatments, a 25.9% ± 0.87% decline, compared to high light treatments, a 19.5 % ± 0.66% decline ($p = 0.041$).

In competition, across all environmental treatments, both *Ochromonas* 584 and 1148 significantly decreased their chlorophyll fluorescence and significantly increased their acidic vacuole content (LGF) when in competition with *P. bandaiensis* (Figure 3.6). Light significantly affected the extent to which phagotrophic investment (as measured by LGF) increased due to competition in *Ochromonas* 584, but not *Ochromonas* 1148 (Figure 3.6). For both strains, light significantly affected the extent to which phototrophic investment decreased in competition (Figure 3.6). *Ochromonas* 1148 increased its investment in phagotrophy more than 584 despite not affecting the growth of *P. bandaiensis* (0.25 ± 0.014 average log-fold increase across treatments versus 0.14 ± 0.016 log-fold increase, $p = 0.0006$).

When in competition with either strain of *Ochromonas*, the LGF of *P. bandaiensis* only differed significantly from values measured alone in high light and high prey environments (Figure 3.7).

Discussion

i. Environmental controls on growth and trophic mode

Though both strains of *Ochromonas* are obligate phagotrophs, *Ochromonas* 584 and 1148 growth rates were controlled by light level and no significant difference was detected between the high and low prey treatments in either light level when grown alone (Figure 3.3). This

suggests, when grown without a competitor, prey abundance was high enough to make light the only limiting factor on growth (Figure 3.3). As expected for a single-guild phagotroph, *P. bandaiensis* growth rates, when not in competition, were dependent only on prey availability and were unaffected by light level (Figure 3.3C). While light has been linked previously to grazing and growth rates of phagotrophic protists (Strom 2001), this has only been shown when engulfing chlorophyll-containing prey.

The observed generally lower chlorophyll fluorescence during exponential phase in high light conditions is consistent with photo-acclimation response of photosynthetic organisms decreasing their pigments when light is abundant to optimize photosynthetic efficiency and reduce photodamage (MacIntyre et al. 2002, Ruban 2015, Friedland et al. 2019, Carrieri et al. 2021). The one exception was higher chlorophyll levels in *Ochromonas* 1148 when both light and prey were abundant (Figure 3.4B). One possible explanation of higher chlorophyll levels in this treatment is the reinvestment of energy between phototrophy and phagotrophy in mixotrophs when prey is abundant. Previous studies have suggested mixotrophs can increase energy efficiency and growth by recycling carbon and other resources between trophic modes, including costs of maintaining photosystem health in high light (Tittle et al. 2003, Cabrerizo et al. 2018, Wilken, Choi, and Worden 2020, Stegemüller et al. 2024). The lack of a similar response in *Ochromonas* 584 may be explained by the findings of Barbaglia et al. (2024) showing *Ochromonas* 584, but not 1148, experiences tradeoffs between trophic pathways where investment in phototrophy leads to a decline in phagotrophy. The same study found *Ochromonas* 584, but not 1148, decreases its carbon use efficiency when prey is abundant, potentially decreasing the energy *Ochromonas* 584 is able to reinvest in phototrophy.

The acidic vacuole content of *Ochromonas* 1148 was determined primarily by light level, but the acidic vacuole content of *Ochromonas* 584 was constant across treatments (Figure 3.4). This is again supported by the findings of Barbaglia et al. (2024) showing *Ochromonas* 1148 generally decreases its attack and ingestion rates with increasing light, but *Ochromonas* 584 does not.

ii. Effects of competition on growth

Both strains of *Ochromonas* experienced decreased growth in competition with *P. bandaiensis* most likely due to the increased competition for prey (Figure 3.5). In this study, when not in competition, *Ochromonas* was not prey-limited. However, the introduction of the voracious single-guild phagotroph *P. bandaiensis* increased competition for prey, apparently forcing *Ochromonas* to occupy a suboptimal realized niche that resulted in decreased growth (Figure 3.5). *P. bandaiensis* has a higher maximum growth rate (Figure 3.5) and has been shown to have generally higher grazing rates than *Ochromonas*, likely explaining its ability to limit *Ochromonas*'s phagotrophic growth (Ochs and Eddy 1998, Selph et al. 2003, Barbaglia et al. 2024). This is reflected in the larger decrease in the growth rate of both strains from competition with *P. bandaiensis* in lower prey treatments (38.3% ± 2.40% decline in low prey treatments versus 17.7% ± 0.928% decline in growth rate in high prey treatments, $p < 0.0001$).

The decrease in growth rate due to competition was not statistically significantly different between *Ochromonas* 584 and 1148 ($p = 0.122$). It would be interesting to see if a facultatively phagotrophic strain of *Ochromonas*, such as *Ochromonas* 1391, would be differently affected by

the presence of the single-guild phagotrophic competitor than the two obligately phagotrophic strains tested here.

Growth of *P. bandaiensis* was inhibited by competition with *Ochromonas* 584, but not 1148 (Figure 3.5C). This was unexpected because of the close evolutionary and ecological relationship between these strains (Barbaglia et al. 2024). Additionally, both strains of *Ochromonas* increased their investment in phagotrophy and decreased their investment in phototrophy in competition with *P. bandaiensis*, presumably leading to increased competition for prey in competition with either strain (Figure 3.6).

The difference in competitive pressure on *P. bandaiensis* between *Ochromonas* 584 and 1148 may be explained by the slight differences in their metabolic preferences. While 1148 increased its food vacuole content to a greater extent under competition, Barbaglia et al. (2024) demonstrated *Ochromonas* 584 has higher attack rates than *Ochromonas* 1148 at light levels similar to this experiment. Additionally, the growth rate of *Ochromonas* 584 was greater than 1148 even in competition, except under severe prey and light limitation (Figure 3.5). We hypothesize the higher attack and growth rates of *Ochromonas* 584 (Barbaglia et al. 2024) likely resulted in greater competition for prey, leading to the observed decrease in *P. bandaiensis* growth rate (Figure 3.5).

iii. Trophic 'doubling down' in competition

Inter-guild competition induced a significant change in phototrophy and phagotrophy in both strains of *Ochromonas* (Figure 3.6). Previous modeling studies have theorized mixotrophs remain competitive in mixed communities through niche displacement towards a more phototrophic niche when competition for phagotrophic resources increases, and vice versa (Crane and Glover 2010, Chu, Moeller, and Archibald 2023). However, in this experiment both mixotrophs significantly *reduced* their investment in phototrophy and significantly *increased* their investment in phagotrophy in competition with the phagotroph *P. bandaiensis* (Figure 3.6).

This 'doubling down' on a more limiting trophic strategy in competition also contrasts with previous laboratory studies on *Ochromonas* and other mixotrophs showing mixotrophs generally shift their trophic balance when resources are limiting in a way that alleviates resource scarcity (Smalley et al. 2013, Cabrerizo et al. 2019, González-Olalla et al. 2021, Barbaglia et al. 2024). However, most of these studies observed mixotrophs in batch culture without competitors. While environmental treatments can act as proxies for the competitive mixed communities of the marine environment, perhaps this experiment demonstrates varying levels of prey in culture is not identical to increasing competition for prey (Figure 3.4, Figure 3.6). Additionally, most studies on mixotrophy are done without any regular addition of nutrients or prey. Batch cultures become more resource limited as experiments continue over days and may conflate increased scarcity with the effects of competition for resources.

As this doubling down result to our knowledge has not been reported previously in controlled culture experiments, we want to briefly consider alternative explanations. We cannot rule out that *Ochromonas* held onto vacuoles for longer periods of time. We assume the lysosome content of *Ochromonas* and *P. bandaiensis* is controlled to a greater extent by prey scarcity and ingestion

than digestion and degradation rates. However, if the presence of the competitor altered the prey digestion and lysosome removal rates of *Ochromonas*, this could explain the measured increase in acidic vacuole content in competition. One possible explanation for this could be reduced prey availability from competition driving regulatory changes for digestive processing and assimilation from prey. With the sparse literature on digestion rates in chrysophytes and even sparser literature on mixotrophic regulation of lysosomes in response to competition, we cannot make any firm conclusions on this theory. This explanation also does not explain the decrease in phototrophy.

While we believe the best current explanation for increased food vacuole content and decreased chlorophyll in *Ochromonas* due to competition in our experiment is a "doubling down" on a phagotrophic strategy, further work is needed to explore and confirm this phenomenon.

iv. Implications for mixotrophic competitive ecology

Our results underscore the growing literature suggesting the direct tradeoffs between mixotrophic investments in phagotrophy and phototrophy is less common than previously thought (Cabrerizo et al. 2019, Wilken, Choi, and Worden 2020, Barbaglia et al. 2024, Stegemüller et al. 2024). Here, we found environmental and competitive treatments where photosynthetic and phagotrophic investment both increased or both decreased in *Ochromonas* (Figure 3.6). Many past models have assumed fixed mixotrophic investments in phagotrophy and phototrophy, but our results suggest investments in trophic mode in mixotrophs is dynamic and highly responsive to competitive pressures.

The observed doubling down phenomenon complicates the common theory that mixotrophs modulate their dual energetic pathways to alleviate competition for resources. In a classical view of resource ratio theory, if both competitors "doubled down" on prey, one might expect the more efficient competitor to exclude the less efficient competitor. Yet, even with the increase in phagotrophic investment and coupled decrease in phototrophic investment, both strains of *Ochromonas* coexisted with *P. bandaiensis* (Figure 3.5, Figure 3.6). Thus, the decreased return on phagotrophic investment (and photosynthetic divestment) in competition must be outweighed by a competitive advantage from doubling down. Whether 'doubling down' is an indirect effect of competition, or a direct recognition of and response to the presence of a competitor is unclear.

Some previous studies have suggested mixotrophs may obtain eco-evolutionary benefits from increasing investment in phagotrophy even when phagotrophy may be the less efficient trophic strategy. A modeling study by Moeller et al. (2024) predicted mixotrophs will invest less in phagotrophy when prey is abundant and more when prey is limiting in nitrogen-scarce gyres. When they accounted for acquisition of the reinvestment of nitrogen acquisition from phagotrophy into phototrophy, they found that when inorganic nitrogen was limited, as in a pelagic environment, greater investment in phagotrophy could relieve this nitrogen-limitation and synergistically support photosynthesis (Moeller et al. 2024). Yet, nutrients were not a limiting factor in this experiment. And, unlike the MOCHA model predicted, we saw the greatest divestment from phototrophy and increased investment in phagotrophy from competition in high light environments (Moeller et al. 2024).

A form of doubling-down was also observed in a mesocosm experiment by Tittle et al. (2003) who suggested one possible advantage is the ability to exclude competitors entirely by grazing down prey. They concluded mixotrophs, even if less efficient grazers, can obtain dominance in a community by using energy from photosynthesis to increase phagotrophic investment and push bacteria concentrations below a critical level where single-guild phagotrophs cannot persist. However, while food vacuole content increased in competition in this experiment, *Ochromonas* also divested from photosynthesis in competition (Figure 3.6). Additionally, the growth rate of both strains of *Ochromonas* decreased due to competition and *P. bandaiensis* growth was affected very little or, in the case of *Ochromonas* 1148, not at all by the competition for prey (Figure 3.5). This suggests *P. bandaiensis* likely played a large role in controlling prey concentrations.

The need to double down on phagotrophy when competition for prey increases may be potentially better by minimum requirements for prey, or for prey quality, in *Ochromonas*. It is possible, as selective grazers, the co-culturing of *Ochromonas* and *P. bandaiensis* not only lead to a decrease in prey availability but increased competition for and predation of higher quality prey. As obligate phagotrophs, *Ochromonas* 584 and 1148 may increase their investment in phagotrophy to ensure they obtain a minimum nutritional quota when competition for prey is high. This necessarily greater investment in phagotrophy could limit the cell's ability to invest in phototrophy, leading to the decline in chlorophyll observed here (Figure 3.6). If this is true, it may warrant greater consideration of the lower bounds of phagotrophic investment when modeling mixotrophic organisms. A better understanding of the nutritional benefits of ingesting prey by mixotrophs from a metabolic perspective, rather than a simple mass balance of carbon, may also shed light on these dynamics.

The decline in mixotrophic growth rates due to competition also indicates there is also a clear trade-off to doubling down (Figure 3.5). The antagonistic dynamics between photosynthetic investment and phagotrophic investment observed in this study have been observed in modeling and culture studies on *Ochromonas* and other mixotrophs previously (Figure 3.6, Edwards, 2019, Barbaglia et al. 2024). Many hypotheses have emerged as to the trade-offs between investment in each trophic pathway including competition for cellular space (Flynn and Mitra 2009) and cell surface area (Ward et al. 2011), as well as the energetic cost associated with maintaining both energetic pathways (Raven 1997). This work suggests that there are some antagonistic effects between trophic pathways in some environments, at least in the two strains of *Ochromonas* tested here. Future studies, such as transcriptomic analysis on direct competition between *Ochromonas* and single guild competitors may shed more light on this question.

It is important to recognize, however, the precariousness of extrapolating studies on model mixotrophs across lineages. The differences between closely related *Ochromonas* strains 584 and 1148 only serve to highlight the warnings of previous studies that mixotrophic dynamics are not easily generalizable across the tree of life (Lie et al. 2018, Wilken, Choi, and Worden 2020, Barbaglia et al. 2024, Flöder et al. 2024). While this study does measure vacuole space in a sense through acidic vacuole staining, we cannot make conclusions about the underlying mechanisms of antagonism between trophic investments in competition.

Finally, this study emphasizes the need to design experiments that directly probe mixotrophic competitive ecology. Evidence of doubling down on phagotrophy in *Ochromonas* was observed only in competitive treatments (Figure 3.6). There was no similar evidence for increased phagotrophy from prey limitation when *Ochromonas* was cultured by itself (Figure 3.4). This suggests that some environmental treatments, such as limiting prey in cultures containing only a mixotroph, may be unreliable proxies for competitive pressures, like direct competition with a phagotroph for prey. We advocate more studies investigating mixotrophic ecology and evolution consider doing so through direct competition experiments.

Acknowledgements

I thank David Caron and Brittany Stewart for providing us with a culture of *Paraphysomonas banaiensis*. I want to thank Holly Moeller for her continued insight and support. Finally, I would like to thank the Woods Hole Oceanographic Institution staff and facilities workers as, without their support, this work would not have been possible.

This work was funded thanks to generous grants from the Woods Hole Oceanographic Institution Ocean Venture Fund. Max Jahns's gradate stipend was funded in part by an NSF Graduate Fellowship.

Figures

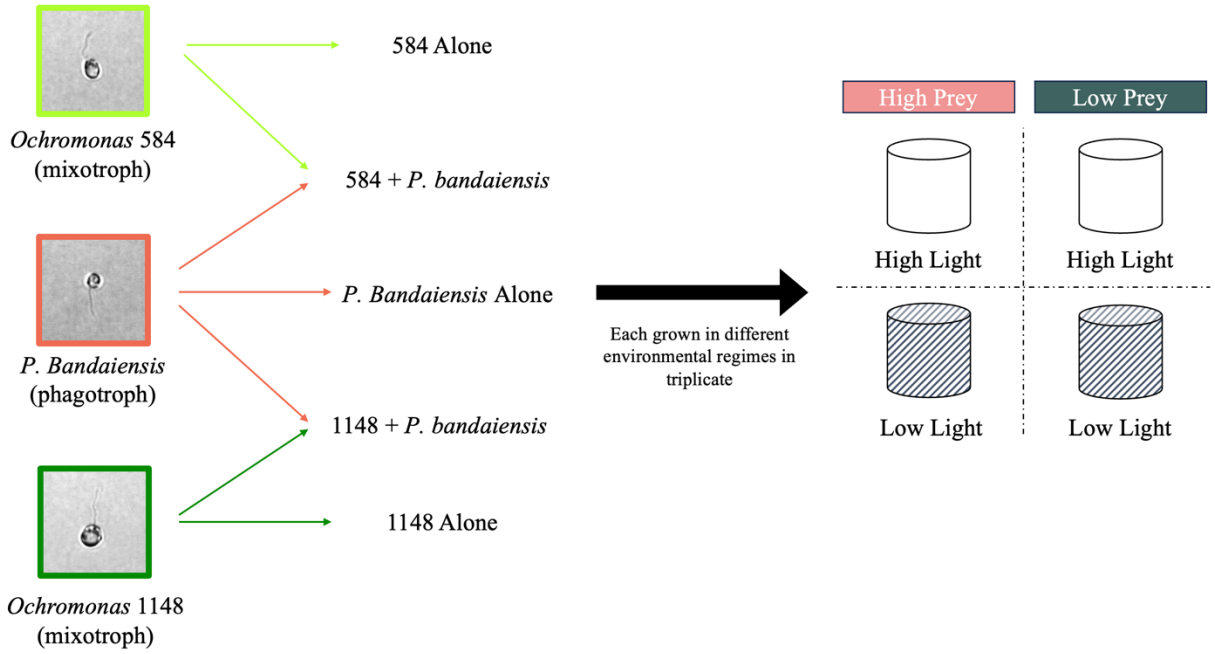

Figure 3.1. Conceptual graphic of the conditions and treatments in the experiment. Briefly, three chrysophytes (*Ochromonas* CCMP 584, *Ochromonas* 1148, and *P. bandaiensis*) were grown alone or a mixotroph was cultured with the addition of *P.* bandaiensis, for a total of five competitive treatments. Each competitive treatment was then cultured in four environmental treatments: either high light (70 µmol photons m^{-2} sec^{-1}) or low light (12 µmol photons m^{-2} sec^{-1}) and either high prey (30 µL in 30 mL of LB daily to control prey growth) or low prey (0.5 µL in 30 mL of LB daily). There were three biological replicates for of each combination of competitive and environmental treatments.

3.2A

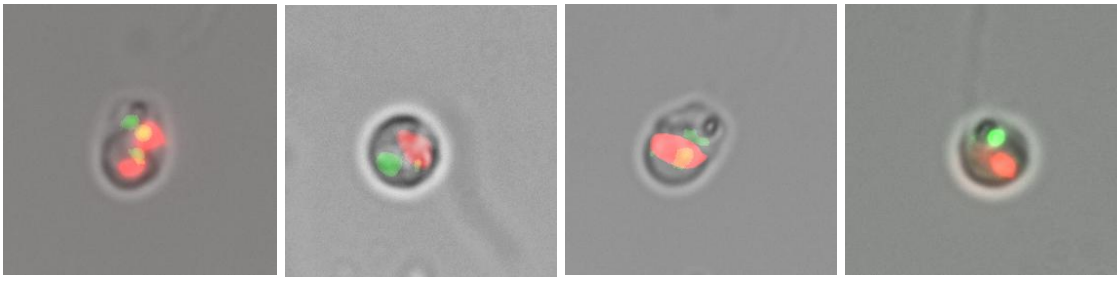

3.2B

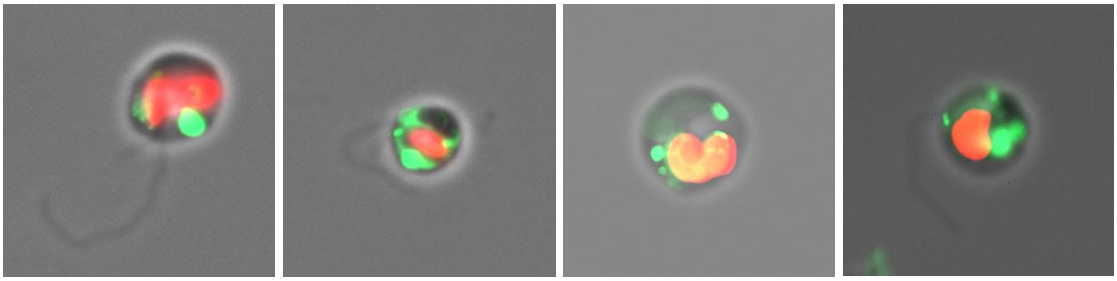

Figure 3.2. Compound microscopy images of (A) *Ochromonas* 584 and (B) *Ochromonas* 1148 false colored with chlorophyll autofluorescence (in red) and Lysotracker Green DND-26 fluorescence (in green). Cells were grown in SOW + K/50 with appended with 5 µL of LB per mL of media and a grain of sterile rice. Cells were imaged in late log phase.

3.3A

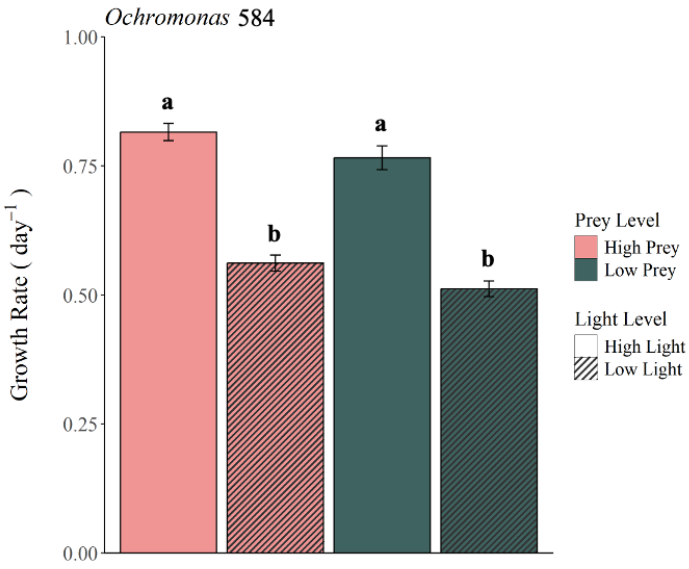

3.3B

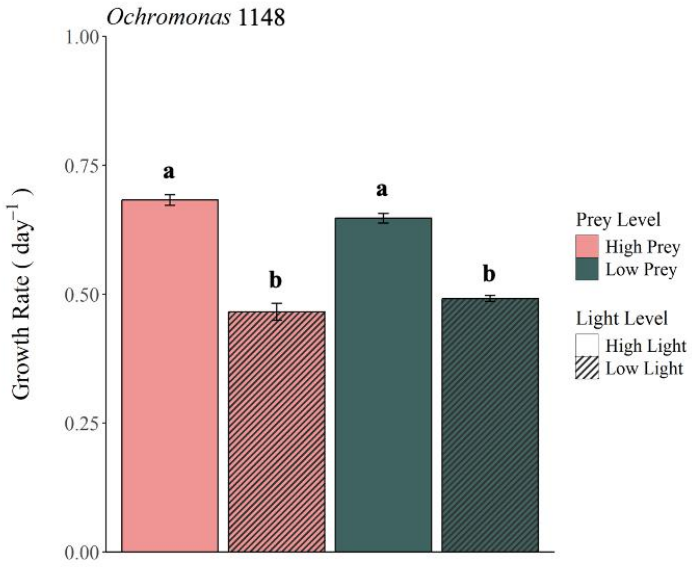

3.3C

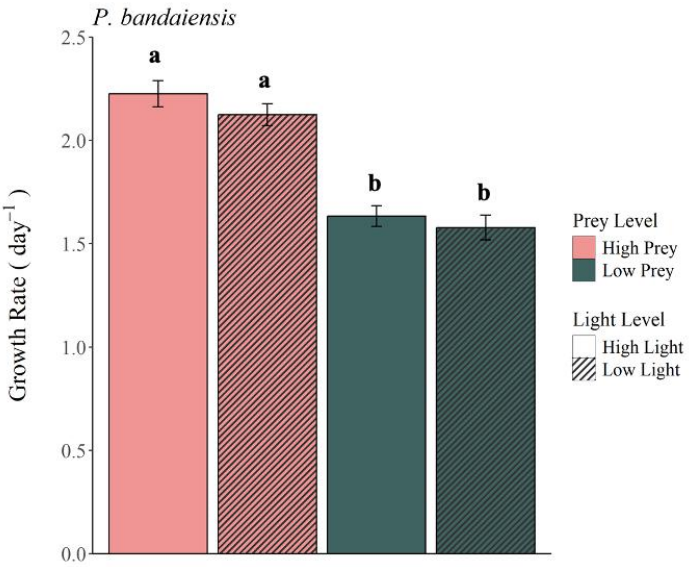

Figure 3.3. The growth rate (1/day) of (A) *Ochromonas* sp. CCMP 584, (B) *Ochromonas* sp. CCMP 1148, and (C) *Paraphysomonas bandaiensis*, when grown separately. Cells were cultured under various nutrient regimes including high prey (pink) and low prey conditions (teal) as well as high light (solid) and low light (shaded) conditions. Letters indicate significantly different groups according to Tukey's Honestly Significantly Different test (HSD test) ($p < 0.05$). Please note the difference in axis scale for *P. bandaiensis* (C).

3.4A

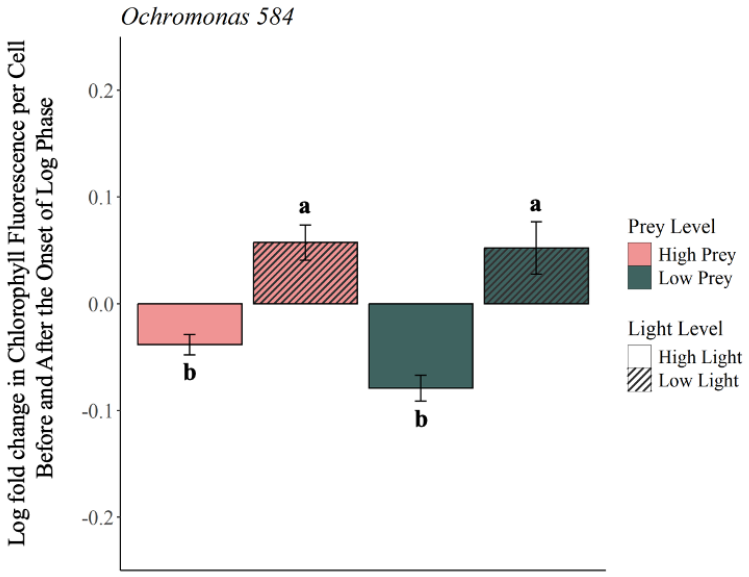
Ochromonas 584
Log fold change in Chlorophyll Fluorescence per Cell Before and After the Onset of Log Phase
0.2
0.1
0.0
-0.1
-0.2
a
a
b
b
Prey Level
High Prey
Low Prey
Light Level
High Light
Low Light

3.4B

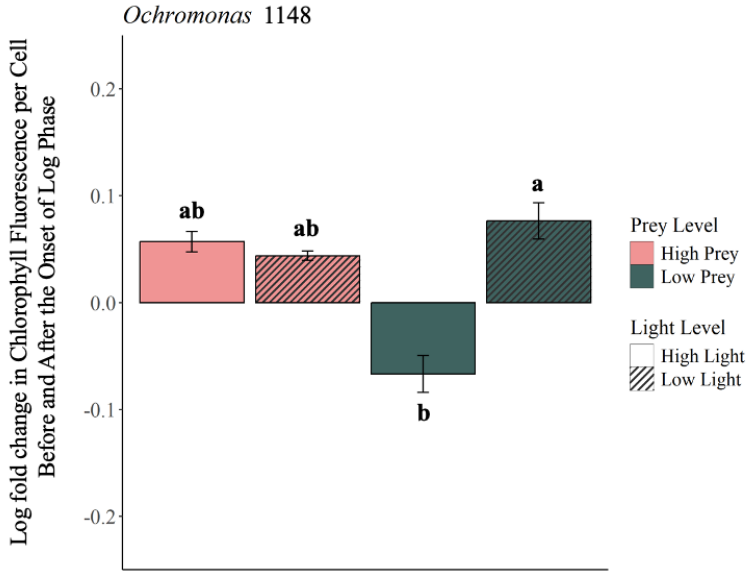
Ochromonas 1148
Log fold change in Chlorophyll Fluorescence per Cell Before and After the Onset of Log Phase
0.2
0.1
0.0
-0.1
-0.2
ab
ab
a
b
Prey Level
High Prey
Low Prey
Light Level
High Light
Low Light

3.4C

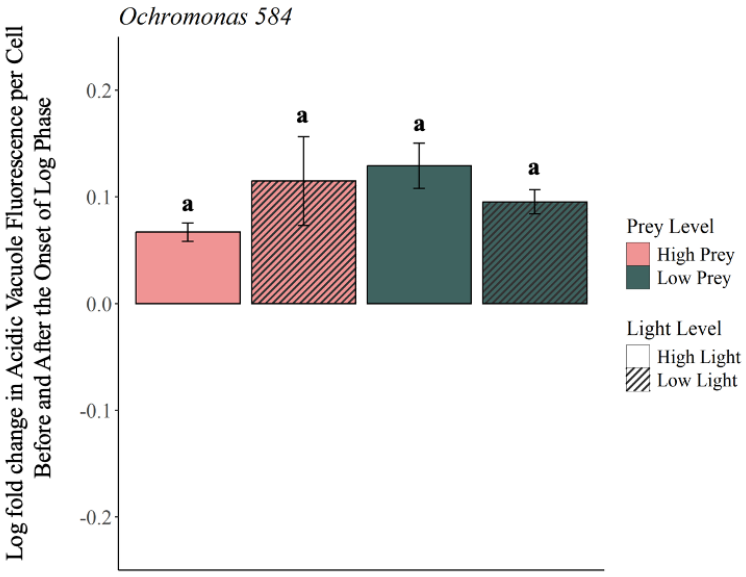
Ochromonas 584
Log fold change in Acidic Vacuole Fluorescence per Cell
Before and After the Onset of Log Phase
0.2
0.1
0.0
-0.1
-0.2
a
a
a
a
Prey Level
High Prey
Low Prey
Light Level
High Light
Low Light

3.4D

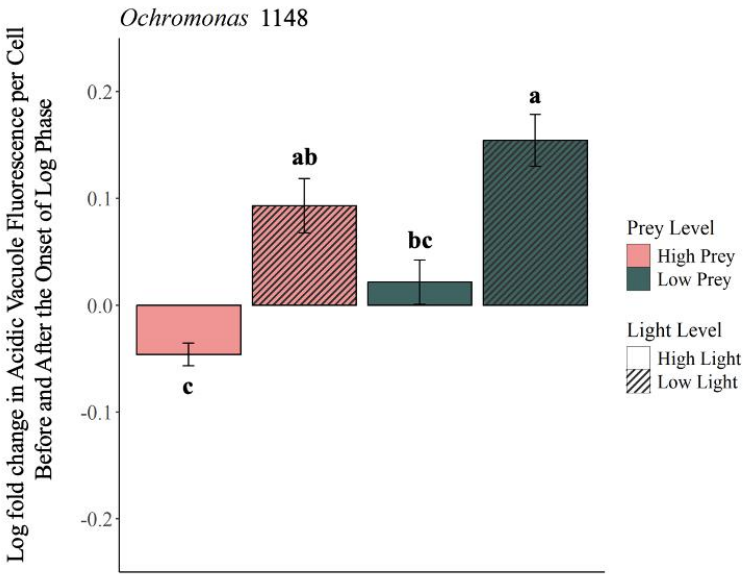

Figure 3.4. The log fold change in average chlorophyll fluorescence per cell (A, B) and acidic vacuole content (as measured by Lysotracker fluorescence) per cell (C, D) between the first two days of the experiment (baseline), and the two days after the onset of log phase in *Ochromonas* 584 (A, C) and *Ochromonas* 1148 (B, D). Cells were cultured under various nutrient regimes including high prey (pink) and low prey conditions (teal) as well as high light (solid bars) and low light (shaded) conditions. Log fold change from an initial baseline was used instead of fluorescence values because of the arbitrary units of raw fluorescence data. Letters indicate significantly different groups according to Tukey's Honestly Significantly Different test (HSD test) ($p < 0.05$).

3.5A

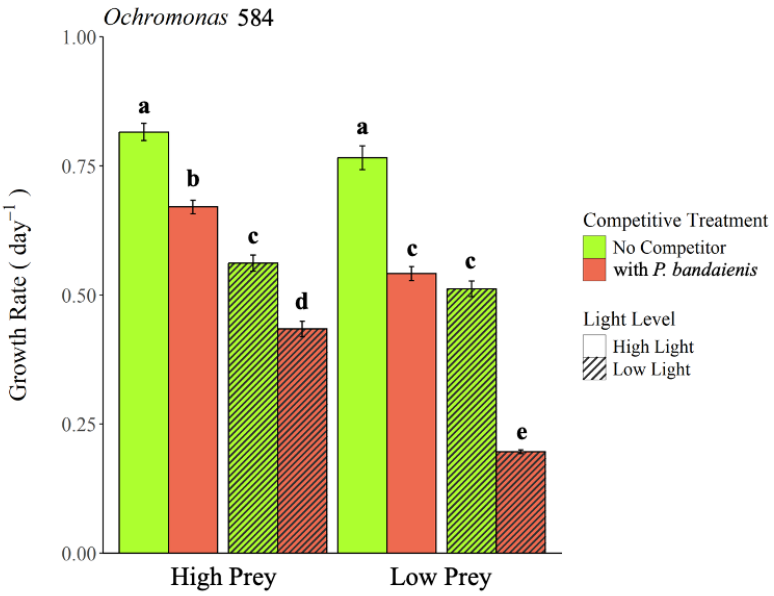
Ochromonas 584
Growth Rate (day^{-1})
1.00
0.75
0.50
0.25
0.00
a
b
c
d
a
c
c
e
High Prey
Low Prey
Competitive Treatment
No Competitor
with P. bandaienis
Light Level
High Light
Low Light

3.5B

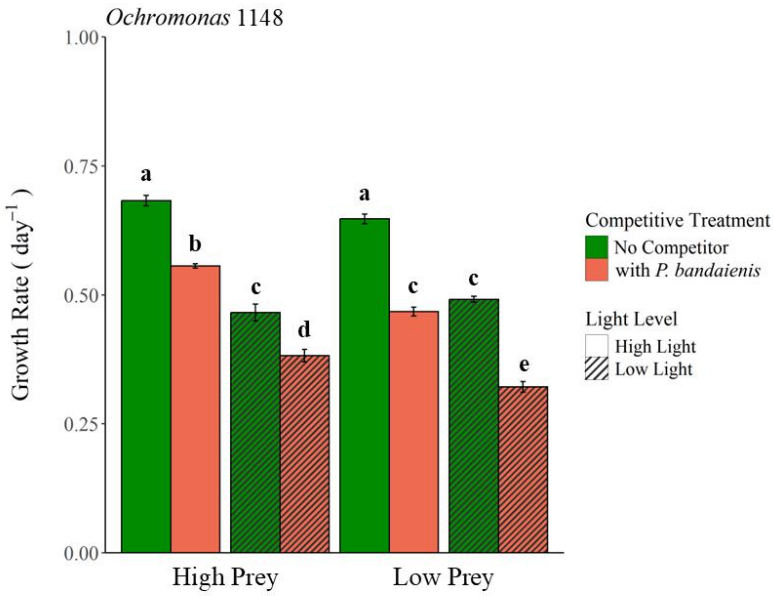
Ochromonas 1148
Growth Rate (day^{-1})
1.00
0.75
0.50
0.25
0.00
a
b
c
d
a
c
c
e
High Prey
Low Prey
Competitive Treatment
No Competitor
with P. bandaienis
Light Level
High Light
Low Light

3.5C

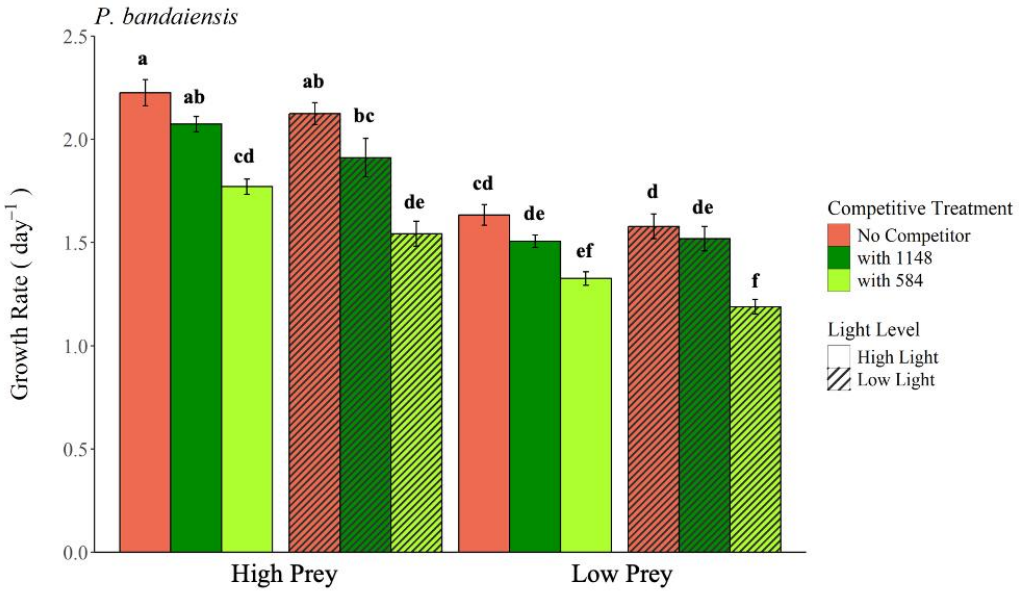

Figure 3.5. (A) The growth rate (1/day) of *Ochromonas* 584 when grown alone (light green) or in competition with *P. bandaiensis* (orange) under different environmental treatments. (B) The growth rate of *Ochromonas* 1148 when grown alone (dark green) or in competition with *P. bandaiensis* (orange) under different environmental treatments. (C) The growth rate of *P. bandaiensis* when grown alone (orange), in competition with *Ochromonas* 1148 (dark green), or in competition with *Ochromonas* 584 (light green) under different environmental treatments. Cells were grown with high or low prey and in high light (solid bars) or low light (shaded). Letters indicate significantly different groups according to Tukey's Honestly Significantly Different test (HSD test) ($p < 0.05$). Note the difference in axis scale for *P. bandaiensis* (C).

3.6A

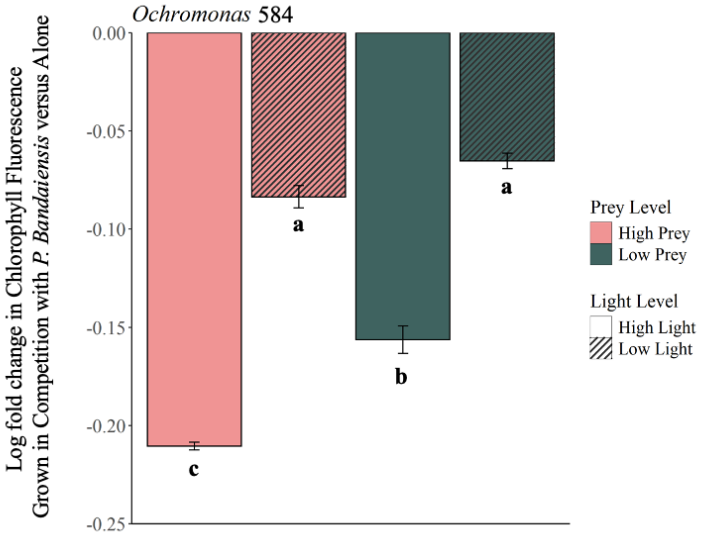
Ochromonas 584
Log fold change in Chlorophyll Fluorescence
Grown in Competition with P. Bandaiensis versus Alone
0.00
-0.05
-0.10
-0.15
-0.20
-0.25
a
a
b
c
Prey Level
High Prey
Low Prey
Light Level
High Light
Low Light

3.6B

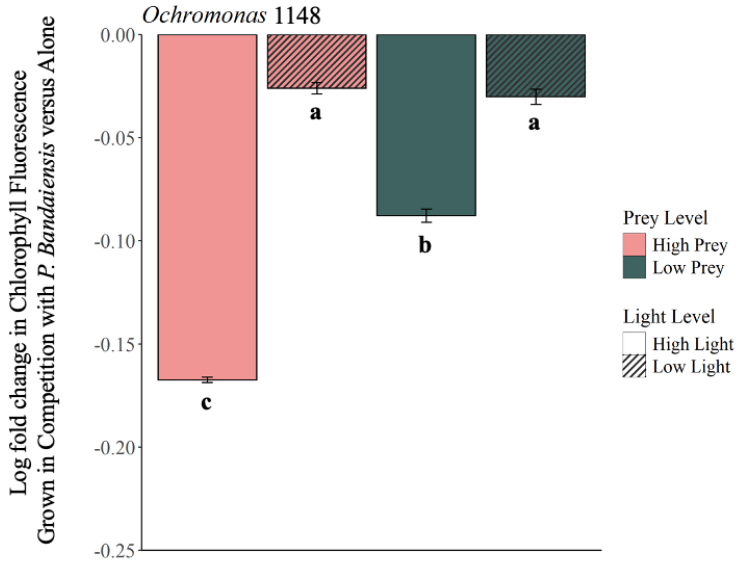
Ochromonas 1148
Log fold change in Chlorophyll Fluorescence
Grown in Competition with P. Bandaiensis versus Alone
0.00
-0.05
-0.10
-0.15
-0.20
-0.25
a
a
b
c
Prey Level
High Prey
Low Prey
Light Level
High Light
Low Light

3.6C

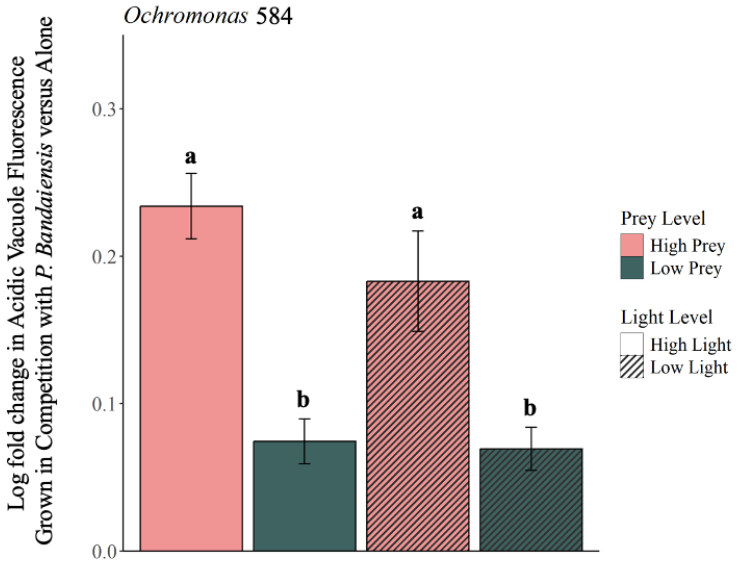

3.6D

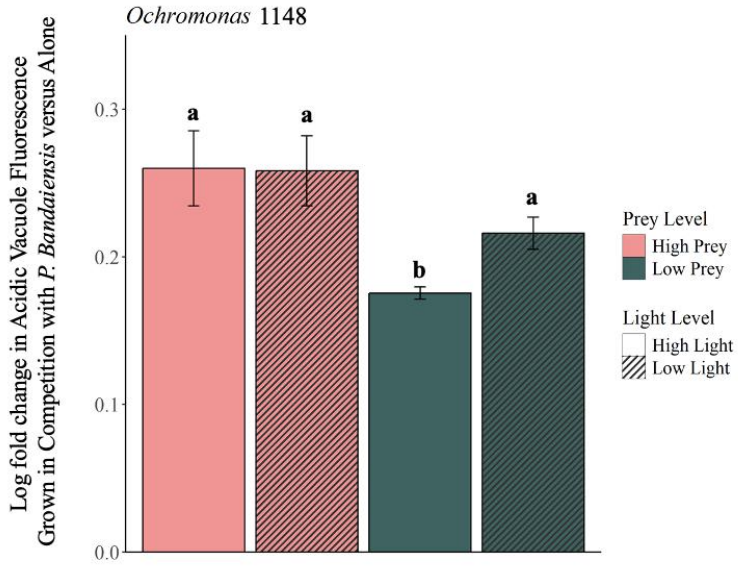

Figure 3.6. The log fold change in chlorophyll fluorescence (A, B) and acidic vacuole content (C, D) in *Ochromonas* 584 (A, C) and *Ochromonas* 1148 (B, D) when grown alone versus in competition with *P. bandaiensis*. Cells were cultured under various nutrient regimes including high prey (pink) and low prey conditions (teal) as well as high light (solid) and low light (shaded) conditions. Letters indicate significantly different groups according to Tukey's Honestly Significantly Different test (HSD test) ($p < 0.05$).

3.7A

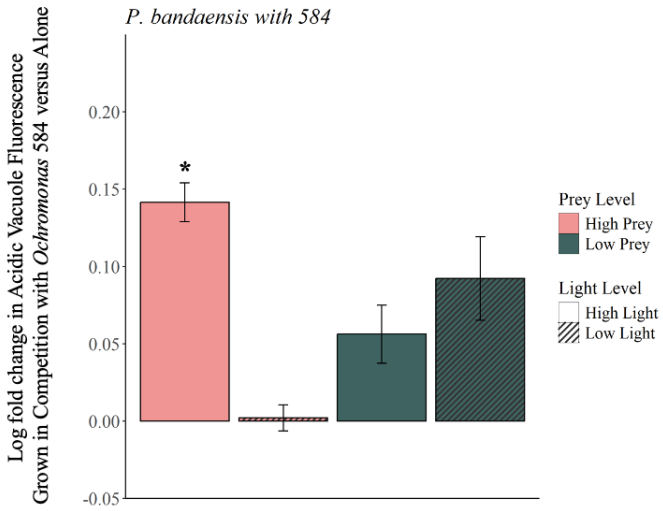

3.7B

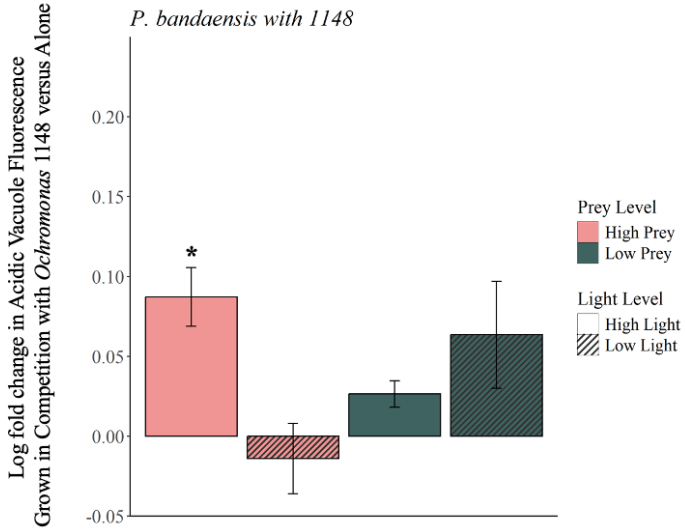

Figure 3.7. The log fold change in acidic vacuole content (as measured by Lysotracker Green DND-26) of *P. bandaiensis* in log phase when grown in competition with *Ochromonas* 584 (A) or *Ochromonas* 1148 (B) versus grown in a monoculture. Cells were cultured under various nutrient regimes including high prey (pink) and low prey conditions (teal) as well as high light (solid bars) and low light (shaded) conditions. Stars indicate means significantly different from zero (one-sample t-test, $p < 0.05$).

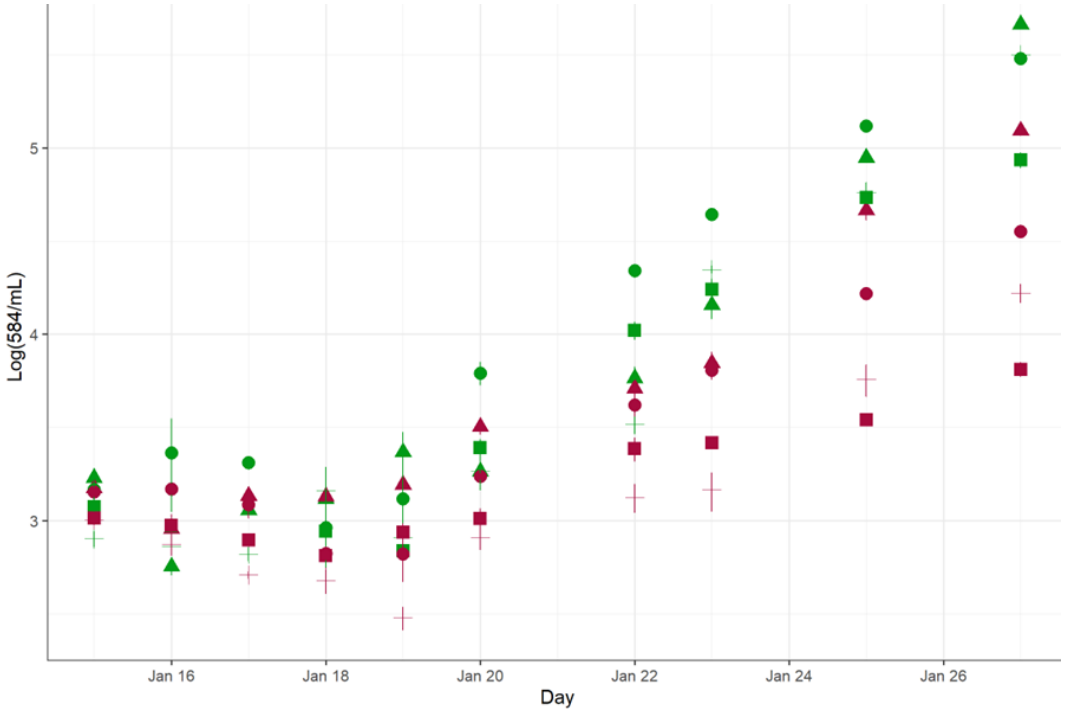

Figure 3.8. Average logarithmic abundances of *Ochromonas* 584 (cells/mL) over the course of the experiment cultured alone (green) and with *P. bandaiensis* (maroon). Cells were grown in different environmental treatments: high light and high prey (triangle, ▲), high light and low prey (cross, +), low light and high prey (circle, ●), and low light and low prey (square, ■). Vertical bars represent standard error.

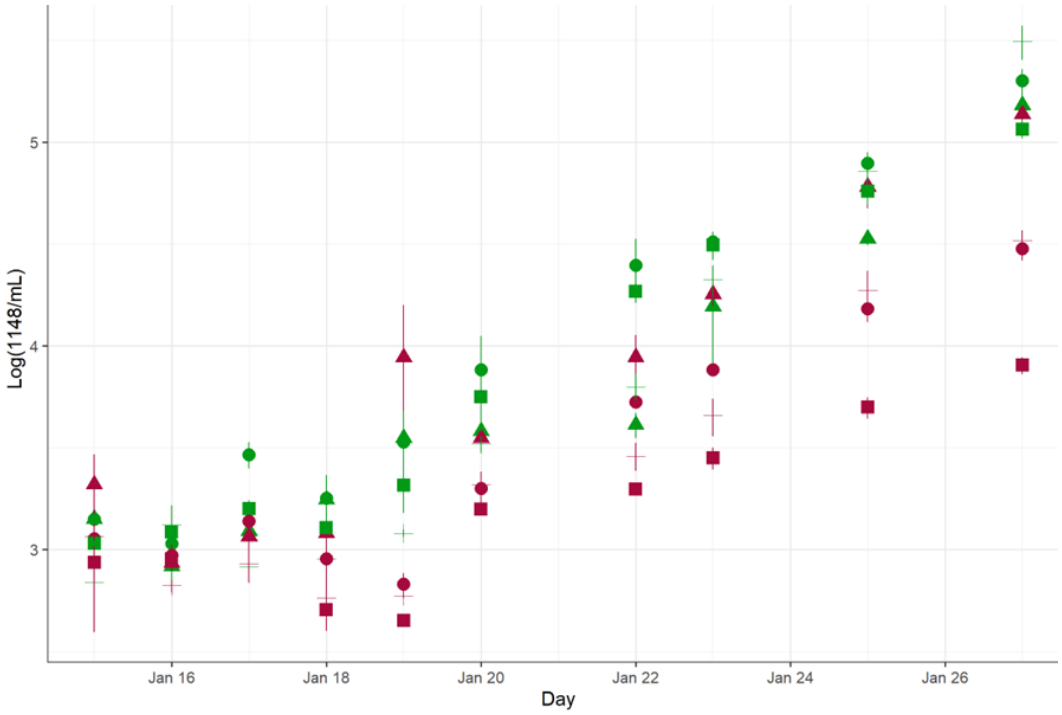

Figure 3.9. Average logarithmic abundances of *Ochromonas* 1148 (cells/mL) over the course of the experiment cultured alone (green) and with *P. bandaiensis* (maroon). Cells were grown in different environmental treatments: high light and high prey (triangle, ▲), high light and low prey (cross, +), low light and high prey (circle, ●), and low light and low prey (square, ■). Vertical bars represent standard error.

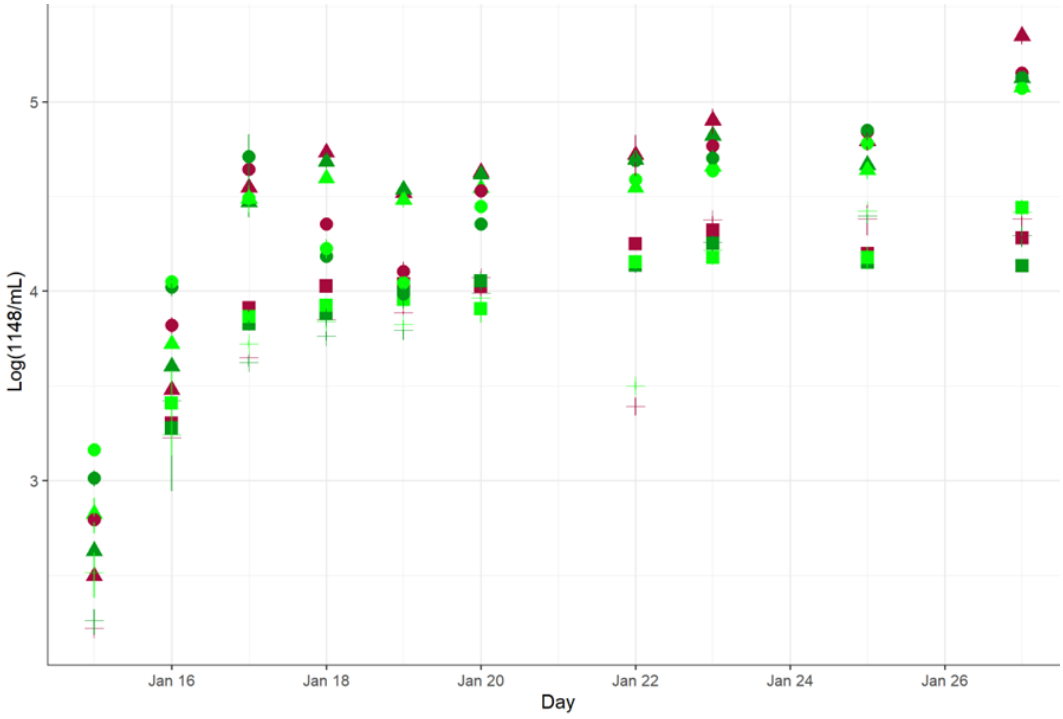

Figure 3.10. Average logarithmic abundances of *P. bandaiensis* (cells/mL) over the course of the experiment cultured alone (maroon), with *Ochromonas* 584 (light green), or with *Ochromonas* 1148 (dark green).Cells were grown in different environmental treatments: high light and high prey (triangle, ▲), high light and low prey (cross, +), low light and high prey (circle, ●), and low light and low prey (square, ■). Vertical bars represent standard error.

References

1. Anderson, R., Jürgens, K. & Hansen, P.J. (2017). Mixotrophic Phytoflagellate Bacterivory Field Measurements Strongly Biased by Standard Approaches: A Case Study. *Front. Microbiol.*, 8.
2. Barbaglia, G.S., Paight, C., Honig, M., Johnson, M.D., Marczak, R., Lepori-Bui, M., and Moeller, H.V. (2024) Environment-dependent metabolic investments in the mixotrophic chrysophyte *Ochromonas*. *Journal of Phycology* **60**: 170–184.
3. Berge, T., Chakraborty, S., Hansen, P.J., and Andersen, K.H. (2017) Modeling succession of key resource-harvesting traits of mixotrophic plankton. *ISME J* **11**: 212–223.
4. Cabrerizo, M.J., González-Olalla, J.M., Hinojosa-López, V.J., Peralta-Cornejo, F.J., and Carrillo, P. (2019) A shifting balance: responses of mixotrophic marine algae to cooling and warming under UVR. *New Phytologist* **221**: 1317–1327.
5. Carrieri, D., Jurista, T., Yazvenko, N., Schafer Medina, A., Strickland, D., and Roberts, J.M. (2021) Overexpression of NblA decreases phycobilisome content and enhances photosynthetic growth of the cyanobacterium *Synechococcus elongatus* PCC 7942. *Algal Research* **60**: 102510.
6. Caron, D.A. (2016) Mixotrophy stirs up our understanding of marine food webs. *Proceedings of the National Academy of Sciences* **113**: 2806–2808.

7. Chu, T., Moeller, H.V., and Archibald, K.M. (2023) Competition between phytoplankton and mixotrophs leads to metabolic character displacement. *Ecological Modelling* **481**:.
8. Costa, M.R.A., Sarmento, H., Becker, V., Bagatini, I.L. & Unrein, F. (2022). Phytoplankton phagotrophy across nutrients and light gradients using different measurement techniques. *Journal of Plankton Research*, 44, 507–520.
9. Crane, K.W. and Grover, J.P. (2010) Coexistence of mixotrophs, autotrophs, and heterotrophs in planktonic microbial communities. *Journal of Theoretical Biology* **262**: 517–527.
10. Cropp, R. and Norbury, J. (2015) Mixotrophy: the missing link in consumer-resource-based ecologies. *Theor Ecol* **8**: 245–260.
11. Curien, G., Lyska, D., Guglielmino, E., Westhoff, P., Janetzko, J., Tardif, M., et al. (2021) Mixotrophic growth of the extremophile *Galdieria sulphuraria* reveals the flexibility of its carbon assimilation metabolism. *New Phytologist* **231**: 326–338.
12. Dorrell, R.G., Azuma, T., Nomura, M., deKerdrel, G.A., Paoli, L., Yang, S., et al. (2019) Principles of plastid reductive evolution illuminated by nonphotosynthetic chrysophytes. *Proceedings of the National Academy of Sciences of the United States of America* **116**: 6914–6923.
13. Edwards, K.F. (2019) Mixotrophy in nanoflagellates across environmental gradients in the ocean. *Proceedings of the National Academy of Sciences* **116**: 6211–6220.
14. Flöder, S., Klauschies, T., Klaassen, M., Stoffers, T., Lambrecht, M., and Moorthi, S. (2024) Competition between mixo- and heterotrophic ciliates under dynamic resource supply. *Ecosphere* **15**: e4950.
15. FC M, and Davis T. (2022). *ggpattern: 'ggplot2' Pattern Geoms*.
16. Florenza, J., Divne, A.-M. & Bertilsson, S. (2024). Fluorescently labeled prey surrogates in combination with fluorescence-activated cell sorting successfully discriminate actively feeding mixotrophs in a lake water sample. *Limnology and Oceanography*, 69, 1030–1044.
17. Flynn, K.J. and Mitra, A. (2009) Building the "perfect beast": modelling mixotrophic plankton. *Journal of Plankton Research* **31**: 965–992.
18. Flynn, K.J., Stoecker, D.K., Mitra, A., Raven, J.A., Glibert, P.M., Hansen, P.J., et al. (2013) Misuse of the phytoplankton–zooplankton dichotomy: the need to assign organisms as mixotrophs within plankton functional types. *Journal of Plankton Research* **35**: 3–11.
19. Friedland, N., Negi, S., Vinogradova-Shah, T., Wu, G., Ma, L., Flynn, S., et al. (2019) Fine-tuning the photosynthetic light harvesting apparatus for improved photosynthetic efficiency and biomass yield. *Sci Rep* **9**: 13028.
20. Ghyoot, C., Flynn, K.J., Mitra, A., Lancelot, C., and Gypens, N. (2017) Modeling Plankton Mixotrophy: A Mechanistic Model Consistent with the Shuter-Type Biochemical Approach. *Front Ecol Evol* **5**:.
21. González-Olalla, J.M., Medina-Sánchez, J.M., Norici, A., and Carrillo, P. (2021) Regulation of Phagotrophy by Prey, Low Nutrients, and Low Light in the Mixotrophic Haptophyte *Isochrysis galbana*. *Microb Ecol* **82**: 981–993.
22. Grolemund, G. and Wickham, H. (2011) Dates and Times Made Easy with lubridate. *Journal of Statistical Software* **40**: 1–25.

23. Hammer, A.C. and Pitchford, J.W. (2005) The role of mixotrophy in plankton bloom dynamics, and the consequences for productivity. *ICES Journal of Marine Science* **62**: 833–840.
24. Hartmann, M., Grob, C., Tarran, G.A., Martin, A.P., Burkill, P.H., Scanlan, D.J., and Zubkov, M.V. (2012) Mixotrophic basis of Atlantic oligotrophic ecosystems. *Proc Natl Acad Sci USA* **109**: 5756–5760.
25. Holen, D.A. (2010) Mixotrophy in two species of *Ochromonas* (Chrysophyceae) *Nova Hedwigia, Beiheft* **136**: 153–165.
26. Honig, M.A., Barbaglia, G.S., Doyle, M.D., and Moeller, H.V. (2025) Effects of mixotroph evolution on trophic transfer. *Journal of Plankton Research* **47**: fbae053.
27. Jost, C., Lawrence, C.A., Campolongo, F., van de Bund, W., Hill, S., and DeAngelis, D.L. (2004) The effects of mixotrophy on the stability and dynamics of a simple planktonic food web model. *Theor Popul Biol* **66**: 37–51.
28. Katechakis, A. and Stibor, H. (2006) The mixotroph *Ochromonas tuberculata* may invade and suppress specialist phago- and phototroph plankton communities depending on nutrient conditions. *Oecologia* **148**: 692–701.
29. Keller, M.D., Selvin, R.C., Claus, W., and Guillard, R.R.L. (1987) Media for the Culture of Oceanic Ultraphytoplankton. *Journal of Phycology* **23**: 633–638.
30. Leles, S.G., Polimene, L., Bruggeman, J., Blackford, J., Ciavatta, S., Mitra, A., and Flynn, K.J. (2018) Modelling mixotrophic functional diversity and implications for ecosystem function. *Journal of Plankton Research* **40**: 627–642.
31. Lie, A.A.Y., Liu, Z., Terrado, R., Tatters, A.O., Heidelberg, K.B., and Caron, D.A. (2017) Effect of light and prey availability on gene expression of the mixotrophic chrysophyte, *Ochromonas* sp. *BMC Genomics* **18**: 163.
32. Lie, A.A.Y., Liu, Z., Terrado, R., Tatters, A.O., Heidelberg, K.B., and Caron, D.A. (2018) A tale of two mixotrophic chrysophytes: Insights into the metabolisms of two *Ochromonas* species (Chrysophyceae) through a comparison of gene expression. *PLoS One* **13**: e0192439.
33. MacIntyre, H.L., Kana, T.M., Anning, T., and Geider, R.J. (2002) Photoacclimation of Photosynthesis Irradiance Response Curves and Photosynthetic Pigments in Microalgae and Cyanobacteria. *Journal of Phycology* **38**: 17–38.
34. Millette, N.C., Leles, S.G., Johnson, M.D., Maloney, A.E., Brownlee, E.F., Cohen, N.R., *et al.* (2024). Recommendations for advancing mixoplankton research through empirical-model integration. *Front. Mar. Sci.*, 11.
35. Moeller, H.V., Neubert, M.G., and Johnson, M.D. (2019) Intraguild predation enables coexistence of competing phytoplankton in a well-mixed water column. *Ecology* **100**: e02874.
36. Ochs, C.A. and Eddy, L.P. (1998) Effects of UV-A (320 to 399 Nanometers) on Grazing Pressure of a Marine Heterotrophic Nanoflagellate on Strains of the Unicellular Cyanobacteria Synechococcus spp. *Appl Environ Microbiol* **64**: 287–293.
37. Posch, T., Simek, K., Vrba, J., Pernthaler, J., Nedoma, J., Sattler, B., et al. (1999) Predator-induced changes of bacterial size-structure and productivity studied on an experimental microbial community. *Aquatic Microbial Ecology* **18**: 235–246.
38. Rothhaupt, K.O. (1996) Laboratorary Experiments with a Mixotrophic Chrysophyte and Obligately Phagotrophic and Photographic Competitors. *Ecology* **77**: 716–724.

39. Rose, J., Caron, D., Sieracki, M. & Poulton, N. (2004). Counting heterotrophic nanoplanktonic protists in cultures and aquatic communities by flow cytometry. *Aquat. Microb. Ecol.*, 34, 263–277.
40. Ruban, A.V. (2015) Evolution under the sun: optimizing light harvesting in photosynthesis. *Journal of Experimental Botany* **66**: 7–23.
41. Safi, K. and Hall, J. (1999) Mixotrophic and heterotrophic nanoflagellate grazing in the convergence zone east of New Zealand. *Aquat Microb Ecol* **20**: 83–93.
42. Schmidtke, A., Bell, E.M., and Weithoff, G. (2006) Potential grazing impact of the mixotrophic flagellate *Ochromonas* sp. (Chrysophyceae) on bacteria in an extremely acidic lake. *Journal of Plankton Research* **28**: 991–1001.
43. Scoble, J.M. and Cavalier-Smith, T. (2014) Scale evolution in Paraphysomonadida (Chrysophyceae): Sequence phylogeny and revised taxonomy of *Paraphysomonas*, new genus *Clathromonas*, and 25 new species. *European Journal of Protistology* **50**: 551–592.
44. Selph, K.E., Landry, M.R., and Laws, E.A. (2003) Heterotrophic nanoflagellate enhancement of bacterial growth through nutrient remineralization in chemostat culture. *Aquatic Microbial Ecology* **32**: 23–37.
45. Shade, A., Peter, H., Allison, S.D., Baho, D., Berga, M., Buergmann, H., et al. (2012) Fundamentals of Microbial Community Resistance and Resilience. *Front Microbiol* **3**:.
46. Sintes, E. & Del Giorgio, P.A. (2010). Community heterogeneity and single-cell digestive activity of estuarine heterotrophic nanoflagellates assessed using lysotracker and flow cytometry. *Environmental Microbiology*, 12, 1913–1925.
47. Smalley, G.W., Coats, D.W., and Stoecker, D.K. (2003) Feeding in the mixotrophic dinoflagellate *Ceratium furca* is influenced by intracellular nutrient concentrations. *Marine Ecology Progress Series* **262**: 137–151.
48. Stegemüller, L., Valverde-Pérez, B., Thygesen, A., and Angelidaki, I. (2024) Synergistic effects of heterotrophic and phototrophic metabolism for *Haematococcus lacustris* grown under mixotrophic conditions. *J Appl Phycol* **36**: 3175–3186.
49. Stickney, H.L., Hood, R.R., and Stoecker, D.K. (2000) The impact of mixotrophy on planktonic marine ecosystems. *Ecological Modelling* **125**: 203–230.
50. Strom, S.L. (2001). Light-aided digestion, grazing and growth in herbivorous protists. *Aquat Microb Ecol* 23, 253-261.
51. Terpis, K.X., Salomaki, E.D., Barcytė, D., Pánek, T., Verbruggen, H., Kolisko, M., et al. (2025) Multiple plastid losses within photosynthetic stramenopiles revealed by comprehensive phylogenomics. *Current Biology* **0**:
52. Terrado, R., Pasulka, A.L., Lie, A.A.-Y., Orphan, V.J., Heidelberg, K.B., and Caron, D.A. (2017) Autotrophic and heterotrophic acquisition of carbon and nitrogen by a mixotrophic chrysophyte established through stable isotope analysis. *ISME J* **11**: 2022–2034.
53. Tittel, J., Bissinger, V., Zippel, B., Gaedke, U., Bell, E., Lorke, A., and Kamjunke, N. (2003) Mixotrophs combine resource use to outcompete specialists: Implications for aquatic food webs. *Proceedings of the National Academy of Sciences* **100**: 12776–12781.
54. Våge, S., Castellani, M., Giske, J., and Thingstad, T.F. (2013) Successful strategies in size structured mixotrophic food webs. *Aquat Ecol* **47**: 329–347.

55. Villanova, V., Fortunato, A.E., Singh, D., Bo, D.D., Conte, M., Obata, T., et al. (2017) Investigating mixotrophic metabolism in the model diatom *Phaeodactylum tricornutum*. *Philos Trans R Soc Lond B Biol Sci* **372**: 20160404.
56. Ward, B.A. (2019) Mixotroph ecology: More than the sum of its parts. *Proceedings of the National Academy of Sciences* **116**: 5846–5848.
57. Ward, B.A. and Follows, M.J. (2016) Marine mixotrophy increases trophic transfer efficiency, mean organism size, and vertical carbon flux. *Proc Natl Acad Sci USA* **113**: 2958–2963.
58. Weithoff, G. and Wacker, A. (2007) The mode of nutrition of mixotrophic flagellates determines the food quality for their consumers. *Functional Ecology* **21**: 1092–1098.
59. Wickham H (2016). *ggplot2: Elegant Graphics for Data Analysis*. Springer-Verlag New York. ISBN 978-3-319-24277-4.
60. Wickham, H. (2020) reshape2: Flexibly Reshape Data: A Reboot of the Reshape Package.
61. Wickham, H., François, R., Henry, L., Müller, K., Vaughan, D., Posit Software, and PBC (2023) dplyr: A Grammar of Data Manipulation.
62. Wickham, H., Hester, J., Francois, R., Bryan, J., Bearrows, S., Posit Software, et al. (2024) readr: Read Rectangular Text Data.
63. Wieczynski, D.J., Moeller, H.V., and Gibert, J.P. (2023) Mixotrophic microbes create carbon tipping points under warming. *Functional Ecology* **37**: 1774–1786.
64. Wilken, S., Verspagen, J.M.H., Naus-Wiezer, S., Van Donk, E., and Huisman, J. (2014) Biological control of toxic cyanobacteria by mixotrophic predators: an experimental test of intraguild predation theory. *Ecological Applications* **24**: 1235–1249.
65. Wilken, S., Soares, M., Urrutia-Cordero, P., Ratcovich, J., Ekvall, M.K., Van Donk, E., and Hansson, L.-A. (2018) Primary producers or consumers? Increasing phytoplankton bacterivory along a gradient of lake warming and browning. *Limnology and Oceanography* **63**: S142–S155.
66. Wilken, S., Yung, C.C.M., Hamilton, M., Hoadley, K., Nzongo, J., Eckmann, C., et al. (2019) The need to account for cell biology in characterizing predatory mixotrophs in aquatic environments. *Philosophical Transactions of the Royal Society B: Biological Sciences* **374**: 20190090.
67. Wilken, S., Choi, C.J., and Worden, A.Z. (2020) Contrasting Mixotrophic Lifestyles Reveal Different Ecological Niches in Two Closely Related Marine Protists. *J Phycol* **56**: 52–67

CHAPTER 4: MIXOTROPHIC METABOLIC LANDSCAPES AND REQUIREMENTS SHAPE TROPHIC INVESTMENT IN COMPETITION

Contributors: Sophia Ahn, Holly Moeller, Matthew D. Johnson

Abstract

Mixotrophic microorganisms combine phototrophy and phagotrophy to occupy unique trophic niches which are inaccessible to single-guild competitors. Many mixotrophs are highly plastic with their metabolic investments and leverage this plasticity to compete for limited resources. However, this plasticity comes with a cost, and often niche displacement leads to less efficient growth. In this experiment we competed the mixotrophic chrysophytes *Ochromonas* 584 (an obligate phagotroph) and *Ochromonas* 1391 (an obligate phototroph) with the solely phagotrophic chrysophyte *Paraphysomonas bandaiensis* in competition in a chemostat and compared these results with the trophic niche occupied by *Ochromonas* when grown alone. We observed opposite niche displacement dynamics in response to competition between the two strains of *Ochromonas,* with one shifting its metabolic investment more towards photosynthesis, while the other doubled down on phagotrophy to directly compete for prey with *P. bandaiensis*. This niche displacement caused both strains to have lower carbon use efficiencies in competition. An investigation of the metabolic landscape of each *Ochromonas* strain demonstrates these results may be explained by prey requirements, prey quality, and mixotrophic tradeoffs.

Introduction

Organismal metabolism is often thought of a dichotomous divide between phototrophy and phagotrophy (Flynn et al. 2013). However, mixotrophs (organisms which can obtain energy from both photosynthesis and phagotrophy) are incredibly abundant in aquatic environments (Flynn et al. 2013).

Mixotrophs have been shown to play a critical role in ecosystem structure and function in aquatic environments (Cropp and Norbury 2015, Worden et al. 2015, Wieczynski, Moeller, and Gilbert 2023). Much of mixotrophs' impact on community dynamics stems from the unique trophic niche they occupy between traditional concepts of producer and consumer (Flynn et al. 2013, Caron 2016). The ability for mixotrophs to contribute to primary and secondary production has important implications for trophic transfer, overall community production, ecosystem stability, bloom dynamics, and nutrient cycling among others (Stickney, Hood, Stoecker 2000, Tittle et al.

2003, Jost et al. 2004, Hammer and Pitchford 2005, Ward and Follows 2016, Stoecker et al. 2017, Leles et al. 2018, Honig et al. 2025).

Constitutive mixotrophic organisms (organisms which innately have the ability to photosynthesize and phagocytize) have two key evolutionary and ecological advantages: the ability to obtain energy from multiple sources and the metabolic plasticity to modulate their trophic investments in response to changing conditions or competition (Tittle et al. 2003, Cropp and Norbury 2015, Selosse, Charpin and Not 2017, Archibald et al. 2024). However, constitutive mixotrophs vary greatly in the extent to which they can efficiently access phototrophic and phagotrophic resources as well as alter their metabolic response to environmental changes (Barbaglia et al. 2024, Millette et al. 2024). How and to what extent mixotrophs are able to alter their trophic niche to remain competitive in mixed communities remains an open question (Millette et al. 2024).

Traditionally, mixotrophic niches are thought of as a "trophic balance" or "relative investment" on a single axis between phototrophy and phagotrophy (Flynn et al. 2013, Edwards 2019, Chu Moeller and Archibald 2023). Mixotrophic metabolism is often thought to confer a trade-off between investments in these dual trophic modes, where investment in one strategy limits investment in the other (Flynn and Mitra 2009). Sometimes, this trade-off is also called the "metabolic cost" of mixotrophy and is used to explain observed inefficiencies in mixotrophic phototrophy or phagotrophy compared to single-guild competitors (Ward et al. 2011, Caron 2016).

Recent research suggests mixotrophic metabolic niches are much more complex, where different mixotrophs experience different multi-dimensional trade-offs between investment in phagotrophy versus phototrophy (Wilken et al. 2019, Barbaglia et al. 2024). Instead of limitations, mixotrophs can experience "synergies" between their dual metabolism where the recycling of energy from one metabolic pathway fuels the other trophic mode (Tittle et al. 2003, Barbaglia et al. 2024).

Mixotrophs coexist and are sometimes outcompeted by single-guild competitors meaning there must be eco-evolutionary limitations to mixotrophic metabolism (Tittle et al. 2003, Mansour and Anestis 2021). This begs the question: if dual tropic pathways enhance survivability and growth, where is the metabolic cost in synergistic mixotrophs?

The cost or trade-offs of mixotrophic metabolism are often thought of as a penalty, sometmes incorporated into models as a single parameter, representing some physiological drawback (Edwards 2019, Mansour and Anestis 2021). While physiological processes no doubt underly the competitive dynamics of mixotrophy, studies demonstrate competitive trade-offs can emerge from niche filling strategies independent of any associated metabolic cost (Archibald et al. 2024). Indeed, in a study by Archibald et al. (2024), incorporating a metabolic penalty into a model which organically produced competitive trade-offs in mixotrophs fundamentally altered the modeled trophic structure in a way which may be unrealistic.

In this study, we attempt to characterize the relationship between mixotrophic niche filling strategies and metabolic tradeoffs in a competitive environment. We compete *Ochromonas* sp.

CCMP 584 and *Ochromonas* sp. CCMP 1391 with the closely related, single-guild competitor *Paraphysomonas bandaiensis* and observe changes to trophic mode and metabolic efficiency in the mixotroph. Studies have demonstrated environmental variation in the laboratory is not equivalent to testing the effects of competition directly (Jahns and Johnson *in prep*). Therefore, we instead compete our organisms within a chemostatic culturing apparatus at steady-state. By comparing the metabolic investments and competitive dynamics of each mixotroph grown alone versus in competition with *P. bandaiensis*, we describe how a mixotroph's metabolic landscape shapes its response to competition and organically leads to competitive tradeoffs.

Methodology

i. Cultures and maintenance

Cultures of *Ochromonas* sp. CCMP 584 (*Ochromonas* 584) and *Ochromonas* sp. CCMP 1391 (*Ochromonas* 1391) were obtained from Bigelow National Center for Marine Algae and Microbiota (NCMA). Cultures of *Paraphysomonas bandaiensis* were graciously provided by the lab of David Caron at the University of Southern California.

Cultures were maintained in a synthetic ocean water (SOW) media made of Instant Ocean Sea Salts (Spectrum Brands, Blackburg, VA, USA) adjusted to 35 practical salinity units (PSU) via refractometer. This media was appended with K/50 from a "K media kit" sold by NMCA, a grain of sterile rice and 5 µL of liquid broth (LB) per mL of media (Keller et al. 1987). Cultures were maintained in constant light at ~70 µmol photons m^{-2} sec^{-1} and 23°C.

ii. Chemostat design

To isolate the effects of competition on mixotrophic metabolism, experiments were conducted in chemostatic culturing apparatuses (chemostats). Our experiment was conducted in chemostats to avoid the confounding variables of fluctuating nutrients and organics in batch cultures due to biological draw-down (Pickell et al. 2009, Le Chevanton et al. 2016, Omta et al. 2017). This ensured steady-state conditions throughout the experiment, after chemostats reached equilibrium, and allowed for careful limitation of resources.

For the chemostat, the culturing vessel was made up of a sterile 2L KIMAX Erlenmeyer flask (DWK Life Sciences, Millville, NJ, USA). The flask contained 1400 mL of phosphorus (P)-scarce media. The media was made of SOW + K/10 + P/85 (Keller et al. 1987) appended with an LB-like mixture made with additional glucose and tryptone (LBGT mixture) to promote bacterial growth supporting the growth of the mixotroph and heterotroph (Table 4.1). A PFTE/silicon septum (WK Life Sciences, Millville, NJ, USA) was attached to the top of the vessel with an open GL45 cap (DWK Life Sciences, Millville, NJ, USA). Four ~0.16" holes were drilled in the septum of the vessel through which three 3mm outer-diameter glass tubes, sheathed in 0.176" outer-diameter Masterflex Transfer Tubing (#06499-48, Cole-Parmer, Vernon Hills, IL, USA), were secured into place. Each rod was cut to a different length and acted as either the media outflow, sampling port, or gas-exchange port (see Figure 4.1). The fourth hole was occupied by Masterflex platinum-coated silicon L/S 13 tubing from the reservoir for media inflow (#96410-

13, Cole-Parmer, Vernon Hills, IL, USA). The vessel remained mixed and oxygenated through the course of the experiment using a sterile 1” stir-bar rotating at 160 rpm.

Media was fed into the vessel from a media reservoir. The reservoir was constructed using a 10000mL FisherBrand glass media bottle (Fisher Scientific, Pittsburg, PA, USA) topped with PFTE/silicon septum (Millipore-Sigma, Burlington, MA, USA) and an open GL45 cap (DWK Life Sciences, Millville, NJ, USA). The reservoirs contained 8L of SOW + K/10 + P/85 with LBGT equivalent to the vessel media (Keller et al. 1987, Table 4.1). Three 0.15” holes were cut in the septum of the vessel, through which three 3mm outer-diameter glass tunes, sheathed in 0.176” outer-diameter Masterflex Transfer Tubing (#06499-48, Cole-Parmer, Vernon Hills, IL, USA), were secured into place. Each rod was cut to a different length and acted as either the media outflow, sampling port, or gas-exchange port (see Figure 4.2).

Flow was controlled by one of two peristaltic pumps: a MasterFlex L/S (07528-10) pump with two attached MasterFlex EZload II two-channel pump heads (77202-60) or a MasterFlex L/S (07528-30) pump with four MasterFlex EZload II two-channel pump heads (Cole-Parmer, Vernon Hills, IL, USA). Inflow tubing (tubing from the reservoir to the vessel) was made of Masterflex platinum-coated silicon L/S 13 tubing from the reservoir for media inflow (#96410-13, Cole-Parmer, Vernon Hills, IL, USA). Outflow tubing (tubing from the vessel to the waste) was made of Masterflex Precision Pump Tubing L/S 14 (#06434-14, Cole-Parmer, Vernon Hills, IL, USA). The pumps were set to 6rpm resulting in a turnover of 518.4 mL each day. The exponential dilution rate of the system was 0.315 day^{-1}. This rate is similar to the turnover rate used in previous chemostat experiments to simulate steady-state gyres (Cermeño et al. 2011). Tubing was secured to the vessel and reservoir using a series of luer locks (see Figure 4.3 and Table 4.2) purchased from Qosina (Ronkonkoma, NY, USA).

To ensure chemostats were not contaminated, sampling was done via a sterile sampling system where two one-way valves ensured that only media could leave, and only sterile air could enter the system (Figure 4.3). After each sample was taken, the tubing was flushed with 20mL of air that passed through a 0.2 micron polycarbonate filter (Whatman, Florham Park, NJ, USA) using a 20mL sterile leur lock syringe (BD, Franklin Lakes, NJ, USA) to ensure no growth in the sampling port.

Chemostats were maintained in constant light at ~130 μmol photons m^{-2} sec^{-1}, which exceeds the growth-saturating irradiance for *Ochromonas sp.*, ensuring light was not a limiting factor during the experiment (Barbaglia et al. 2024). Cultures were grown at 23°C. All components were rinsed with milli-Q water then sterilized in an autoclave prior to assembly. Chemostats were assembled in a laminar hood to ensure sterility. Reservoirs were also sampled periodically to confirm the absence of contaminant bacteria.

The overall chemostat design can be found in Figure 4.4 and the complete parts list can be found in Table 4.2.

iii. Experimental design and sampling

Prior to the experiment, cells were grown for at least eight generations in P-scarce media made of SOW + K/10 + P/50 appended with the LBGT mixture (Keller et al. 1987, Table 4.3). Cultures were grown at 23°C and in constant light at ~130 µmol photons m^{-2} sec^{-1}. Cells were inoculated into the chemostats in log phase at a stating concentration of 10^2-10^3 cells per mL. Each chemostat contained one of five combinations of strains: 1) *Ochromonas* 584 alone, 2) *Ochromonas* 584 + *P. bandaiensis*, 3) *Ochromonas* 1391 alone, 4) *Ochromonas* 1391 + *P. bandaiensis*, or 5) *P. bandaiensis* alone. Three replicates were conducted for each treatment.

Samples were taken from chemostats with the sterile sampling system (Figure 4.3) using either a 5, 10, or 20 mL sterile luer-lock syringe (BD, Franklin Lakes, NJ, USA), depending on the sampling requirements. The entire syringe was flushed once with culture and emptied before sampling. Each experiment lasted until treatments reached equilibrium (see below).

iv. Flow cytometry

Cell counts were taken via flow cytometry each day on a Guava easyCyte HT. *Ochromonas* cells were identified via their chlorophyll red fluorescence. To identify *Paraphysomonas bandaiensis* cells (which lack pigments) aliquots were stained with SYBR Green I Nucleic Acid Gel Stain (ThermoFisher Scientific) to a concentration of 0.5x, incubated in the dark for at least 15 minutes, and then run on the flow cytometer.

Other aliquots of sample were stained with the acidic vacuole stain Lysotracker Green DND-26 (ThermoFisher Scientific) at a concentration of 100 nM then immediately run on the flow cytometer. Previous studies show lysotracker can be used as a proxy for food vacuoles and grazing (Sintes and Del Georgio 2010, Jahns and Johnson *in prep*) and we have used it to monitor grazing activity in the past (Jahns and Johnson *in prep*). While other studies have indicated Lysotracker Green DND-26 may also stain acidic thylakoid membrane in mixotrophs' chloroplasts (Wilken et al. 2019, Millette et al. 2023), we find no evidence for this in the strains of *Ochromonas* we used (Figure 3.2).

v. Growth rates and equilibrium

Instantaneous growth rates for each day were calculated as the slope of the linear least squares regression between the log cell abundance of that day and the two nearest data points. For example, the instantaneous growth rate of a culture at day 7 would be the slope of the line of best fit on log cell abundance for days 6, 7, and 8.

Experiments were stopped when the culture reached equilibrium for at least three days. A day was considered to be "at equilibrium" if it satisfied at least two of the following conditions:

1. The instantaneous growth rate was not significantly different from zero.
2. The instantaneous growth rate was not significantly different from the average instantaneous growth rate of the last three days.
3. The log concentration of cells was not significantly different from the log concentration of cells on the final day of the experiment.

This definition was chosen to account for limit cycles or oscillating growth dynamics that can occur in chemostats (Lenas and Pavlou 1994, Jost et al. 2004, Toth and Kot 2006, Fekih-Salem, Rapaport, and Sari 2016, Felpeto, Roy, and Vasconcelos 2018, etc.). We then determined the equilibrium period, which is the period during which the growth rate of the competitors was equivalent to the dilution rate. We defined the equilibrium period as the last day of the experiment until the latest day which was still in equilibrium. Reported means during the equilibrium period are the mean of all measured values of the variable during the period.

vi. Bacteria and grazing: phagotrophic investment

Grazing rates of *Ochromonas* were obtained using methods with live, fluorescently labeled bacteria following methods described by First et al. (2011) and Bock et al. (2021). Live, fluorescently labeled bacterial prey was chosen because of evidence suggesting other proxies, such as beads and heat-killed bacteria, can be inadequate for accurately quantifying grazing rates in marine mixotrophic flagellettes (Boenigk et al. 2005, Jimenez et al. 2020, Bock et al. 2021).

Spores of *Pelagibaca bermudensis* HTCC2601 were inoculated in a yeast extract-tryptone-sea salt (YTSS) media and allowed to grow until late-exponential phase (Gonzalez et al. 1996). Bacterial cells were then stained with CellTracker Green CMFDA (CMFDA) to a final concentration of 25 µM. They were then mixed via inversion and incubated in the dark at 23°C for at least three hours. After incubation, ~1 mL of bacteria was filtered onto a 0.2 µm GTTP filter (Millipore, Bedford, MA) and washed with at least 3 mL of 0.2µm-filtered SOW (f-SOW). The washed cells were then resuspended in ~1 mL of f-SOW via vortexing at maximum speed in the dark for 30 seconds. The concentration of stained bacteria was determined by diluting stained bacteria 1:200 or 1:400 (depending on concentration) in f-SOW and counted on an Attune CytPix imaging flow cytometer (Thermo Fisher Scientific, Waltham, MA, USA) at a flow rate of 25 µL/min.

Bacteria concentrations in chemostats were calculated by first diluting the sample 1:100 in f-SOW and staining with SYBR Green I Nucleic Acid Gel Stain (ThermoFisher Scientific) to a concentration of 0.5x. Diluted samples were placed in the dark for at least fifteen minutes and then counted on an Attune CytPix imaging flow cytometer (Thermo Fisher Scientific, Waltham, MA, USA) at a flow rate of 25 µL/min.

At the start of each grazing experiment, stained prey was added to 1 mL of sample collected from a chemostat such that the final concentration of fluorescently labeled *P. bermudensis* made up 10% of the total bacteria in the sample, then mixed via inversion. Over the duration of the experiment, aliquots of the sample with stained prey was diluted ~1:6 in f-SOW, inverted three times, and counted on an Attune CytPix imaging flow cytometer (Thermo Fisher Scientific, Waltham, MA, USA) at a flow rate of 100 µL/min. *Ochromonas* cells were identified via red fluorescence. *Ochromonas* cells that also fluoresced green with CMFDA (above the baseline before stained prey was added) were considered to have ingested a labeled bacterium. In our experiments we rarely observed *Ochromonas* cells with two ingested CMFDA stained bacteria within the first thirty minutes (Figure 4.13). From previous work we also find that the growth rates of bacteria grown without predators are negligible and does not influence our calculations (Ahn, personal communication). Ingestion rates were calculated during the linear portion of

ingestion versus time (usually ~30 minutes). From the increase in *Ochromonas* with ingested prey over time, the concentration of bacteria (labeled and unlabeled), and the concentration of *Ochromonas*, the ingestion rate in each sample could be calculated (Bock et al. 2021).

The grazing rates of *P. bandaiensis* were not quantified due to the restriction on our method that, to accurately count *Ochromonas* cells, red fluorescence and size thresholds were turned on during flow cytometry. Additionally, we find over 30 minutes *P. bandaiensis* cells often ingest more than one labeled bacterium and thus the assumptions we use to calculate grazing rate using our methods do not hold (Figure A.1). We instead use a previously measured representative grazing rate in *P. bandaiensis* of 12.6 prey ingested per hour as an estimate of the *P. bandaiensis* grazing rate in our experiment.

Total carbon acquisition rates from grazing were estimated based on an average of 113.6 fg C per bacterium from reported elemental compositions of bacteria in similar *Ochromonas* cultures (Lepori-Bui et al. 2022, Barbaglia et al. 2024).

vii. Photo-physiology and primary production: phototrophic investment

Approximately every two days, and at the end of the experiment, the primary productivity and photosynthetic health of samples from chemostats were assessed via a Fluorescence Induction and Relaxation (FIRe) system (Satlantic, Halifax, Nova Scotia, Canada) (Gorbunov and Falkowski 2020). Briefly, a 3mL quartz cuvette was washed once with milli-q water, once with sterile seawater, and thrice with sample. 3mL of sample was then added to the cuvette and placed in the dark for at least fifteen minutes. The sample was then run at PAR levels between 0-425 µmol photons m^{-2} sec^{-1}. A complete list of settings used is listed in Table 4.4.

Electron transport rates per reaction center (ETR_{RC}) were calculated for each sample as described by the following equation (Gorbunov et al. 2000, Gorbunov et al. 2001):

$$ETR_{RC} = I \times \sigma_{PSII} \times \frac{F_v'}{F_m'} \div \frac{F_v}{F_m} \times 2.04 \times 0.00602$$

In this equation, 2.04 and 0.00602 are conversion factors to convert the measured photo-system II absorbance cross section (σ_{PSII}) into absolute units of area (in m^2) and quanta into electron units. The resulting ETR_{rc} is measured in electrons/sec/reaction center.

To ensure accurate ETR measurements, acquisitions that returned ETRs which were physiologically impossible or biologically improbable were excluded. Negative ETRs and acquisitions with negative F_vs were excluded from further analysis. Similarly, ETRs greater than 400 electrons/sec/reaction center were excluded from further analysis because they are above reported values for the strains of *Ochromonas* used in these conditions (Barbaglia et al. 2024) and tended to occur in photo-stressed samples at high light intensities.

Photosynthetic rates were computed from this data by fitting the ETR_{rc} data for each PAR level to the equation from Jassby and Platt (1976) via non-linear regression (see xi. Analytical Methods):

$$ETR_{rc} = P_{max} \times \tanh\left(\frac{\alpha I}{P_{max}}\right)$$

Here, P_{max} is the maximum electron transport rate and alpha (α) is the initial slope of ETR_{rc} versus PAR (I).

Electron transport rates were converted into absolute units of pg C/pg chlorophyll *a*/hr following the procedure outlined in Gorbunuv and Falkowski (2020) and Lepori-Bui et al. (2022). Because we did not measure the size of the photosynthetic unit, the quantum yield of O_2 evolution, and the photosynthetic quotient (PQ), we use estimates based on previous literature as described by Barbaglia et al. (2024). We also assume these parameters do not vary in response to competition.

Approximately every other day, chlorophyll was collected by filtering 10 mL of sample onto a GF/C filter (Whatman, Marlborough, MA, USA). The filter was then folded, placed in aluminum foil, and stored at -20 °C until extraction. To extract the chlorophyll from the sample, the filter was removed from the foil and placed into 10 mL of 90% acetone overnight. Chlorophyll was quantified via a TD-700 Laboratory Fluorometer (Turner Designs, Sunnyvale, CA, USA).

Primary productivity (pg C/cell/hr) was computed by multiplying the ETR_{max} (pg C/pg chlorophyll *a*/hr) for each sample by the cellular chlorophyll concentration (pg chlorophyll *a*/cell).

viii. Imaging and cell size

Samples were run daily on an Attune CytPix imaging flow cytometer (Thermo Fisher Scientific, Waltham, MA, USA). *Ochromonas* cells were identified via red fluorescence, and *P. bandaiensis* cells were identified via SYBR staining as described above.

At least 10,000 images were taken of each sample. Images which were identified as *Ochromonas* or *P. bandaiensis* particles were then analyzed using the Attune Cells_Full_Resolution_v23 image processing software packaged with Attune Cytometric Software v.7.1.0. Pictures where the particle overlapped with the border were discarded. As were pictures where more than one particle was identified. Pictures were further filtered by circularity (at least 75%) and the standard deviation of pixel intensity (at least 150) to separate out dead cells, cells with associated bacteria, out of focus cells, and cells attached to TEP or other particles (see Figure 4.5).

The average area of cells identified in the quality-controlled pictures was computed for each sample and converted into spherical biovolume, by assuming the image took a cross-section of a spherical cell.

ix. Elemental analysis

For elemental analysis, GF/D filters (Whatman, Marlborough, MA, USA) were furnaced in aluminum foil at 500 °C for two hours and stored at room temperature in a sealed container before use to remove residual organic matter. On the final day of each experiment, 20 mL of sample were filtered onto the GF/D filters (Whatman, Marlborough, MA, USA) and placed into aluminum foil that had been thoroughly rinsed with HPLC-grade methanol (Fischer Chemical,

Fair Lawn, NJ, USA) to remove residual organic matter on the foil. Filters were then stored at -20 °C.

Before shipping, samples were dried at 50°C overnight and stored in a container with desiccant to ensure stability. Filters (including blanks) were analyzed for carbon, nitrogen, and phosphorus content at Chesapeake Biological Laboratory (Solomon, MD, USA) according to their procedures (www.umces.edu/nasl/methods).

Estimates of cellular biomass for flagellates were calculated using cell volume data (see viii.) and known relationships between biovolume and biomass in nanoflagelletes (Menden-Deuer and Lessard 2000, Liu et al. 2023, Tas 2023).

The inorganic nutrient content of the media was directly calculated from the known K media additions since SOW was devoid of nutrients. The organic nutrient content was computed using previously published elemental analysis of yeast extract (Thompson et al. 2017), the manufacturer specified nitrogen content of tryptone, and the known chemical formulas of all other organics used. Because we assume vitamins are not being catabolized, we do not include vitamins as a major source of carbon or nitrogen in the media. We assume the phosphorus content of tryptone is negligible. The total nitrogen, phosphorus, and organic carbon contents of the media is listed in Table 4.5.

x. Metabolic investments

Total carbon acquisition rate (CAR) was defined by the sum of the carbon obtained from grazing and from photosynthesis (see iv. and v. above). The relative investment in each trophic mode (phagotrophy or phototrophy) is defined as the rate at which carbon was obtained from a single trophic mode over the total rate of carbon acquisition.

Similarly, the carbon use efficiency (CUE), the amount of carbon used for growth versus carbon obtained, was calculated using the following equation:

$$CUE = \frac{\mu}{P + G}$$

For these equations, total carbon obtained via photosynthesis and grazing (P + G) is compared to the carbon used for the observed cell growth (converted from cells into carbon units using the procedure described above). Growth rate is represented by μ. All parameters are measured in units of carbon/cell/day.

Because grazing and photosynthetic rates were not always taken on the same day, if one measurement but not the other was taken on any given day during the non-equilibrium period, the carbon use efficiency was calculated using the average of the other measurement from adjacent days.

xi. Analytical methods

All data analysis was conducted in RStudio (version 2023.12.0) using R (version 4.3.2) or in Microsoft Excel for Microsoft 365 (Version 2502). R analysis utilized the packages readxls (Wickham and Bryan 2025) for importing excel files into R; dplyr (Wickham et al. 2023),

reshape2 (Wickham 2007), and stringr (Wickham 2023) for data handling; ggplot2 (Wickham 2016) to produce figures; and nlstools (Baty et al. 2015) for non-linear analysis. Linear extrapolation of the metabolic landscape (Figure 12) was done using the akima R package (Akima 2025).

Except where stated, all error bars and confidence intervals represent standard error (SE), and statistical significance was determined using an alpha of 0.05.

Results

i. Chemostatic culturing

Chemostats took 4-14 days to reach equilibrium (Figure 4.6). In chemostats where mixotrophs competed with *P. bandaiensis*, both flagellates were able to coexist at equilibrium (Figure 4.6). Bacteria concentrations also reached equilibrium and at similar levels (Figure 4.6C). The one exception was when *P. bandaiensis* was grown alone where bacteria concentrations were lower than chemostats with mixotrophs (Figure 4.6C, $p < 0.001$).

ii. Community composition

The total biomass and production in each chemostat were mainly controlled by the mixotroph, and the mixotroph made up the vast majority of biological carbon in all chemostats where it was present (Figure 4.7). Both strains of *Ochromonas* were larger than *P. bandaiensis* as expected (Figure 4.9C). *Ochromonas* 584 was also larger than 1391 (Figure 4.9C). Interestingly, when in competition both strains of *Ochromonas* and *P. bandaiensis* were larger at equilibrium than when grown alone (Figure 4.9C).

iii. Trophic displacement

In competition with *P. bandaiensis*, *Ochromonas* 1391 and 584 displayed contrasting niche displacement strategies. *Ochromonas* 1391 significantly divested from phagotrophy, growing more autotrophically (Figure 4.8A). Whereas *Ochromonas* 584 increased its relative investment in phagotrophy (Figure 4.8A). In *Ochromonas* 584, these trends were mainly driven by changes in phagotrophy carbon acquisition, as phototrophic carbon acquisition was not significantly different grown alone versus in competition (Figure 4.8).

Changes in photo- versus phagotrophic growth in *Ochromonas* 1391 were illuminated by physiological measurements. *Ochromonas* 1391 had higher photosynthetic rates in competition, corresponding with an increase in chlorophyll *a* content (4.9A). Similarly, *Ochromonas* 1391 had lower ingestion rates in competition corresponding with lower acidic food vacuole content as measured by LysoTracker Green fluorescence (4.9B). The positive relationship between food vacuole content and phagotrophy was also consistent in *Ochromonas* 584 (4.9B). However, *Ochromonas* 584 significantly decreased its investment in chlorophyll in competition (4.9A). This mirrors its increase in relative investment in phagotrophy under competition but contrasted with its similar rates of primary production to when 584 was grown alone (Figures 4.8A, 4.9A). These dynamics demonstrate *Ochromonas* 584 had higher electron transport rates (ETRs) in competition ($p < 0.05$).

We did not measure the grazing rates of *P. bandaiensis* through the course of our experiment, due to difficulties in differentiating this species from bacteria using flow cytometry without nucleic acid stains, which shared fluorescence emission spectra with CMFDA used for staining FLB. However, if we use acidic food vacuole content as a proxy for phagotrophy, we can assume *P. bandaiensis* increased its ingestion rate in competition with *Ochromonas* 1391, but not *Ochromonas* 584 (Figure 4.9B).

iv. Growth efficiency and metabolic landscapes

Overall, *Ochromonas* 1391 had a higher carbon use efficiency than *Ochromonas* 584 (Figure 4.10). The average carbon use efficiency of both strains of *Ochromonas* declined in competition with *P. bandaiensis*, though the change was only significant in *Ochromonas* 584 (Figure 4.10). *Ochromonas* 584, but not 1391, exhibited a significantly negative relationship between relative investment in phagotrophy and growth efficiency (Figure 4.11).

A quadratic model on all observations over the duration of the experiment predicts a maximum carbon use efficiency of 0.654 at a relative investment in phagotrophy of 53.05% ($p = 0.2662$) for *Ochromonas* 1391 (Figure 4.11A). This is remarkably similar to the 0.631 ± 0.042 carbon use efficiency observed at equilibrium when 1391 is grown alone (Figures 4.8A, 4.10). Alone *Ochromonas* 1391 had an average phagotrophic investment, or percent of total carbon obtained that was obtained via phagotrophy, of 37.02 ± 2.83% (Figure 4.8A). But, because of the model's predicted weak relationship between phagotrophic investment and carbon use efficiency, at the observed relative phagotrophic investment of 37.02%, our model predicts a carbon use efficiency of 0.646, again similar to the observed carbon use efficiency 0.631 of in *Ochromonas* 1391 (Figures 4.8A, 4.10, 4.11A).

Applying a similar quadratic model to *Ochromonas* 584 revealed a negative relationship between increased investment in phagotrophy and growth efficiency over the conditions tested in this experiment ($p < 0.0001$, Figure 4.11B). Our model predicts a maximum carbon use efficiency of 0.662 at a relative investment in phagotrophy of 11.90%. This is well above the observed growth efficiencies and well below the observed relative phagotrophic investment of *Ochromonas* 584 both alone and in competition at equilibrium (Figures 4.8, 4.10). At equilibrium, *Ochromonas* 584 obtains 73.53 ± 1.82% of its carbon from phagotrophy when grown alone and 82.19 ± 2.70% in competition. Our model predicts carbon use efficiencies of 0.338 and 0.240 in these treatments respectively. These align well with the observed carbon use efficiencies in *Ochromonas* 584 at equilibrium of 0.333 ± 0.027 grown alone and 0.271 ± 0.018 in competition.

To examine the tradeoffs of mixotrophic metabolism and plasticity, we wanted to investigate three key related variables for each mixotroph: phagotrophic carbon capture, phototrophic carbon capture, and carbon use efficiency. Combining all observations of carbon acquisition for each strain, we created a 3D surface via linear extrapolation and visualized it using contour plots (Figure 4.12). We call this each mixotroph's metabolic landscape.

This analysis supports that while *Ochromonas* 1391 occupied a more contained metabolic space over the course of the experiment, it was more successful in retaining high carbon use efficiencies regardless of relative investment between trophic modes (Figure 4.12). Similarly, the

trade-off between phagotrophic growth and carbon use efficiency in *Ochromonas* 584 can be visualized by the horizontal bands in decreasing carbon use efficiency as phagotrophy increased in Figure 4.12B.

For further analysis we assembled an extrapolated 3D surface at a scale of 0.01 pg photosynthetic carbon per cell per day by 0.01 pg phagotrophic carbon per cell per day. *Ochromonas* 1391 had a much smaller observed metabolic space than 584. The area where the model predicted 90% or higher growth efficiency, as well as 80% or higher growth efficiency, was significantly larger in *Ochromonas* 1391 than 584 ($p < 0.001$).

Discussion

In this study, we observed that the trophic displacement of closely related mixotrophs allowed them to remain competitive in mixed environments, and how the new realized niches affected their metabolism. Previous studies on mixotrophs tend to treat mixotrophic metabolic tradeoffs as a problem of resource partitioning between trophic modes and assume mixotrophic investment is fixed over the lifetime of an organism (Berge et al. 2017, Edwards 2019). Yet, other research suggests the eco-evolutionary tradeoffs to mixotrophy may be rooted in synergies, not penalties, from the possession of two trophic pathways and competitive benefits and disadvantages may be emergent properties of the trophic plasticity inherent in many constitutive mixotrophs (Chu, Moeller, and Archibald 2023, Mitra and Flynn 2023, Archibald et al. 2024). Reconciling the perceived costs and the eco-evolutionary advantages of dual metabolisms is a vital question in the field of mixotrophy (Millette et al. 2024). How these tradeoffs manifest have an impact on the nutrient cycling and ecosystem structure of aquatic communities (Livanou et al. 2020, Mitra and Flynn 2023, Archibald et al. 2024, Millette et al. 2024). Our study provides insight into how constitutive mixotrophs utilize their trophic duality to persist in competitive environments and the associated costs.

i. Trophic displacement due to competition explained through metabolic landscapes

The contrasting response to competition between *Ochromonas* 1391 and 584 is informed by the metabolic landscape and requirements of each strain. The shape of trophic investment in the metabolic landscape of *Ochromonas* 1391 reveals an ability to supplement a loss in phagotrophy with increased phototrophic investment without losing growth efficiency (Figure 4.12). This explains the displacement from a more phagotrophic to a more phototrophic mode in equilibrium in response to competition with a single-guild phagotroph (Figure 4.8). It can also explain why the carbon use efficiency of 1391 did not decrease due to competition (Figure 4.10). Whereas in *Ochromonas* 584 the tradeoff between phagotrophic investment and growth efficiency is highly negative (Figure 4.11, Figure 4.12). The investment in photosynthesis does not have the same tradeoff (Figure 4.12).

A metabolic landscape of this shape at first glance suggests a divestment from phagotrophy, similar to 1391, could improve 584's competitive dynamics. However, unlike *Ochromonas* 1391, 584 is an obligate phagotroph and thus presumably must satisfy certain metabolic requirements through phagotrophy, limiting its ability to divest from this trophic mode. *Ochromonas* 584 has also been shown to have a negative relationship between phagotrophy and phototrophy, where

direct investment in one trophic strategy leads to a characteristic divestment in the other (Barbaglia et al. 2024). In competition with *P. bandaiensis*, *Ochromonas* 584 presumably must more actively compete, not only for prey availability, but possibly also for ingestion of higher quality prey. If this requires a greater investment in phagotrophy, with 584's negative relationship between trophic investments, this explains the decrease in phototrophy we observed (Figure 4.8). And, with *Ochromonas* 584's decreasing growth efficiency as phagotrophic investment increases, this may underlie the decreasing growth efficiency from competition (Figure 4.8, 4.11, 4.12).

This result is contrary to the traditional view of mixotrophic niche displacement strategies where mixotrophs invest relatively more in the trophic strategy where competition is lowest (Jost et al. 2004, Chu, Moeller, and Archibald 2024). However, this 'doubling down' in response to competition agrees with more recent studies showing, under some conditions, the optimal strategy for mixotrophs is to increase investment in the more limiting trophic mode (Moeller et al. 2024, Jahns and Johnson *in prep*). Such dynamics could be driven by prey nutritional requirements and diminished returns on phagotrophic investment due to competition for active prey, however we did not assess qualitative changes in the bacterial prey community. Because our chemostats were maintained under phosphorous (P) limitation, P content of prey may have played a major role in driving 584 towards increased phagotrophy.

The high prey requirements of *Ochromonas* 584 compared to 1391 are further reflected in the higher grazing rates and lower equilibrium bacteria concentrations when grown alone (Figures 4.7, 4.8). While *Ochromonas* strains in competition did not differ in their bacteria concentration, bacteria were more abundant in chemostats where *Ochromonas* 1391 was grown alone and grazed less than 584 across all treatments, suggesting 1391 has lower prey requirements in these conditions (Figures 4.7, 4.9, 4.10, 4.12). If this is true, being a facultative phagotroph likely protects it from needing to 'double down' on less efficient trophic strategies in competitions. For the obligate phagotroph, *Ochromonas* 584, even small metabolic displacement causes decreased growth efficiency. *Ochromonas* 1391, on the other hand, displayed lower energy costs related to its metabolic plasticity.

Chu, Moeller, and Archibald (2023) parameterized this trait in a model as 'z' which represented the shape of the tradeoff between relative investment in phagotrophy and attack rate. A 'generalist' mixotroph would have a lower decline in attack rate than a 'specialist' if both divested equally in energy from phagotrophy. In this framework, *Ochromonas* 1391 could be classified as a generalist mixotroph as its carbon use efficiency remained high no matter its relative investment in phagotrophy. On the other hand, *Ochromonas* 584 experienced a sharp tradeoff between investment in phagotrophy and energy efficiency, categorizing it as a 'specialist'. Notably however, the Chu, Moeller, and Archibald (2023) model predicts a shift away from the more competitive trophic mode in all mixotrophs in response to competition with a single-guild competitor which we did not see in our chemostats.

ii. Mechanisms underlying metabolic tradeoffs

If energy efficiency and prey requirements can partially explain observed niche displacement in *Ochromonas* in response to competition, the next question is why?

While *Ochromonas* 584 showed decreasing carbon efficiency in response to competition, it was not carbon limited (Table 4.5). More likely, *Ochromonas* 584's prey requirement was dictated by a need for another limiting nutrient. While it is possible *Ochromonas* 584 required a vitamin or other vital compound that cannot be produced by photosynthesis, we find it more likely that *Ochromonas* 584 relies on prey for phosphorus in the phosphorus scare media in which *Ochromonas* was grown (Table 4.5). *Ochromonas* 1391 is likely able to either better obtain or more efficiently utilize dissolved phosphorus obtained via uptake than 584. This meant *Ochromonas* 584 could not divest from phagotrophy under competition. However, this does not explain the increased grazing.

Obligately phagotrophic mixotrophs have been shown to benefit from doubling-down on grazing when both nutrients and prey are limiting, as they are here (Moeller et al. 2024, Table 4.5). While the model of Moeller et al. (2024) used nitrogen limitation its reasoning applies equally well to phosphorus limitation. Interestingly though, the increased investment in phagotrophy described by Moeller et al. (2024) occurred through differences in the availability of bacteria, while we observed similar bacterial concentrations at equilibrium when *Ochromonas* 584 competed with *P. bandaiensis* compared to *Ochromonas* 584 in culture by itself (Figure 4.7).

Chemostats were grown xenically with a natural community of bacteria. Assuming different bacteria have different nutritional qualities, it is possible that the voracious grazer *P. bandaiensis* removed many of the highest quality prey forcing the increased grazing in *Ochromonas* 584 in competition (Selph, Landry, and Laws 2003). Foster and Chrzanowski (2012) found that prey quality was vitally important to the fitness of another strain of *Ochromonas*.

Cell-size is a complicating factor in this analysis. Phytoplankton cell size tends to decrease under nutrient limitation, like the phosphorus-scarce environment tested here (Higini Peter and Sommer 2013). *Ochromonas* 1391 did not change in cell size due to competition, while *P. bandaiensis* did decrease in size due to competition (Figure 4.9). However, the size of *Ochromonas* 584 increased in competition with *P. bandaiensis* (Figure 4.9). This may suggest that *Ochromonas* 584 was more carbon limited in competition, or perhaps limited in a compound such as a vitamin, cofactor, or fatty acid, as opposed to phosphorus.

Whatever underlies the metabolic inefficiency of increased phagotrophic investment in *Ochromonas* 584 (i.e. Figure 4.11B), it seems apparent that *Ochromonas* 584 was pushed to the edge of its ability to remain competitive in this environment (Figure 4.12). While *Ochromonas* 584, more so than 1391, remained dominant in competition with *P. bandaiensis* and suppressed the growth of *P. bandaiensis*, at a certain point it would presumably become limited, in the ability to find and ingest enough prey to support its growth, or perhaps the intracellular space or resources needed to produce and process the many food vacuoles(Figure 4.6).

We did not observe the limits of *Ochromonas* 1391's metabolic investment and growth efficiency. Future studies should investigate whether increased pressure for phototrophic resources in competition with a single-guild phototroph causes metabolic efficiency tradeoffs in doubling-down analogous to *Ochromonas* 584 in competition with the single-guild phagotroph *P. bandaiensis*.

Despite the longstanding view of tradeoffs between dual trophic modes and trophic efficiency, we find that there are contours of the metabolic space of both strains of *Ochromonas* along which *Ochromonas* can achieve high grazing or photosynthetic rates without losing energetic efficiency (Figures 4.11, 4.12). Further, while there are observable energetic tradeoffs to metabolic plasticity, these tradeoffs do not always manifest in relative metabolic investment between phototrophy and phagotrophy (Figure 4.11, 4.12). This further supports the growing body of research suggesting that, if mixotrophs are less efficient than single-guild competitors, tradeoffs associated with mixotrophic metabolism are more likely an emergent property from their complex metabolism than a direct penalty due to the maintenance of dual trophic pathways (Barbaglia et al. 2024, Flöder et al. 2024, Chu, Moeller, and Archibald 2024, Archibald et al. 2024).

What tradeoffs exist do not appear related to increased basal metabolic costs (Raven 1997), as metabolic efficiency was able to stay the same or, in some dimensions for *Ochromonas* 1391, increase with increased investment in phototrophy and/or phagotrophy (Figure 4.12). We find that proposed hypotheses of mixotrophic tradeoffs in membrane space are also unlikely (Ward et al. 2011). *Ochromonas* has not been shown to ingest more than one prey at a time and often feeds via ambush feeding (personal observation). Thus, there is an upper limit on the membrane-space return-on-investment in *Ochromonas* for phagotrophy. Yet, we saw the greatest trade-offs in increased investment in phagotrophy in this environment (Figure 4.12). On the other hand, the amount of phosphorus needed for photosynthetic growth is believed to be roughly proportional to its carbon fixation rate (Armin, Kim, and Inomura 2023). Alternatively, Ward et al. (2011) also predicted in low-nutrient environment, mixotrophs could increase efficiency by not needing to invest more in phosphorus-uptake transporters since such uptake is diffusion not transporter limited. This may be reflected in the only minor costs to increasing phototrophic investment in our mixotrophs grown in this P-limited media (Figure 4.12).

iii. Community-level impacts

Total biological carbon in each chemostat was dictated by which mixotroph was present. Many studies predict increased community production with the inclusion of mixotrophs in mixed community models (Hammer and Pitchford 2005, Ward and Follows 2016). However, we found no significant differences in equilibrium carbon concentration when *Ochromonas* was grown alone or in competition (Figure 4.7). Further, although *Ochromonas* 584 grew more phagotrophically and had lower carbon use efficiencies, chemostats containing *Ochromonas* 584 had the highest total biomass (Figures 4.7, 4.10). We infer that as *Ochromonas* 584 had higher growth rates in the pre-equilibrium period of the experiment, it was able to reach a higher total biomass at carrying capacity and obscure any productivity difference that we may have been able to observe otherwise (Figure 4.6).

The presence of the mixotroph greatly suppressed the yield of the grazer, *P. bandaiensis* (Figures 4.6, 4.7). Despite *P. bandaiensis* having higher grazing rates than *Ochromonas*, the prey-limited environments, combined with the inability to relieve the competitive pressures through another nutritional source and being less metabolically plastic, decreased the fitness of *P. bandaiensis* (Selph, Landry, and Laws 2003). This is in line with other studies which have shown the

advantages of mixotrophy over pure heterotrophy in highly limiting environments (Ward et al. 2011, Edwards 2019).

Bacteria concentrations were also higher in cultures where a mixotroph was present than with *P. bandaiensis* alone. This again could be an artefact of the high growth rates, high grazing rates, and shorter time to reach equilibrium of *P. bandaiensis*. Alternatively, this may reflect the release of organic carbon from the mixotrophs that stimulated bacterial growth. The growth of the bacteria in chemostats were controlled in part by organic carbon availability (Table 4.5). Mixotrophs can contribute to the microbial loop by transforming inorganic carbon otherwise inaccessible to heterotrophic bacteria and excreting organic compounds, thus increasing the carbon available for bacterial growth (Azam et al. 1983, Worden et al. 2015, Gilbert and Mitra 2022). This may explain why bacterial concentrations were significantly higher when *Ochromonas* 1391 was grown alone, as its excretions contributed greatly to bacterial growth and the bacteria experienced less top-down pressure due to *Ochromonas* 1391 low grazing rate relative to *P. bandaiensis* and *Ochromonas* 584 (Selph, Landry, and Laws 2003, Figure 4.7, 4.8).

Ultimately, the most productive mixotroph in terms of the balance of carbon fixation to respiration was *Ochromonas* 1391. This is unsurprising because *Ochromonas* 1391 was generally more autotrophic and had higher growth efficiencies than *Ochromonas* 584. Additionally, as a more phagotrophic specialist, *Ochromonas* 584 experienced a greater carbon efficiency penalty in competition with *P. bandaiensis* than *Ochromonas* 1391. It would be interesting to observe if the opposite pattern exists when *Ochromonas* 1391 competes with a solely phototrophic organism.

iv. Evolutionary implications

Ochromonas 1391 and 584 have nearly identical 18S ribosomal RNA sequences (Barbaglia et al. 2024). Both strains were isolated from the same location in the Sargasso Sea at the same time (NCMA 2025) and thus were presumably subject to similar evolutionary pressures. Yet, the metabolic strategies and responses to competition of these strains are distinct (Figures 4.8, 4.11, 4.12).

The evolutionary drivers of mixotrophic metabolism are elusive, but this is perhaps not surprising considering the immense diversity of mixotrophs and the complexities of integrated organismal metabolism (Millette et al. 2024). Archibald et al. (2024) suggest a potential mechanism for the coexistence of diverse mixotrophs could be the time it takes mixotrophs to remodel their metabolism to shifting environmental conditions. Such a response is difficult to measure and assumes the coexistence of mixotrophs that occupy similar metabolic landscapes and with identical tradeoffs. While both strains here reached equilibrium around the same time, this is dictated by their growth, not necessarily their metabolic activity (Figure 4.6). That said, in equilibrium investments in phototrophy and phagotrophy were stable.

Though ribosomal 18S sequences suggest close evolutionary relationships between *Ochromonas* 1391 and 584, we cannot rule out that these strains are unique species. Other studies have demonstrated even organisms with extremely similar 18S sequences may have more diverse evolutionary relationships revealed through the sequencing of other loci (Schoenle et al. 2025). It

is possible that the metabolic preferences of these strains are a result of events that occurred after the divergence of these strains from their ancestor which pushed them into different evolutionary trajectories. Alternatively, these two strains were found in the same environment and niche filling pressures may have driven their divergence as both organisms compete for the same limited resources (White and Butlin 2021).

v. Summary

These results underscore the need to take organismal metabolism into account when modeling community production and competitive dynamics. The metabolic landscapes of mixotrophs are more informative than simple relationships between fitness, environment, and growth efficiencies. There exists a multidimensional trophic space which mixotrophs leverage to compete with single-guild organisms. Following the results of Jahns and Johnson (*in prep*), this study shows that even in steady-state environments competitors affect the trophic modes of mixotrophic organisms. As an increasingly large body of research suggests, mixotrophs, and the ways they modulate their metabolism, play key roles in our aquatic ecosystems, and to understand their impact and dynamics direct competition experiments coupled with the quantification of trophic energy capture are vital.

Acknowledgements

I'd like to thank Paul Berube for sharing his chemostat expertise with me and helping me with the sampling port design. Holly Moeller's guidance on photo-physiology, *Ochromonas* behavior, and overall scientific advice were indispensable. I'd also like to the entire Johnson Lab – Matt, Sophia, Brittany, and Julia – for keeping me sane during this process and lending a hand when they could.

This work was made possible by the generous support of the Woods Hole Oceanographic Institution's Ocean Venture Fund. Max Jahns's gradate stipend was funded in part by an NSF Graduate Fellowship.

Figures

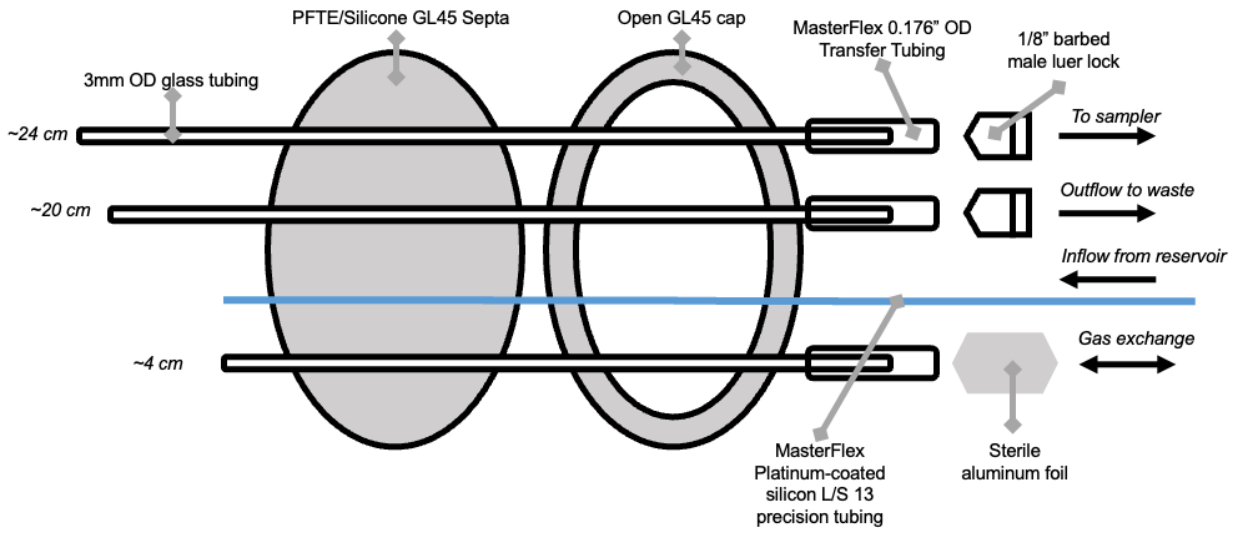

Figure 4.1 Schematic of chemostat vessel cap. See Table 4.2 for a list of parts used.

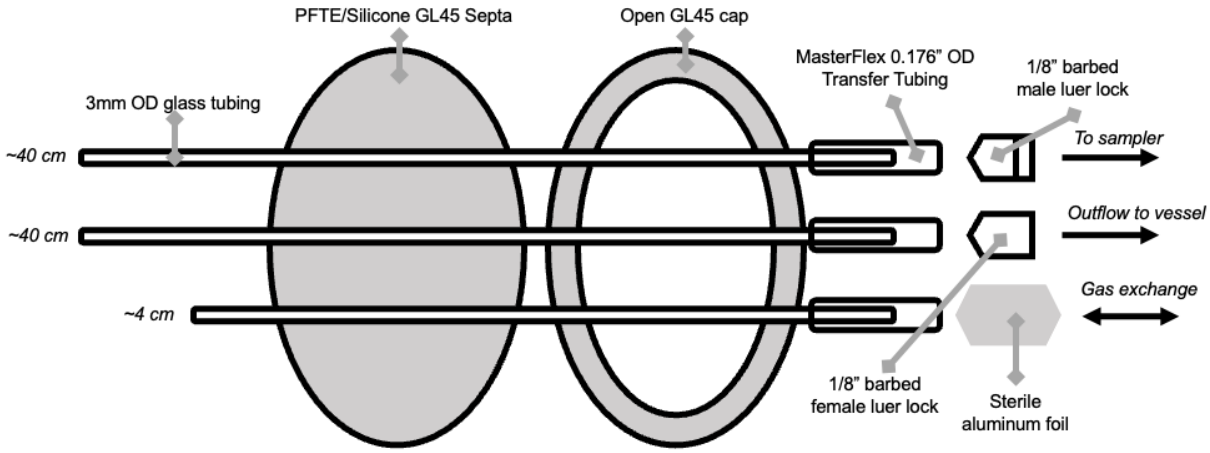

Figure 4.2 Schematic of chemostat reservoir cap. See table 4.2 for list of parts used.

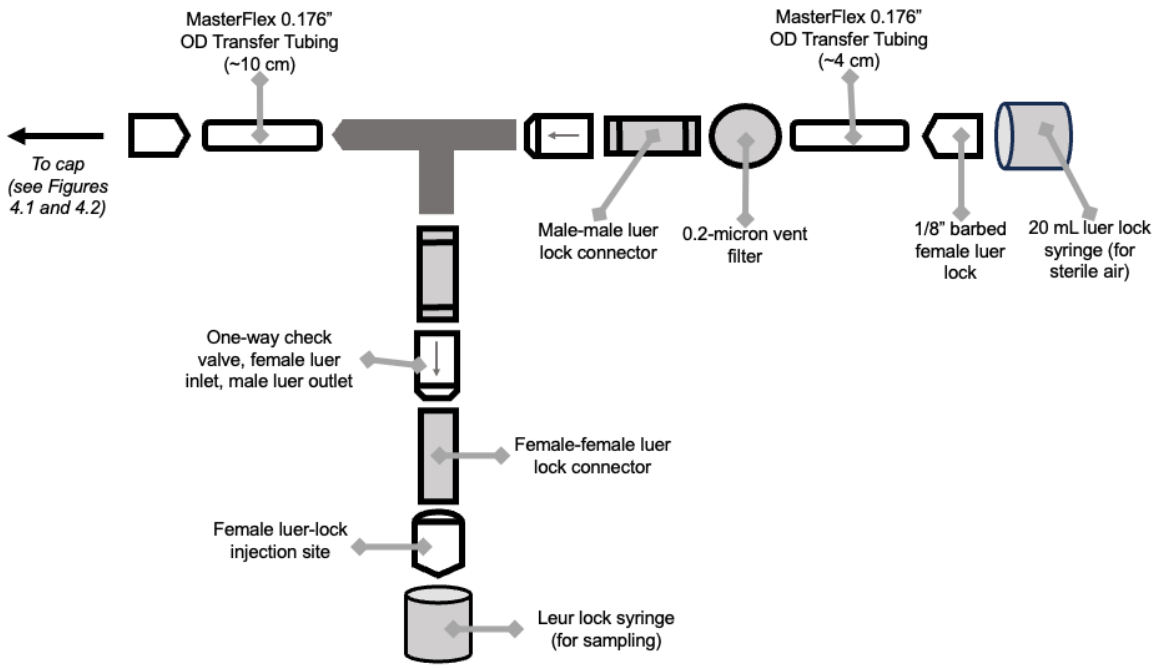

Figure 4.3 Schematic of sterile sampling system. See Table 4.2 for a list of parts used.

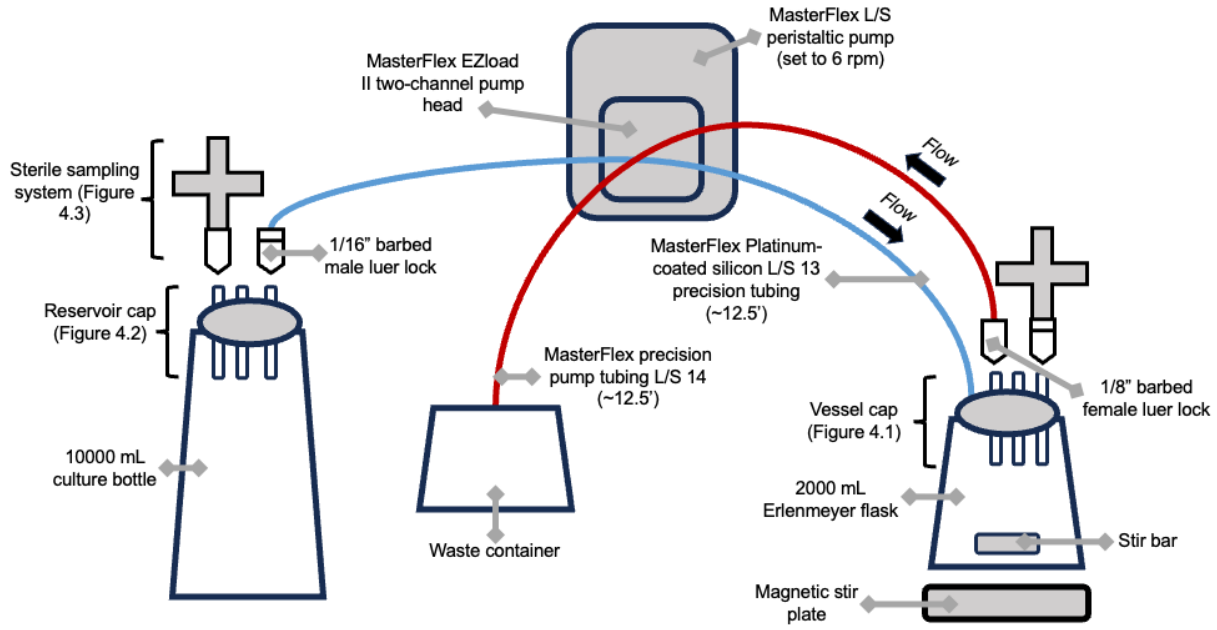

Figure 4.4 Schematic of chemostat assembly and flow. See Table 4.2 for a list of parts used.

4.5A

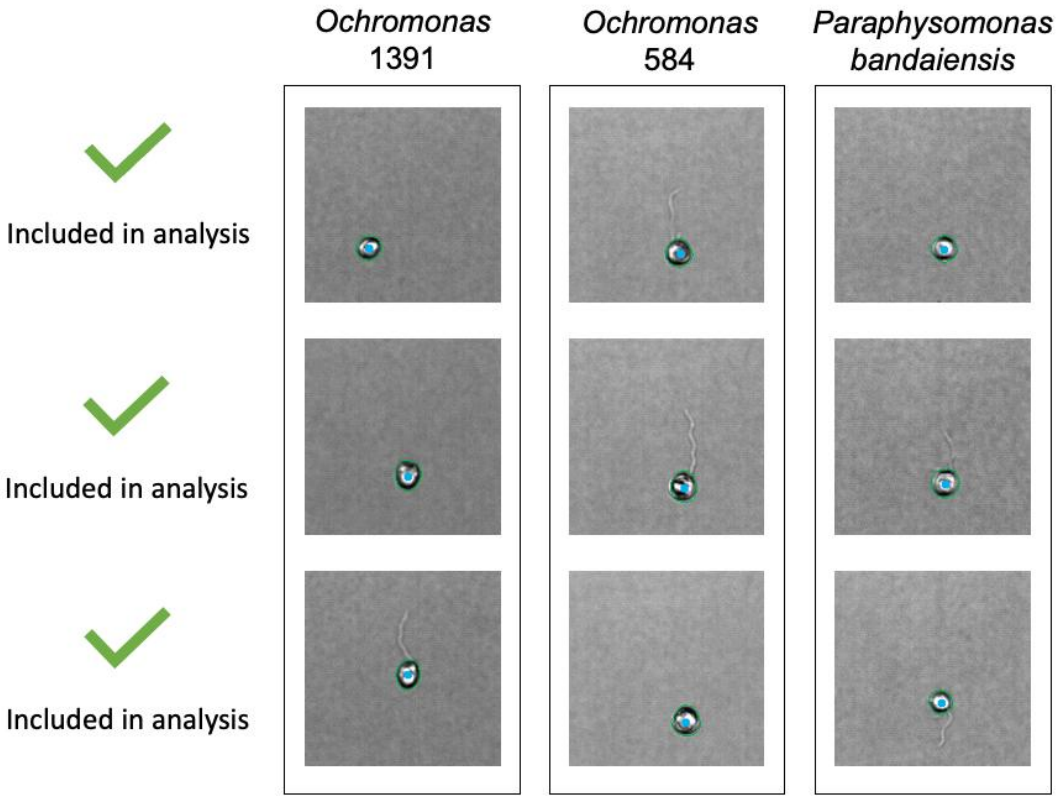
Ochromonas 1391
Ochromonas 584
Paraphysomonas bandaiensis
Included in analysis
Included in analysis
Included in analysis

4.5B

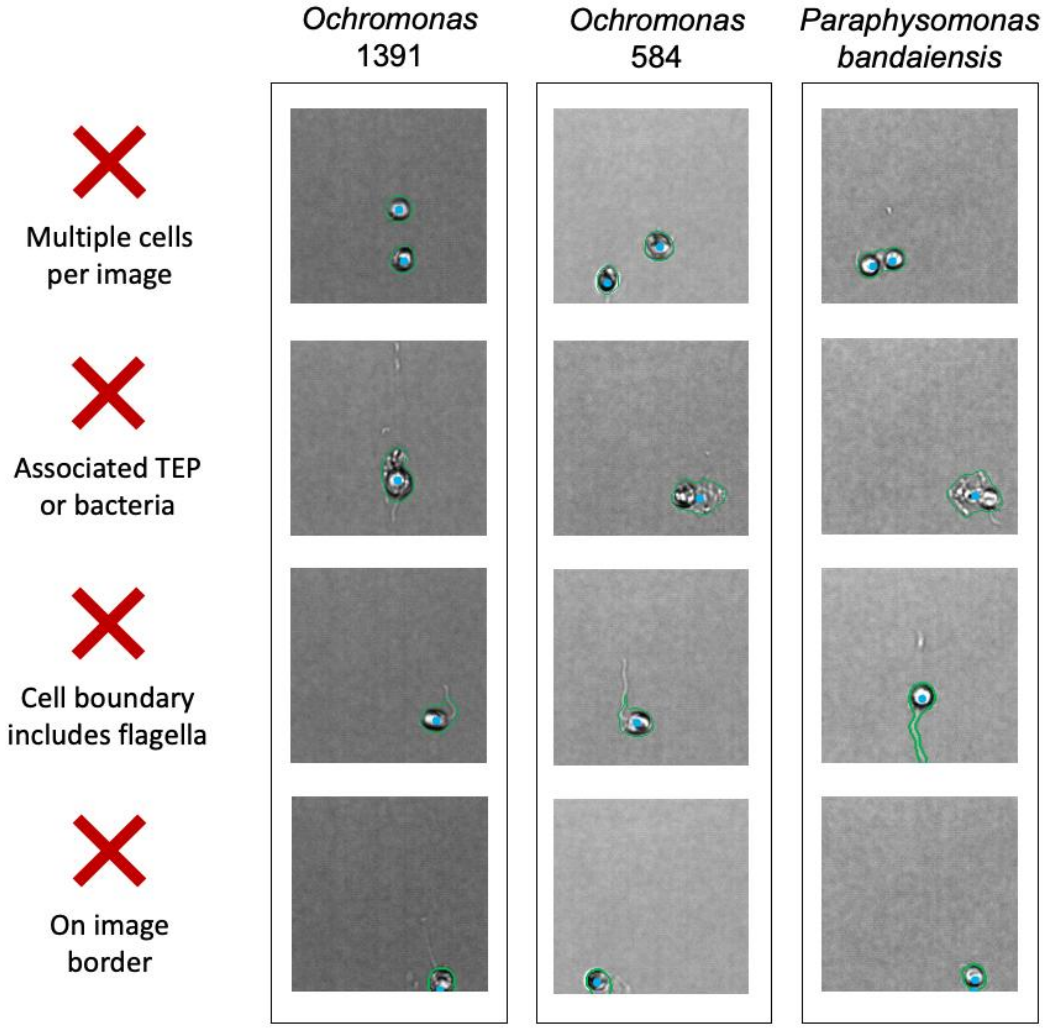

Figure 4.5 Example processed images of *Ochromonas* 1381, *Ochromonas* 584, and *P. bandaiensis* that were (A) included in analysis or (B) excluded from analysis. Colored lines are the boundary (green) and centroid (blue) of the cell as determined by the Attune Cells_Full_Resolution_v23 image processing algorithm.

4.6A

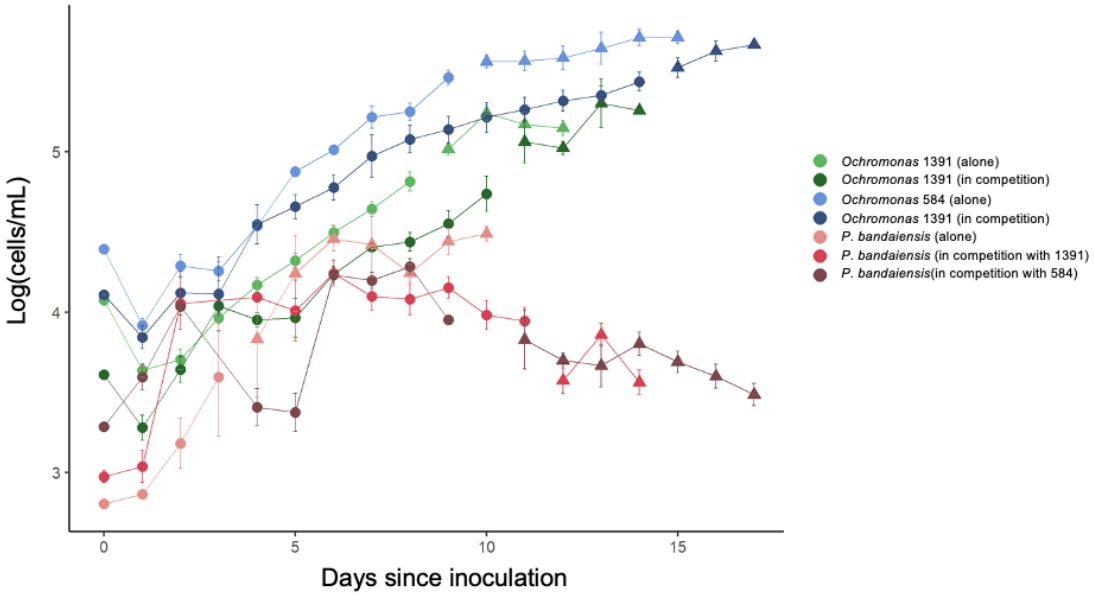
Log(cells/mL)
5
4
3
0
5
10
15
Days since inoculation
Ochromonas 1391 (alone)
Ochromonas 1391 (in competition)
Ochromonas 584 (alone)
Ochromonas 1391 (in competition)
P. bandaiensis (alone)
P. bandaiensis (in competition with 1391)
P. bandaiensis(in competition with 584)

4.6B

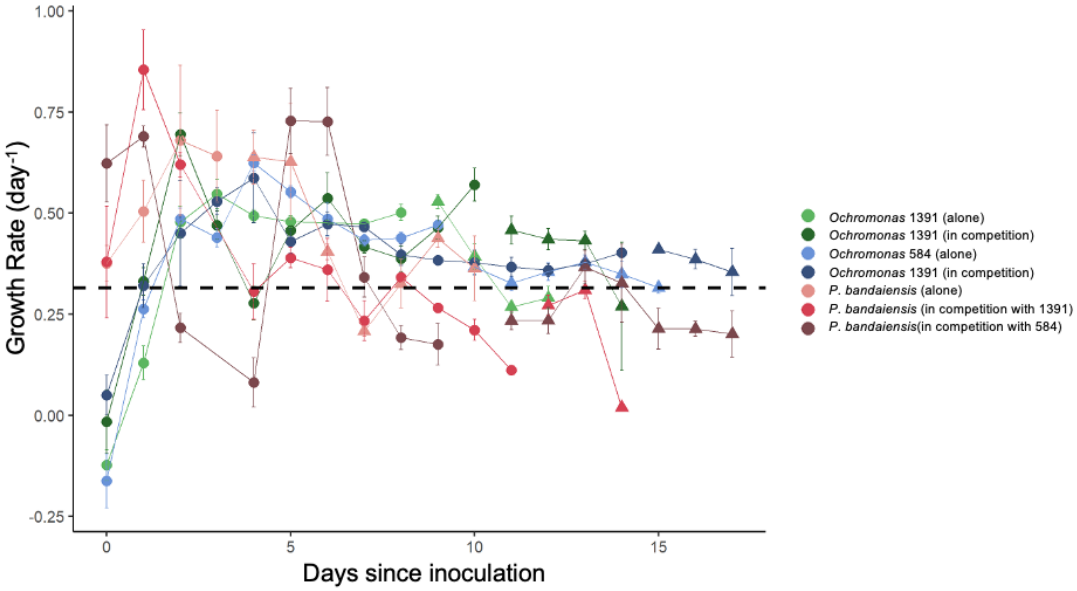
Growth Rate (day-1)
1.00
0.75
0.50
0.25
0.00
-0.25
0
5
10
15
Days since inoculation
Ochromonas 1391 (alone)
Ochromonas 1391 (in competition)
Ochromonas 584 (alone)
Ochromonas 1391 (in competition)
P. bandaiensis (alone)
P. bandaiensis (in competition with 1391)
P. bandaiensis(in competition with 584)

4.6C

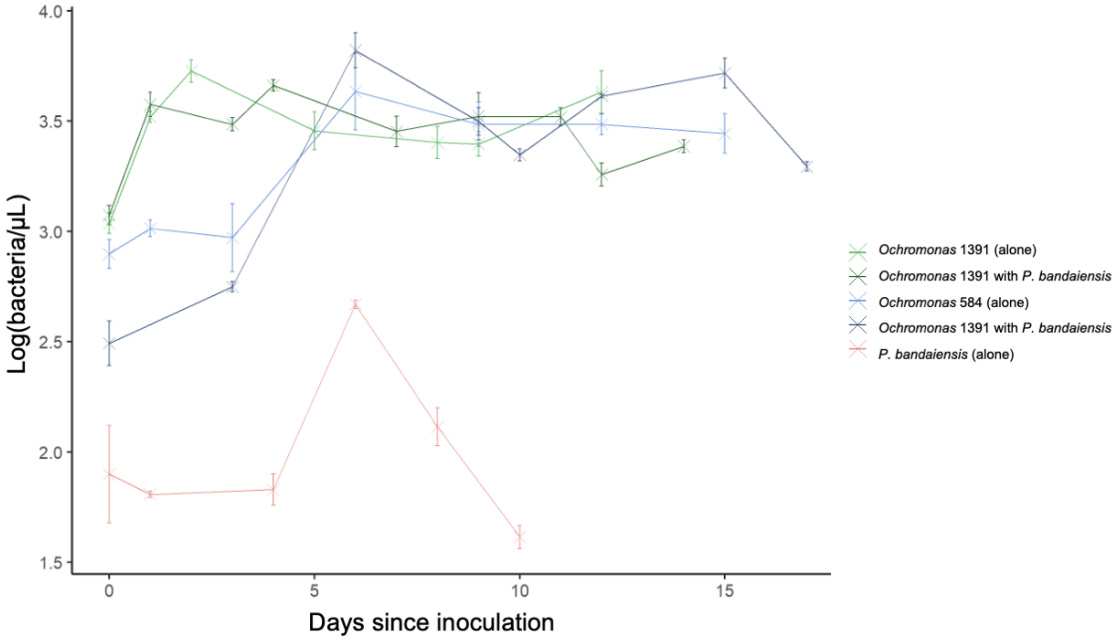

4.6D

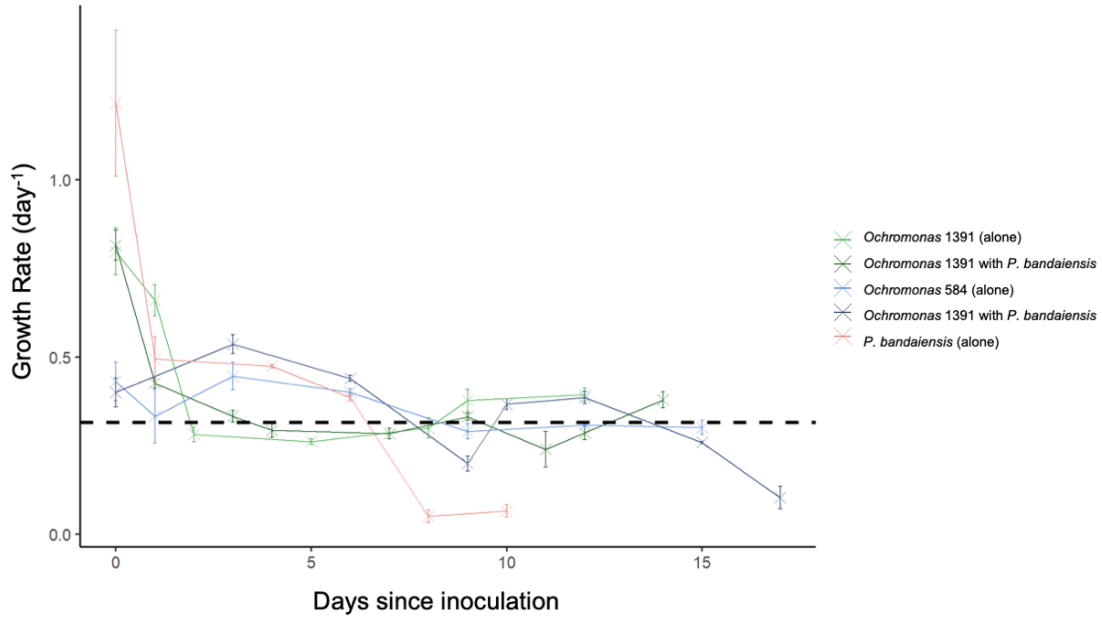

Figure 4.6 (A,C) Concentration (in log cells per mL) and (B,D) growth rate of (A,B) flagellate cells and (C,D) bacteria over the course of the experiment. Colors correspond to the treatment and flagellate counted. For flagellate cells (A,B), the equilibrium period is denoted with triangles (▲) while non-equilibrium points are circles (●) (see Methodology.*v.*). The dashed line is the dilution rate (0.315 day^{-1}).

4.7A

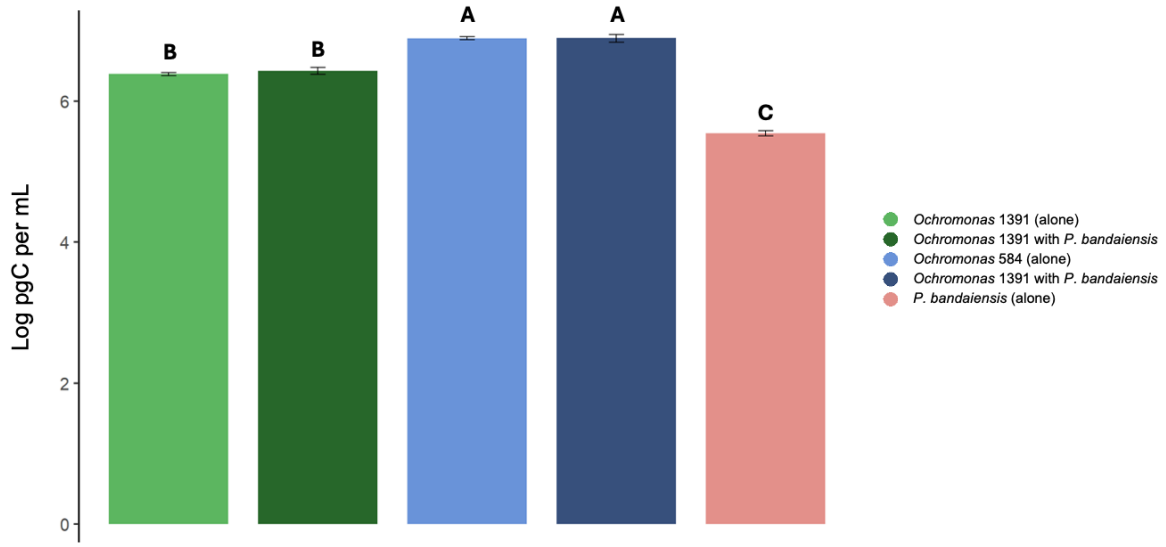

4.7B

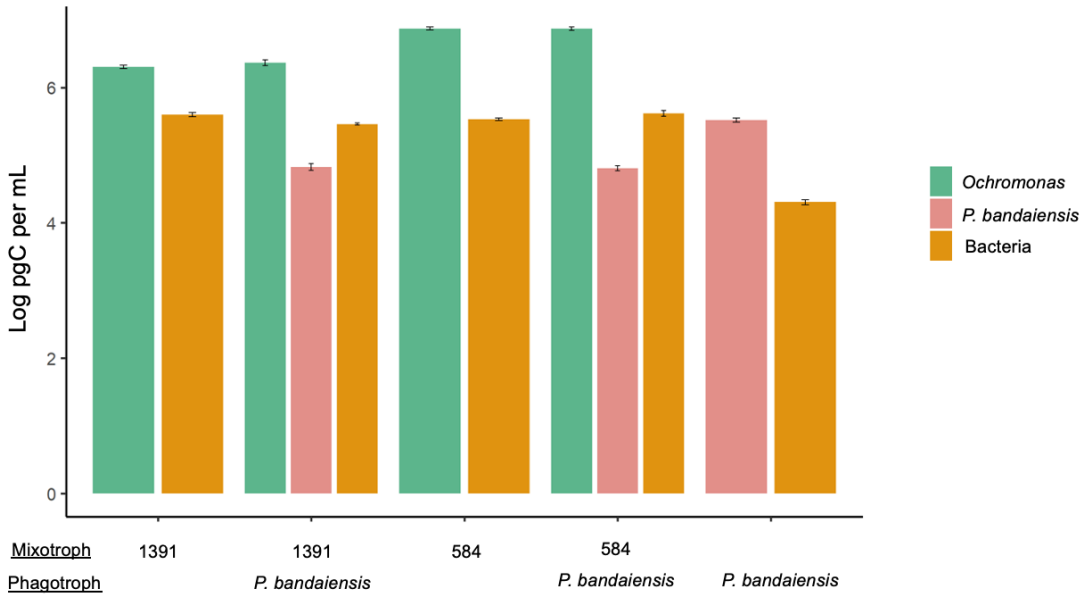

Figure 4.7 The concentration of (A) total biological carbon and (B) biological carbon in each competitor in chemostatic cultures at equilibrium. Letters indicate significantly different groups according to Tukey's Honestly Significantly Different test (HSD test) ($p < 0.05$).

4.8A

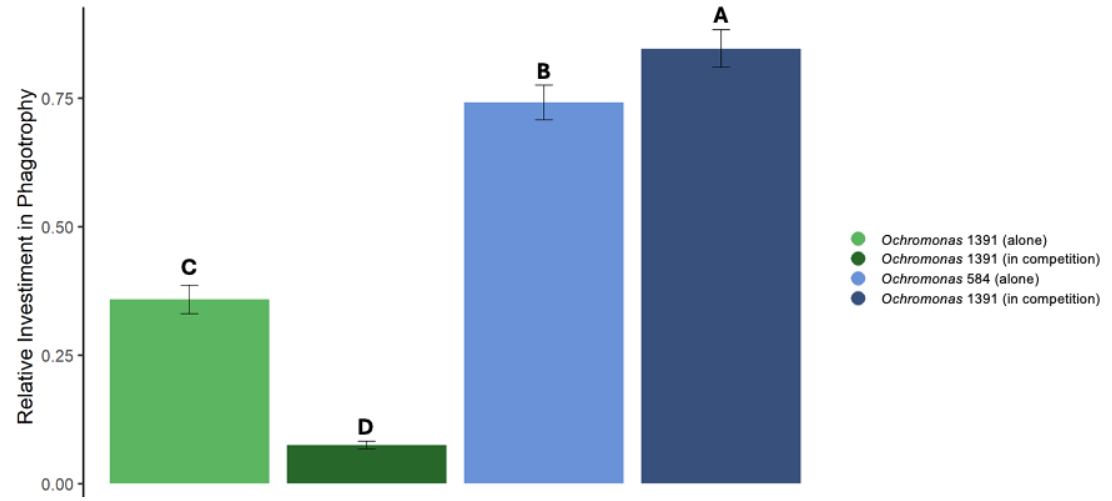
Relative Investiment in Phagotrophy
0.00
0.25
0.50
0.75
C
D
B
A
Ochromonas 1391 (alone)
Ochromonas 1391 (in competition)
Ochromonas 584 (alone)
Ochromonas 1391 (in competition)

4.8B

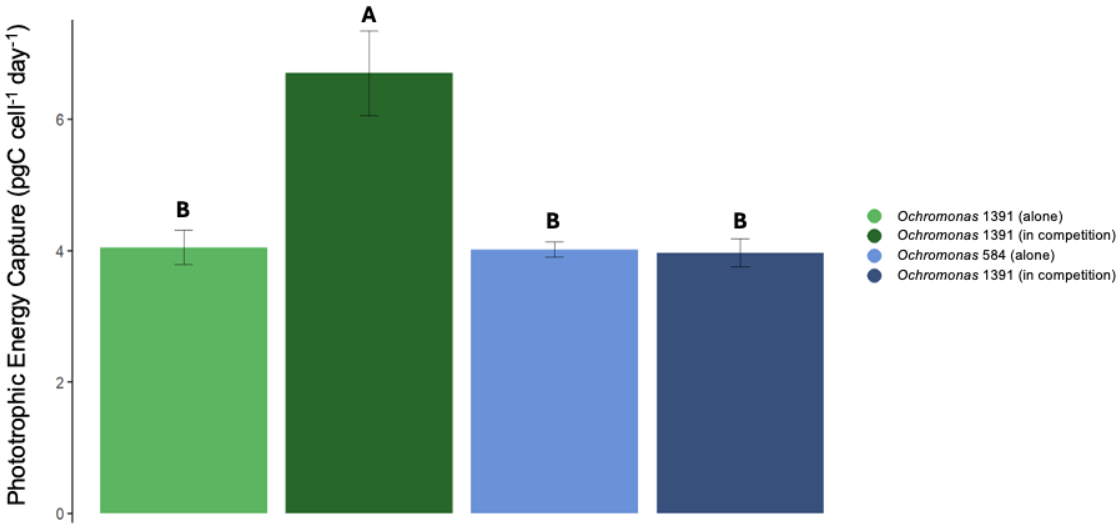
Phototrophic Energy Capture (pgC cell-1 day-1)
0
2
4
6
B
A
B
B
Ochromonas 1391 (alone)
Ochromonas 1391 (in competition)
Ochromonas 584 (alone)
Ochromonas 1391 (in competition)

4.8C

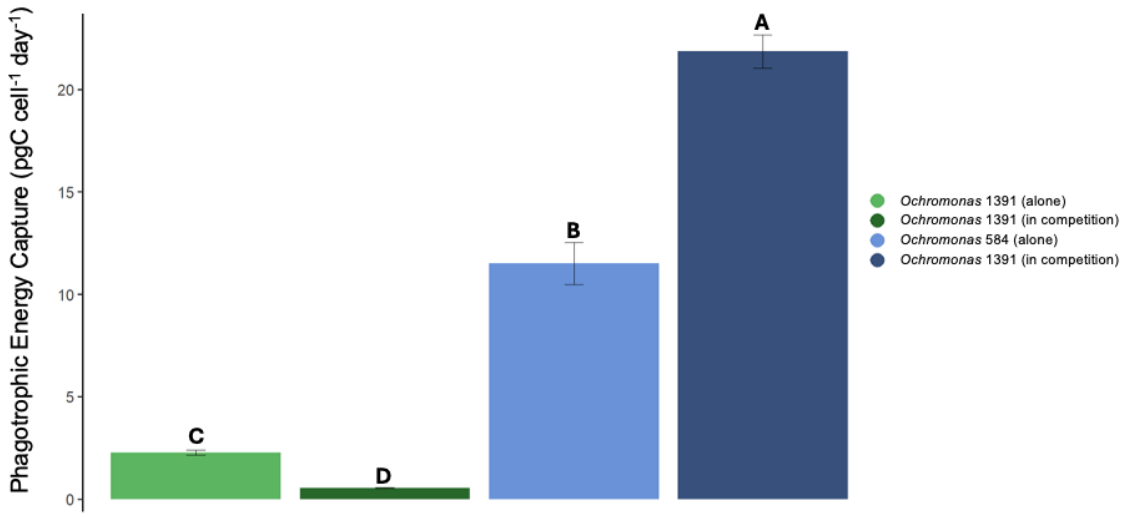

Figure 4.8 The relative investment in phagotrophy (A), phototrophic carbon acquisition (B) and phagotrophic carbon acquisition (C) per cell per day in *Ochromonas* at equilibrium. Letters indicate significantly different groups according to Tukey's Honestly Significantly Different test (HSD test) ($p < 0.05$).

4.9A

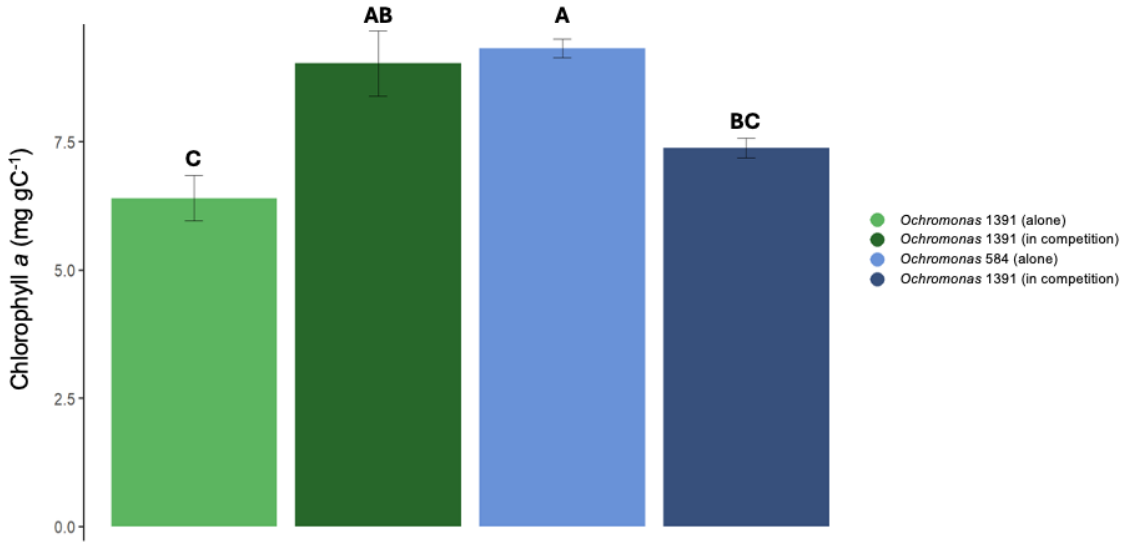
Chlorophyll a (mg gC-1)
0.0
2.5
5.0
7.5
C
AB
A
BC
Ochromonas 1391 (alone)
Ochromonas 1391 (in competition)
Ochromonas 584 (alone)
Ochromonas 1391 (in competition)

4.9B

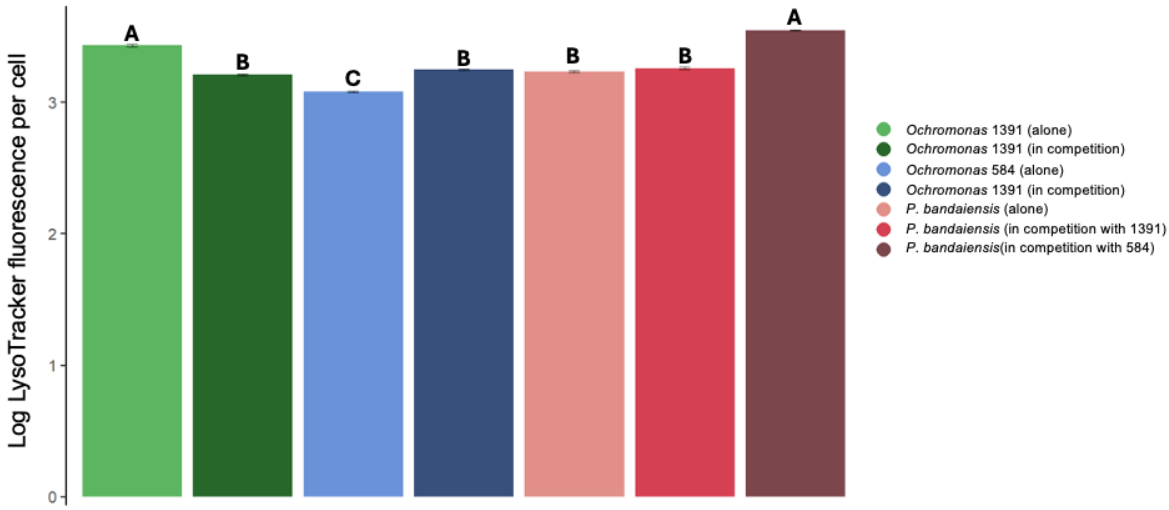
Log LysoTracker fluorescence per cell
0
1
2
3
A
B
C
B
B
B
A
Ochromonas 1391 (alone)
Ochromonas 1391 (in competition)
Ochromonas 584 (alone)
Ochromonas 1391 (in competition)
P. bandaiensis (alone)
P. bandaiensis (in competition with 1391)
P. bandaiensis(in competition with 584)

4.9C

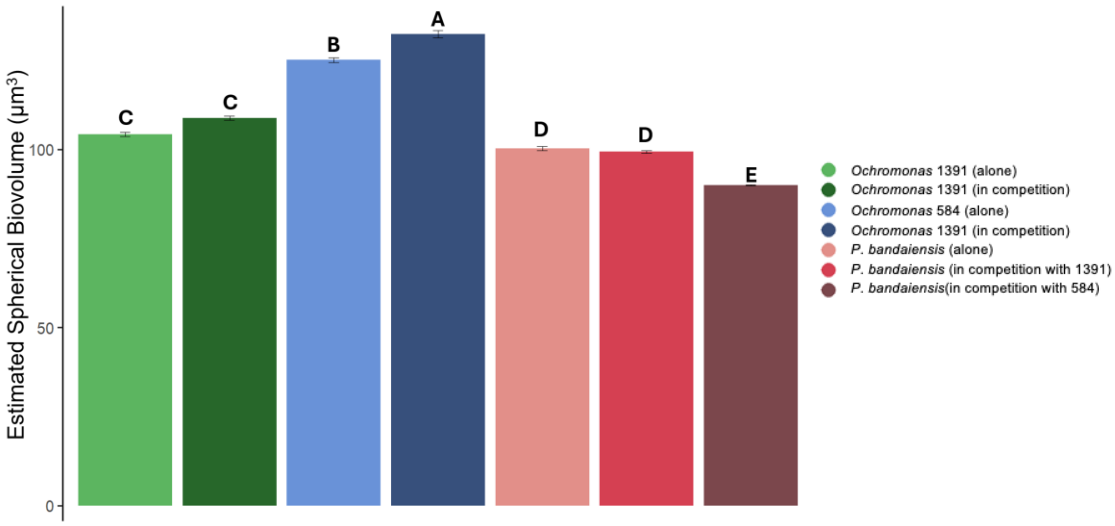

Figure 4.9 (A) The phototrophic investment (mg chlorophyll *a* per gram of cellular carbon) at equilibrium in *Ochromonas* across each treatment. (B) The acidic food vacuole content (log LysoTracker Green fluorescence) at equilibrium in each flagellate across each treatment. (C) The estimated spherical biovolume at equilibrium based on analysis of two-dimensional images on an Attune Imaging Flow Cytometer. Letters indicate significantly different groups according to Tukey's Honestly Significantly Different test (HSD test) ($p < 0.05$).

4.10

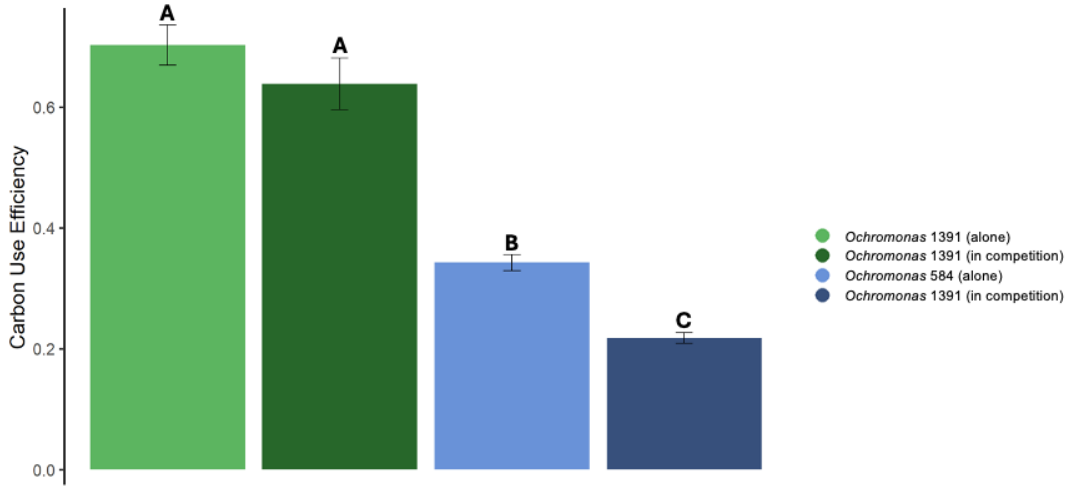

Figure 4.10 The carbon use efficiency of *Ochromonas* at equilibrium. Letters indicate significantly different groups according to Tukey's Honestly Significantly Different test (HSD test) ($p < 0.05$).

4.11A

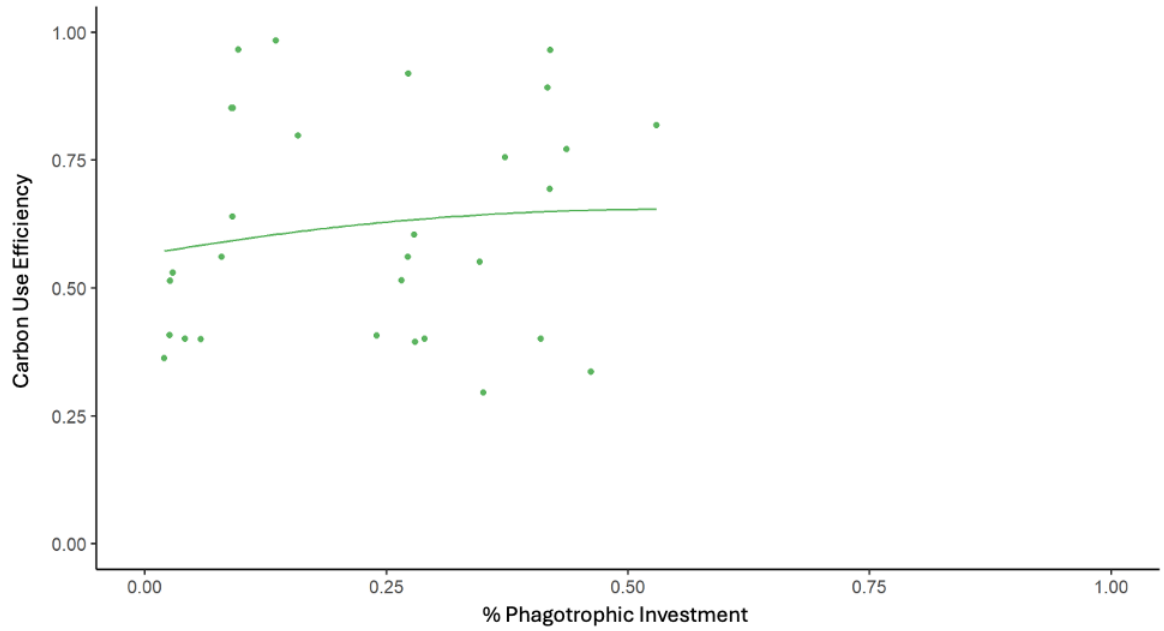

4.11B

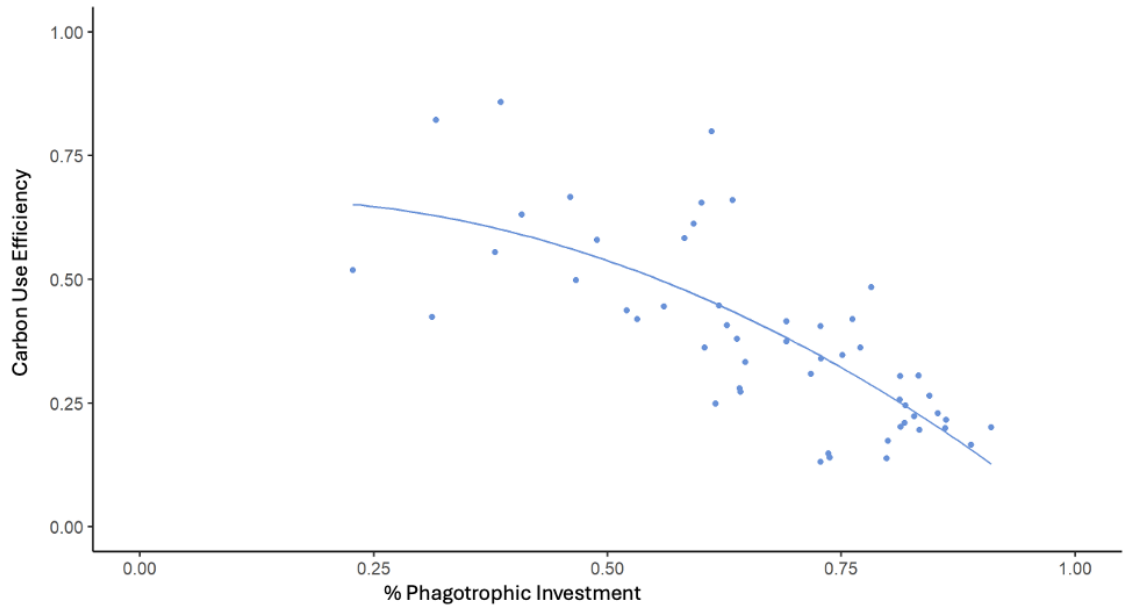

Figure 4.11 The relationship between phagotrophic investment and carbon use efficiency in *Ochromonas* (A) 1391 and (B) 584 for all measurements taken. The trendline is the quadratic best fit. This model predicts a maximum carbon use efficiency of 0.6535 ($p = 0.2662$, adjusted $r^2 = 0.0500$) at a 53.03% investment in phagotrophy for 1391 and a maximum carbon use efficiency of 0.6618 ($p < 0.0001$, adjusted $r^2 = 0.5467$) at a 11.90% investment in phagotrophy for 584.

4.12A

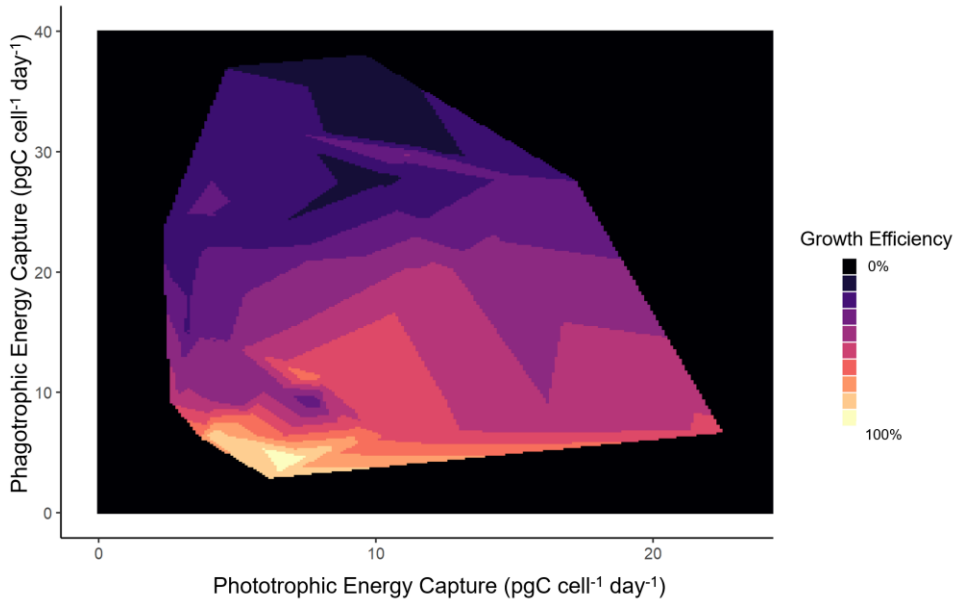

4.12B

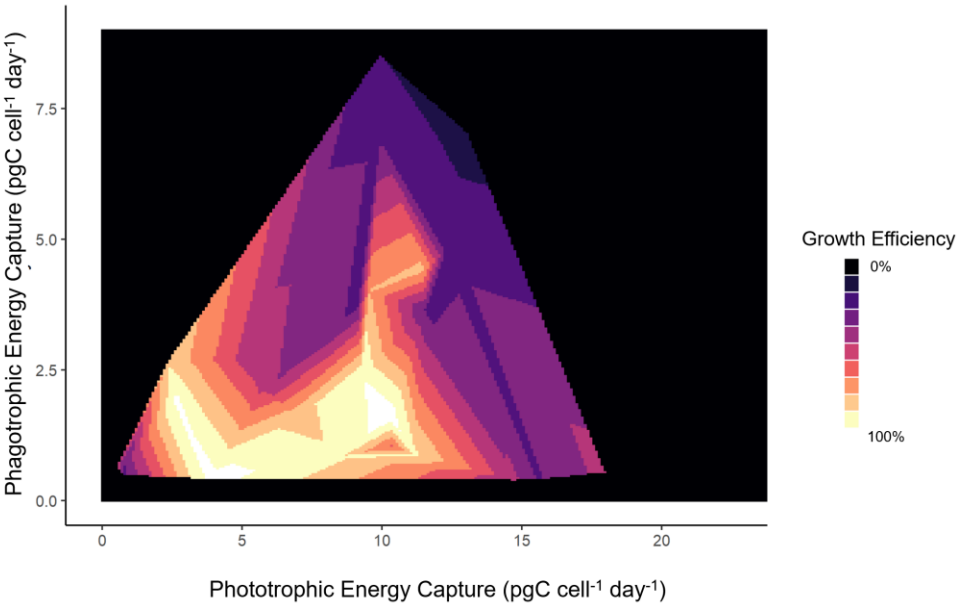

Figure 4.12 The metabolic landscapes of (A) *Ochromonas sp.* 1391 and (B) *Ochromonas sp.* 584. Each point represents an estimated carbon use efficiency in this environment for any given investment in phagotrophy and phototrophy as determined by a linear extrapolation in three-dimensional space using the R package akima (Akima 2025). Lighter colors indicate higher expected carbon use efficiencies. Note the difference in scale alone y-axes.

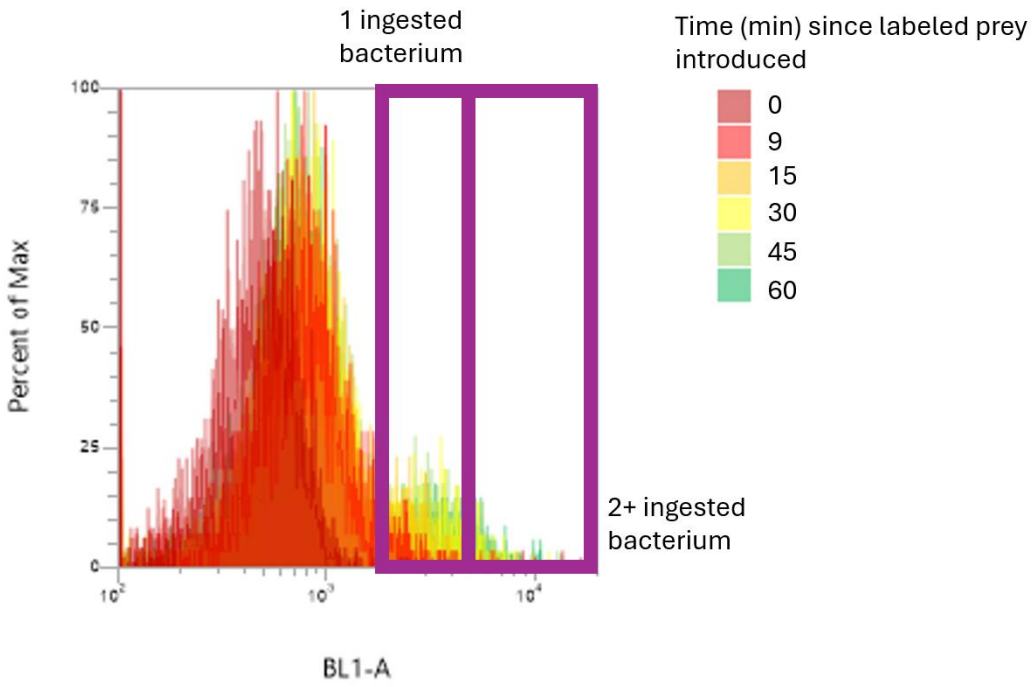

Figure 4.13 Overlayed histogram of *Ochromonas* 584 flow cytometry green fluorescence during a grazing measurement (as described in *vi. Bacteria and grazing: phagotrophic investment*). Color indicated the minutes elapsed since the introduction of labeled *Pelagibaca bermudensis* HTCC2601 prey into the sample. Note the lack of *Ochromonas* cells in the 'ingested' regions during t0 and the small number of cells appearing in the 2+ ingested region before t45.

Tables

Component	Stock Solution (g/L)	Quantity Added (µL/L)	Final Concentration
$NaNO_3$	75.00	100	8.82×10^{-5} M
NH_4Cl	2.67	100	5.00×10^{-6} M
Na_2 b-glycerophosphate	2.16	11.76	1.18×10^{-7} M
$Na_2SiO_3 \bullet 9H_2O$	15.35	100	5.04×10^{-5} M
H_2SeO_3	1.92×10^{-3}	100	1.00×10^{-9} M
Tris-base (pH 7.2)	121.10	100	1.00×10^{-4} M
Yeast extract	5.00	300	1.50×10^{-3} g/L
Glucose	0.14	300	1.4×10^{-6} M
Tryptone	13.0	300	3.90×10^{-3} g/L
K trace metal solution	-	100	-
f/2 vitamin solution	-	100	-

Table 4.1 K/10 + P/85 + LBGT media used in chemostat experiments. For the K trace metal and f/2 vitamin solutions see Keller et al. (1987) and Guillard (1975). Components which differ in concentration from the maintenance media outlined in Table 4.3 are highlighted in grey.

Component	Supplier	Part number	Amount per one chemostat
2000mL KIMAX Erlenmeyer flask	DWK Life Sciences	26720-2000	1
10000 mL FisherBrand glass media	Fisher Scientific	FB80010000	1
PFTE/silicon septum for GL45 caps	DWK Life Sciences	292483005	2
Open GL45 cap	DWK Life Sciences	292271007	2
3mm OD borosilicate glass tubing	Whale Apparatus	BS-002	~135 inches
MasterFlex 0.176” OD Transfer Tubing	Cole-Palmer	06499-48	~12 inches
MasterFlex Platinum-coated silicon L/S 13 precision tubing	Cole-Palmer	96410-13	~12.5 feet
MasterFlex precision pump tubing L/S 14	Cole-Palmer	06434-14	~12.5 feet
2” length magnetic stir bar	Fisher Scientific	14-513-61	1
MasterFlex EZload II two-channel pump head	Cole-Palmer	77202-60	1
0.2-micron vent filter (1/8” barb and luer lock)	Tisch Scientific	6713-0425	2
1/8” barbed female luer lock	Qosina	11536	7
1/8” barbed male luer lock	Qosina	11537	4
1/16” barbed male luer lock	Qosina	11533	1
Male-male luer connector	Qosina	12090	4
Female-female luer connector	Qosina	17642	2
Female luer-lock injection site	Qosina	80147	2
One-way check valve, female luer inlet, male luer outlet	Qosina	80107	4
T-connector with 2 female luer locks and a male slip	Qosina	80144	2
Cimarec+ 7”x7” ceramic stirrer	ThermoFischer	SP88857100	1

Table 4.2. Complete parts list used in the assembly of a chemostat as used in this study. This list does not include a compatible pump, aluminum foil, autoclave supplies, a container for waste, and other incidentals.

Component	Stock Solution (g/L)	Quantity Added (µL/L)	Final Concentration
$NaNO_3$	75.00	100	8.82×10^{-5} M
NH_4Cl	2.67	100	5.00×10^{-6} M
Na_2 b-glycerophosphate	2.16	20.0	2.00×10^{-7}M
$Na_2SiO_3 \bullet 9H_2O$	15.35	100	5.04×10^{-5} M
H_2SeO_3	1.92×10^{-3}	100	1.00×10^{-9} M
Tris-base (pH 7.2)	121.10	100	1.00×10^{-4} M
Yeast extract	5.00	600	3.00×10^{-3} g/L
Glucose	0.14	600	2.8×10^{-6} M
Tryptone	13.0	600	7.80×10^{-3} g/L
K trace metal solution	-	1000	-
f/2 vitamin solution	-	1000	-

Table 4.3 K/10 + P/50 + LBGT media used in maintenance. For the K trace metal and f/2 vitamin solutions see Keller et al. (1987) and Guillard (1975). Components which differ in concentration from the chemostat media outlined in Table 4.1 are highlighted in grey.

Parameter	Explanation	Value
LED Color	The LED to be used to stimulate photosynthesis. .	"blue"
Gain	The relative gain of the detector.	*varied*
Sample Delay	The interval between acquisitions to allow for "recovery" of the photosystem in milliseconds.	1000
Number of Samples	The number of acquisitions to be taken at each PAR level.	15
STF	The duration of the single turnover flash (STF) in microseconds.	80
STRP	The number of pulses in the STF relaxation sequence.	40
STRI	The interval between relaxation pulses in microseconds.	60
PAR	The maximum PAR level of the actinic light source for this sample.	425
Num PAR Steps	The number of PAR levels between 0 and the maximum PAR (inclusive) to be taken for this sample.	25
PAR Off Int	The interval the actinic light source is turned off between PAR levels in seconds.	0
PAR On Int	The interval the actinic light source is turned on between PAR levels in seconds to allow for acclimation in seconds.	15

Table 4.4 List of parameters used for Fv/Fm and ETR measurements on the FIRe. The gain was adjusted according to the chlorophyll content of the sample to ensure an accurate reading. Note that multiple turnover flash (MTF) was turned off (including during data analysis). On rare occasions the maximum PAR level (PAR) was altered to ensure accurate ETR measurements.

Component	Contributors	Concentration in media
	Carbon	
Organic Carbon	Yeast extract	4.61×10^{-5} M C
	Glucose	1.40×10^{-6} M C
	Tryptone	6.69×10^{-5} M C
	Na_2 b-glycerophosphate	3.53×10^{-7} M C
	TOTAL DOC	**1.17×10^{-4} M C**
	Nitrogen	
Inorganic nitrogen	$NaNO_3$	8.82×10^{-5} M N
	NH_4Cl	5.00×10^{-6} M N
	TOTAL DIN	**9.32×10^{-5} M N**
Organic Nitrogen	Yeast extract	1.07×10^{-5} M N
	Tryptone	2.78×10^{-5} M N
	TOTAL DON	**3.86×10^{-5} M N**
	TOTAL N	**1.32×10^{-4} M N**
	Phosphorus	
Organic Phosphorus	Na_2 b-glycerophosphate	1.18×10^{-7} M P
	Yeast extract	8.72×10^{-7} M P
	TOTAL P	**9.89×10^{-7} M P**

Table 4.5 Composition of nitrogen, phosphorus, and organic carbon in the media. Inorganic carbon is omitted as the cultures were continuously mixed with the air and inorganic carbon was not limiting. The elemental composition of yeast extract was estimated from previous yeast extract elemental analysis (Thompson et al. 2017). The CN content of tryptone was taken from the manufacture's website. We assume vitamins are not being catabolized; as such we do not include vitamins as a major source of carbon or nitrogen in the media. We assume the phosphorus content of tryptone is negligible. The final C:N:P ratio was 119:31:1, making the chemostat P-limited, with a secondary organic carbon limitation (Redfield, Ketchum, and Richards 1963). Since the culture was in contact with sterile air and well-mixed, there was no inorganic carbon limitation.

References

1. Akima, H. (2025). Interpolation of Irregularly and Regularly Spaced Data.
2. Amado, A., Fernández, L., Huang, W., Ferreira, F.F. & Campos, P.R.A. (2016). Competing metabolic strategies in a multilevel selection model. *Royal Society Open Science*, 3, 160544.
3. Archibald, K.M., Dutkiewicz, S., Laufkötter, C. & Moeller, H.V. (2024). Emergent trade-offs among plasticity strategies in mixotrophs. *J Theor Biol*, 590, 111854.
4. Armin, G., Kim, J. & Inomura, K. (2023). Saturating growth rate against phosphorus concentration explained by macromolecular allocation. *mSystems*, 8, e00611-23.
5. Azam, F., Fenchel, T., Field, J., Gray, J., Meyer-Reil, L. & Thingstad, F. (1983). The Ecological Role of Water-Column Microbes in the Sea. *Mar. Ecol. Prog. Ser.*, 10, 257–263.

6. Baldauf, S.A., Engqvist, L. & Weissing, F.J. (2014). Diversifying evolution of competitiveness. *Nat Commun*, 5, 5233.
7. Barbaglia, G.S., Paight, C., Honig, M., Johnson, M.D., Marczak, R., Lepori-Bui, M., *et al.* (2024). Environment-dependent metabolic investments in the mixotrophic chrysophyte *Ochromonas*. *Journal of Phycology*, 60, 170–184.
8. Baron, R., Davie, A., Gaines, A., Grant, D., Okay, O. & Ozsoy, E. (2014). Continuous cultures of phytoplankton. *Int Aquat Res*, 6, 95–111.
9. Baty, F., Ritz, C., Charles, S., Brutsche, M., Flandrois, J.-P. & Delignette-Muller, M.-L. (2015). A Toolbox for Nonlinear Regression in *R* : The Package **nlstools**. *J. Stat. Soft.*, 66.
10. Berge, T., Chakraborty, S., Hansen, P.J. & Andersen, K.H. (2017). Modeling succession of key resource-harvesting traits of mixotrophic plankton. *ISME J*, 11, 212–223.
11. Bernhardt, J.R., Kratina, P., Pereira, A.L., Tamminen, M., Thomas, M.K. & Narwani, A. (2020). The evolution of competitive ability for essential resources. *Philosophical Transactions of the Royal Society B: Biological Sciences*, 375, 20190247.
12. Bigelow National Center for Marine Algea and Microbiota (NCMA). (2025). *National Center for Marine Algea and Microbiota*. Available at: https://ncma.bigelow.org/. Last accessed 8 August 2025.
13. Bock, N.A., Charvet, S., Burns, J., Gyaltshen, Y., Rozenberg, A., Duhamel, S., *et al.* (2021). Experimental identification and in silico prediction of bacterivory in green algae. *The ISME Journal*, 15, 1987–2000.
14. Boenigk, J., Pfandl, K., Stadler, P. & Chatzinotas, A. (2005). High diversity of the '*Spumella*-like' flagellates: an investigation based on the SSU rRNA gene sequences of isolates from habitats located in six different geographic regions. *Environmental Microbiology*, 7, 685–697.
15. Caron, D.A. (2016). Mixotrophy stirs up our understanding of marine food webs. *Proceedings of the National Academy of Sciences*, 113, 2806–2808.
16. Caron, D.A., Lim, E.L., Dennett, M.R., Gast, R.J., Kosman, C. & DeLong, E.F. (1999). Molecular phylogenetic analysis of the heterotrophic chrysophyte genus *Paraphysomonas* (Chrysophyceae), and the design of RRNA-targeted oligonucleotide probes for two species. *Journal of Phycology*, 35, 824–837.
17. Cermeño, P., Lee, J., Wyman, K., Schofield, O. & Falkowski, P. (2011). Competitive dynamics in two species of marine phytoplankton under non-equilibrium conditions. *Mar. Ecol. Prog. Ser.*, 429, 19–28.
18. Chu, T., Moeller, H.V. & Archibald, K.M. (2023). Competition between phytoplankton and mixotrophs leads to metabolic character displacement. *Ecological Modelling*, 481, 110331.
19. Cropp, R. & Norbury, J. (2015). Mixotrophy: the missing link in consumer-resource-based ecologies. *Theor Ecol*, 8, 245–260.
20. Edwards, K.F. (2019). Mixotrophy in nanoflagellates across environmental gradients in the ocean. *Proc Natl Acad Sci U S A*, 116, 6211–6220.

21. Fekih-Salem, R., Rapaport, A. & Sari, T. (2016). Emergence of coexistence and limit cycles in the chemostat model with flocculation for a general class of functional responses. *Applied Mathematical Modelling*, 40, 7656–7677.
22. Felpeto, A.B., Roy, S. & Vasconcelos, V.M. (2018). Allelopathy prevents competitive exclusion and promotes phytoplankton biodiversity. *Oikos*, 127, 85–98.
23. First, M.R., Park, N.Y., Berrang, M.E., Meinersmann, R.J., Bernhard, J.M., Gast, R.J., *et al.* (2012). Ciliate Ingestion and Digestion: Flow Cytometric Measurements and Regrowth of a Digestion-Resistant Campylobacter jejuni. *Journal of Eukaryotic Microbiology*, 59, 12–19.
24. Flöder, S., Klauschies, T., Klaassen, M., Stoffers, T., Lambrecht, M. & Moorthi, S. (2024). Competition between mixo- and heterotrophic ciliates under dynamic resource supply. *Ecosphere*, 15, e4950.
25. Flynn, K.J. & Mitra, A. (2009). Building the "perfect beast": modelling mixotrophic plankton. *Journal of Plankton Research*, 31, 965–992.
26. Flynn, K.J., Stoecker, D.K., Mitra, A., Raven, J.A., Glibert, P.M., Hansen, P.J., *et al.* (2013). Misuse of the phytoplankton–zooplankton dichotomy: the need to assign organisms as mixotrophs within plankton functional types. *Journal of Plankton Research*, 35, 3–11.
27. García-Oliva, O., Hantzsche, F.M., Boersma, M. & Wirtz, K.W. (2022). Phytoplankton and particle size spectra indicate intense mixotrophic dinoflagellates grazing from summer to winter. *Journal of Plankton Research*, 44, 224–240.
28. Glibert, P.M. & Mitra, A. (2022). From webs, loops, shunts, and pumps to microbial multitasking: Evolving concepts of marine microbial ecology, the mixoplankton paradigm, and implications for a future ocean. *Limnology and Oceanography*, 67, 585–597.
29. González, J.M., Whitman, W.B., Hodson, R.E. & Moran, M.A. (1996). Identifying numerically abundant culturable bacteria from complex communities: an example from a lignin enrichment culture. *Appl Environ Microbiol*, 62, 4433–4440.
30. Gorbunov, M.Y. & Falkowski, P.G. (2021). Using chlorophyll fluorescence kinetics to determine photosynthesis in aquatic ecosystems. *Limnology and Oceanography*, 66, 1–13.
31. Gorbunov, M.Y., Falkowski, P.G. & Kolber, Z.S. (2000). Measurement of photosynthetic parameters in benthic organisms in situ using a SCUBA-based fast repetition rate fluorometer. *Limnology and Oceanography*, 45, 242–245.
32. Gorbunov, M.Y., Kolber, Z.S., Lesser, M.P. & Falkowski, P.G. (2001). Photosynthesis and photoprotection in symbiotic corals. *Limnol. Oceanogr.*, 46, 75–85.
33. Guillard, R.R.L. (1975). Culture of Phytoplankton for Feeding Marine Invertebrates. In: *Culture of Marine Invertebrate Animals: Proceedings — 1st Conference on Culture of Marine Invertebrate Animals Greenport* (eds. Smith, W.L. & Chanley, M.H.). Springer US, Boston, MA, pp. 29–60.
34. Hahn, M.W. & Höfle, M.G. (1999). Flagellate Predation on a Bacterial Model Community: Interplay of Size-Selective Grazing, Specific Bacterial Cell Size, and Bacterial Community Composition. *Appl Environ Microbiol*, 65, 4863–4872.

35. Hammer, A.C. & Pitchford, J.W. (2005). The role of mixotrophy in plankton bloom dynamics, and the consequences for productivity. *ICES Journal of Marine Science*, 62, 833–840.
36. Harris, J.R.W. (1981). Competition relatedness and efficiency. *Nature*, 292, 54–55.
37. Higini Peter, K. & Sommer, U. (2013). Phytoplankton cell size reduction in response to warming mediated by nutrient limitation. PLOS One. (8)9,
38. Honig, M.A., Barbaglia, G.S., Doyle, M.D. & Moeller, H.V. (2025). Effects of mixotroph evolution on trophic transfer. *Journal of Plankton Research*, 47, fbae053.
39. Jahns, M. & Johnson, M. (Unpublished). Competition for prey drives a 'doubling down' on phagotrophy in the mixotroph *Ochromonas*. *In prep.*
40. Jimenez, V., Burns, J.A., Le Gall, F., Not, F. & Vaulot, D. (2021). No evidence of Phago-mixotropy in *Micromonas polaris* (Mamiellophyceae), the Dominant Picophytoplankton Species in the Arctic. *Journal of Phycology*, 57, 435–446.
41. Jost, C., Lawrence, C.A., Campolongo, F., Van De Bund, W., Hill, S. & DeAngelis, D.L. (2004). The effects of mixotrophy on the stability and dynamics of a simple planktonic food web model. *Theoretical Population Biology*, 66, 37–51.
42. Keller, M.D., Selvin, R.C., Claus, W. & Guillard, R.R.L. (1987). Media for the Culture of Oceanic Ultraphytoplankton. *Journal of Phycology*, 23, 633–638.
43. Le Chevanton, M., Garnier, M., Lukomska, E., Schreiber, N., Cadoret, J.-P., Saint-Jean, B., *et al.* (2016). Effects of Nitrogen Limitation on Dunaliella sp.–Alteromonas sp. Interactions: From Mutualistic to Competitive Relationships. *Front. Mar. Sci.*, 3.
44. Lenas, P. & Pavlou, S. (1994). Periodic, quasi-periodic, and chaotic coexistence of two competing microbial populations in a periodically operated chemostat. *Math Biosci*, 121, 61–110.
45. Lepori-Bui, M., Paight, C., Eberhard, E., Mertz, C.M. & Moeller, H.V. (2022). Evidence for evolutionary adaptation of mixotrophic nanoflagellates to warmer temperatures.
46. Lindsay, R.J., Holder, P.J., Talbot, N.J. & Gudelj, I. (2023). Metabolic efficiency reshapes the seminal relationship between pathogen growth rate and virulence. *Ecology Letters*, 26, 896–907.
47. Liu, X., Sun, J., Wei, Y. & Liu, Y. (2023). Relationship between cell volume and particulate organic matter for different size phytoplankton. *Marine Pollution Bulletin*, 194, 115298.
48. Livanou, E., Barsakis, K., Psarra, S. & Lika, K. (2020). Modelling the nutritional strategies in mixotrophic nanoflagellates. *Ecological Modelling*, 428, 109053.
49. Malard, L.A. & Guisan, A. (2023). Into the microbial niche. *Trends in Ecology & Evolution*, 38, 936–945.
50. Mansour, J.S. & Anestis, K. (2021). Eco-Evolutionary Perspectives on Mixoplankton. *Front. Mar. Sci.*, 8.
51. Menden-Deuer, S. & Lessard, E.J. (2000). Carbon to volume relationships for dinoflagellates, diatoms, and other protist plankton. *Limnology and Oceanography*, 45, 569–579.

52. Millette, N.C., Leles, S.G., Johnson, M.D., Maloney, A.E., Brownlee, E.F., Cohen, N.R., *et al.* (2024). Recommendations for advancing mixoplankton research through empirical-model integration. *Front. Mar. Sci.*, 11.
53. Mitra, A. & Flynn, K.J. (2023). Low rates of bacterivory enhances phototrophy and competitive advantage for mixoplankton growing in oligotrophic waters. *Sci Rep*, 13, 6900.
54. Moeller, H. (2022). *ID 798096 - BioProject - NCBI*. *National Center for Biotechnology Information*. Available at: https://www-ncbi-nlm-nih-gov.libproxy.mit.edu/bioproject?LinkName=biosample_bioproject&from_uid=25046786. Last accessed 1 August 2025.
55. Moeller, H.V., Archibald, K.M., Leles, S.G. & Pfab, F. (2024). Predicting optimal mixotrophic metabolic strategies in the global ocean. *Science Advances*, 10, eadr0664.
56. Omta, A.W., Talmy, D., Sher, D., Finkel, Z.V., Irwin, A.J. & Follows, M.J. (2017). Extracting phytoplankton physiological traits from batch and chemostat culture data. *Limnology and Oceanography: Methods*, 15, 453–466.
57. Pickell, L.D., Wells, M.L., Trick, C.G. & Cochlan, W.P. (2009). A sea-going continuous culture system for investigating phytoplankton community response to macro- and micro-nutrient manipulations. *Limnology and Oceanography: Methods*, 7, 21–32.
58. Raven, J.A. (1997). Phagotrophy in phototrophs. *Limnology and Oceanography*, 42, 198–205.
59. Redfield, A.C., Ketchum, B.H. & Richards, F.A. (1963). The Influence of Organisms on the Composition of the Sea Water. *The Sea*, 2, 26–77.
60. Roller, B.R. & Schmidt, T.M. (2015). The physiology and ecological implications of efficient growth. *ISME J*, 9, 1481–1487.
61. Schenone, L., Aarons, Z.S., García-Martínez, M., Happe, A. & Redoglio, A. (2024). Mixotrophic protists and ecological stoichiometry: connecting homeostasis and nutrient limitation from organisms to communities. *Front. Ecol. Evol.*, 12.
62. Schoenle, A., Francis, O., Archibald, J.M., Burki, F., de Vries, J., Dumack, K., *et al.* (2025). Protist genomics: key to understanding eukaryotic evolution. *Trends in Genetics*.
63. Selosse, M.-A., Charpin, M. & Not, F. (2017). Mixotrophy everywhere on land and in water: the grand écart hypothesis. *Ecology Letters*, 20, 246–263.
64. Selph, K.E., Landry, M.R. & Laws, E.A. (2003). Heterotrophic nanoflagellate enhancement of bacterial growth through nutrient remineralization in chemostat culture. *Aquatic Microbial Ecology*, 32, 23–37.
65. Sintes, E. & Del Giorgio, P.A. (2010). Community heterogeneity and single-cell digestive activity of estuarine heterotrophic nanoflagellates assessed using lysotracker and flow cytometry. *Environmental Microbiology*, 12, 1913–1925.
66. Stickney, H.L., Hood, R.R. & Stoecker, D.K. (2000). The impact of mixotrophy on planktonic marine ecosystems. *Ecological Modelling*, 125, 203–230.
67. Stoecker, D.K., Hansen, P.J., Caron, D.A. & Mitra, A. (2017). Mixotrophy in the Marine Plankton. *Annu. Rev. Mar. Sci.*, 9, 311–335.

68. Tas, S. (2023). Estimation of cellular carbon content based on the cell biovolume of microalgae from a eutrophic estuary (Sea of Marmara, Türkiye). *Environ Monit Assess*, 195, 1–14.
69. Thompson, K.A., Summers, R.S. & Cook, S.M. (2017). Development and experimental validation of the composition and treatability of a new synthetic bathroom greywater (SynGrey). *Environ. Sci.: Water Res. Technol.*, 3, 1120–1131.
70. Tittel, J., Bissinger, V., Zippel, B., Gaedke, U., Bell, E., Lorke, A., *et al.* (2003). Mixotrophs combine resource use to outcompete specialists: Implications for aquatic food webs. *Proceedings of the National Academy of Sciences*, 100, 12776–12781.
71. Toth, D. & Kot, M. (2006). Limit cycles in a chemostat model for a single species with age structure. *Math Biosci*, 202, 194–217.
72. Trappes, R., Nematipour, B., Kaiser, M.I., Krohs, U., van Benthem, K.J., Ernst, U.R., *et al.* (2022). How Individualized Niches Arise: Defining Mechanisms of Niche Construction, Niche Choice, and Niche Conformance. *Bioscience*, 72, 538–548.
73. Troost, T.A., Kooi, B.W. & Kooijman, S.A.L.M. (2005). When do mixotrophs specialize? Adaptive dynamics theory applied to a dynamic energy budget model. *Mathematical Biosciences*, 193, 159–182.
74. Ward, B.A., Dutkiewicz, S., Barton, A.D. & Follows, M.J. (2011). Biophysical aspects of resource acquisition and competition in algal mixotrophs. *Am Nat*, 178, 98–112.
75. Ward, B.A. & Follows, M.J. (2016). Marine mixotrophy increases trophic transfer efficiency, mean organism size, and vertical carbon flux. *Proc. Natl. Acad. Sci. U.S.A.*, 113, 2958–2963.
76. White, N.J. & Butlin, R.K. (2021). Multidimensional divergent selection, local adaptation, and speciation. *Evol*, 75, 2167–2178.
77. Wickham, H. (2007). Reshaping data with the reshape package. *Journal of Statistical Software*, 21, 1–20.
78. Wickham, H. (2016). *ggplot2: Elegant Graphics for Data Analysis*. Springer-Verlag New York.
79. Wickham, H. (2023). stringr: Simple, Consistent Wrappers for Common String Operations.
80. Wickham, H. & Bryan, J. (2025). readxl: Read Excel Files.
81. Wickham, H., François, R., Henry, L., Müller, K. & Vaughan, D. (2025). dplyr: A Grammar of Data Manipulation.
82. Wieczynski, D.J., Moeller, H.V. & Gibert, J.P. (2023). Mixotrophic microbes create carbon tipping points under warming. *Functional Ecology*, 37, 1774–1786.
83. Wilken, S., Yung, C.C.M., Hamilton, M., Hoadley, K., Nzongo, J., Eckmann, C., *et al.* (2019). The need to account for cell biology in characterizing predatory mixotrophs in aquatic environments. *Philosophical Transactions of the Royal Society B: Biological Sciences*, 374, 20190090.
84. Worden, A.Z., Follows, M.J., Giovannoni, S.J., Wilken, S., Zimmerman, A.E. & Keeling, P.J. (2015). Rethinking the marine carbon cycle: Factoring in the multifarious lifestyles of microbes. *Science*, 347, 1257594.

85. Ye, Z.-P., Robakowski, P. & Suggett, D.J. (2013). A mechanistic model for the light response of photosynthetic electron transport rate based on light harvesting properties of photosynthetic pigment molecules. *Planta*, 237, 837–847.

CHAPTER 5: CONCLUSIONS AND FURTHER WORK

Summary and implications

This thesis aimed to describe some of the mechanisms by which organismal metabolism shapes and is shaped by community structure in microbial communities. We used representative model laboratory systems and added realistic complexity through the introduction of multiple community members. In Chapter 2, we examined the metabolic underpinnings of predation and parasitism. In Chapters 3 we introduced competition and environmental change to observe niche displacement in a model mixotroph, *Ochromonas*. And, in Chapter 4, we continued competition experiments in a chemostatic environment to control for environmental impacts on metabolism and isolate the direct effects of competition on *Ochromonas's* metabolic niche.

i. Chapter 2

Cyanophages are key parasites of some of the most productive phytoplankton in the ocean (Ankrah et al. 2014). Cyanophages alter the metabolism of their host both through their own viral genes and the host auxiliary metabolic genes they carry in their genomes (Lindell et al. 2007). We investigated how cyanophages shape the metabolism of *Prochlorococcus* MED4 and alter the structure of the microbial community.

Grown alone, the ideal metabolism of *Prochlorococcus* MED4 was revealed through the extremely low investment in phospholipids compared to many other bacteria (Chapter 2). We also demonstrated that much of the *Prochlorococcus* lipidome is made up of a few key compounds (Chapter 2).

Then, we cultured the same strain of *Prochlorococcus* with P-SSP7, a T7-like phage. P-SSP7 greatly altered the lipid metabolism of its host. We identified lipid compounds which were particularly affected by the phage which we called the "modular lipidome". In particular, we found an unknown lipid compound, OML-321, in the modular lipidome which was highly responsive to infection and demonstrated it may be a viable biomarker of phage infection in future field studies (Chapter 2). We also observed a shift towards more phosphorus in the lipid fraction (Chapter 2). We contend that even though P-SSP4 does not carry the phosphorus-stress auxiliary metabolic genes carried by many other cyanophages (Chapter 2).

Finally, we observed a metabolic niche displacement in a predator of *Prochlorococcus* MED4, *Paraphysomonas bandaiensis* in response to infected prey. *P. bandaiensis* declined greatly in its concentration of triacylglycerols (TAGs), which are key energy storage molecules (Chapter 2). This previously undescribed indirect mechanism of a parasite on a host predator's metabolism has wide-reaching implications for the cycling of lipids and energy in the ocean, as diel TAG

cycling in the NPSG is equivalent to 4-6% of global net primary production (Chapter 2, Becker et al. 2018).

The lipidome of *Prochlorococcus* was not greatly altered by the presence of the predator. The presence of the parasite on the other hand greatly affected the lipidome and metabolism of *Prochlorococcus*. This suggests complexity and nuance is required for understanding metabolic interactions between community members. It also indicates that phage infection is a highly effective method for altering communities and may play a key role in carbon and nutrient cycling in these environments.

In that vein, the discovery that phage alteration of host metabolism effects the metabolic niche of the host's predator has important implications for understanding marine community dynamics. Though the frequency of viral infection in the ocean is unknown, whatever the rate, models of predators on only uninfected prey will not capture the realized niche of these organisms in the environment and may lead to misleading results (Vincent and Vardi 2023). Additionally, these results underscore how the metabolic niche is responsive to and shaped by far-removed community members. The predator and the phage are not likely to interact directly, yet the phage altered how the predatory stored and used energy through infection of its prey. This type of interaction is rarely included in ecological or evolutionary models and may be a powerful force driving the metabolic niches of phagotrophs.

ii. Chapter 3

Like phages, the importance of mixotrophs in the structure and function of aquatic microbial communities is well appreciated (Millette et al. 2024). However, the eco-evolutionary dynamics of mixotrophs remains an evolving topic of study (Millette et al. 2024). Mixotrophs are also interesting study systems for investigating the role of the metabolic niche, as their investments in both phototrophy and phagotrophy are easily observed and are key to their competitive success.

Culturing two obligately phagotrophic strains of the aquatic mixotrophic chrysophyte *Ochromonas* alone we characterized each strain's ideal niche. As expected, strains survived using a balance of phototrophy and phagotrophy. Then, we introduced *P. bandaiensis* as a representative of a single-guild competitor and observed, to our surprise, both strains did not occupy new more phototrophic niches to relieve the competitive pressure for resources. Instead, *Ochromonas* 'doubled-down', investing more in phagotrophy in competition despite phagotrophy presumably being a less efficient strategy for growth.

Though their growth was significantly decreased in competition, both mixotrophs were able to coexist with *P. bandaiensis*, suggesting there must exist some eco-evolutionary benefit to this strategy. Modern literature suggests direct trade-offs between phagotrophy and phototrophy are rarer than once thought (Smalley et al. 2003, Cabrerizo et al. 2019, González-Olalla et al. 2021, Barbaglia et al. 2024). We believe our findings support this conclusion, as the 'doubling down' strategy is likely better explained by a prey requirement or prey quota as both strains were obligate phagotrophs.

iii. Chapter 4

To test the hypothesis that prey nutritional requirements are responsible for the doubling-down we observed in Chapter 3, we conducted a similar competition experiment between *Ochromonas* and *P. bandaiensis* in co-culture, but we substituted *Ochromonas* 1148 for *Ochromonas* 1391, which is not an obligate phagotroph. These experiments were caried out in a chemostatic culture apparatus we designed to control for environmental confounding environmental variables and to isolate the direct effects of competition on the realized niche of our mixotrophs.

Ochromonas 584, the obligate phagotroph, followed the same pattern in competition with *P. bandaiensis* we observed in Chapter 3. Namely, in competition *Ochromonas* 584 doubled-down on phagotrophy, going so far as to decrease its growth efficiency by nearly 50%. *Ochromonas* 1391, on the other hand, displayed niche displacement away from the more limiting resource, exhibiting a classical mixotrophic response more akin to niche displacement models like Chu, Moeller, and Archibald (2023).

The extent to which each strain's growth was affected by competition, and thus how the community was structured, was determined in part by their metabolic landscape. To conceptualize the ideal and realized niches of *Ochromonas* in competition, we reduced the metabolic niche to tradeoffs in investment between their two trophic modes. Growth efficiency and energy investment were key variables in the competitive dynamics of the two *Ochromonas* strains tested here and their occupied niche in competition.

Again, we hypothesize the doubling down in *Ochromonas* 584 in response to competition is related to its prey quota as an obligate phagotroph. *Ochromonas* 1391, in not doubling down, did not decrease its carbon use efficiency in response to competition. Also, in this environment the ideal niche space of *Ochromonas* 1391, or the metabolic states where *Ochromonas* 1391 experienced little decline in return on energy investment, was significantly larger than *Ochromonas* 584. A possible explanation is that there is a spectrum of prey quality in these natural bacterial communities and in competition *Ochromonas* 584 needs to graze more voraciously to achieve the same nutritional requirement.

Unlike in Chapter 3, we found the growth of *P. bandaiensis* was greatly limited by the presence of both mixotrophs. Whether this is an artefact of the different environment, the saturating light at which the mixotrophs were grown, or some other mechanism is unknown. It is possible that the presence of the mixotroph did affect the ability of *P. bandaiensis* in this environment, however in cultures with *Ochromonas*, more bacteria were available at equilibrium than in cultures with only *P. bandaiensis*.

In terms of overall community impacts, contrary to our hypothesis, we only saw evidence for increased net productivity in competition in cultures with *Ochromonas* 1391, and no evidence in cultures containing *Ochromonas* 584. One possible explanation is the great carbon use efficiency of *Ochromonas* 1391. While the total biomass of each chemostat was determined by which mixotrophic strain was present, both mixotrophs varied greatly in size and *Ochromonas* was also always the largest fraction of biomass in each chemostat at equilibrium.

We find that this competitive chemostat system containing different strains of *Ochromonas* is ripe for further exploration, and we anticipate further experiments in this system, including the introduction of a solely phototrophic competitor.

Ochromonas as a non-traditional 'model system' for mixotrophic metabolism and ecology

The study of constitutive mixotrophy is important to fields as diverse as ecology, evolution, microbiology, environmental science, and biofuel production. Since the discovery that many organisms possess the capability to photosynthesize and ingest prey, there has been a growing appreciation that mixotrophic organisms play key roles in our environment (Raven 1997, Stickney et al. 2000, Caron 2016). In an era of global change, more and more studies demonstrate the importance of mixotrophic organisms in how our ecosystems will respond to perturbation (Jost et al. 2004, Hammer and Pitchford 2005, Mitra et al. 2014, Wieczynski, Gilbert and Moeller 2023, Schenone et al. 2024, Honig et al. 2025). Additionally, mixotrophic microorganisms have been shown to have a direct impact on human health through shaping environmental events like red tides and energy transfer to higher trophic levels (Wilken et al. 2014, Cropp and Norbury 2015, Ward and Follows 2016, Yoo et al. 2017, Flynn et al. 2019). The evolution of metabolic strategies as well as the acquisition and retention of plastids is also informed by mixotrophic research (Mansour and Anestis 2021, Millette et al. 2024).

While there is a growing field of mixotrophic science, many open questions remain about the metabolism, eco-evolutionary trade-offs, biogeography, and characterization of mixotrophic organisms (Millette et al. 2024). While many applied, theoretical, and environmental studies have been key for understanding mixotrophic organisms (Millette et al. 2024). In this review we argue the importance of controlled laboratory studies for advancing our knowledge of mixotrophy. In particular, we present an overview of how and why the mixotrophic nanoflagellete *Ochromonas* sp. can be used as a particularly effective organism for the study of constitutive phagophototrophic metabolism and ecology. We encourage the community to think of *Ochromonas*, in a non-traditional sense, as a model system. While *Ochromonas* lacks some of the key features normally associated with model systems we show how and why these drawbacks can be overcome by features unique to a *Ochromonas* study system. We call this system a "non-traditional model".

i. The choice of mixotrophic study systems

Laboratory researchers interested in a biological process or phenomenon cannot investigate how it manifests in all organisms. Yet often the choice of organism to study can impact the success of the research (Krogh 1929, Burian 1993, Dietrich et al. 2020). Therefore, it is vital researchers take care in choosing which organisms to invest time and resources into when investigating the underpinnings of mixotrophic metabolism and ecology.

Studies on mixotrophy cover a wide-range of organisms- from unicellular to multicellular, bacteria to animals to protists, pico-scale to macro-scale, etc. (Caron 2016, Sellose, Charpin and Not 2017, Millette et al. 2024). The diversity of mixotrophy on the planet and its implications

remains an open question properly explored only through exploring a diversity of mixotrophic life. Many fundamental biological questions about mixotrophy also benefit from phylogenetic variety including, for example:

1. How does evolutionary history shape mixotrophic physiology?
2. What genes, if any, are common among mixotrophic organisms?
3. How can mixotrophic organisms be best divided into functional groups?

However, when it comes to certain questions of fundamental biological phenomenon, general acceptance of a few key organisms with broad biological applicability can greatly help advance a field's understanding (Jenner and Willis 2007, Russel et al. 2017, Ackney and Leonelli 2020). Here we argue for the coalescence of constitutive mixotrophy researchers in our choice of study organisms. As recent reviews have highlighted, a multitude of experimental systems means differing perspectives must be reconciled by exploration of a more fundamental biological truth (Ward 2019, Ackney and Leonelli 2020, Millette et al. 2024). Therefore, we are especially convinced of the benefits of the establishment of a model system for probing fundamental constitutive mixotrophy.

ii. Importance of model systems

Model systems are a key advancement that accelerated the rate of biological discovery during the 20th and into the 21st centuries (Russel et al. 2017, Matthews and Vosshall 2020). While the definition of a 'model organism' varies, generally a model organism is distinct from the choice of a purely 'experimental organism'. Model organisms share key traits that allow researchers to build a large knowledgebase studying evolutionary or ecologically conserved functions extrapolated from a well-known species (Ackney and Leonelli 2020, Bertile et al. 2023). Experimental organisms on the other hand are chosen to investigate a specific biological process or interaction only extrapolated to closely related species (Ackney and Leonelli 2020).

While model organisms are often thought of as analogs which can be extrapolated to fundamental biological processes that affect humans, such as cell structure or genetics, here we focus on the more diverse emerging definition of model organisms which includes systems that are not equipped to advance our understand on human biology or are do not have all the normal traits associated with a model organism but none-the-less provide insights into fundamental processes that are widely applicable (Russel et al. 2017, Duffy et al. 2021). These organisms are sometimes called non-model model organisms (NMMOs) because they are useful to study as a 'model system' of a biological process but are still emerging in their acceptance as a model system or do not conform to traditional standards of 'model systems' used in the field of biomedicine (Russel et al. 2017). Recently, studies have highlighted NMMOs for expanding the biological questions that can be probed by model organisms (Russel et al. 2017, Duffy et al. 2021). As such, we will not use a particular definition of model organism, instead choosing to focus on identifying whether an organism is useful and broadly applicable as model for a particular research question. Instead, we choose to use "non-traditional model system", focusing on the ability for a constitutive mixotroph to emerge with the utility of a model system, but without satisfying all the traditional criteria. We also use this term as well because it is descriptive of the type of broad acceptance, we hope to generate from the field to work together

on addressing questions of constitutive mixotrophic metabolism. Studies have shown that acceptance of a 'model organism' in a field (perhaps even a non-traditional one) can support funding to development of that research area, scientific coordination, and breakthroughs (Russel et al. 2017, Ankeny and Leonelli 2020, Matthews and Vosshall 2022).

The work of model system scholars Russel et al. (2017), Ankeny and Leonelli (2020), and Matthews and Vosshall (2022) on the criteria of an organism for becoming a more classical 'model organism' status can be summarized in five points:

I. Addressing the fundamental question and applicability
    a. Does the organism directly address the open question?
    b. Is research on the organism applicable to lifeforms more diverse than immediate evolutionary relatives?
II. Ease and access
    a. Is the organism accessible to all scientists?
    b. Is the organism easily culturable?
    c. Is the organism robust to laboratory conditions?
III. Stability and predictability
    a. Does the organism act predictably similar in similar conditions?
    b. Is the organism's behavior stable over many generations in culture?
    c. Is study of the organism not impeded by the organism's genetic drift in culture?
IV. Knowledgebase
    a. Is the organism well-described by an existing body of research?
    b. Are there well-established methods for probing the biological question of interest in the organism?
    c. Are these methods standardized?
V. Genetic characterization and manipulation
    a. Is the genome of the organism published and the genetics well-described?
    b. Can the organism be genetically manipulated to investigate the biological question of interest (i.e. knock-outs, etc.)?

In this framework, we must define research questions which are appropriate for the development of a model system. We believe there are several open questions concerning mixotrophic metabolism and ecology which are suitable to model system, or non-traditional model system, research. After careful review, we find there are three research questions vital to the advancement of mixotrophic research proposed by Millette et al. (2024) which are ripe for the acceptance of a non-traditional model system:

1. What are the tradeoffs that mixotrophic plankton experience?
2. What are the drivers of mixotrophic eco-evolutionary tradeoffs?
3. How does cellular composition vary as mixotrophic plankton navigate the metabolic landscape and how does extracellular biogeochemistry help to shape it?

Each of these three questions speak to the fundamental biological processes underlying mixotrophic metabolism, their role in community ecology, and their role in evolution. These

study areas also frequently employ well-established methods in laboratory settings (Millette et al. 2024). Laboratory data has also been successfully incorporated into theoretical models which generate foundational theories for mixotrophic traits and metabolism (Millette et al. 2024). All these factors make these questions particularly ripe for development of a model system.

Model systems are not perfect replicas of the real world, but are efficient and useful (Krogh 1929, Russel et al. 2017, Ackney and Leonelli 2020, Matthews and Vosshall 2022). Exploring each of these questions across the tree of life is incredibly important; to truly understand a biological phenomenon we must characterize all its contours and caveats (Jenner and Willis 2007, Dietrich et al. 2020, Duffy et al. 2021). However, studies have demonstrated that, especially in the microbial environment, discovering relatively simplistic foundational 'rules' can have powerful applicability in modeling and predicting biological outcomes (Duarte, Gasol and Vaqué 1997, Datta et al. 2016, Russel et al. 2017, Edwards et al. 2023, Lee, Bloxham and Gore 2023, Moeller et al. 2024). In this sense, as mixotrophic researchers probe these three questions for underlying principles, utilizing a standardized model system could be incredibly useful.

iii. Ochromonas *as a non-model model system*

Ochromonas is a genus of aquatic nano-flagellate chrysophytes thought to entirely contain mixotrophs (Terpis et al. 2025). *Ochromonas* engages in photophagotrophy and is thought to be robust to many different environments (Andersen et al. 2017, Bargalia et al. 2024). *Ochromonas* is extremely widespread in fresh- and saltwater environments, and in some communities can account for the majority of bacterivory or primary production (Aaronson 1973, Boenigk et al. 2005, Schmidtke, Bell and Weifhoff 2006, Andersen et al. 2017, GBIF Secretariat 2025). Importantly, *Ochromonas* species are relatively closely related evolutionarily, and are all constitutive mixotrophs, but have vastly different metabolic landscapes (Holen 2010, Dorell et al. 2019, Bargalia et al. 2024, Jahns and Johnson *in prep*, Chapter 4). Some strains of *Ochromonas* are facultatively phagotrophic and obligately phototrophic, obligately phagotrophic and facultatively phototrophic, or both obligately phototrophic and phagotrophic (Lie et al. 2018, Bargalia et al. 2024, Jahns and Johnson *in prep*). A summary of characteristics for highlighted *Ochromonas* strains can be found in Table 5.1.

The utility of *Ochromonas* for the study of mixotrophy has been long recognized. Many studies have used *Ochromonas* as a representative constitutive mixotroph (Holen 2010, Wilken, Choi, and Worden 2020, Honig et al. 2025, Jahns and Johnson *in prep*). Additionally, experimental methods in *Ochromonas* systems are well described and easily applicable between strains, making *Ochromonas* a great choice for researchers choosing a system to study (Table 5.2).

For these reasons and more, we believe *Ochromonas* can be adapted into a non-traditional model system for constitutive phagophototrophs. While *Ochromonas* is a genus, and not a species as a model system is traditionally defined, as we will explain we believe this is a feature of having multiple labs investigate *Ochromonas* in comparable ways. Indeed, multiple non-model model systems or non-traditional model systems employ species diversity in representative systems (Russel et al. 2017, Duffy et al. 2021).

To explore the efficacy of *Ochromonas* as a potential non-traditional model system, we will now address the extent to which *Ochromonas* could be properly utilized as a model organism following the five criteria laid out above.

I. *Addressing the fundamental question and applicability*
    a. Yes. *Ochromonas* has already been used to study the three scientific questions we identified, and studies have spoken directly to the implications of *Ochromonas* on mixotrophy as a whole (Corno 2006, Lie et al. 2018, Wilken et al. 2020, Jahns and Johnson *in prep*, etc.).
    b. Yes. Laboratory findings in *Ochromonas* have been applied to models which can accurately predict actual field observations on diverse mixotrophs, underscoring the applicability of an *Ochromonas* system to broad and fundamental biological questions about constitutive mixotrophy (Simonds, Grover, and Chrzanowski 2010, Wilken et al. 2014, Moeller et al. 2024, etc.).

II. *Ease and access*
    a. Yes. Strains of *Ochromonas* are commercially available for purchase from algal culture collections such as the National Center for Marine Algae and Microbiota (Bigelow Laboratory, East Boothbay, ME, USA), Roscoff Culture Collection (Station Biologique de Roscoff, Roscoff, France), and UTEX Culture Collection of Algae (The University of Texas at Austin, Austin, TX, USA).
    b. Yes. Depending on the strain *Ochromonas* culturing can be done in small volumes, using inexpensive nutrient kits, under a variety of light and temperature levels, and with low maintenance (transfers taking place every two to four weeks).
    c. Yes. Among strains of *Ochromonas* are those with the ability to survive in the dark, without organics, in artificial seawater, under nutrient-stress, in the presence of a competitor or predator, under thermal stress, and a variety of other robust environmental conditions, showing *Ochromonas* is a resilient organism that can be used under a large variety of experimental parameters.

III. *Stability and predictability*
    a. Yes. Studies on the same strains of *Ochromonas* by independent labs have demonstrated predictably similar results (Terrado et al. 2017, Lie et al. 2018, Wilken, Choi, and Worden 2020, Barbaglia et al. 2024, Honig et al. 2024, Jahns and Johnson *in prep*, etc.).
    b. Yes. Having acquired the same strains of *Ochromonas* from multiple sources and monitoring strains for many generations we find no evidence for any changes to the behavior or morphology of *Ochromonas* from laboratory domestication (personal observation).
    c. Unknown. To our knowledge, no study has investigated the potential genetic drift of *Ochromonas* strains in culture. Such studies are rare for protists in general, but should become more common as the application of genomics and transcriptomics are becoming increasingly routine.

IV. *Knowledgebase*
    a. Yes. As described above, many studies have used a variety of strains of *Ochromonas* to probe difficult metabolic questions. The phylogeny, morphology,

behavior, trophic characteristics, and energy usage has been described for many strains of *Ochromonas* by multiple laboratories.

b. Yes. Studies have demonstrated the ability to quantify *Ochromonas* grazing, photosynthesis, morphology, growth, growth efficiency, elemental composition, etc. (see Table 4.2)

c. No. Little to no attempt has been made by the community of *Ochromonas* researchers to agree upon acceptable or preferred standard methodologies for assessing *Ochromonas* traits and processes.

V. Genetic characterization and manipulation

a. Yes and no. There are published, assembled genomes for multiple strains of *Ochromonas* (Worden and Wilken 2014, Busi et al. 2022, Dorrell et al. 2022, etc.). Plastid and mitochondrial genomes are also available (Coleman, Thompson and Coff 1991, Ševčíková et al. 2015, etc.). There exists abundant existing data on the transcriptomes of *Ochromonas* strains and gene regulation (Lie et al. 2017, etc.). However, the functional characterization of those genes is done almost entirely based on homology. See: www-ncbi-nlm-nih-gov.libproxy.mit.edu/Taxonomy/Browser/wwwtax.cgi?mode=Undef&id=2985&lvl=3&keep=1&srchmode=1&unlock

b. No. To the best of our knowledge no system has been devised for reliably transforming or knocking-out genes in *Ochromonas*.

The most obvious short-coming of thinking of *Ochromonas* as a more traditional model system is the lack of a system to transform *Ochromonas*. This is generally considered essential for model systems (Ankeny and Leonelli 2020, Matthews and Vosshall 2020). While such a tool would undoubtably be powerful, we believe it is still worth thinking of *Ochromonas* as a non-traditional system in some ways analogous to a model system by utilizing the diversity of the genus itself.

Mixotrophy is an emergent phenomenon from complex interconnected metabolic pathways (Millette et al. 2024). One could, for example, knockout a gene integral to photosynthesis to observe changes to an organism, but this is not the same thing as transforming the mixotroph into a single-guild organism. The theorized energetic, spatial, and membrane surface area trade-offs would still exist even though the organism could not photosynthesize (Raven 1997, Flynn and Mitra 2009, Ward et al. 2011). These studies are obviously still informative but limited in their ability to address the research questions directly.

The reason genetic editing is thought to be central to a model system is because it allows for well-controlled manipulation of underlying mechanisms (Ankeny and Leonelli 2020, Matthews and Vosshall 2020). As mentioned, editing a metabolic pathway out of a mixotroph's genome or changing the mixotroph's metabolic landscape would require bioengineering entire trophic modes. While theoretically possible, this defeats the purpose of having a model organism as such techniques would be expensive and inaccessible to many labs.

As an alternative, we advocate utilizing the natural variety in *Ochromonas* trophic landscapes as an alternative to metabolic engineering. The *Ochromonas* genus is functionally diverse enough

to encompass a wide range of mixotrophic strategies while simultaneously being morphologically and phylogenetically similar enough to warrant direct comparison. *Ochromonas* strains share grazing rates, metabolic requirements, elemental composition, etc. within similar ranges, but are measurably distinct (Holen 2010, Dorell et al. 2019, Wilken et al. 2020, Barbaglia et al. 2024, Jahns and Johnson *in prep*). In some sense, swapping one strain of *Ochromonas* for an evolutionarily related but metabolically district strain can be analogous to observing genetic variation without need for genetic manipulation. In other words, treating each strain as a naturally genetically edited homologs of one another allows us to still create a 'model system' for studying mixotrophic trade-offs and metabolism without needing extensive artificial remodeling of multiple metabolic pathways. Such strain comparison can be common in traditional and non-traditional model systems as well (Russel et al. 2017, Ankney and Leonelli 2020).

This approach is not without drawbacks, but such work will be useful for advancing our body of knowledge. To take advantage of this approach, strains must be phylogenetically closely related and well-characterized. Obviously, there will be confounding variables associated with recent evolutionary history. As always, it is important to recognize the possibility that an unknown difference between strains, but many studies have already employed strain comparison techniques to great effect (Lie et al. 2018, Wilken, Choi, and Worden 2020, Barbaglia et al. 2024, Jahns and Johnson *in prep*, etc.).

iv. Research methods for using an Ochromonas *model system*

For those wishing to adopt *Ochromonas* as a non-traditional model system, there exists a wealth of knowledge and resources for establishing an experimental regime. Many established methodologies in microbial ecology have already been applied to *Ochromonas*, and we review some of them here and in Table 5.2.

Ochromonas can be grown in a variety of aquatic media depending on the strain, including freshwater (ex. Simonds, Grover and Chrzanowski 2010), seawater (ex. Flöder, Hansen and Ptacnik 2006), artificial seawater/Aquil salts (ex. Nodwell and Price 2001), and Instant Ocean (ex. Jahns and Johnson *in prep*). Many *Ochromonas* strains can survive under a range of nutrient concentrations and compositions (Flöder, Hansen and Ptacnik 2006, Barbaglia et al. 2024, Jahns and Johnson *in prep*, etc.). Most commonly used for freshwater cultures of *Ochromonas* is what is called "Ochromonas medium" (OM) made of natural freshwater and a mixture of organics (Starr 1978) or "WC medium" which includes additional nutrients (Guillard and Lorenzen 1972). In seawater, *Ochromonas* is often grown with the addition of other nutrients, most commonly K (Keller et al. 1987), with an organic addition to support phagotrophic growth such as heat-killed prey (ex. Wilken, Choi, and Worden 2020), small organic compounds (ex. Jahns and Johnson *in prep*) or sterile rice (ex. Barbaglia et al. 2024). *Ochromonas* can be grown in batch culture or chemostat (Chapter 4).

We have summarized many of the common and accessible techniques used to study mixotrophy in *Ochromonas* in Table 5.2. We believe there are ample established ways to appropriately evaluate both at phototrophy and phagotrophy indirectly or directly depending on the specific

research question. That does not mean our tools cannot expand and as *Ochromonas* increases in popularity as a study we are excited to see the procedures that develop.

Recent advances also highlight potential experimental pitfalls. For instance, the "prey" used for grazing measurements has varied greatly. Bacteria-sized fluorescence beads, stained heat-killed bacteria, and stained live bacteria have all been used. Because previous work from Boenigk et al. (2001), Johnke et al. (2017), Bock et al. (2021), Jimenez et al. (2021) and others have demonstrated inert prey, like beads and heat-killed bacteria, are not as accurate for quantification of grazing, we advocate all studies moving forward use only live bacteria as prey for *Ochromonas*. As for what bacteria are used as live prey, natural populations or single-strain bacteria that *Ochromonas* is known to graze upon, such as *Escherichia coli* K-12 and *Pelagibaca bermudensis* HTCC2601, have been used (ex. Hahn and Höfle 1997, Barbaglia et al. 2024, Jahns and Johnson *in prep*, etc.). It is important to consider prey type as it can considerably alter the growth and grazing rates of *Ochromonas* (Foster and Chrzanowski 2012).

Additionally, while competing strains of *Ochromonas* in coculture could be incredibly informative, those who wish to do so should carefully evaluate how to separate the two populations experimentally. Closely related strains of *Ochromonas* tend to have similar sizes and chlorophyll content making their distinction difficult (Barbaglia et al. 2024, Jahns and Johnson *in prep*, Chapter 4). One possible methodology to separate *Ochromonas* strains in co-culture is qPCR. Anderson et al. (2017) was able to separate and quantify multiple groups of *Ochromonas* strains via 18S rRNA sequencing in an environmental sample. However, using qPCR to determine cell abundances in a mixed-strain culture would likely require more phylogenetically distant strain as Barbaglia et al. (2024) showed strains which are metabolically unique may share 18S sequences which are not significantly distinct. Better gene markers for distinguishing between closely related strains could also be identified.

Combining experimental methods with models based on real observations has proven extremely powerful for understanding the mechanisms of mixotrophy in *Ochromonas* (Moeller et al. 2024). As the research in the field expands, we recommend the construction of more complex models based on even more real-life measurements.

Finally, in our mind, the gold standard for assessing mixotrophic tradeoffs and metabolic landscapes is direct competition with competitors. As Jahns and Johnson (*in prep*) demonstrate, varying the environment to induce resource pressure is not equivalent to competitive pressures for resources from a competitor like the single-guild phagotroph *Paraphysomonas bandaiensis*. Going forward, we recommend studies interested in competitive tradeoffs of mixotrophic metabolism design studies which directly test the effects of competition on *Ochromonas*.

v. Looking towards the future

Establishing an accepted model around a scientific question can lead to more interdisciplinary collaboration (Ankney and Leonelli 2020), greater standardization and infrastructure in the field (Russel et al. 2017), new methodologies (Matthews and Vosshall 2020) and greater funding in the research area (Ankney and Leonelli 2020). However, to realize the benefits of a non-traditional model system, it must reach a level of acceptance within the field (Russel et al. 2017,

Ankney and Leonelli 2020). A unified understanding of how the model system operates must also be achieved (Russel et al. 2017, Ankney and Leonelli 2020).

With this in mind, there remains important work to be done on characterizing *Ochromonas* strains. Genomes of more strains of *Ochromonas* must be assembled and published in easily accessible formats. Key genes thought to underly mixotrophy should be investigated directly to confirm their function. The genetic drift tendencies of strains in culture must also be better described. And finally, a consensus must be reached on the trophic niches and metabolic requirements of key strains to standardize comparisons and analyses across lab groups (see Table 5.1). These studies will also provide insight into the evolutionary trajectories of these organisms and may help elucidate the evolutionary drivers of mixotrophy in *Ochromonas*. Looking beyond *Ochromonas* to other Chrysophytes, including comparisons with closely related but solely phagotrophic clades like *Paraphysomonas*, may also offer fruitful avenues of research to contextualize the evolution of *Ochromonas* and mixotrophy in this lineage (Scoble and Cavalier-Smith 2014, Dorrell et al. 2019, Terpis et al. 2025).

With continued focus on solidifying *Ochromonas* as a non-traditional model system, *Ochromonas* gives our field a springboard towards future advancement. Early career scientists and researchers coming from other disciplines or systems will benefit from the wealth of current knowledge on the system and how to experimentally manipulate *Ochromonas*. And continued research into the question of mixotrophic tradeoffs and metabolic underpinnings will only grow that knowledgebase, further lowering barriers to entry for probing interesting mixotrophic questions using *Ochromonas*. This can create a positive feedback loop, where research into open questions on mixotrophic metabolism will become easier to study and more inviting to new researchers (Russel et al. 2017).

We want to reiterate that even after a non-traditional model organism is established, continued research on diverse organisms is and will remain incredibly important for advancing our knowledge of mixotrophic trade-offs and metabolism. *Ochromonas* represents only a specific subset of mixotrophs, constitutive mixotrophs, and results from *Ochromonas* must be extrapolated to non-constitutive mixotrophs with extreme care, if at all. Additionally, studies have demonstrated the utility of variety in study system on the robustness of a field's findings (Duffy et al. 2021). We believe it is most beneficial to invite scientists from across disciplines to engage with our model mixotroph, and not to discourage the vital research on other organisms in our field. Fortunately, historical evidence suggests the establishment of a model system does not decrease the study on diverse non-model organisms (Dietrich, Ankeny, and Chen 2014).

In summary, based on evidence from research in *Ochromonas* and studies examining the benefits of model systems, we believe there is a great potential benefit in standardizing our field's approach to studying mixotrophic trade-offs and metabolism, as well as developing *Ochromonas* into a non-traditional model system for wide use. We do not proclaim *Ochromonas* to be a magic key which will unlock the secret underpinnings of mixotrophy which have otherwise eluded our research. Instead, we believe there are several interesting experimental approaches – in genetics, competition, evolution, and biochemistry – which, combined with the "model organism-like characteristics" of *Ochromonas*, make *Ochromonas* a particularly compelling genus for research.

With some time and resources, a greater understanding of *Ochromonas* can be developed, and the non-traditional model *Ochromonas* system may help our field continue progressing our understanding of the mechanisms underlying mixotrophy.

Future work

i. Investigating the pathways involved in T4-like phage lipid remodeling

In Chapter 1 we demonstrated P-SSP4, a T4-like cyanophage, remodeled the *Prochlorococcus* MED4 lipidome in ways as predicted by a transcriptomic study on a T7-like phage (Lindell et al. 2007). Namely it altered both the fatty acid metabolism and phosphorus partitioning of its host (Chapter 1). Yet, unlike P-SSP7, the phage used in that study, P-SSP4 lacks the auxiliary metabolic genes thought to be associated with these metabolic changes, like a Pho-regulon phosphorus stress gene (Lindell et al. 2007, Sullivan et al. 2005). There are two possible explanations: either there is an auxiliary metabolic gene of mislabeled or unknown function in the P-SSP4 genome that performs these metabolic functions or the genes P-SSP4 does carry has the same downstream effects despite not being directly involved in these metabolic pathways.

Both possibilities are intriguing as they indicate we need to better characterize the how cyanophage genes interact with host metabolism or that cyanophage genomes possess genes with functions that are difficult to annotate due to higher evolutionary rates or unknown origins. This would be especially interesting as it may indicate a convergent evolution towards manipulation of the same metabolic process but through diverse means. Perhaps, even though Pho-like genes are very prevalent in marine phages (appearing in 40% of phage genomes) the number of phages which leverage this host metabolic pathway is underestimated as seemingly unrelated genes serve similar functions.

We recommend assembling the complete lipidomes of other strains of *Prochlorococcus* as infected by other cyanophages, especially the P-SSP7 used by Lindell et al. (2007). Additionally, we recommend studies use modern genetic manipulation techniques to investigate the true function of the auxiliary metabolic genes in common to cyanophage genomes.

ii. Cyanophage infection biomarker verification and field use

One of the most immediately applicable findings presented in Chapter 1 is the identification of OML-321 in the *Prochlorococcus* lipidome, a MGDG-like lipid of unknown structure with a mass corresponding to an oxidized MGDG. OML-321 was significantly correlated with phage infection of *Prochlorococcus*. The cursory analysis tying OML-321 to the diel-patterns of phage infection in the Pacific Ocean should be expanded in more sample sites and compared to direct measurements of infection in the open ocean. This compound may be a new way for field researchers to estimate phage infection but much more ground-truthing is needed to consider OML-321 a biomarker of this process.

iii. Complex competitive communities in chemostat culturing

In establishing *Ochromonas* as a non-traditional model system, we created a chemostat culturing apparatus for competition experiments with *Ochromonas* (Chapter 4).

In Chapter 4 we used the plastidless chrysophytes *Paraphysomonas bandaiensis* as a single-guild phagotrophic competitor for *Ochromonas* because of its similar size, environment, and evolutionary relationship (Scoble and Cavalier-Smith 2014, Dorrell et al. 2019, Terpis et al. 2025). However, we believe this competitive chemostat system is ripe for exploration with a greater diversity of organisms and trophic strategies. Dual *Ochromonas* strains in competition could provide insight into the evolutionary tradeoffs of different mixotrophic metabolic strategies. Additionally, we only looked at competition with a single-guild competitor, but there are a variety of phototrophs that could be informative to investigate. Expanding on this work to include three or more competitors in a single environment could also be incredibly informative for exploring community dynamics and nutrient cycling in more realistic mixed communities.

iv. Determining the metabolic pathways involved in mixotrophic competitive tradeoffs via transcriptomics

Underlying mechanisms of mixotrophic metabolic tradeoffs are poorly characterized (Millette et al. 2024). In Chapters 3 and 4 we overserved significant niche displacement in all *Ochromonas* strains in response to competition. In some of these plastic strains, namely 584 and 1148, this trophic shift came at a huge energetic cost. While we were able to develop some theories about how the energy and nutrient use and requirements of *Ochromonas* inform the metabolic landscapes of these organisms in Chapter 4, this system provides an ample opportunity to get at the specific metabolic landscapes involved in these tradeoffs.

Identifying up- or downregulation of specific metabolic pathways when mixotrophs compete with specialists for resources, would allow for a more specific description of the metabolic and biochemical trade-offs of mixotrophy. Transcriptomic analysis can pinpoint and describe the specific metabolic processes that contribute to the competitive dynamics of mixotrophs in mixed communities. For example, as some studies suggest, if investment in phosphate transporters limits mixotrophic competitiveness, one would expect to see tight regulatory control of these expensive proteins, and significantly lower expression when the mixotroph is in competition with the phototroph, than when it is in competition with the phagotroph (Ward et al. 2011). On the other hand, it is theorized mixotrophs may have more selectivity in the organic compounds they can break down. If this is the case, changes to metabolite catabolism and excretion pathways would be more likely (Crawford and Stoecker 1996).

We have already undertaken the sampling and extractions required for shotgun transcriptomic sequencing of each chemostat experiment in Chapter 4. After sequencing, we hope to separate the reads through assembled reference transcriptomes, and analyze them using differential expression and metabolic pathway analysis.

v. A model to predict competitive metabolic tradeoffs in mixotrophs

There are a wealth of impressive models investigating the metabolic landscapes and competitive dynamics of *Ochromonas* and mixotrophs in general (Flynn and Mitra 2009, Crane and Grover 2010, Vage et al. 2013, Edwards 2019, Chu, Moeller, and Archibald 2023, Archibald et al. 2024, Honig et al. 2024, Moeller et al. 2024, Schenone et al. 2024, etc.). Some of the most compelling, in our opinion, are those which incorporate real observations into confining the parameters of the

model, almost like a test set. We believe the chemostat cultures in Chapter 4, because of their tightly controlled environment and abundant measurements, can be converted into a simulated model effectively. Especially interesting would be varying the parameters associated with specialization (as in Chu, Moeller, and Archibald 2024) and plasticity kinetics (as in Archibald et al. 2024).

Concluding remarks on community dynamics and the metabolic niche

The multidimensional niche space encapsulating the 'metabolic niche' remains a powerful tool for conceptualizing community dynamics. Understanding the tradeoffs between metabolic efficiency and investment can help elucidate the responses of organisms to disturbance (Chapter 4). These 'metabolic landscapes' help to outline the contours of possible metabolic states in organisms and the tradeoffs associated with plasticity and niche displacement (Chapter 4).

Some mixotrophic researchers have recently cast doubt upon the idea that trait-based tradeoffs as a basis for understanding mixotrophs (Mitra et al. 2024). Mitra et al. (2024) argue against trait trade-offs and the need for the field to move away from considering trait-based approaches to mixotrophic competitiveness. Yet, Chapter 3 and Chapter 4 demonstrate the importance of trait-based approaches to mixotrophic ecology and that tradeoffs in growth, growth efficiency, and investment can shape the metabolic landscape of mixotrophs. At least in this system, we find that trait-based tradeoffs may not be as simple as a single growth penalty parameter (as trait-based tradeoffs are often modeled) but are still important to the eco-evolutionary strategies driving mixotrophic competitiveness and survival (Chapter 3, Chapter 4). As Mitra et al. (2024) mention, comparing mixotrophs across phylogenies may obscure the mechanisms underlying mixotrophic ecology as mixotrophy did not emerge from a single common ancestor of all mixotrophs. While this point is well taken, we believe our *Ochromonas* system, a non-traditional model system of closely related species or strains (e.g. Barbaglia et al, 2024), controls for this potentially confounding variable and this thesis demonstrates the utility of trait-based approaches to study closely related mixotrophs (Chapter 3, Chapter 4).

This work contributes to the growing literature that shows an organism's metabolic niche shapes and is shaped by its interactions with other organisms (Chapter 2, Chapter 3, Chapter 4). Organismal metabolic alteration may have a cascading effect that alters the metabolic niche of another organism several trophic levels removed (Chapter 2). Additionally, metabolically plastic organisms may utilize their flexible metabolism to relieve resource pressure in competition (Chapter 4). But plasticity for all living beings is limited, and some organisms may benefit from 'doubling down' on more competitive energy acquisition strategies, especially when resource quotas require a certain level of investment for the microbe to persist (Chapter 3, Chapter 4).

Additionally, we hypothesize that prey availability and nutritional value is a key component of community dynamics and organismal metabolic responses (Chapter 2, Chapter 3, Chapter 4). Average prey nutritional quality, whether through viral infection or lack of available nutritious prey, likely played a key role in the alteration of *Paraphysomonas bandaiensis* lipid biochemistry and energy storage (Chapter 2), as well as limiting the growth and metabolic efficiency of *Ochromonas* 584 (Chapter 3, Chapter 4).

In summary, this work examined three key ecological relationships between community members, parasitism, predation, and competition, and their interplay with organisms' metabolic landscape. We found that metabolic strategies shape and are shaped by community dynamics. We explored the benefits and drawbacks of metabolic plasticity in responding to changes in the abiotic environment. Finally, we created novel experimental systems for studying the dynamics of complex, mixed communities in laboratory settings and demonstrated their utility.

Tables

Scientific name	*Ochromonas sp.*	*Ochromonas sp.*	*Ochromonas sp.*	*Ochromonas sp.*	*Ochromonas danica*	*Ochromonas sp.*	*Ochromonas triangulata* (formerly *O. distigma*)[18]
Strain	CCMP 584	CCMP 1391	CCMP 1393	CCMP 2951	UTEX 1298, SAG 933-7 (both cultures are from the same isolate)	BG-1	RCC21
Availability	NCMA	NCMA	NCMA	NCMA	UTEX and SAG	Not publicly available[16]	RCC
Isolation location	Sargasso Sea[1]	Sargasso Sea[1]	Gulf Stream[1]	Okinawa, Japan[1]	Everdrup, Denmark[10]	Malaysia[16]	Bay of Biscay[18]
Approximate longitude, latitude	(34N, -65W)[1]	(34N, -65W)[1]	(39N, -72W)[1]	(25N, 125W)[1]	(55N, 12W)[23]	Unknown	(48N, 4W)[18]
Known growth media	K, K/50, K/10 + P/85, PROV50, ASM3, ASM4, L1 Prov100, L1-Si[1,3,4]	K, ASM2, K/10 + P/85, K-Si -Tris, ASM4, L1, L1-Si[1,3,4,5]	K, ASM2, K-Si -Tris, ASM4, L1, L1-Si[1,3,5]	K, K-Si -Tris, L1, L1-Si[1,3,5]	OM, Mineral Media, Aaronson & Baker Media (1959), DY-V[10,11,12,15,24]	DY-IV, DY-V[16,17]	f/2, L1, K/2[18,19,20,21]
Known temperature range (ºC)	22-26[1]	18-23[1,6]	18-23[1,3]	18-30[1,9]	21-25[12,13,24]	20[16]	13-20[19,21]
Obligately phototrophic	No[2,3]	Yes[2,3]	Conflicting accounts: No[2], Yes[7,8]	No[2,8]	No[14]	No[16]	Unknown
Obligately phagotrophic	Yes[3]	No[3]	Conflicting accounts: No[7], Yes[8]	No[8]	Conflicting accounts: No[14], Yes[13]	Yes[16]	Unknown
Estimated cell length (microns, approx.)	3-8[1,5]	3-6[1,6]	4-6[1]	3-7[1,3]	Unknown	5-8[16]	4-7[22]
Selected sequencing studies		Moeller (2022)	Worden and Wilken (2014), Lie et al. (2018), Ševčíková et al. (2015)	Lepori-Bui et al. (2022)	Terauchi et al. (2010), Majda, Beisser, and Boenigk (2021)	Lie et al. (2017)	Lepere et al. (2011), Andersen et al. (2017), Jeevannavar et al. (2025)

Table 5.1 An introduction to selected, commonly studied strains of Ochromonas that are ripe for continued research. Obligately phototrophic is defined as being able to grow in certain conditions in the absence of light. Obligately phagotrophic is defined as being able to grow in certain conditions in the absence of prey. NCMA is short for the National Center for Marine Algae and Microbiota (Bigelow Laboratory, East Boothbay, ME, USA). UTEX is short for the UTEX Culture Collection of Algae (The University of Texas at Austin, Austin, TX, USA). SAG is short for Department Experimental Phycology and Culture Collection of Algae at Georg-August-Universität Göttingen (Göttingen, Germany). RCC is short for the Roscoff Culture Collection (Station Biologirque de Roscoff, Roscoff, France). [1](Bigelow NCMA). [2](Barbaglia et al. 2024). [3](Personal observation). [4](Jahns and Johnson *in prep*). [5](Slomka et al. 2025). [6](Chapter 4). [7](Lie

et al. 2018). [8](Wilken, Choi, and Worden 2020). [9](Lepori-Bui et al. 2022). [10](UTEX Culture Collection of Algae). [11](White et al. 2016). [12](Aaronson 1971). [13](Chrzanowski and Foster 2014). [14](Coleman, Thompson, and Coff 1991). [15](Miao et al. 2010). [16](Sanders et al. 2001). [17](Lie et al. 2017). [18](Andersen et al. 2017). [19](Jimenez et al. 2021). [20](Jeevannavar et al. 2025). [21](Syhapanha et al. 2025). [22](Roscoff Culture Collection). [23](Department Experimental Phycology and Culture Collection of Algae). [24](Wilken, Schurrmans, and Matthijs 2014).

Method	Explanation	Example Studies
Cell Counting and Morphology		
Flow cytometry and microscopy	Ochromonas can be easily counted using red fluoresce and size on either a flow cytometer or a microscope.	Lie et al. 2018, Wilken, Choi, and Worden 2020, Barbaglia et al. 2024
qPCR	It is possible to count some Ochromonas strains via qPCR in mixed environments. However, Barbaglia et al. (2024) some Ochromonas strains share such similar 18S sequences they likely cannot be separated via qPCR.	Anderson et al. 2017
Primary Production		
Isotope labeling	^{13}C, ^{14}C, and ^{18}O are among the isotopes used to label spiked substrates for photosynthesis (such as carbonate) to quantify primary production.	Andersson et al. 1989, Weis and Brown 1959
Electron transport rates	Combining an electron transport rate from, for example, a Fluorescence Induction and Relaxation (FIRe) system with chlorophyll measurements can produce a carbon fixation rate.	Wilken, Chjoi and Worden 2020, Barbaglia et al. 2024, Chapter 4
Chlorophyll	If primary productivity does not need to be quantified with certainty (i.e. relative changes), cellular chlorophyll *a* content is often used as a proxy for phototrophic investment. This should be used with caution as chlorophyll content does not always have a direct relationship with primary production.	Tittle et al. 2003
Bacteria in Xenic Cultures		
DAPI	This stain attaches to adenine-thymine rich regions of DNA to visualize nucleic acids.	Corno 2009
SYBR Green	Another bright DNA-binding stain used to visualize bacteria.	Jahns and Johnson *in prep*
Food Vacuoles		
LysoTracker	LysoTracker green stains acidic vacuoles in the cell and has been shown to correlate with phagotrophic investment within the same strain of *Ochromonas*.	Jahns and Johnson *in prep*, Chapter 4
Bacterivory		

Bacteria ingestion rates	Bacterivory can be estimated through the counting of ingested labeled (usually fluorescent) prey over time through either microscopy or flow cytometry.	Jimenez et al. 2020, Costa et al. 2022, Chapter 4
Bacteria removal rates	Similar to above, bacterivory can be estimated by comparing the disappearance of labeled bacteria from the experiment (relative to the growth rate of the bacteria).	Tittle et al. 2003, Barbaglia et al. 2024
Shotgun Sequencing		
Genomics	Several published genomes of *Ochromonas* strains are assembled and published. Other studies have found success assembling metagenomes of mixed strain communities.	Worden and Wilken 2014, Busi et al. 2022
Transcriptomics	Transcriptomics is a powerful and well-used tool in *Ochromonas* systems for understanding metabolic responses to disturbance. Methods are proven and well established.	Liu et al. 2016, Zhang et al. 2018, Jeevannavar et al. 2025
Phylogeny		
18S ribosomal subunit sequence comparison	Most phylogenetic trees have been constructed using 18S sequences. Comparisons of trophic strategy and 18S phylogeny have proven useful to understanding the evolution and speciation of *Ochromonas* strains.	Andersen et al. 2017, Barbaglia et al. 2024
Functional gene sequence comparison	Sequencing of functional genes have also revealed convergent evolution and horizontal gene transfer between strains of *Ochromonas*. These may also provide more nuanced views on phylogeny and evolutionary history.	Dorrell et al. 2022
Experimental Evolution		
Long-term evolution experiments	One of the most exciting recent develops in *Ochromonas* experimentation is demonstrating *Ochromonas* can be an effective subject for long-term evolution experiments maintained over years.	Lepori-Bui et al. 2022
Metabolism		
Biochemical characterization	Lipidomes, metabolomes, exo-metabolomes, and proteomes have been characterized for a variety of strains of *Ochromonas*. The best practices for these methods are not well establish and vary by field and research question.	Aaronson et al. 1971, Vogel and Eichenberg 1992, Yamagishi et al. 2009, Princiotta et al. 2025
Carbon use efficiency and respiration	The carbon usage efficiency of *Ochromonas*, or the amount of captured carbon that is used for growth (as opposed to excreted or respired), is one of the more interesting potential tradeoffs of mixotrophy that continues to be investigated.	Barbaglia et al. 2024, Chapter 4

Table 5.2 A review of some of the methods commonly employed to study mixotrophy in *Ochromonas*.

References

1. Aaronson, S. (1971). The Synthesis of Extracellular Macromolecules and Membranes by a Population of the Phytoflagellate *Ochromonas danica*. *Limnology and Oceanography*, 16, 1–9.
2. Aaronson, S. (1973). Ochromonas: A Model System for the Study of Phytoflagellate and Algal Secretion into the Environment. *Bulletins from the Ecological Research Committee*, 367–370.
3. Aaronson, S., DeAngelis, B., Frank, O. & Baker, H. (1971). Secretion of Vitamins and Amino Acids into the Environment by Ochromonas Danica. *Journal of Phycology*, 7, 215–218.
4. Andersen, R.A., Graf, L., Malakhov, Y. & Yoon, H.S. (2017). Rediscovery of the *Ochromonas* type species *Ochromonas triangulata* (Chrysophyceae) from its type locality (Lake Veysove, Donetsk region, Ukraine). *Phycologia*, 56, 591–604.
5. Andersson, A., Falk, S., Samuelsson, G. & Hagström, Å. (1989). Nutritional characteristics of a mixotrophic nanoflagellate, *Ochromonas* sp. *Microb Ecol*, 17, 251–262.
6. Ankeny, R. & Leonelli, S. (2020). *Model Organisms*. 1st edn. Cambridge University Press.
7. Ankrah, N.Y.D., May, A.L., Middleton, J.L., Jones, D.R., Hadden, M.K., Gooding, J.R., *et al.* (2014). Phage infection of an environmentally relevant marine bacterium alters host metabolism and lysate composition. *ISME J*, 8, 1089–1100.
8. Archibald, K.M., Dutkiewicz, S., Laufkötter, C. & Moeller, H.V. (2024). Emergent trade-offs among plasticity strategies in mixotrophs. *Journal of Theoretical Biology*, 590, 111854.
9. Barbaglia, G.S., Paight, C., Honig, M., Johnson, M.D., Marczak, R., Lepori-Bui, M., *et al.* (2024). Environment-dependent metabolic investments in the mixotrophic chrysophyte *Ochromonas*. *Journal of Phycology*, 60, 170–184.
10. Becker, K.W., Collins, J.R., Durham, B.P., Groussman, R.D., White, A.E., Fredricks, H.F., *et al.* (2018). Daily changes in phytoplankton lipidomes reveal mechanisms of energy storage in the open ocean. *Nat Commun*, 9, 5179.
11. Bertile, F., Matallana-Surget, S., Tholey, A., Cristobal, S. & Armengaud, J. (2023). Diversifying the concept of model organisms in the age of -omics. *Commun Biol*, 6, 1062.
12. Bock, N.A., Charvet, S., Burns, J., Gyaltshen, Y., Rozenberg, A., Duhamel, S., *et al.* (2021). Experimental identification and in silico prediction of bacterivory in green algae. *The ISME Journal*, 15, 1987–2000.
13. Boenigk, J., Matz, A.C., Jurgens, K. & Arndt, H. (2001). Confusing selective feeding with differential digestion in bacterivorous nanoflagellates. *J Eukaryot Microbiol*, 48, 425–432.
14. Boenigk, J., Pfandl, K., Stadler, P. & Chatzinotas, A. (2005). High diversity of the '*Spumella*-like' flagellates: an investigation based on the SSU rRNA gene sequences of isolates from habitats located in six different geographic regions. *Environmental Microbiology*, 7, 685–697.

15. Burian, R.M. (1993). How the Choice of Experimental Organism Matters: Epistemological Reflections on an Aspect of Biological Practice. *Journal of the History of Biology*, 26, 351–367.
16. Busi, S.B., Bourquin, M., Fodelianakis, S., Michoud, G., Kohler, T.J., Peter, H., *et al.* (2022a). Genomic and metabolic adaptations of biofilms to ecological windows of opportunity in glacier-fed streams. *Nat Commun*, 13, 2168.
17. Busi, S.B., Bourquin, M., Fodelianakis, S., Michoud, G., Kohler, T.J., Peter, H., *et al.* (2022b). Genomic and metabolic adaptations of biofilms to ecological windows of opportunity in glacier-fed streams. *Nat Commun*, 13, 2168.
18. Cabrerizo, M.J., González-Olalla, J.M., Hinojosa-López, V.J., Peralta-Cornejo, F.J. & Carrillo, P. (2019). A shifting balance: responses of mixotrophic marine algae to cooling and warming under UVR. *New Phytologist*, 221, 1317–1327.
19. Caron, D.A. (2016). Mixotrophy stirs up our understanding of marine food webs. *Proceedings of the National Academy of Sciences*, 113, 2806–2808.
20. Castillo, T., Ramos, D., García-Beltrán, T., Brito-Bazan, M. & Galindo, E. (2021). Mixotrophic cultivation of microalgae: An alternative to produce high-value metabolites. *Biochemical Engineering Journal*, 176, 108183.
21. Chrzanowski, T.H. & Foster, B.L.L. (2014). Prey element stoichiometry controls ecological fitness of the flagellate *Ochromonas danica*. *Aquatic Microbial Ecology*, 71, 257–269.
22. Chu, T., Moeller, H.V. & Archibald, K.M. (2023). Competition between phytoplankton and mixotrophs leads to metabolic character displacement. *Ecological Modelling*, 481.
23. Coleman, A.W., Thompson, W.F. & Coff, L.J. (1991). Identification of the Mitochondrial Genome in the Chrysophyte Alga *Ochromonas danica*. *The Journal of Protozoology*, 38, 129–135.
24. Corno, G. (2006). Effects of nutrient availability and *Ochromonas* sp. predation on size and composition of a simplified aquatic bacterial community. *FEMS Microbiology Ecology*, 58, 354–363.
25. Costa, M.R.A., Sarmento, H., Becker, V., Bagatini, I.L. & Unrein, F. (2022). Phytoplankton phagotrophy across nutrients and light gradients using different measurement techniques. *Journal of Plankton Research*, 44, 507–520.
26. Crane, K.W. & Grover, J.P. (2010). Coexistence of mixotrophs, autotrophs, and heterotrophs in planktonic microbial communities. *Journal of Theoretical Biology*, 262, 517–527.
27. Crawford, D.W. & Stoecker, D.K. (1996). Carbon content, dark respiration and mortality of the mixotrophic planktonic ciliate *Strombidium capitatum*. *Marine Biology*, 126, 415–422.
28. Cropp, R. & Norbury, J. (2015). Mixotrophy: the missing link in consumer-resource-based ecologies. *Theor Ecol*, 8, 245–260.
29. Datta, M.S., Sliwerska, E., Gore, J., Polz, M.F. & Cordero, O.X. (2016). Microbial interactions lead to rapid micro-scale successions on model marine particles. *Nat Commun*, 7, 11965.

30. Department Experimental Phycology and Culture Collection of Algae. (2025). *RCC21 Ochromonas triangulata*. *Department Experimental Phycology and Culture Collection of Algae*. Available at: https://roscoff-culture-collection.org/rcc-strain-details/21. Last accessed 1 August 2025.
31. Dietrich, M.R., Ankeny, R.A. & Chen, P.M. (2014). Publication Trends in Model Organism Research. *Genetics*, 198, 787–794.
32. Dietrich, M.R., Ankeny, R.A., Crowe, N., Green, S. & Leonelli, S. (2020). How to choose your research organism. *Studies in History and Philosophy of Science Part C: Studies in History and Philosophy of Biological and Biomedical Sciences*, 80, 101227.
33. Dorrell, R.G., Azuma, T., Nomura, M., deKerdrel, G.A., Paoli, L., Yang, S., *et al.* (2019). Principles of plastid reductive evolution illuminated by nonphotosynthetic chrysophytes. *Proceedings of the National Academy of Sciences of the United States of America*, 116, 6914–6923.
34. Dorrell, R.G., Kuo, A., Füssy, Z., Richardson, E.H., Salamov, A., Zarevski, N., *et al.* (2022). Convergent evolution and horizontal gene transfer in Arctic Ocean microalgae. *Life Science Alliance*, 6.
35. Duarte, C., Gasol, J. & Vaqué, D. (1997). Role of experimental approaches in marine microbial ecology. *Aquat. Microb. Ecol.*, 13, 101–111.
36. Duffy, M.A., García-Robledo, C., Gordon, S.P., Grant, N.A., Green, D.A., Kamath, A., *et al.* (2021). Model Systems in Ecology, Evolution, and Behavior: A Call for Diversity in Our Model Systems and Discipline. *The American Naturalist*, 198, 53–68.
37. Edwards, K.F. (2019). Mixotrophy in nanoflagellates across environmental gradients in the ocean. *Proceedings of the National Academy of Sciences*, 116, 6211–6220.
38. Edwards, K.F., Li, Q., McBeain, K.A., Schvarcz, C.R. & Steward, G.F. (2023). Trophic strategies explain the ocean niches of small eukaryotic phytoplankton. *Proc Biol Sci*, 290, 20222021.
39. Flöder, S., Hansen, T. & Ptacnik, R. (2006). Energy–Dependent Bacterivory in *Ochromonas minima*–A Strategy Promoting the Use of Substitutable Resources and Survival at Insufficient Light Supply. *Protist*, 157, 291–302.
40. Flynn, K.J. & Mitra, A. (2009). Building the "perfect beast": modelling mixotrophic plankton. *Journal of Plankton Research*, 31, 965–992.
41. Flynn, K.J., Mitra, A., Anestis, K., Anschütz, A.A., Calbet, A., Ferreira, G.D., *et al.* (2019). Mixotrophic protists and a new paradigm for marine ecology: where does plankton research go now? *Journal of Plankton Research*, 41, 375–391.
42. Foster, B.L.L. & Chrzanowski, T.H. (2012). The mixotrophic protist Ochromonas danica is an indiscriminant predator whose fitness is influenced by prey type. *Aquatic Microbial Ecology*, 68, 1–11.
43. Gilmour, D.J. (2019). Chapter One - Microalgae for biofuel production. In: *Advances in Applied Microbiology* (eds. Gadd, G.M. & Sariaslani, S.). Academic Press, pp. 1–30.
44. González-Olalla, J.M., Medina-Sánchez, J.M., Norici, A. & Carrillo, P. (2021). Regulation of Phagotrophy by Prey, Low Nutrients, and Low Light in the Mixotrophic Haptophyte *Isochrysis galbana*. *Microb Ecol*, 82, 981–993.

45. Guillard, R.R.L. & Lorenzen, C.J. (1972). Yellow-Green Algae with Chlorophyllide C. *Journal of Phycology*, 8, 10–14.
46. Hahn, M.W. & Höfle, M.G. (1999). Flagellate Predation on a Bacterial Model Community: Interplay of Size-Selective Grazing, Specific Bacterial Cell Size, and Bacterial Community Composition. *Appl Environ Microbiol*, 65, 4863–4872.
47. Hammer, A.C. & Pitchford, J.W. (2005). The role of mixotrophy in plankton bloom dynamics, and the consequences for productivity. *ICES Journal of Marine Science*, 62, 833–840.
48. Holen, D.A. (2010). Mixotrophy in two species of *Ochromonas* (Chrysophyceae). *Nova Hedwigia, Beihefte*, 153–165.
49. Honig, M.A., Barbaglia, G.S., Doyle, M.D. & Moeller, H.V. (2024). Effects of mixotroph evolution on trophic transfer. *Journal of Plankton Research*, 47, fbae053.
50. in GBIF Secretariat. (2025). *Ochromonas vysotskii*.
51. Jahns, M. & Johnson, M. (Unpublished). Competition for prey drives a 'doubling down' on phagotrophy in the mixotroph *Ochromonas*. *In prep.*
52. Jeevannavar, A., Florenza, J., Divne, A.-M., Tamminen, M. & Bertilsson, S. (2025). Cellular heterogeneity in metabolism and associated microbiome of a non-model phytoflagellate. *The ISME Journal*, 19, wraf046.
53. Jenner, R.A. & Wills, M.A. (2007). The choice of model organisms in evo–devo. *Nat Rev Genet*, 8, 311–314.
54. Jimenez, V., Burns, J.A., Le Gall, F., Not, F. & Vaulot, D. (2021). No evidence of Phago-mixotropy in *Micromonas polaris* (Mamiellophyceae), the Dominant Picophytoplankton Species in the Arctic. *Journal of Phycology*, 57, 435–446.
55. Johnke, J., Boenigk, J., Harms, H. & Chatzinotas, A. (2017). Killing the killer: predation between protists and predatory bacteria. *FEMS Microbiology Letters*, 364, fnx089.
56. Jost, C., Lawrence, C.A., Campolongo, F., van de Bund, W., Hill, S. & DeAngelis, D.L. (2004). The effects of mixotrophy on the stability and dynamics of a simple planktonic food web model. *Theor Popul Biol*, 66, 37–51.
57. Keller, M.D., Selvin, R.C., Claus, W. & Guillard, R.R.L. (1987). Media for the Culture of Oceanic Ultraphytoplankton. *Journal of Phycology*, 23, 633–638.
58. Krogh, A. (1929). The progress of physiology. *American Journal of Physiology-Legacy Content*, 90, 243–251.
59. Lee, H., Bloxham, B. & Gore, J. (2023). Resource competition can explain simplicity in microbial community assembly. *Proceedings of the National Academy of Sciences*, 120, e2212113120.
60. Lepere, C., Demura, M., Kawachi, M., Romac, S., Probert, I. & Vaulot, D. (2011). Whole-genome amplification (WGA) of marine photosynthetic eukaryote populations. *FEMS Microbiology Ecology*, 76, 513–523.
61. Lepori-Bui, M., Paight, C., Eberhard, E., Mertz, C.M. & Moeller, H.V. (2022). Evidence for evolutionary adaptation of mixotrophic nanoflagellates to warmer temperatures. *Global Change Biology*, 28, 7094–7107.

62. Lie, A.A.Y., Liu, Z., Terrado, R., Tatters, A.O., Heidelberg, K.B. & Caron, D.A. (2017). Effect of light and prey availability on gene expression of the mixotrophic chrysophyte, *Ochromonas* sp. *BMC Genomics*, 18, 163.
63. Lie, A.A.Y., Liu, Z., Terrado, R., Tatters, A.O., Heidelberg, K.B. & Caron, D.A. (2018). A tale of two mixotrophic chrysophytes: Insights into the metabolisms of two *Ochromonas* species (Chrysophyceae) through a comparison of gene expression. *PLoS One*, 13, e0192439.
64. Lindell, D., Jaffe, J.D., Coleman, M.L., Futschik, M.E., Axmann, I.M., Rector, T., *et al.* (2007). Genome-wide expression dynamics of a marine virus and host reveal features of co-evolution. *Nature*, 449, 83–86.
65. Liu, Z., Campbell, V., Heidelberg, K.B. & Caron, D.A. (2016). Gene expression characterizes different nutritional strategies among three mixotrophic protists. *FEMS Microbiology Ecology*, 92, fiw106.
66. Majda, S., Beisser, D. & Boenigk, J. (2021). Nutrient-driven genome evolution revealed by comparative genomics of chrysomonad flagellates. *Commun Biol*, 4, 328.
67. Mansour, J.S. & Anestis, K. (2021). Eco-Evolutionary Perspectives on Mixoplankton. *Front. Mar. Sci.*, 8.
68. Matthews, B.J. & Vosshall, L.B. (2020). How to turn an organism into a model organism in 10 'easy' steps. *Journal of Experimental Biology*, 223, jeb218198.
69. Miao, A.-J., Luo, Z., Chen, C.-S., Chin, W.-C., Santschi, P.H. & Quigg, A. (2010). Intracellular Uptake: A Possible Mechanism for Silver Engineered Nanoparticle Toxicity to a Freshwater Alga Ochromonas danica. *PLOS ONE*, 5, e15196.
70. Millette, N.C., Leles, S.G., Johnson, M.D., Maloney, A.E., Brownlee, E.F., Cohen, N.R., *et al.* (2024). Recommendations for advancing mixoplankton research through empirical-model integration. *Front. Mar. Sci.*, 11.
71. Mitra, A., Flynn, K.J., Burkholder, J.M., Berge, T., Calbet, A., Raven, J.A., *et al.* (2014). The role of mixotrophic protists in the biological carbon pump. *Biogeosciences*, 11, 995–1005.
72. Mitra, A., Flynn, K.J., Stoecker, D.K., & Raven, J.A. (2024). Trait trade-offs in phagotrophic microalgae: the mixoplankton conundrum. *European Journal of Phycology*, 59(1), 51-70.
73. Moeller, H.V., Archibald, K.M., Leles, S.G. & Pfab, F. (2024). Predicting optimal mixotrophic metabolic strategies in the global ocean. *Science Advances*, 10, eadr0664.
74. Nodwell, L.M. & Price, N.M. (2001). Direct use of inorganic colloidal iron by marine mixotrophic phytoplankton. *Limnology and Oceanography*, 46, 765–777.
75. Patel, A.K., Choi, Y.Y. & Sim, S.J. (2020). Emerging prospects of mixotrophic microalgae: Way forward to sustainable bioprocess for environmental remediation and cost-effective biofuels. *Bioresource Technology*, 300, 122741.
76. Patel, A.K., Singhania, R.R., Sim, S.J. & Dong, C.D. (2021). Recent advancements in mixotrophic bioprocessing for production of high value microalgal products. *Bioresource Technology*, 320, 124421.
77. Princiotta, S.D., Hiripitiyage, Y., Holen, D., Kellogg, J.J., Sturm, B. & Harris, T.D. (2025). Nutrient limitation determines biological interactions between a mixotrophic

Chrysophyte and toxin-producing *Microcystis*. *Journal of Plankton Research*, 47, fbae067.
78. Raven, J.A. (1997). Phagotrophy in phototrophs. *Limnology and Oceanography*, 42, 198–205.
79. Roscoff Culture Collection. (2025). *SAG 933-7 Ochromonas danica*. *UTEX Culture Collection of Algae*. Available at: https://sagdb.uni-goettingen.de/detailedList.php?str_number=933-7. Last accessed 1 August 2025.
80. Russell, J.J., Theriot, J.A., Sood, P., Marshall, W.F., Landweber, L.F., Fritz-Laylin, L., *et al.* (2017). Non-model model organisms. *BMC Biology*, 15, 55.
81. Sanders, R.W., Caron, D.A., Davidson, J.M., Dennett, M.R. & Moran, D.M. (2001). Nutrient Acquisition and Population Growth of a Mixotrophic Alga in Axenic and Bacterized Cultures. *Microb Ecol*, 42, 513–523.
82. Schenone, L., Aarons, Z.S., García-Martínez, M., Happe, A. & Redoglio, A. (2024). Mixotrophic protists and ecological stoichiometry: connecting homeostasis and nutrient limitation from organisms to communities. *Front. Ecol. Evol.*, 12.
83. Schmidtke, A., Bell, E.M. & Weithoff, G. (2006). Potential grazing impact of the mixotrophic flagellate *Ochromonas* sp. (Chrysophyceae) on bacteria in an extremely acidic lake. *J PLANKTON RES*, 28, 991–1001.
84. Scoble, J.M. & Cavalier-Smith, T. (2014). Scale evolution in Paraphysomonadida (Chrysophyceae): Sequence phylogeny and revised taxonomy of *Paraphysomonas*, new genus *Clathromonas*, and 25 new species. *European Journal of Protistology*, 50, 551–592.
85. Ševčíková, T., Horák, A., Klimeš, V., Zbránková, V., Demir-Hilton, E., Sudek, S., *et al.* (2015). Updating algal evolutionary relationships through plastid genome sequencing: did alveolate plastids emerge through endosymbiosis of an ochrophyte? *Sci Rep*, 5, 10134.
86. Simonds, S., Grover, J.P. & Chrzanowski, T.H. (2010). Element content of *Ochromonas* danica: a replicated chemostat study controlling the growth rate and temperature. *FEMS Microbiology Ecology*, 74, 346–352.
87. Slomka, S., Verspagen, J.M.H., Huisman, J. & Wilken, S. (2025). Variable responses to ocean acidification among mixotrophic protists with different lifestyles. *ISME Commun*, 5, ycaf064.
88. Smalley, G.W., Coats, D.W. & Stoecker, D. (2003). Feeding in the mixotrophic dinoflagellate Ceratium furca is influenced by intracellular nutrient concentrations.
89. Starr, R. (1978). Culture Collection of Algae at the University-of-Texas at Austin. *J. Phycol.*, 14, 47–100.
90. Stickney, H.L., Hood, R.R. & Stoecker, D.K. (2000). The impact of mixotrophy on planktonic marine ecosystems. *Ecological Modelling*, 125, 203–230.
91. Stoltze, H.J., Lui, N.S.T., Anderson, O.R. & Roels, O.A. (1969). The influence of the mode of nutrition on the digestive system of *Ochromonas malhamensis*. *The Journal of Cell Biology*, 43, 396–409.
92. Sullivan, M.B., Coleman, M.L., Weigele, P., Rohwer, F. & Chisholm, S.W. (2005). Three Prochlorococcus Cyanophage Genomes: Signature Features and Ecological Interpretations. *PLoS Biol*, 3, e144.

93. Syhapanha, K.S., Poulin, R.X., Russo, D.A., Wong, W.Y.F. & Pohnert, G. (2025). Context-dependent allelopathy in algal interactions: Insights from laboratory and natural phytoplankton communities. *Harmful Algae*, 148, 102886.
94. Terauchi, M., Kato, A., Nagasato, C. & Motomura, T. (2010). Research note: Analysis of expressed sequence tags from the chrysophycean alga Ochromonas danica (Heterokontophyta). *Phycological Research*, 58, 217–221.
95. Terpis, K.X., Salomaki, E.D., Barcytė, D., Pánek, T., Verbruggen, H., Kolisko, M., *et al.* (2025). Multiple plastid losses within photosynthetic stramenopiles revealed by comprehensive phylogenomics. *Current Biology*, 0.
96. Terrado, R., Pasulka, A.L., Lie, A.A.-Y., Orphan, V.J., Heidelberg, K.B. & Caron, D.A. (2017). Autotrophic and heterotrophic acquisition of carbon and nitrogen by a mixotrophic chrysophyte established through stable isotope analysis. *ISME J*, 11, 2022–2034.
97. Tittel, J., Bissinger, V., Zippel, B., Gaedke, U., Bell, E., Lorke, A., *et al.* (2003). Mixotrophs combine resource use to outcompete specialists: Implications for aquatic food webs. *Proceedings of the National Academy of Sciences*, 100, 12776–12781.
98. UTEX Culture Collection of Algae. (2025). *UTEX LB 1298 Ochromonas danica*. *UTEX Culture Collection of Algae*. Available at: https://utex.org/products/utex-lb-1298. Last accessed 1 August 2025.
99. Våge, S., Castellani, M., Giske, J. & Thingstad, T.F. (2013). Successful strategies in size structured mixotrophic food webs. *Aquat Ecol*, 47, 329–347.
100. Vincent, F. & Vardi, A. (2023). Viral infection in the ocean—A journey across scales. *PLOS Biology*, 21, e3001966.
101. Vogel, G. & Eichenberger, W. (1992). Betaine Lipids in Lower Plants. Biosynthesis of DGTS and DGTA in Ochromonas danica (Chrysophyceae) and the Possible Role of DGTS in Lipid Metabolism. *Plant and Cell Physiology*, 33, 427–436.
102. Wang, J., Yang, H. & Wang, F. (2014). Mixotrophic cultivation of microalgae for biodiesel production: status and prospects. *Appl Biochem Biotechnol*, 172, 3307–3329.
103. Ward, B.A. (2019). Mixotroph ecology: More than the sum of its parts. *Proceedings of the National Academy of Sciences*, 116, 5846–5848.
104. Ward, B.A., Dutkiewicz, S., Barton, A.D. & Follows, M.J. (2011). Biophysical Aspects of Resource Acquisition and Competition in Algal Mixotrophs. *The American Naturalist*, 178, 98–112.
105. Ward, B.A. & Follows, M.J. (2016). Marine mixotrophy increases trophic transfer efficiency, mean organism size, and vertical carbon flux. *Proc. Natl. Acad. Sci. U.S.A.*, 113, 2958–2963.
106. Weis, D. & Brown, A.H. (1959). Kinetic Relationships between Photosynthesis and Respiration in the Algal Flagellate, *Ochromonas malhamensis*. *Plant Physiology*, 34, 235–239.
107. White, A.R., Duggan, B.M., Tsai, S.-C. & Vanderwal, C.D. (2016). The Alga *Ochromonas danica* Produces Bromosulfolipids. *Org. Lett.*, 18, 1124–1127.
108. Wieczynski, D.J., Moeller, H.V. & Gibert, J.P. (2023). Mixotrophic microbes create carbon tipping points under warming. *Functional Ecology*, 37, 1774–1786.

109. Wilken, S., Choi, C.J. & Worden, A.Z. (2020). Contrasting Mixotrophic Lifestyles Reveal Different Ecological Niches in Two Closely Related Marine Protists. *J Phycol*, 56, 52–67.
110. Wilken, S., Schuurmans, J.M. & Matthijs, H.C.P. (2014a). Do mixotrophs grow as photoheterotrophs? Photophysiological acclimation of the chrysophyte *Ochromonas danica* after feeding. *New Phytologist*, 204, 882–889.
111. Wilken, S., Verspagen, J.M.H., Naus-Wiezer, S., Van Donk, E. & Huisman, J. (2014b). Biological control of toxic cyanobacteria by mixotrophic predators: an experimental test of intraguild predation theory. *Ecological Applications*, 24, 1235–1249.
112. Worden, A. & Wilken, S. (2014). *Ochromonas CCMP1393 Annotated Standard Draft*. *JGI*. Available at: https://genome.jgi.doe.gov/portal/OchCCMStandDraft_FD/OchCCMStandDraft_FD.info.html. Last accessed 30 July 2025.
113. Yamagishi, T., Motomura, T., Nagasato, C. & Kawai, H. (2009). Novel Proteins Comprising the Stramenopile Tripartite Mastigoneme in Ochromonas Danica (chrysophyceae). *Journal of Phycology*, 45, 1110–1115.
114. Yoo, Y., Seong, K., Jeong, H., Yih, W., Rho, J., Nam, S., *et al.* (2017). Mixotrophy in the marine red-tide cryptophyte Teleaulax amphioxeia and ingestion and grazing impact of cryptophytes on natural populations of bacteria in Korean coastal waters. *Harmful Algae*, 68, 105–117.
115. Zhang, L., Lyu, K., Wang, N., Gu, L., Sun, Y., Zhu, X., *et al.* (2018). Transcriptomic Analysis Reveals the Pathways Associated with Resisting and Degrading Microcystin in Ochromonas. *Environ Sci Technol*, 52, 11102–11113.